Electronic Supplementary Material (ESI) for Organic & Biomolecular Chemistry

Supplementary Information

Chemo-enzymatic synthesis and glycosidase inhibitory properties of DAB and LAB derivatives

Alda Lisa Concia[a], Livia Gomez[a], Jordi Bujons[a], Teodor Parella[b], Cristina Vilaplana[c], Pere Joan Cardona[c], Jesús Joglar[a] and Pere Clapés[a*]

[a]Dept Química Biológica y Modelización Molecular. Instituto de Química Avanzada de Cataluña, IQAC-CSIC. Jordi Girona 18-26, 08034 Barcelona, Spain.

[b]Servei de Ressonància Magnètica Nuclear, Departament de Química. Universitat Autònoma de Barcelona, Bellaterra, Spain.

[c]Unitat de Tuberculosi Experimental. Fundació Institut d'Investigació en Ciències de la Salut Germans Trias i Pujol. Universitat Autònoma de Barcelona. CIBERES. Edifici Laboratoris de Recerca. Crtra. de Can Ruti, Camí de les Escoles, s/n, 08916, Badalona (Spain)

Materials. *Synthesis*. Aniline, benzylamine, quinolin-3-amine and N^1-methylbenzene-1,2-diamine, aminoalcohols and amino acid derivatives were purchased from Sigma-Aldrich. Dihydroxyacetone (DHA) was purchased from Merck. *N*-Cbz-2-amino ethanal (*N*-Cbz-glycinal) was synthesized in our lab using procedures published in previous works.[1] L-Rhamnulose-1-phosphate aldolase [Co^{II}] (RhuA) (3.8 U mg^{-1} protein) (1 Unit (U) catalyses the cleavage of 1 μmol of L-rhamnulose-1-phosphate per minute at 25 ºC and pH 7.5 (100 mM Tris·HCl + 150 mM KCl)) was produced in our lab using standard procedures.[2] FSA A165G (0.9 U mg^{-1} protein; 1U catalysed the formation of 1 μmol of D-fructose-6-phosphate (D-F6P) per minute from DHA (300 mM) and D,L-glyceraldehyde-3-phosphate at 30 ºC in 50 mM glycylglycine buffer pH 8.5, containing 1 mM DTT) was produced in our lab using standard procedures.[3] Aqueous borate solutions were prepared by adjusting the desired pH of a solution of boric acid with 2 M aq NaOH. Water for analytical and preparative HPLC and for the preparation of buffers and other assay solutions was obtained from an Arium® Pro Ultrapure Water Purification System (SartoriusStedim Biotech). All other solvents used were of analytical grade.

Biological activity: Ketamine chlorhydrate and Imalgene 1000 were from Merial Laboratorios S.A. (Barcelona, Spain). Xylacine and Rompun 2% were from Química Farmacéutica S.A. (Barcelona, Spain). Starch from potatoes, starch azure, 4-hydroxybenzoic acid, 4-aminoantipyrine, Glucose oxydase Type II-S from *Aspergillus niger*, Peroxidase Type II from horseradish, α-D-Glucosidase from baker's yeast, α-D-glucosidase from rice, β-D-glucosidase from sweet almonds, β-D-galactosidase from bovine liver, α-D-mannosidase from jack beans, α-L-rhamnosidase from *Penicillium decumbens*, α-L-fucosidase from bovine kidney and the synthetic substrates *p*-nitrophenyl-α-D-glucopyranoside, *p*-nitrophenyl-β-D-glucopyranoside, *p*-nitrophenyl-β-D-galactopyranoside, *p*-nitrophenyl-α-D-mannopyranoside, *p*-nitrophenyl-α-

D-rhamnopyranoside, and *p*-nitrophenyl-α-D-fucopyranoside were purchase from Sigma-Aldrich.

HPLC analyses. HPLC analyses were performed on a RP-HPLC XBridge® C18, 5 μm, 4.6 x 250 mm column (Waters). Samples (25 μL) were withdrawn from the aldol reactions, dissolved in MeOH (1 mL) to stop the reaction and analysed by HPLC. The solvent system used was: solvent (A): 0.1 % (v/v) trifluoroacetic acid (TFA) in H_2O and solvent (B): 0.095 % (v/v) TFA in ACN/H_2O 4:1, flow rate 1 mL min^{-1}, detection 215 nm, column temperature 30 ºC. Gradient conditions are given for each compound. The amount of aldol adduct produced was quantified from the peak areas using an external standard methodology.

Methods

Enzymatic inhibition assays against commercial glycosidases

Commercial glycosidase solutions were prepared with the appropriate buffer and incubated in 96-well plates at 37ºC without (control) or with inhibitor (1.0 mM to 2.0 nM) during 3 min for α-D-glucosidase from *Saccharomyces cerevisiae*, β-D-glucosidase, α-D-mannosidase, α-L-rhamnosidase, α-L-fucosidase and 5 min for β-D-galactosidase. After addition of the corresponding substrate solution, incubations were prolonged during different time periods: 10 min for α-D-glucosidase from rice, 3 min for β-D-glucosidase, 6 min for α-D-mannosidase, 5 min for α-L-rhamnosidase, 7 min for α-L-fucosidase and 16 min for β-D-galactosidase and stopped by addition of Tris solution (50 μL, 1 M) or glycine buffer (180 μL, 100 mM, pH 10), depending on the enzymatic inhibition assay. The amount of *p*-nitrophenol formed was determined at 405 nm with UV/VIS Spectramax Plus (Molecular Devices Corporation) spectrophotometer. α-D-glucosidase from *Saccharomyces cerevisiae* activity was determined with *p*-nitrophenyl-α-D-glucopyranoside (1 mM) in phosphate buffer (100 mM; pH 7.2). α-D-Glucosidase from rice activity was determined with *p*-nitrophenyl-α-D-glucopyranoside (1 mM) in sodium acetate buffer (50 mM, pH 5.0). β-D-Glucosidase activity was determined with

p-nitrophenyl-β-D-glucopyranoside (1 mM) in sodium acetate buffer (100 mM, pH 5.0). β-D-Galactosidase activity was determined with *p*-nitrophenyl-β-D-galactopyranoside (1 mM) in sodium phosphate buffer (100 mM, 0.1 mM $MgCl_2$, pH 7.2). α-D-Mannosidase activity was determined with *p*-nitrophenyl-α-D-mannopyranoside (1 mM) in sodium acetate buffer (50 mM, pH 5.0). α-L-Rhamnosidase activity was determined with *p*-nitrophenyl-α-D-rhamnopyranoside (1 mM) in sodium acetate buffer (50 mM, pH 5.0). α-L-Fucosidase activity was determined with *p*-nitrophenyl-α-D-fucopyranoside (0.15 mM) in sodium acetate buffer (50 mM, pH 5.0). The commercial glycosidase solutions were prepared as follows: α-D-glucosidase from *Saccharomyces cerevisiae* (0.15 mg mL^{-1} buffer); α-D-glucosidase from rice $(NH_4)_2SO_4$ suspension (100 μL) in buffer (5 mL); β-D-glucosidase: (0.1 mg mL^{-1} buffer), β-D-galactosidase from *Aspergillus oryzae* (0.5 mg mL^{-1} buffer), α-L-rhamnosidase (naringinase) (0.3 mg mL^{-1} buffer); α-D-mannosidase $(NH_4)_2SO_4$ suspension (25 μL) in buffer (10 mL); β-D-galactosidase from bovine liver (0.1 mg mL^{-1} buffer), and α-L-fucosidase $(NH_4)_2SO_4$ suspension (33 μL) in buffer (10 mL).

Kinetics of inhibition. The nature of the inhibition against enzymes and the K_i values were determined from the Lineweaver-Burk plots.

Inhibition assays against rat intestinal disacharidases. *Animals*. Adult male Sprague-Dawley rats weighing 200 g (n=2) (Harlan Ibèrica, Barcelona, Spain) were housed in cages (n=2/cage) under controlled conditions of a 12 hours light:dark cycle, with a temperature of 22 ± 3 ºC and a relative humidity of 40-70%. Rats were fed on a standard diet (Panlab A04, Panlab, Barcelona, Spain) and water *ad libitum*. Handling and sacrificing of the animals were in full accordance with the European Community guidelines for the care and management of laboratory animals and the pertinent permission was obtained from the CSIC Subcommittee of Bioethical issues (permit number: CTQ2009-07359). Rats were fasted overnight and then

anesthetized by intramuscular injection of ketamine hydrochloride (0.1 % v/weight of rat, (90 mg/kg body wt ip) and xylacine (0.01 % v/weight of rat, 10 mg/kg body wt). The samples were diluted with ice-cold isotonic saline (50 mg mucosa mL^{-1}) and homogenized (T10 basic Ultra-Turrax , IKA, Staufen, Germany).

Preparation of gut mucosal suspension. Small intestine was removed, and carefully divided into duodenum, jejunum and ileum. The jejunum was washed with ice-cold isotonic saline, opened lengthwise and the mucosa scraped off with a microscope slide. The jejunum mucosa was stored at –80ºC. The samples were diluted with ice-cold isotonic saline (50 mg mucosa mL^{-1}) and homogenized (T10 basic Ultra-Turrax , IKA, Staufen, Germany).

Assay of disacharidase activity. Disacharidase activities, i.e. sucrase, lactase, maltase and trehalase, in the homogenized jejunum mucosa were determined by the method of Dalqhvist.[4] Enzyme activity (μmoles of substrate hydrolysed per hour) were normalized to protein content evaluated by the method of Bradford.[5] The disaccharide substrates, sucrose, lactose, maltose and trehalose, were purchased at the highest purity available (Sigma Chemical Co.) Substrates and inhibitors were prepared in distilled water. The concentrations used in the assay were 0.02 M for disaccharides, and a range from 2 mM down for inhibitors. The homogenized mucosa was diluted four times for the sucrose and trehalase assays; one time for the lactase assay and 25 times for the maltase activity and protein determination assays. Inhibitors and suitably diluted homogenized mucosa were pre incubated for 30 minutes at 37 ºC. Then, the reaction was carried out by the addition of the substrate in phosphate buffer pH 6.8. Substrate, inhibitor and homogenized mucosa were incubated together for 30 min at 37 ºC and agitation (250 r.p.m.). The reaction was terminated by the addition of Tris-glucose oxidase-peroxidase reagent: Tris 0.5 M; 4-hydroxybenzoic acid 10 mM; 4-aminoantipyrine 0.4 mM; glucose oxidase 1480 UI L^{-1}, peroxidase 250 UI L^{-1}, pH 7.3. Glucose is transformed in gluconic acid and hydrogen peroxide by glucose oxidase. Peroxidase catalyses the

combination of hydrogen peroxide with 4-aminoantipiryne generating a stable and coloured compound. After a further incubation of 2 hours this product was measured spectrophotometrically at 505 nm.

Minimum inhibitory concentration (MIC) determination. REMA plate method. Mycobateria strain (H37RvPasteur *M. tuberculosis* laboratory strain)

The resazurin microtiter assay (REMA) plate method[6] was performed in Middlebrook 7H9 Broth medium supplemented with 0.2% glycerol, 0.5% albumin-dextrose catalase (Becton Dickinson) and 0.05% Tween 80 (7H9-S). Resazurin sodium salt powder (Sigma-Aldrich 199303-1G) was prepared at (0.01% w/v) concentration in distilled water and sterilized by filtration trough a 0.2 μm membrane. The inoculum was prepared as follows: *M. tuberculosis* H37Rv Pasteur was grown in 250 mL PYREX bottles in a shaking incubator at 37ºC and 120 rpm in 7H9-S, it was left grow to mid-log phase, and stored at –70ºC. The inoculum was prepared by diluting an aliquot (3 mL) of the previous solution down to 10^6 CFU mL^{-1} in 7H9-S.

Serial of two-fold dilutions of each inhibitor in 7H9-S medium (100 μL) were prepared directly in 96-well plates at concentrations ranging from 2.5 mg mL^{-1} to 0.078 mg mL^{-1}. Growth controls containing no antibiotic, sterility controls without inoculation and inhibition controls containing isoniazide (1 μg mL^{-1}) were also included in the assay.

The assay was conducted as follows: The inoculum (100 μL) was added to the wells containing the inhibitors and to the corresponding control assays, the plates were covered, sealed, and incubated at 37°C in the standard atmosphere. After 6 days of incubation, resazurin solution (100 μL) added to each well, incubated during 2 days at 37°C, and assessed for colour development. A change from blue to pink indicates reduction of resazurin and therefore bacterial growth. The MIC was defined as the lowest drug concentration that prevented this colour change. Experiments were performed in triplicate.

*DAB and LAB aromatic 2-aminomethyl derivatives **24**.*

(2*S*,3*S*,4*S*)-3,4-dihydroxy-2-((phenylamino)methyl)pyrrolidine (24a). The precursor (2*S*,3*S*,4*S*)-*N*-benzyloxycarbonyl-3,4-dihydroxy-2-((phenylamino)methyl)pyrrolidine (115 mg, 40% yield) was purified by HPLC: gradient elution from 30 to 80% B in 30 min. HPLC analysis: identical to that of **23a**. The title compound (60 mg, 85% yield) was prepared according to the general procedure described above. HPLC Purification: gradient elution from 0 to 60% B in 40 min. $[\alpha]_D^{22} = -41.5$ (*c* 1.1 in MeOH). ^{1}H NMR (600 MHz, MeOD) δ= 7.15 (dd, *J* = 8.6, 7.4 Hz, 2H), 6.78 – 6.59 (m, 3H), 4.24 – 4.23 (m, 1H), 4.11 (d, *J* = 1.0 Hz, 1H), 3.72 (ddd, *J* = 9.5, 5.4, 1.6 Hz, 1H), 3.58 (dd, *J* = 14.0, 5.5 Hz, 1H), 3.53 (dd, *J* = 14.0, 9.7 Hz, 1H), 3.48 (dd, *J* = 12.0, 3.7 Hz, 1H), 3.34 (d, *J* = 12.4 Hz, 1H). ^{13}C NMR (101 MHz, CD_3OD) δ= 148.8, 130.2, 119.0, 114.11, 78.5, 76.3, 67.3, 52.3, 45.1. HRMS (ESI-TOF): *m*/*z* $[M+H]^+$ for $C_{11}H_{17}N_2O_2^+$ calculated 209.1285; observed 209.1276.

(2*S*,3*S*,4*S*)-2-((benzylamino)methyl)-3,4-dihydroxypyrrolidine (24b). The precursor (2*S*,3*S*,4*S*)-*N*-benzyloxycarbonyl-2-((benzylamino)methyl)-3,4-dihydroxypyrrolidine (133 mg, 48% yield) was purified by HPLC: gradient elution from 0 to 70% B in 40 min. HPLC analysis: identical to that of **12b**. The title compound (64 mg, 85% yield) was prepared according to the general procedure described above. HPLC Purification: gradient elution from 0 to 60% B in 40 min. $[\alpha]_D^{22} = -14.4$ (*c* 1.3 in MeOH). ^{1}H NMR (500 MHz, CD_3OD) δ= 7.55 – 7.43 (m, 5H), 4.27 (s, 2H), 4.25 – 4.22 (m, 1H), 4.20 (s, 1H), 3.82 (t, *J* = 6.4 Hz, 1H), 3.57 (dd, *J* = 9.2, 5.1 Hz, 3H), 3.40 (d, *J* = 12.1 Hz, 1H). ^{13}C NMR (101 MHz, CD_3OD) δ= 132.2, 131.1, 130.8, 130.3, 79.3, 75.7, 64.62, 53.1, 53.0, 48.4. HRMS (ESI-TOF): *m*/*z* $[M+H]^+$ for $C_{12}H_{19}N_2O_2^+$ calculated 223.1441; observed 223.1440.

(2*S*,3*S*,4*S*)-3,4-dihydroxy-2-((quinolin-3-ylamino)methyl)pyrrolidine (24c). The precursor (2*S*,3*S*,4*S*)-*N*-benzyloxycarbonyl-3,4-dihydroxy-2-((quinolin-3-ylamino)methyl)pyrrolidine (170 mg, 57% yield) was purified by HPLC: gradient elution from 0 to 65% B in 35 min.

HPLC analysis: identical to that of **23c**. The title compound (540 mg, 95% yield) was prepared according to the general procedure described above. HPLC Purification: gradient elution from 0 to 50% B in 40 min. $[\alpha]_D^{22}$ = – 35.0 (*c* 1.0 in MeOH). ^{1}H NMR (500 MHz, CD_3OD) δ= 8.72 (d, *J* = 2.7 Hz, 1H), 8.06 – 7.83 (m, 3H), 7.79 – 7.62 (m, 2H), 4.31 – 4.27 (m, 1H), 4.21 (d, *J* = 0.9 Hz, 1H), 3.88 – 3.77 (m, 3H), 3.57 (dd, *J* = 12.0, 3.7 Hz, 1H), 3.42 (d, *J* = 12.0 Hz, 1H). ^{13}C NMR (101 MHz, CD_3OD) δ= 143.76, 137.88, 134.73, 131.64, 130.64, 130.16, 128.14, 122.47, 119.95, 78.62, 76.27, 66.46, 52.62, 44.47. HRMS (ESI-TOF): *m*/*z* $[M+H]^+$ for $C_{14}H_{18}N_3O_2^+$ calculated 260.1393; observed 260.1404.

(2*S*,3*S*,4*S*)-3,4-dihydroxy-2-(1-methyl-1H-benzo[d]imidazol-2-yl)pyrrolidine (24d). The precursor (2*S*,3*S*,4*S*)-*N*-benzyloxycarbonyl-3,4-dihydroxy-2-(1-methyl-1*H*-benzo[*d*]imidazol-2-yl)pyrrolidine (152 mg, 55% yield) was obtained as described for compound **23d** purified by HPLC: gradient elution from 10 to 70% B in 40 min. HPLC analysis: identical to that of **23d**. The title compound (58 mg, 74% yield) was prepared following the procedure described for **23d**. HPLC Purification: gradient elution from 0 to 60% B in 40 min. $[\alpha]_D^{22}$ = + 2.6 (*c* 0.9 in MeOH). ^{1}H NMR (500 MHz, CD_3OD) δ= 7.68 (d, *J* = 8.0 Hz, 1H), 7.57 (d, *J* = 8.1 Hz, 1H), 7.40 – 7.35 (m, 1H), 7.33 – 7.29 (m, 1H), 5.01 (d, *J* = 3.2 Hz, 1H), 4.51 (t, *J* = 2.6 Hz, 1H), 4.36 (dt, *J* = 4.8, 2.4 Hz, 1H), 3.94 (s, 3H), 3.74 (dd, *J* = 12.0, 4.7 Hz, 1H), 3.58 (dd, *J* = 11.9, 2.4 Hz, 1H). ^{13}C NMR (101 MHz, CD_3OD) δ= 149.6, 141.6, 137.7, 125.0, 124.3, 119.9, 111.4, 81.0, 76.7, 62.7, 52.7, 30.8. HRMS (ESI-TOF): *m*/*z* $[M+H]^+$ for $C_{12}H_{16}N_3O_2^+$ calculated 234.1237; observed 234.1230.

(2*S*,3*S*,4*S*)-2-(aminomethyl)-1-(quinolin-3-yl)pyrrolidine-3,4-diol (24e). The title compound (28 mg, 5% yield) was prepared according to the general procedure described above. HPLC Purification: gradient elution from 0 to 60% B in 40 min. $[\alpha]_D^{22}$ = + 17.7 (*c* 0.7 in MeOH). ^{1}H NMR (400 MHz, CD_3OD) δ= 8.87 (d, *J* = 2.9 Hz, 1H), 8.20 (d, *J* = 2.8 Hz, 1H), 8.11 – 8.04 (m, 2H), 7.83 – 7.70 (m, 2H), 4.38 (d, *J* = 4.1 Hz, 1H), 4.36 (s, 1H), 4.17 (dd,

J = 7.1, 1.8 Hz, 1H), 3.88 – 3.74 (m, 2H), 3.68 (dd, *J* = 13.9, 7.3 Hz, 1H), 3.37 (dd, *J* = 13.9, 2.0 Hz, 1H). ^{13}C NMR (101 MHz, CD_3OD) δ= 143.3, 137.3, 137.3, 131.3, 130.0, 129.5, 128.1, 124.3, 120.43, 80.8, 75.3, 66.5, 57.7, 39.7. HRMS (ESI-TOF): *m*/*z* $[M+H]^+$ for $C_{14}H_{17}N_3O_2^+$ calculated 260.1399; observed 260.1390.

Figure 1. Observed NMR spectra of 1,4-dideoxy-1,4-imino-L-xylitol (**22**): a) ^{1}H, b) ^{13}C, c) 2D ^{1}H-^{1}H COSY and 2D multiplicity-edited HSQC.

a)

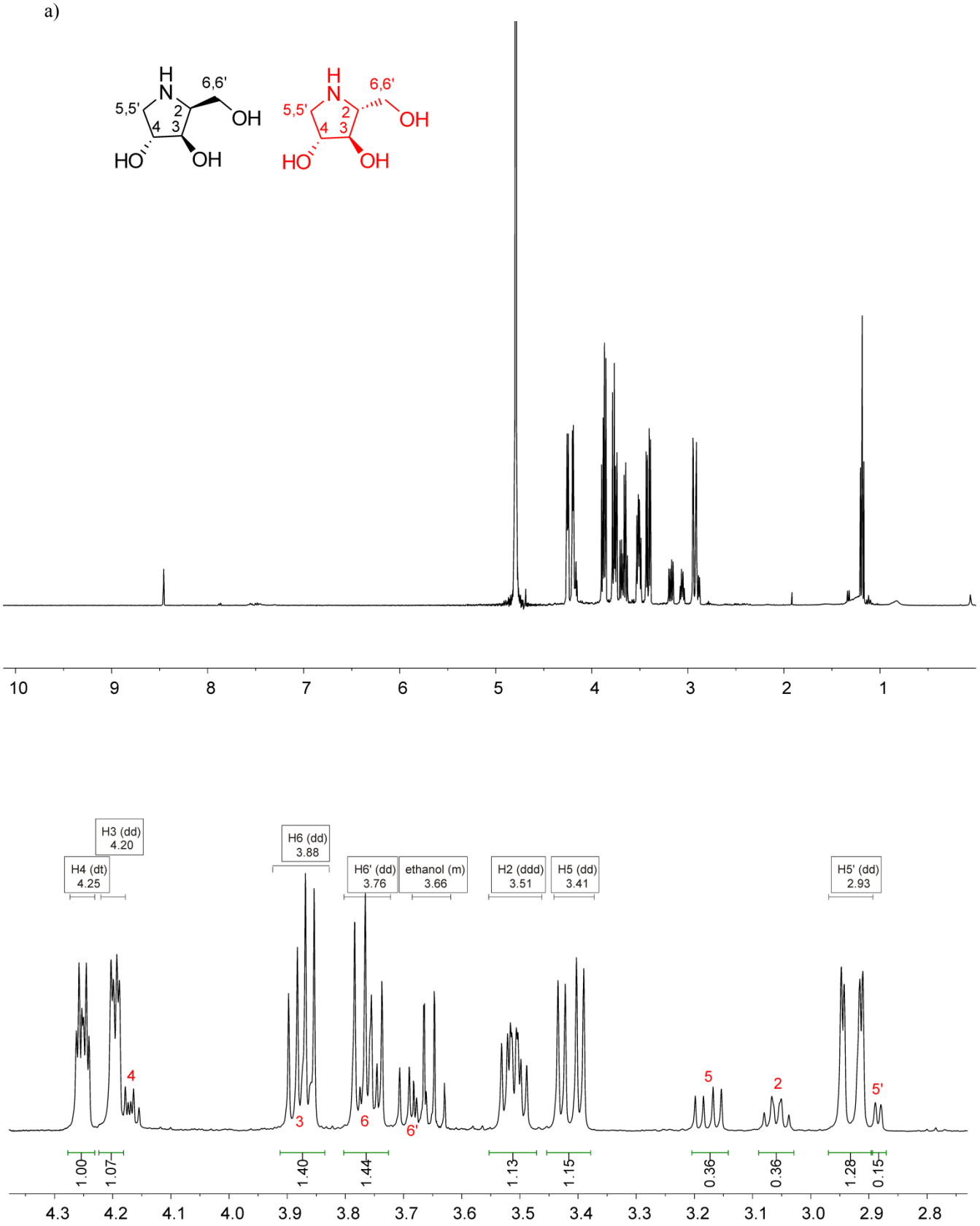

b)

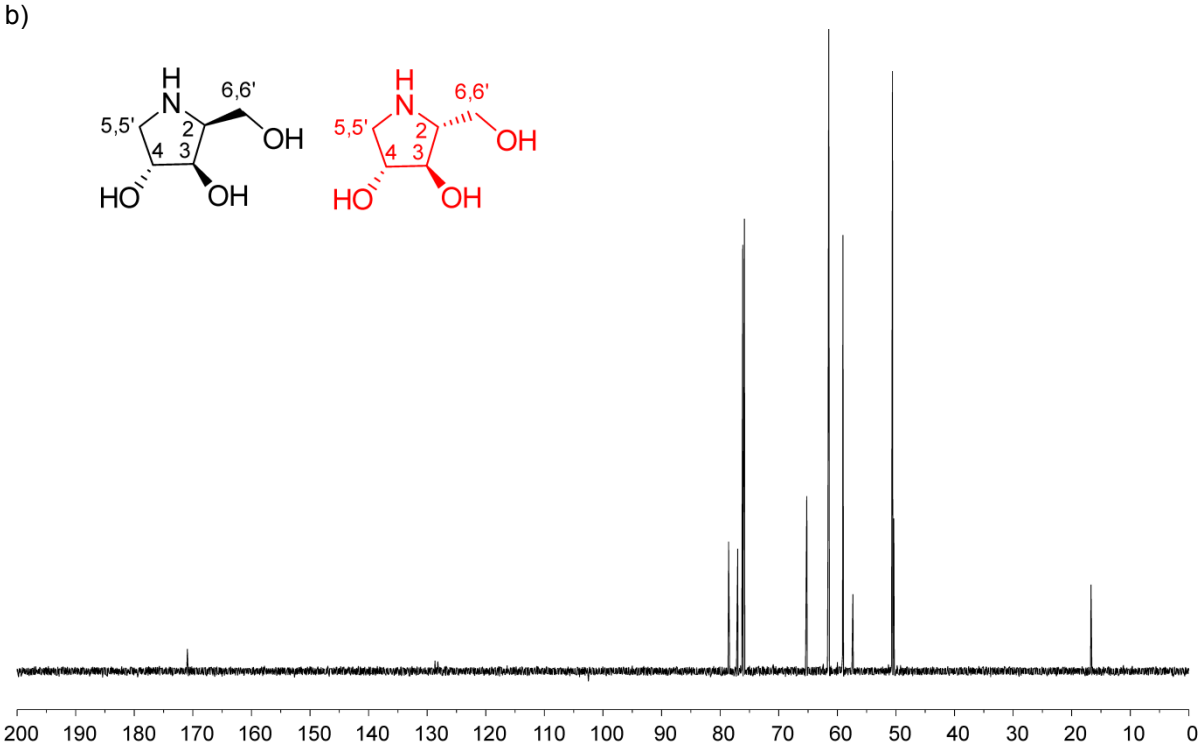

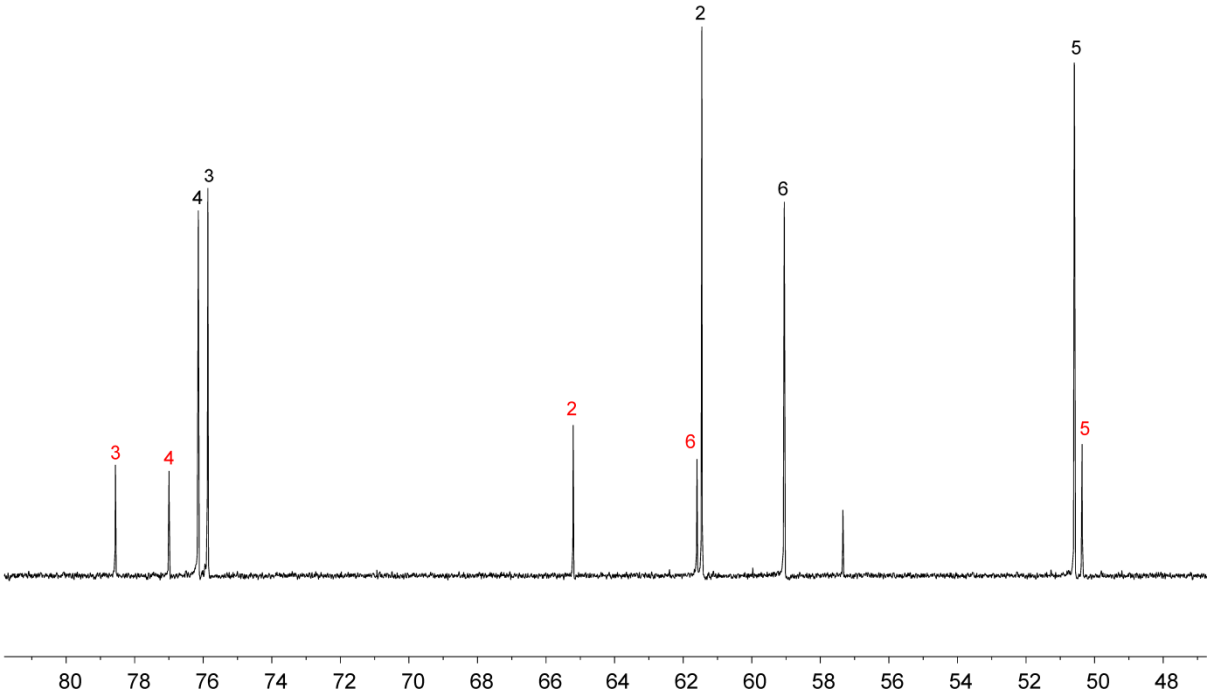

c)

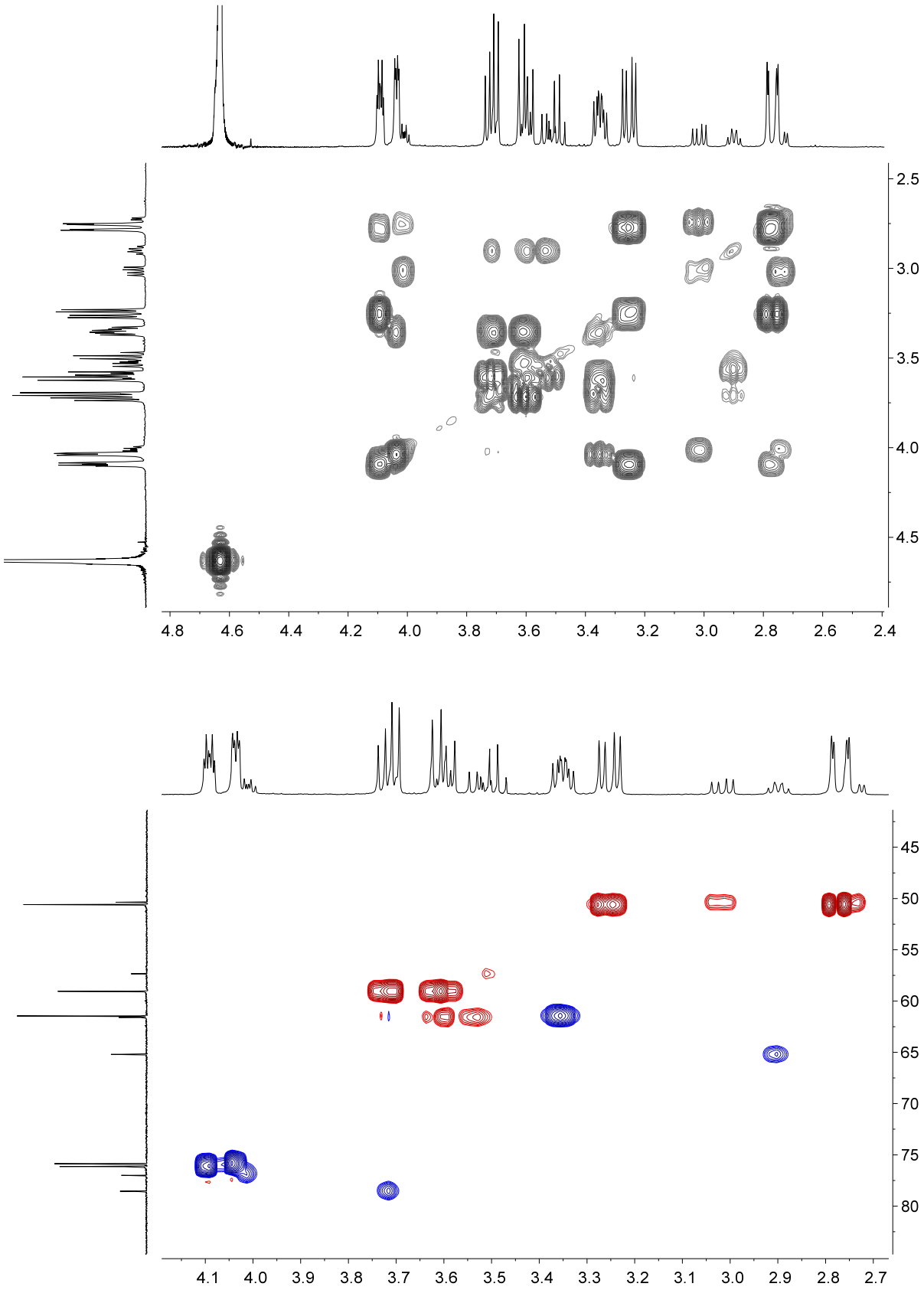

The full NMR characterization was conducted for compounds **24a**-**e**. Those spectra are shown first. The NMR spectra of the corresponding enantiomers **23a**-**e** are shown immediately after.

Figure 2. Observed NMR spectra of **24a**: a) ^{1}H, b) ^{13}C, c) 2D ^{1}H-^{1}H COSY and 2D multiplicity-edited HSQC.

a)

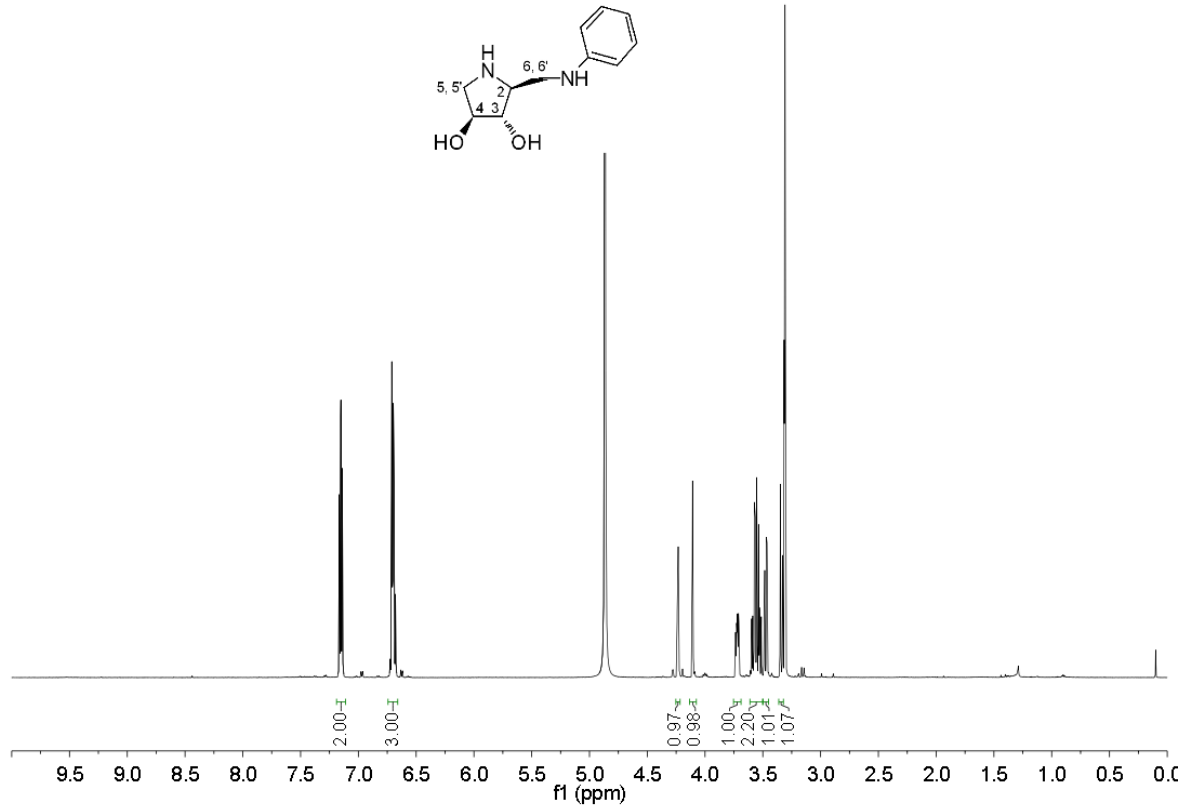

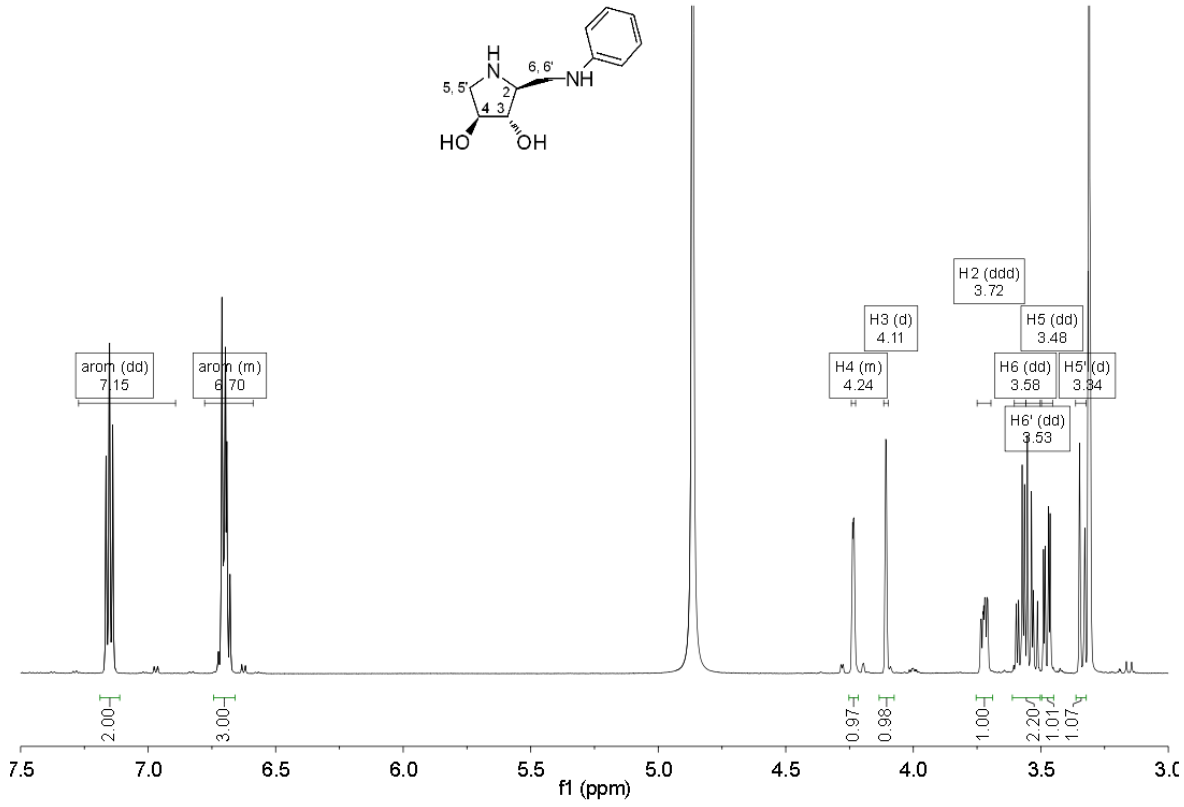

b)

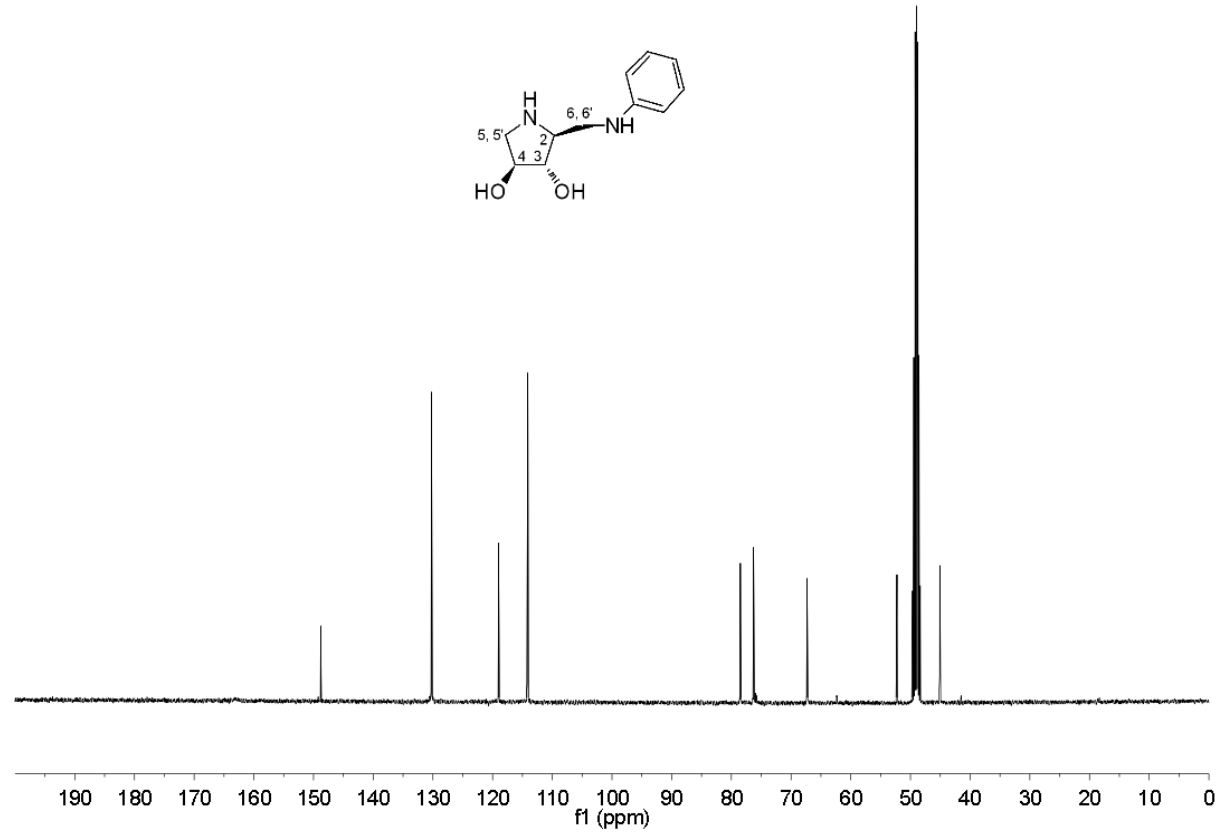

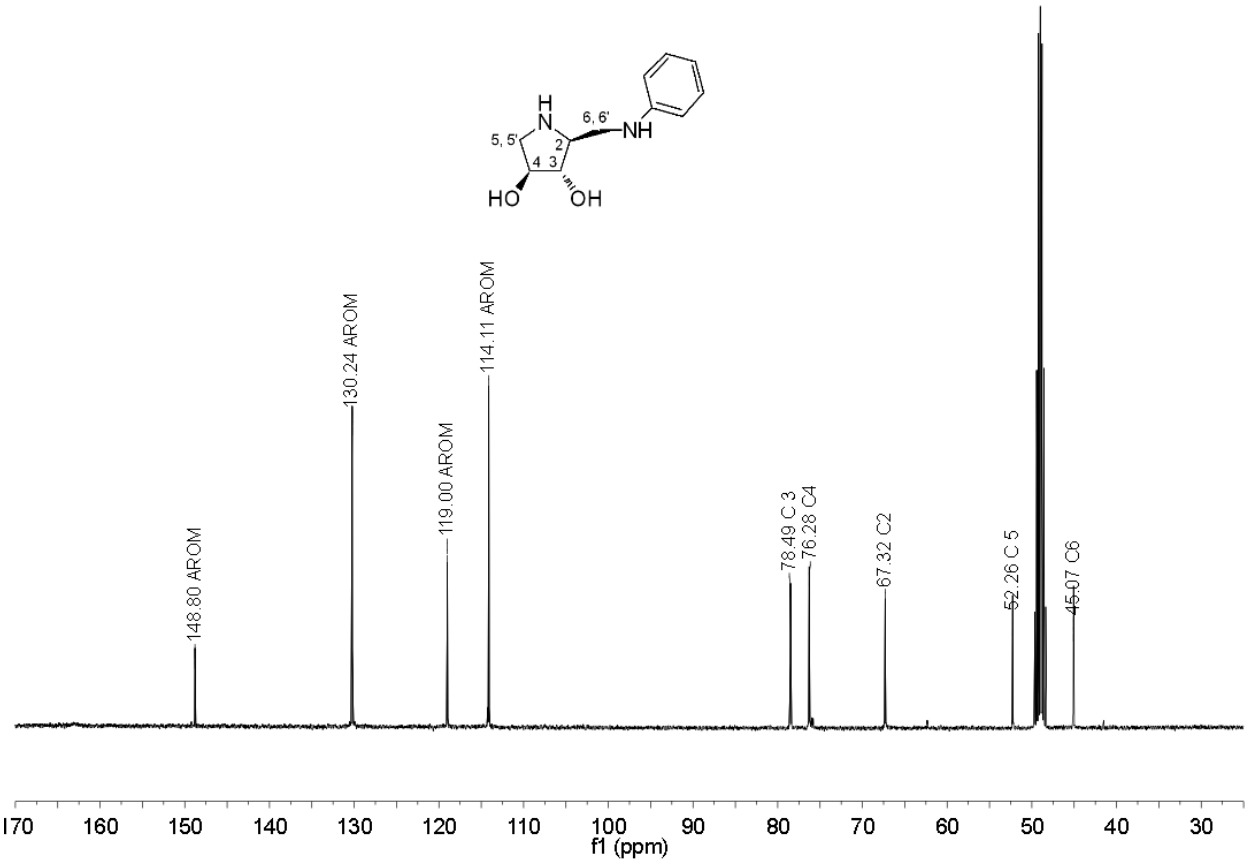

c)

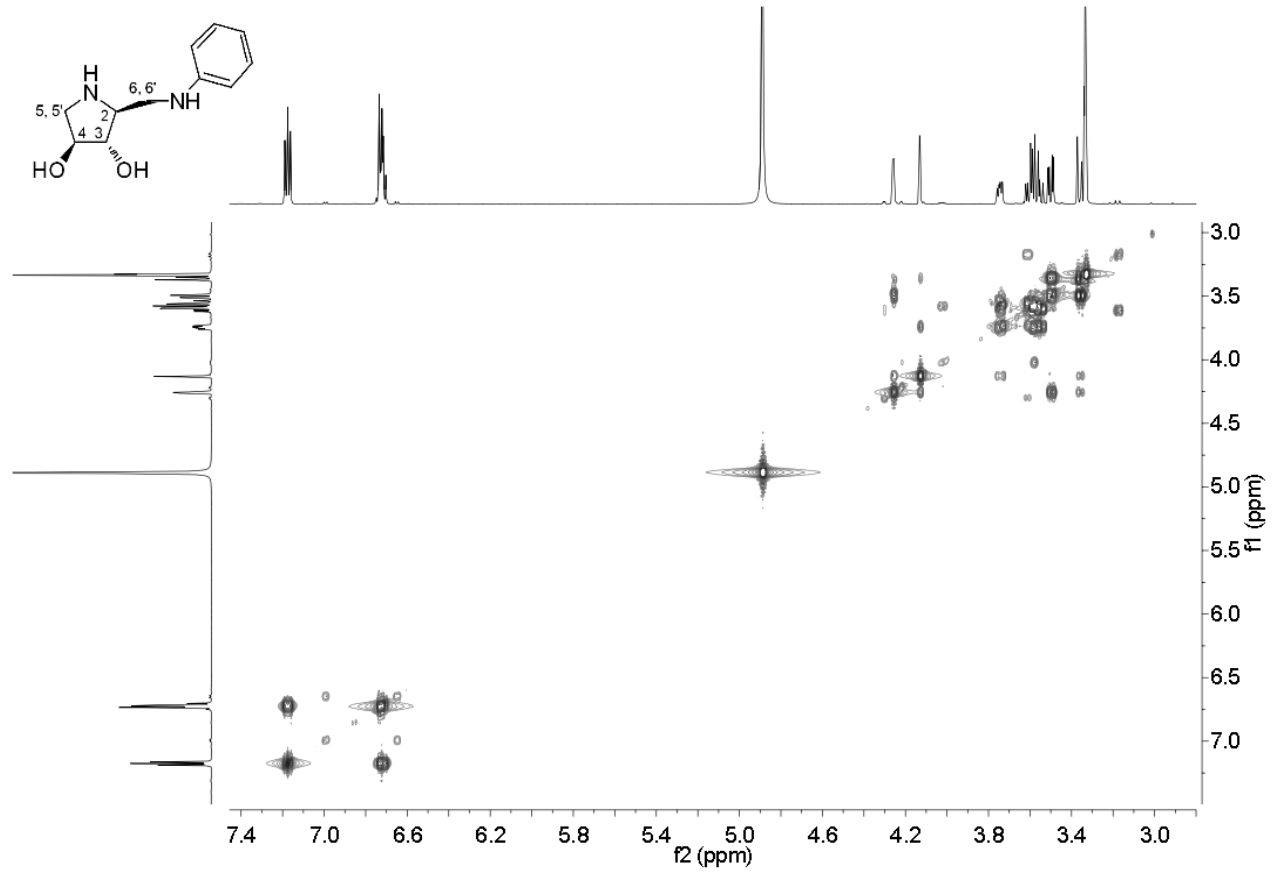

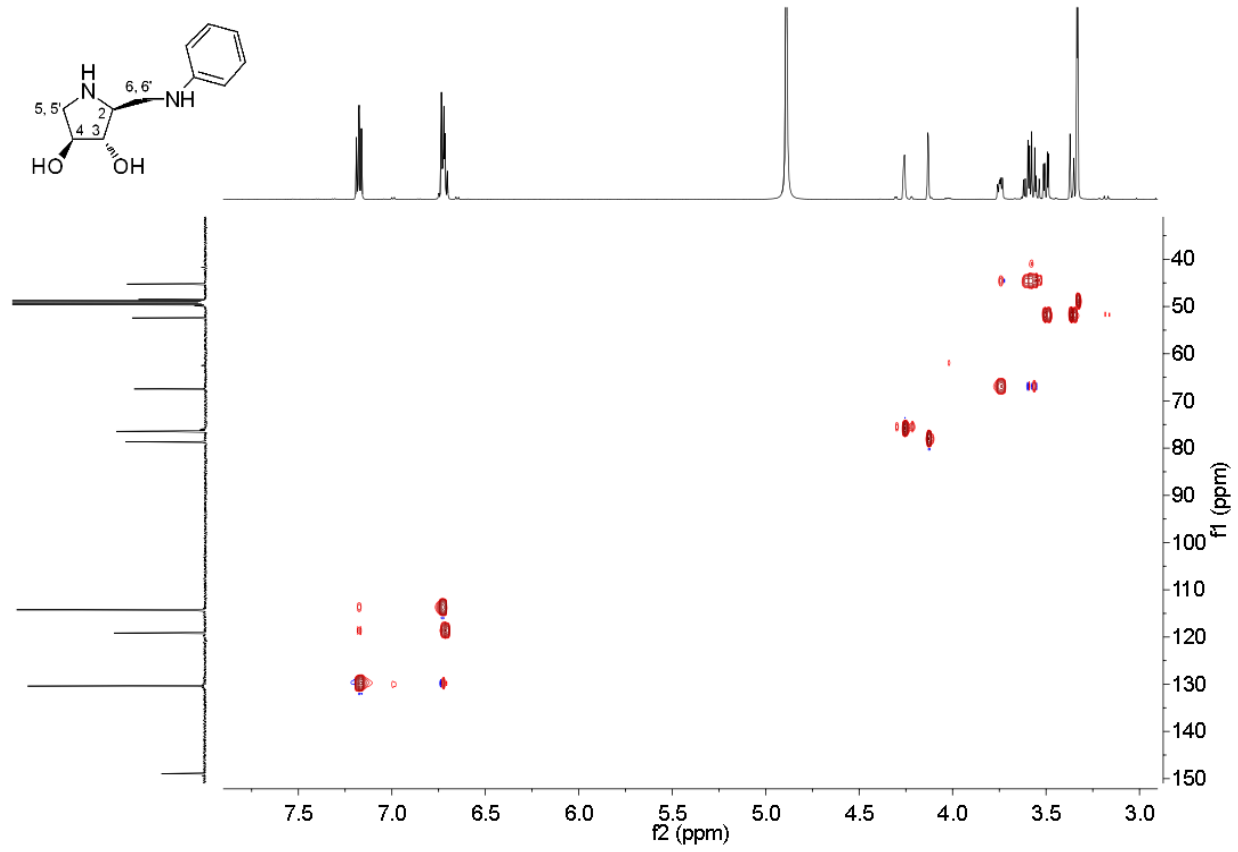

Figure 3. Observed NMR spectra of **23a** enantiomer of **24a**: a) ^{1}H and, b) ^{13}C.

a)

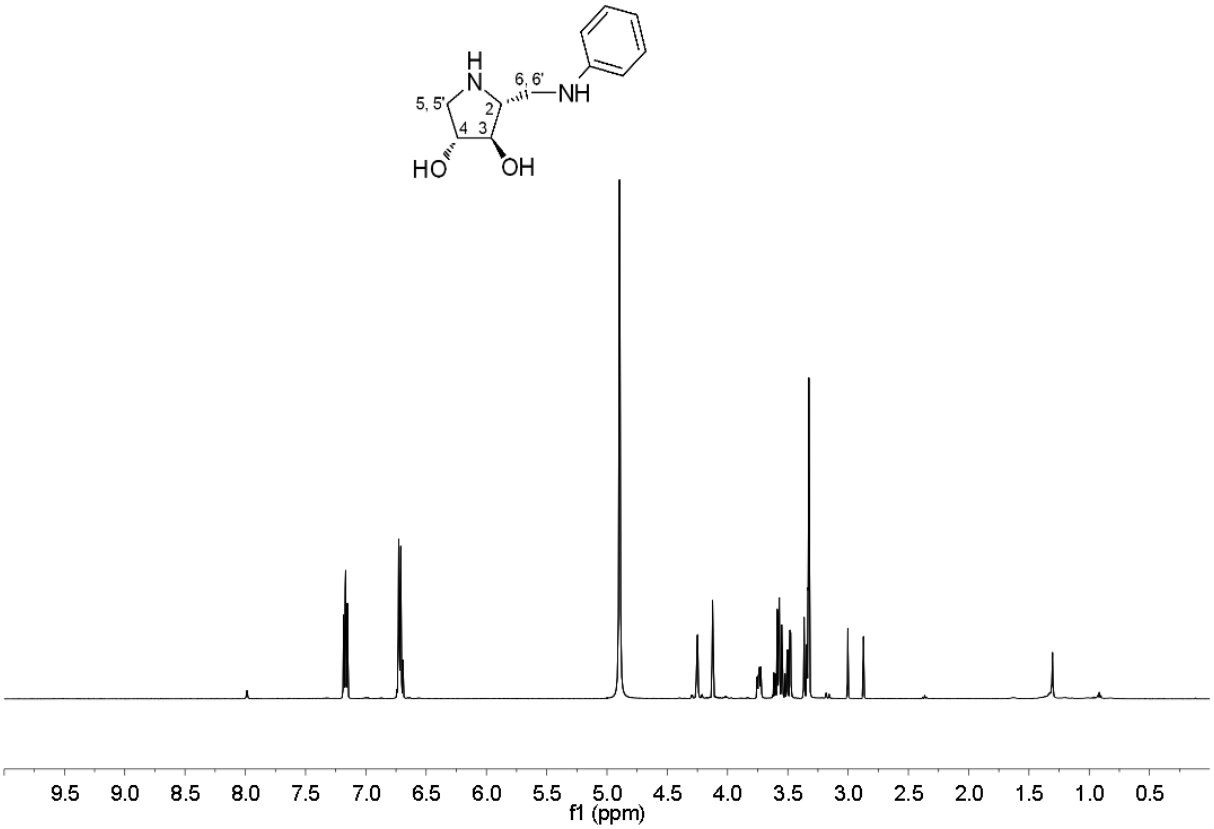

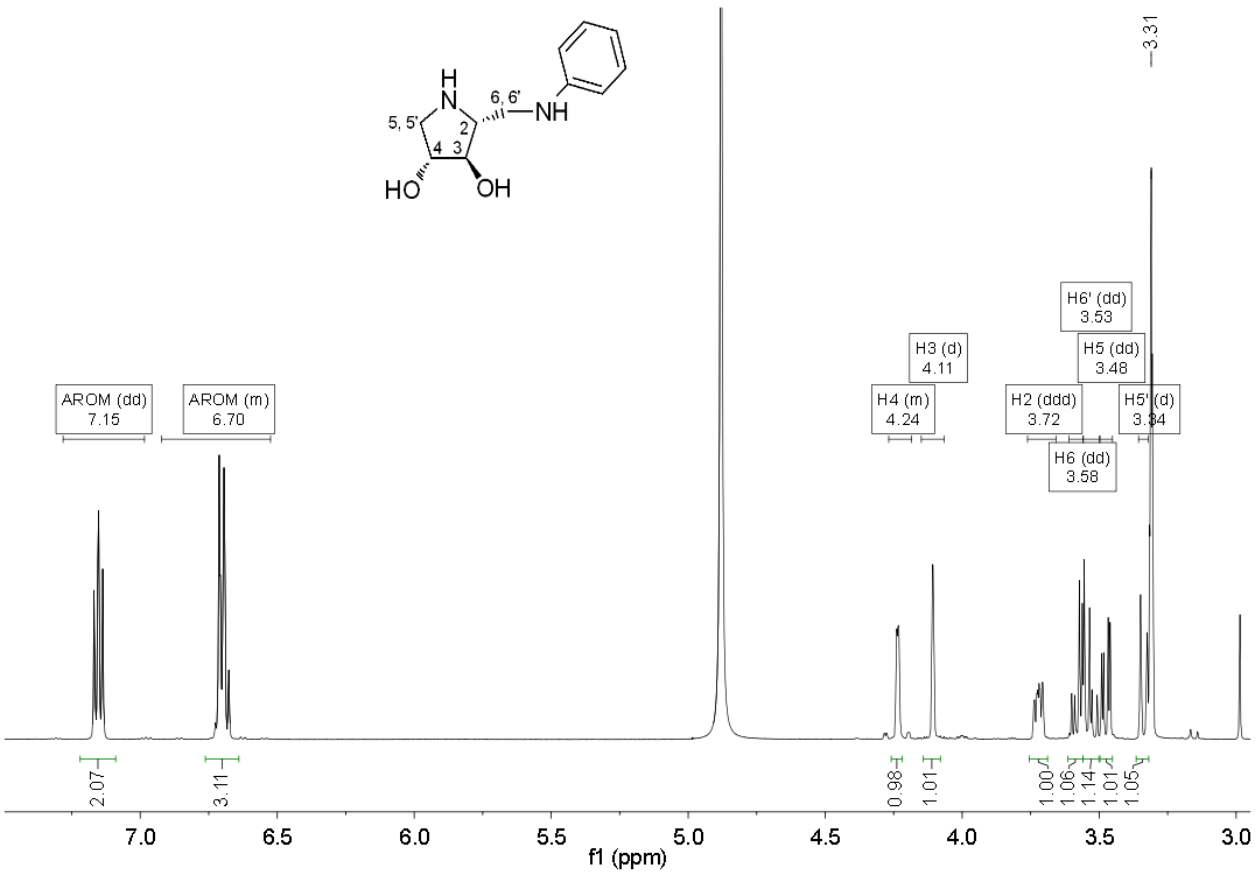

b)

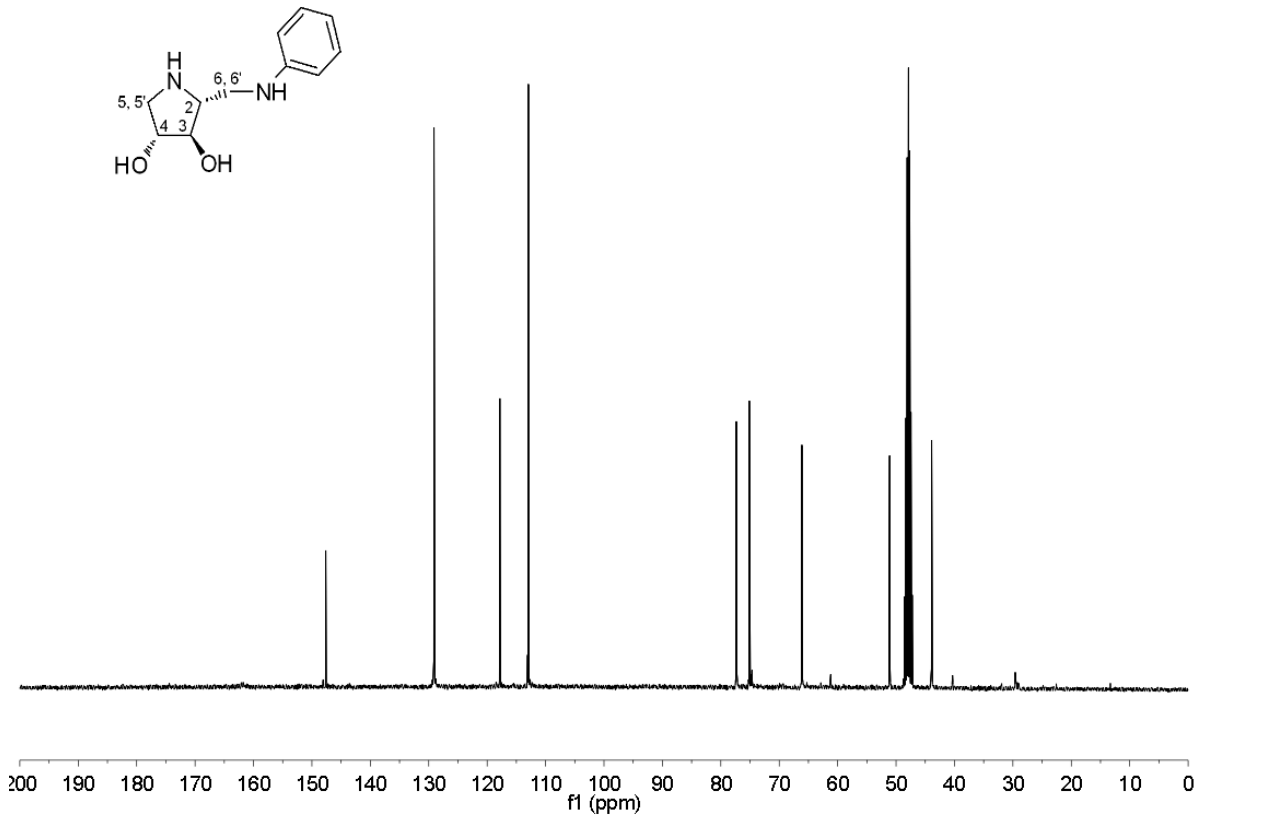

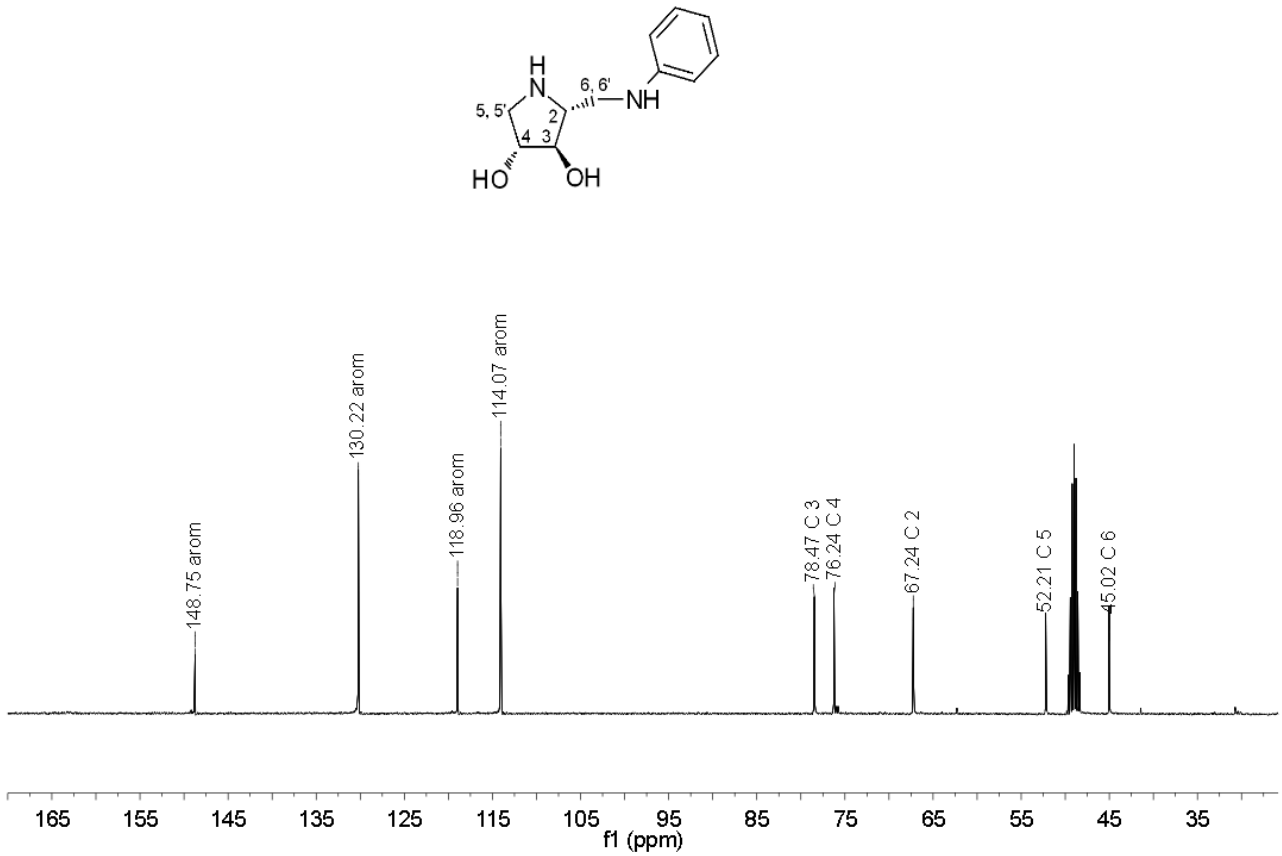

Figure 4. Observed NMR spectra of **24b**: a) ^{1}H, b) ^{13}C, c) 2D ^{1}H-^{1}H COSY and 2D multiplicity-edited HSQC.

a)

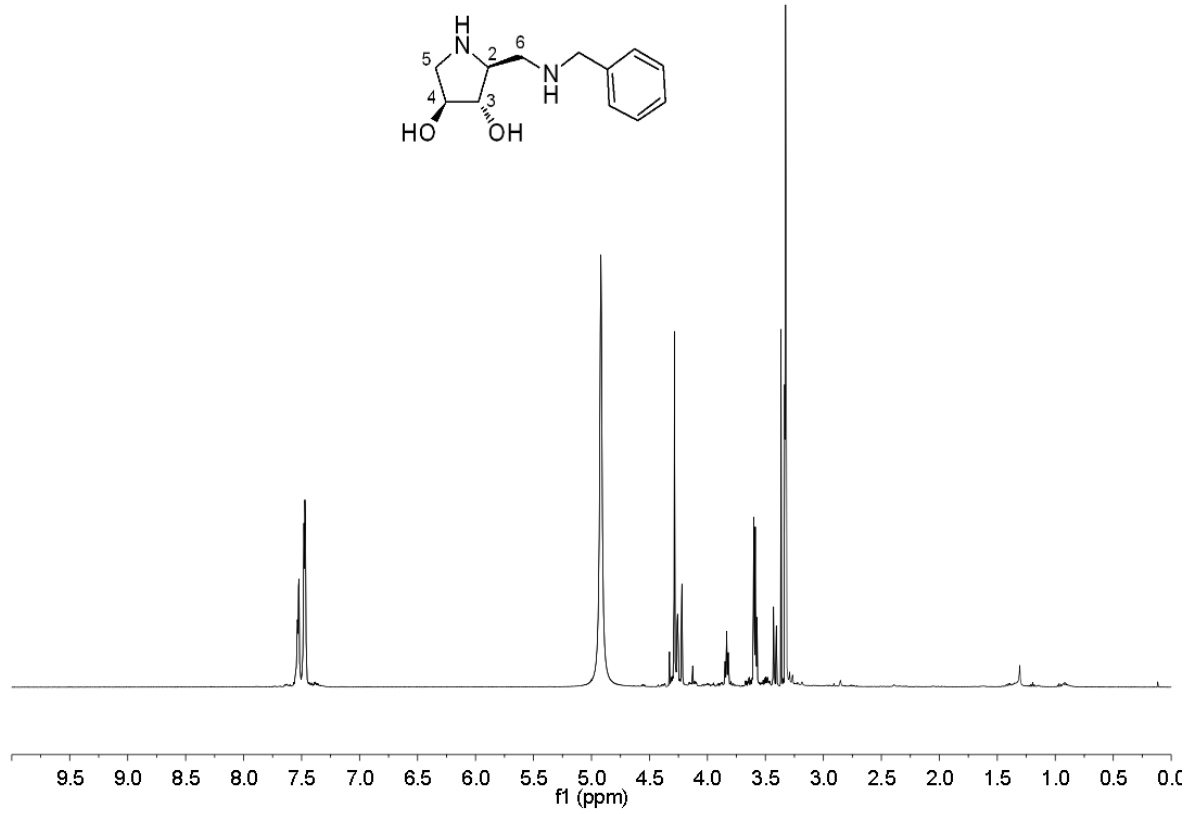

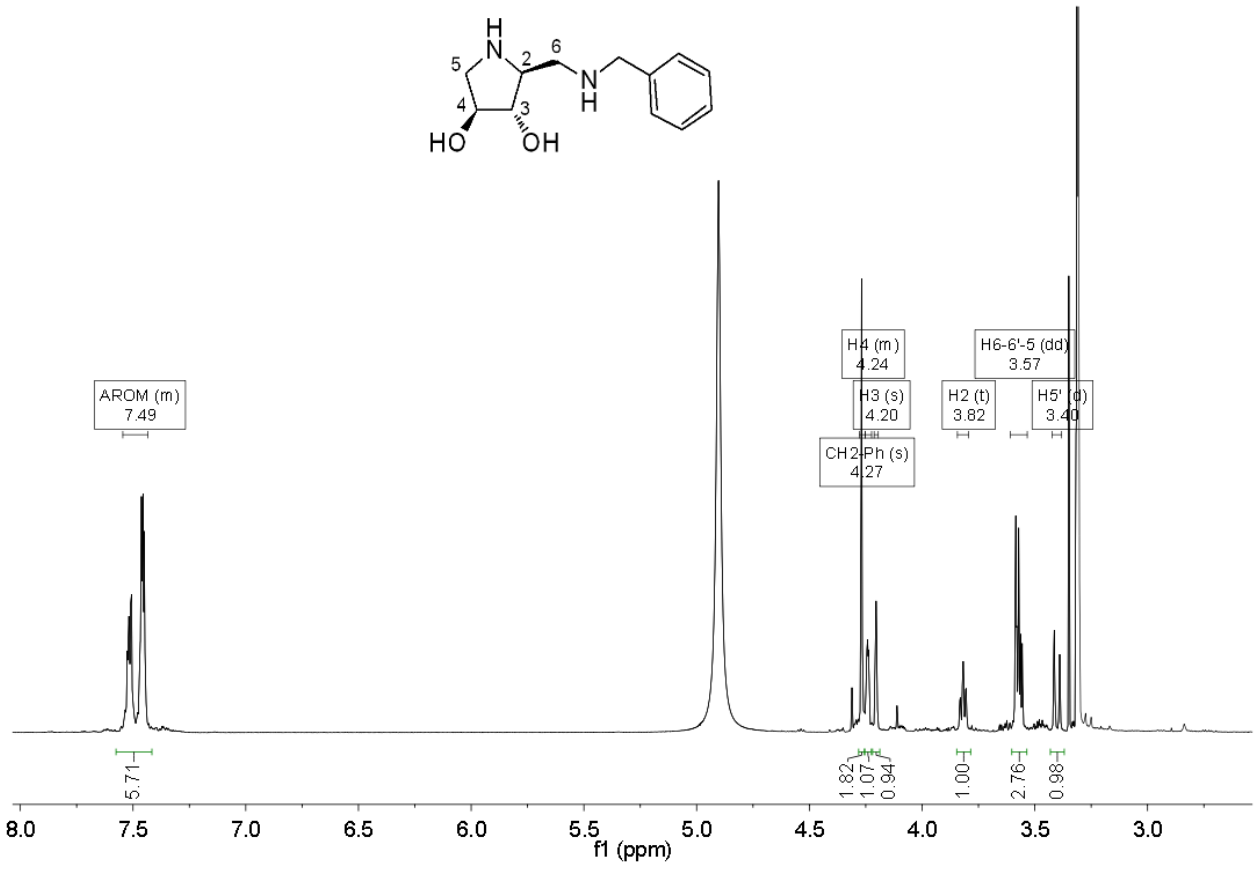

b)

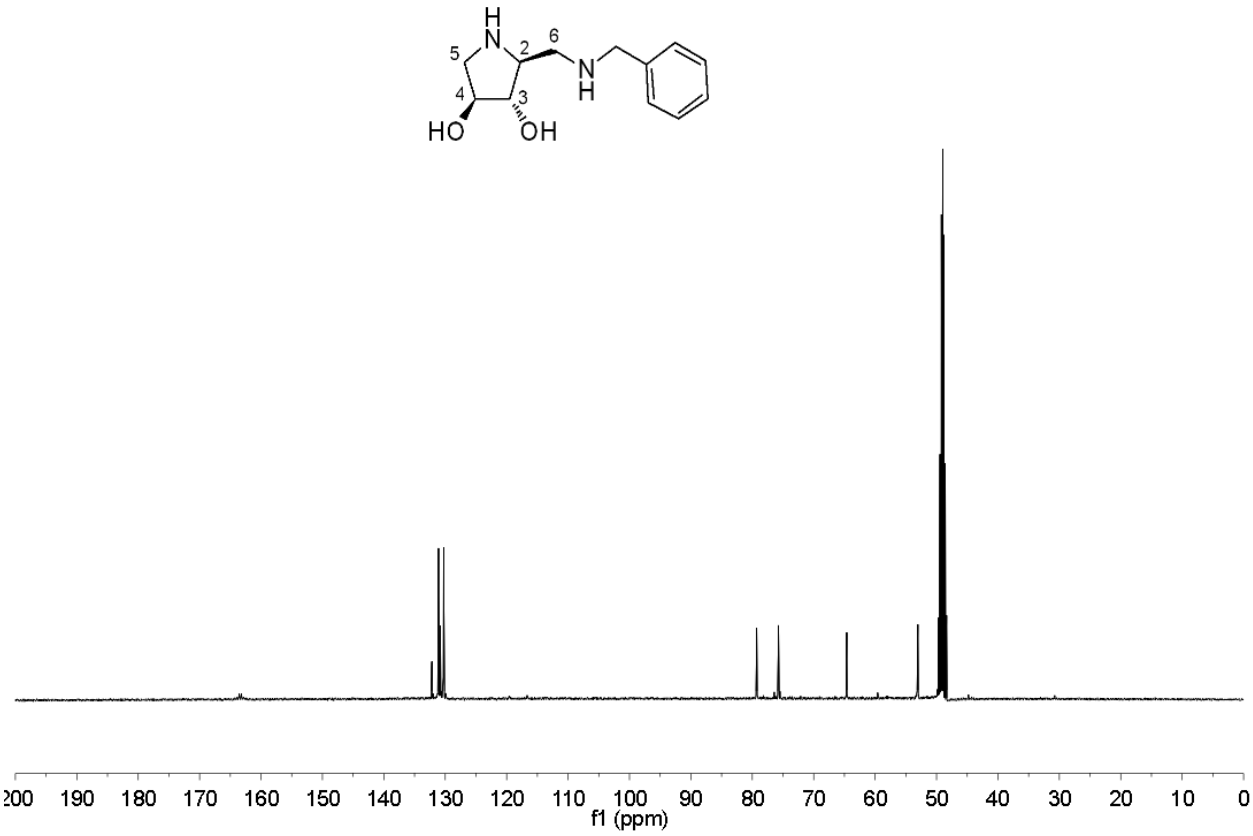
H
N
2
6
5
4
3
N
H
HO
OH
200 190 180 170 160 150 140 130 120 110 100 90 80 70 60 50 40 30 20 10 0
f1 (ppm)

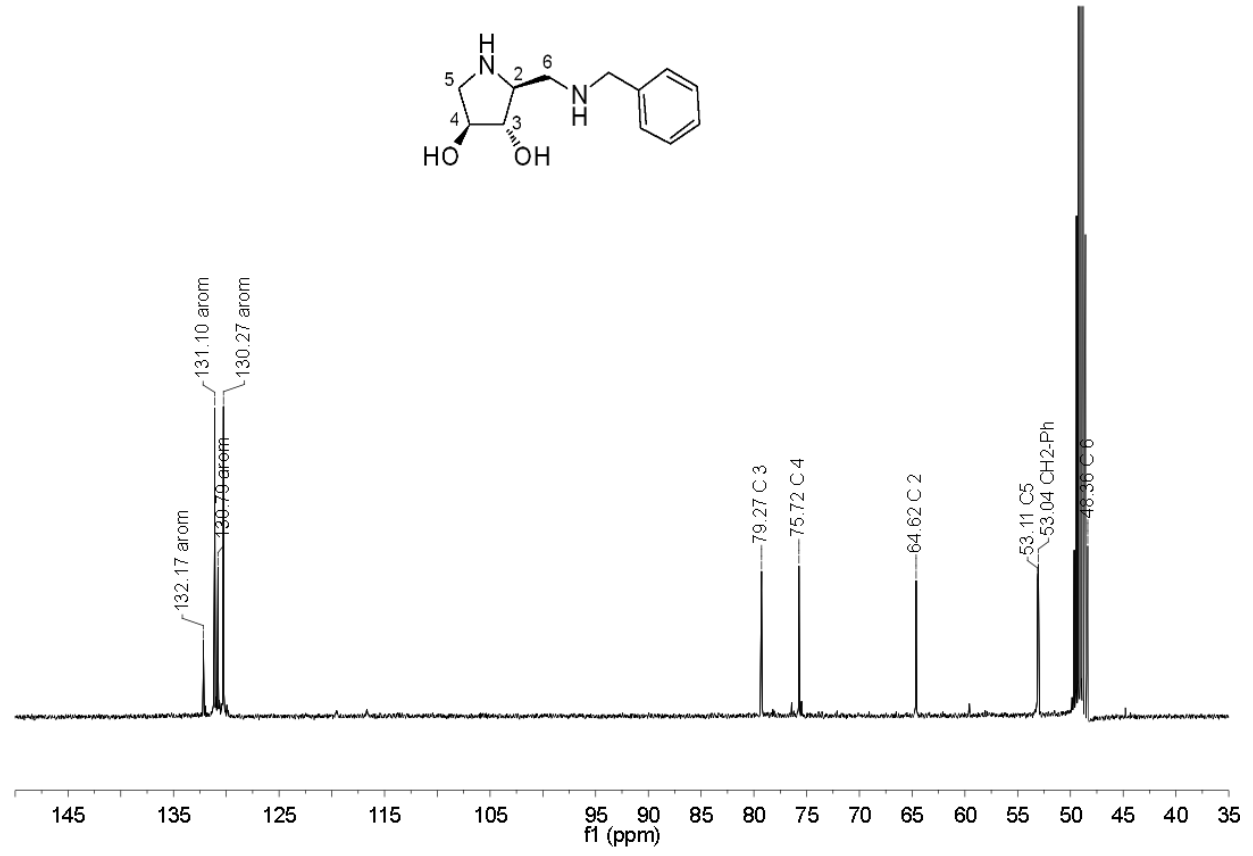
H
N
2
6
5
4
3
N
H
HO
OH
131.10 arom
130.27 arom
132.17 arom
130.70 arom
79.27 C 3
75.72 C 4
64.62 C 2
53.11 C5
53.04 CH2-Ph
48.36 C 6
145 135 125 115 105 95 90 85 80 75 70 65 60 55 50 45 40 35
f1 (ppm)

c)

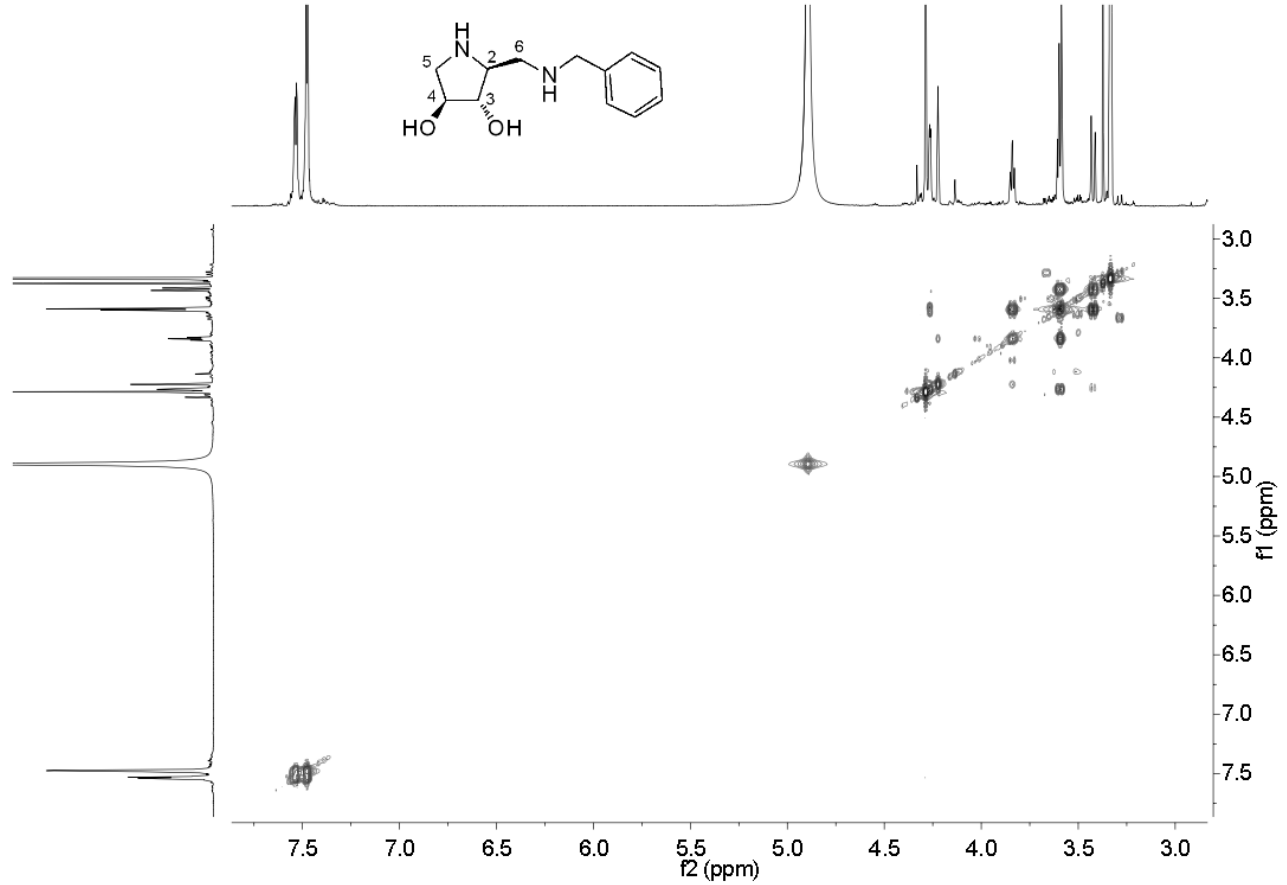

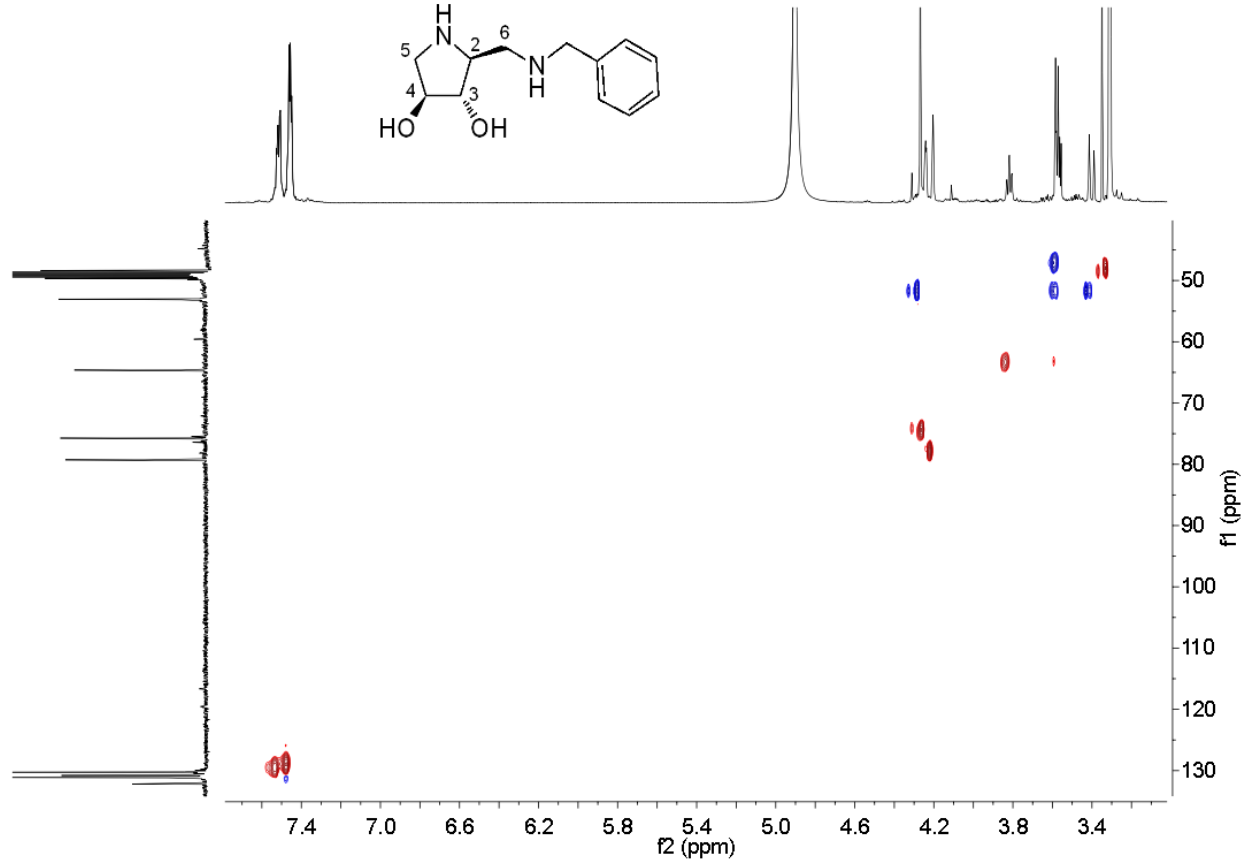

Figure 5. Observed NMR spectra of **23b** enantiomer of **24b**: a) ^{1}H and, b) ^{13}C.

a)

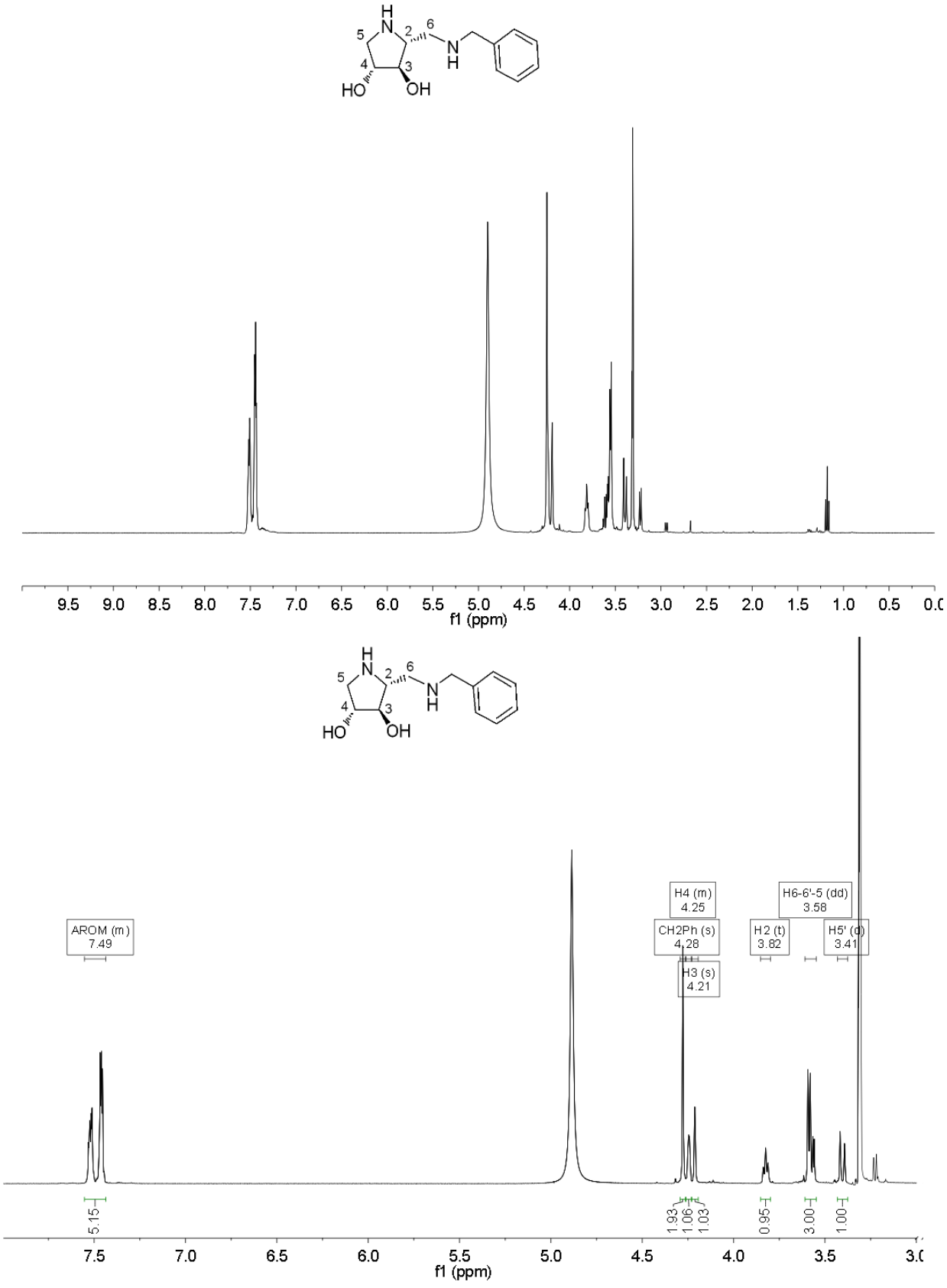

b)

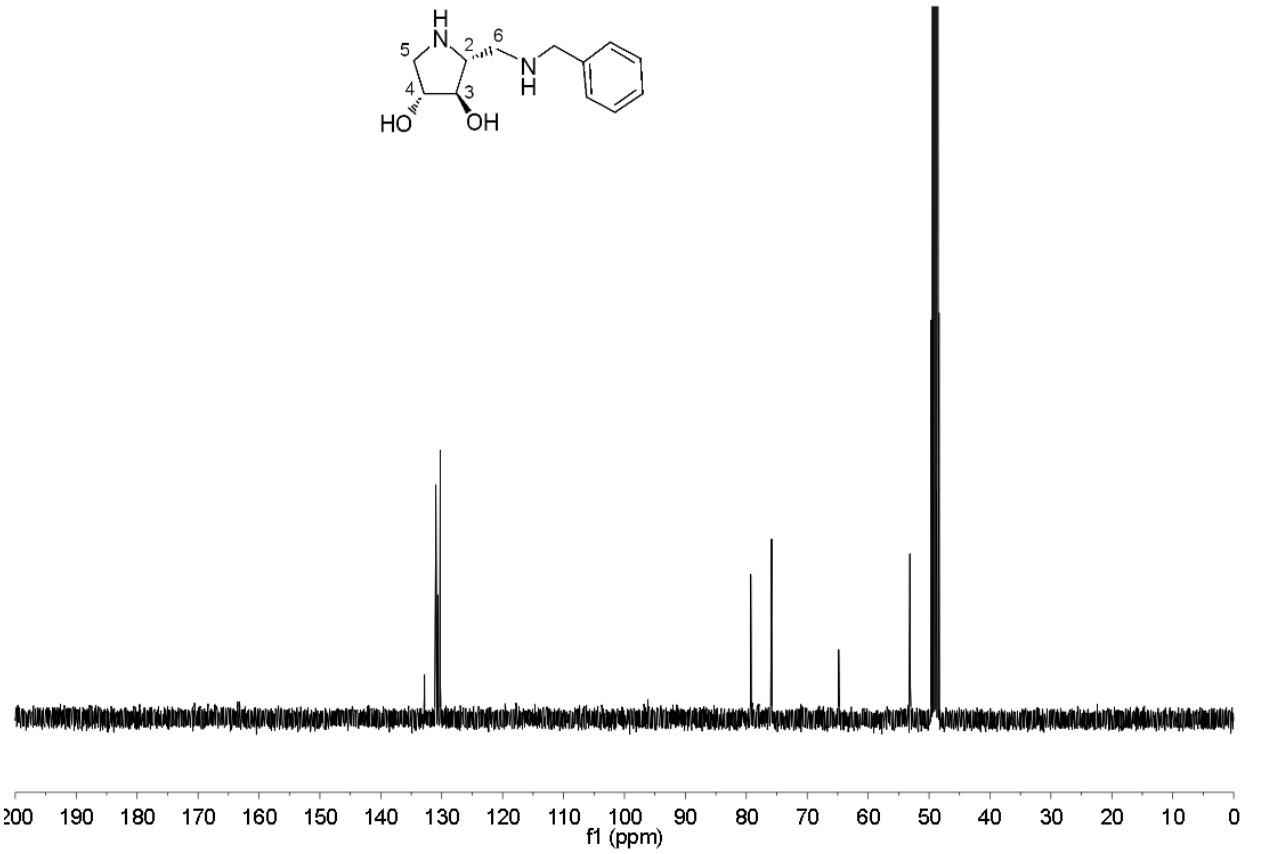

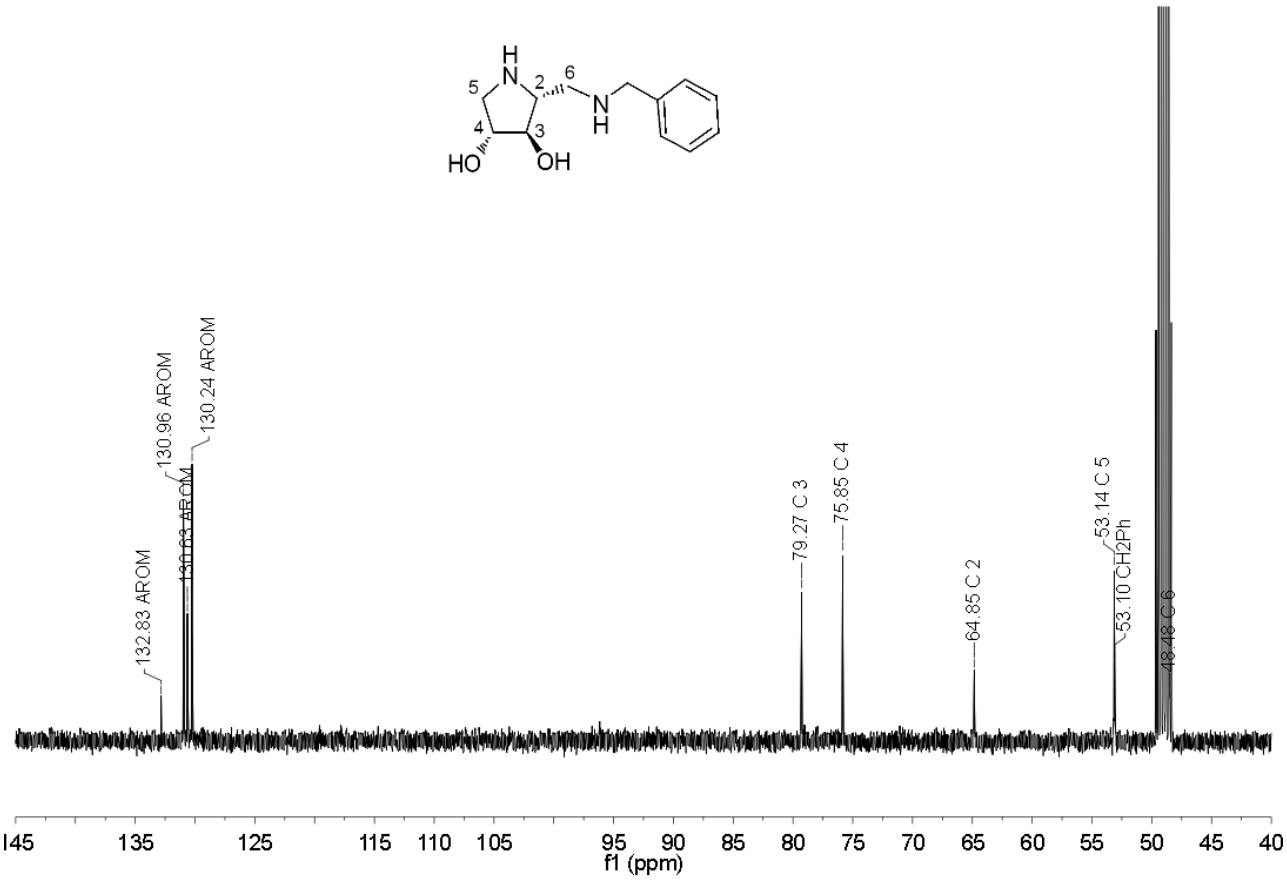

Figure 6. Observed NMR spectra of **24c**: a) ^{1}H, b) ^{13}C, c) 2D ^{1}H-^{1}H COSY and 2D multiplicity-edited HSQC.

a)

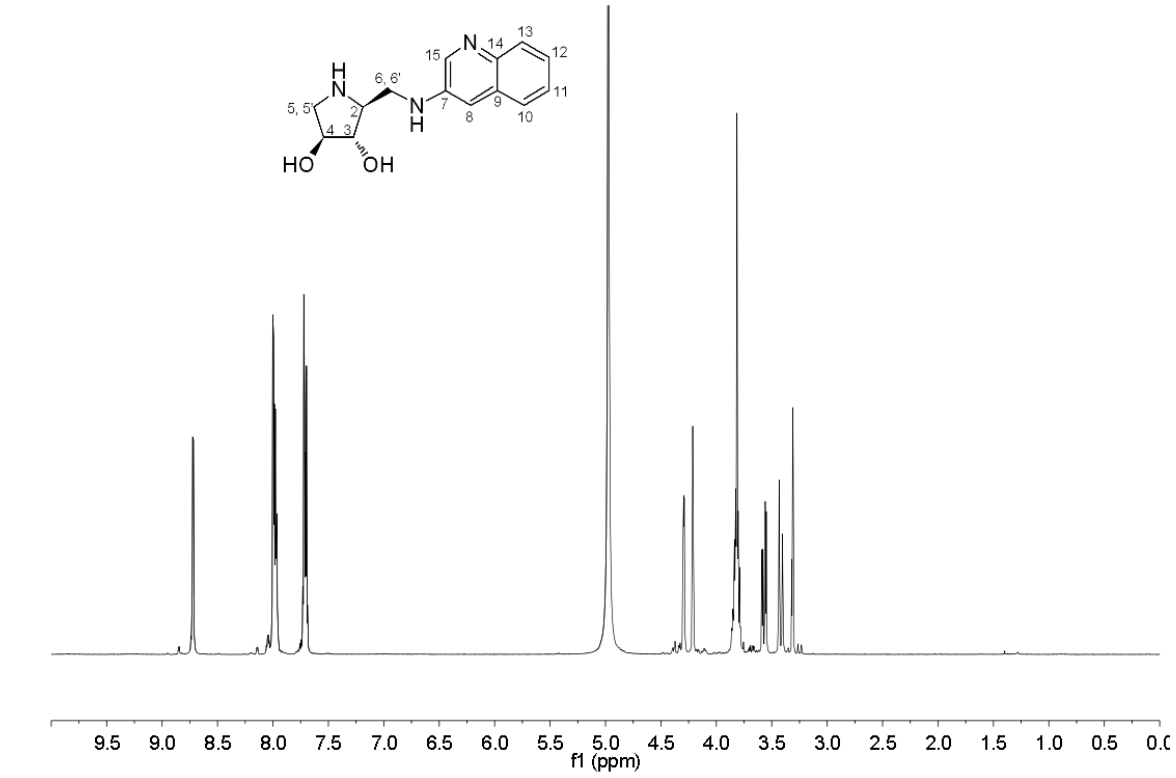

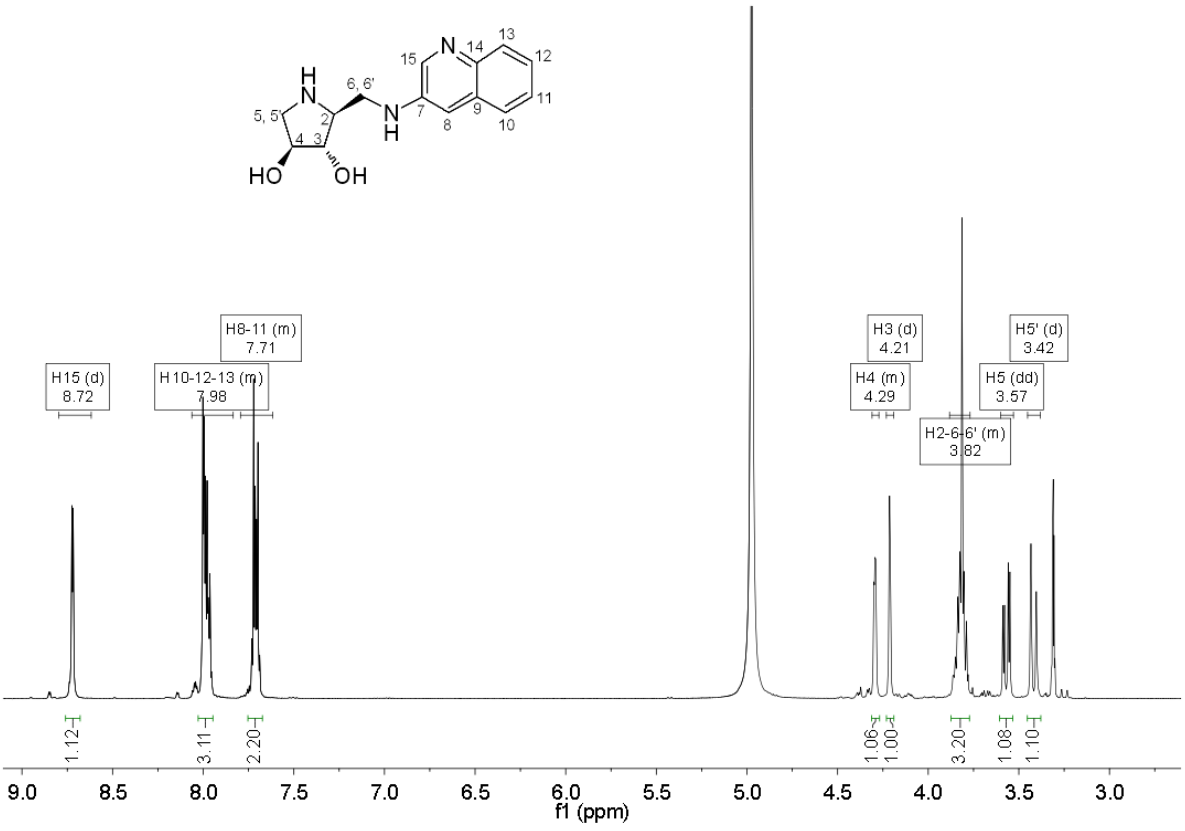

b)

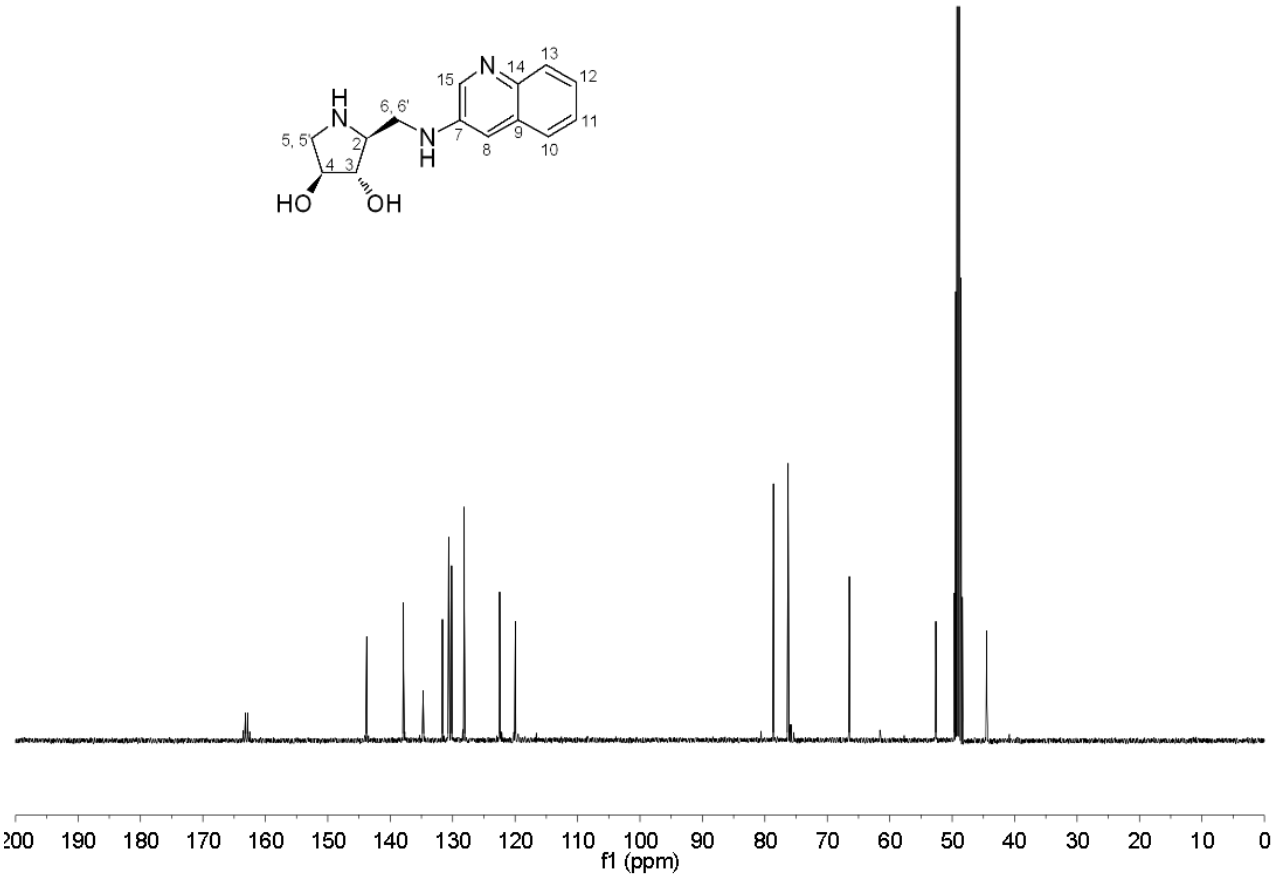

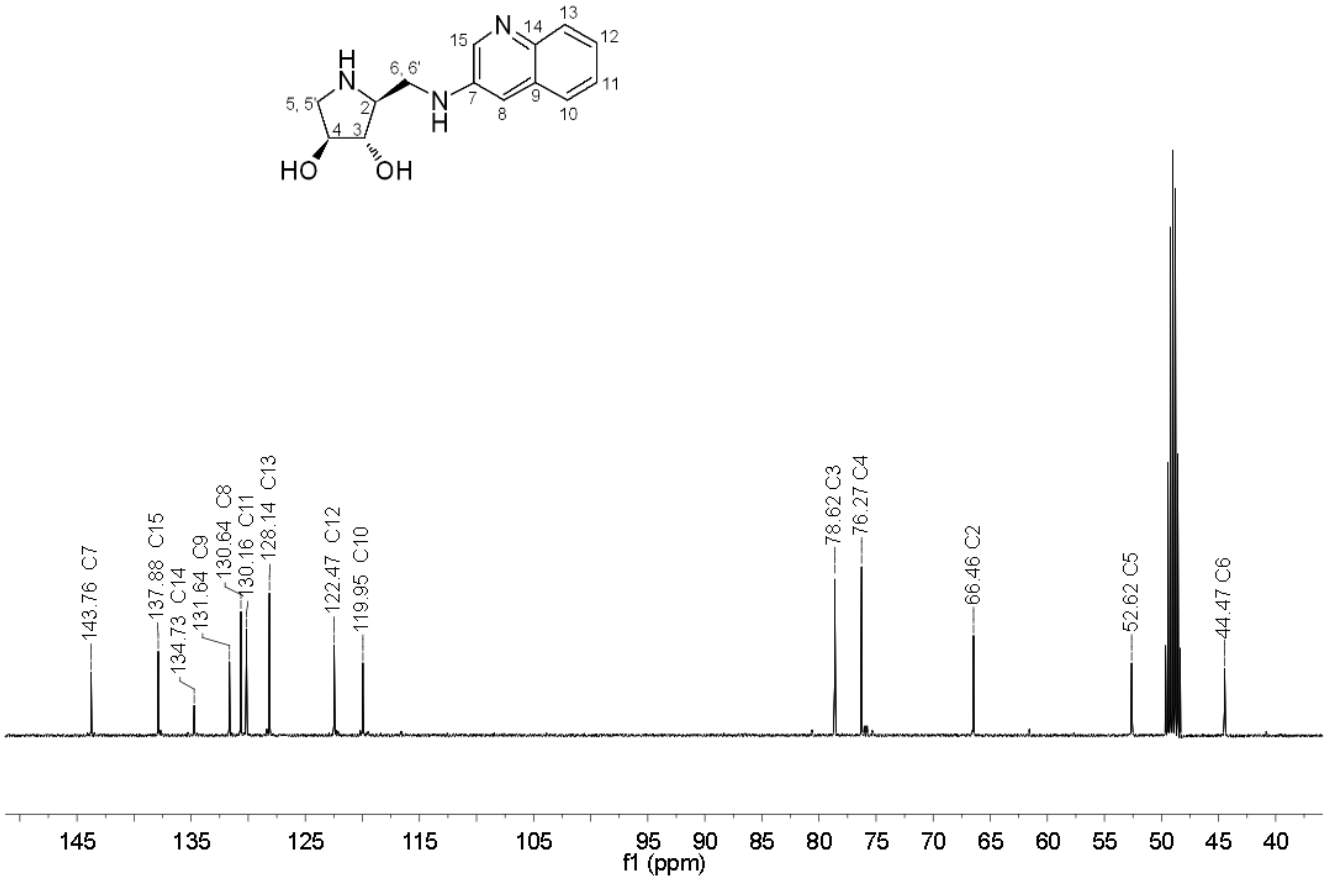

c)

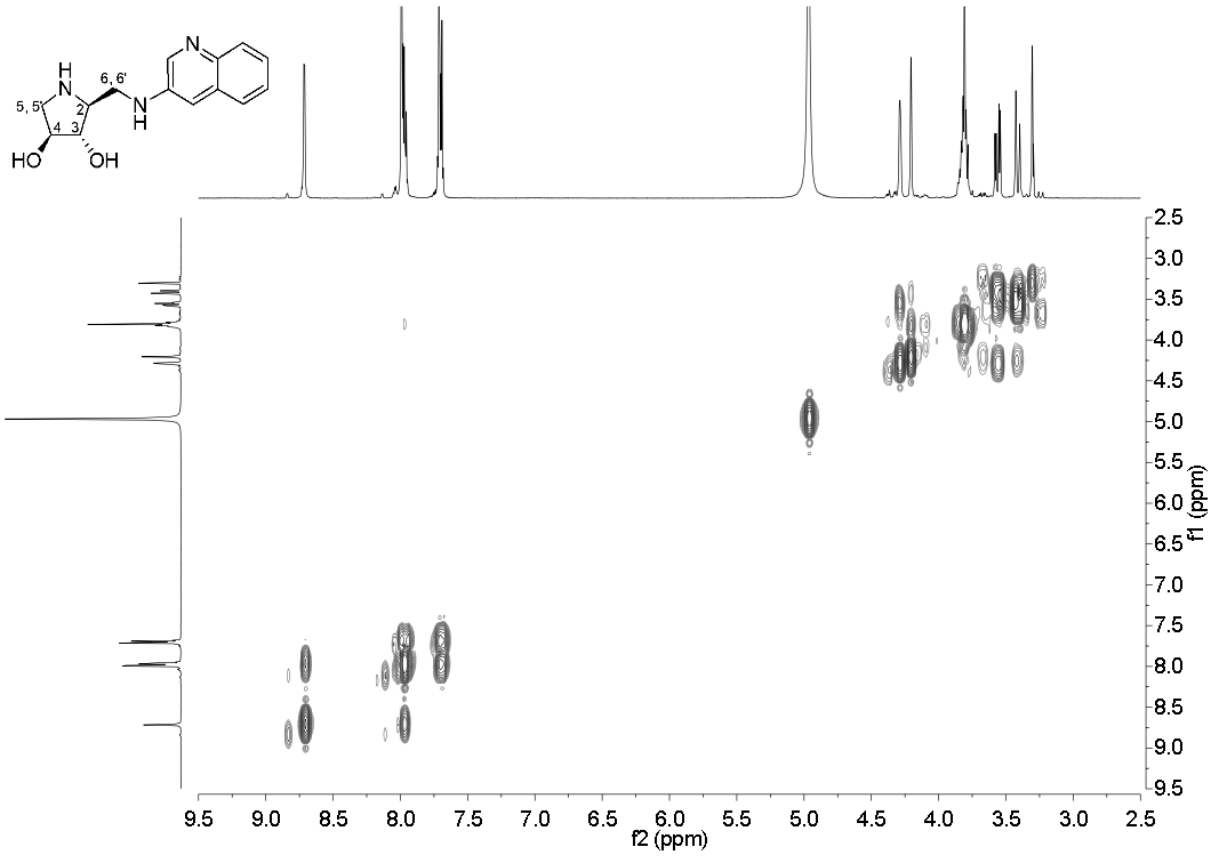
H
N
6, 6'
N
H
5, 5'
2
4
3
HO
OH
N
f2 (ppm)
f1 (ppm)

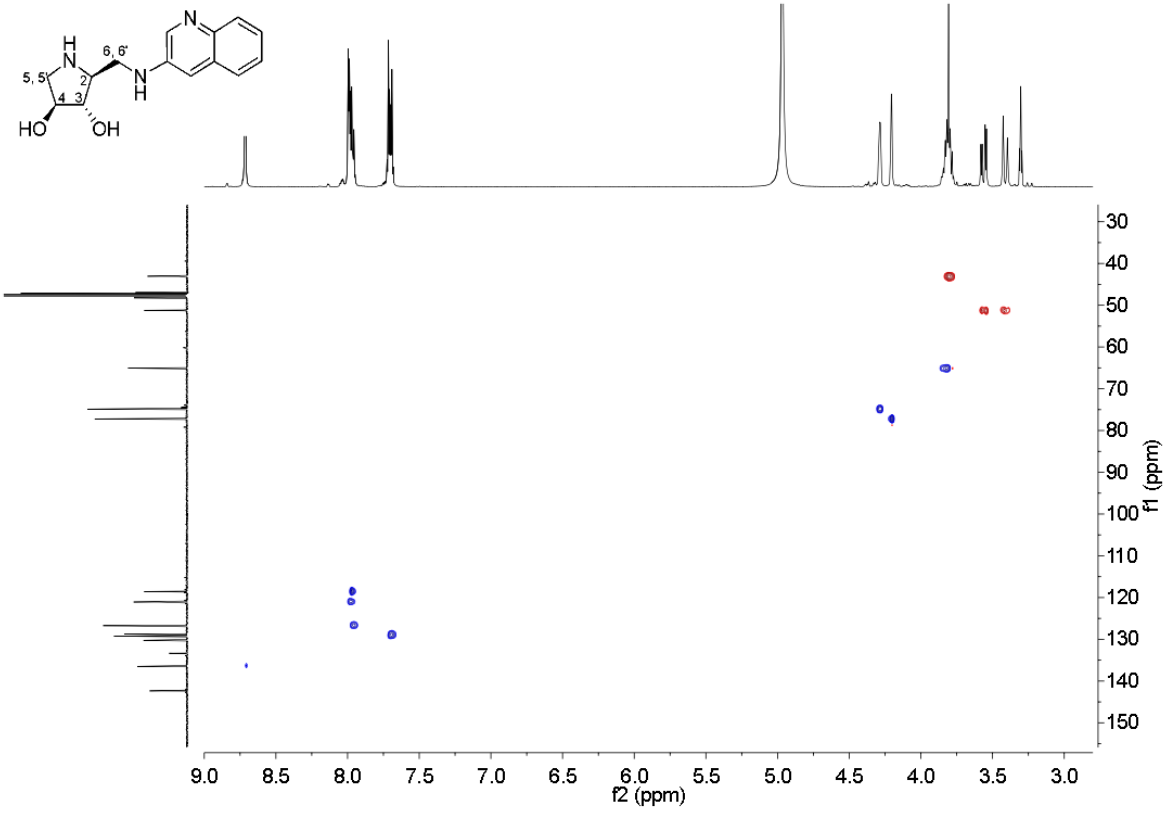
H
N
6, 6'
N
H
5, 5'
2
4
3
HO
OH
N
f2 (ppm)
f1 (ppm)

Figure 7. Observed NMR spectra of **23c** enantiomer of **24c**: a) ^{1}H and, b) ^{13}C, c) 2D ^{1}H-^{1}H COSY and 2D multiplicity-edited HSQC and d) HMBC and selective NOE spectra.

a)

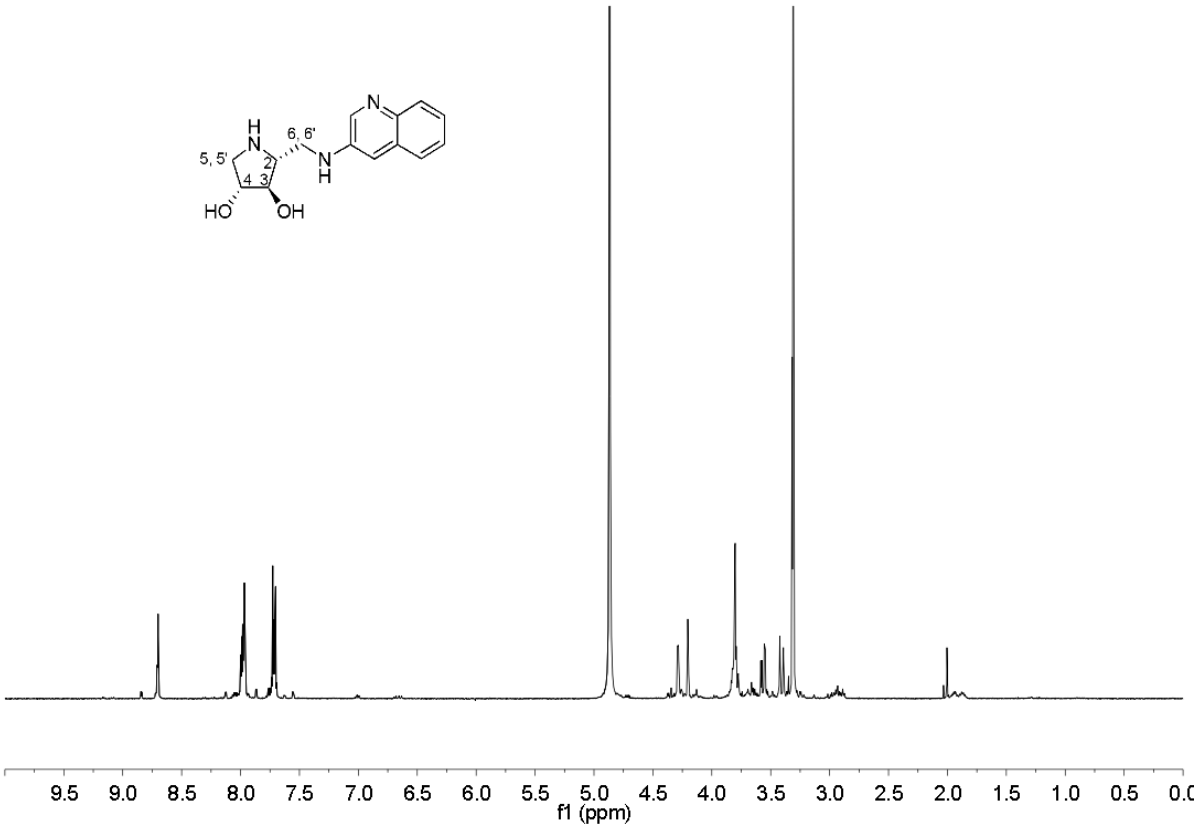

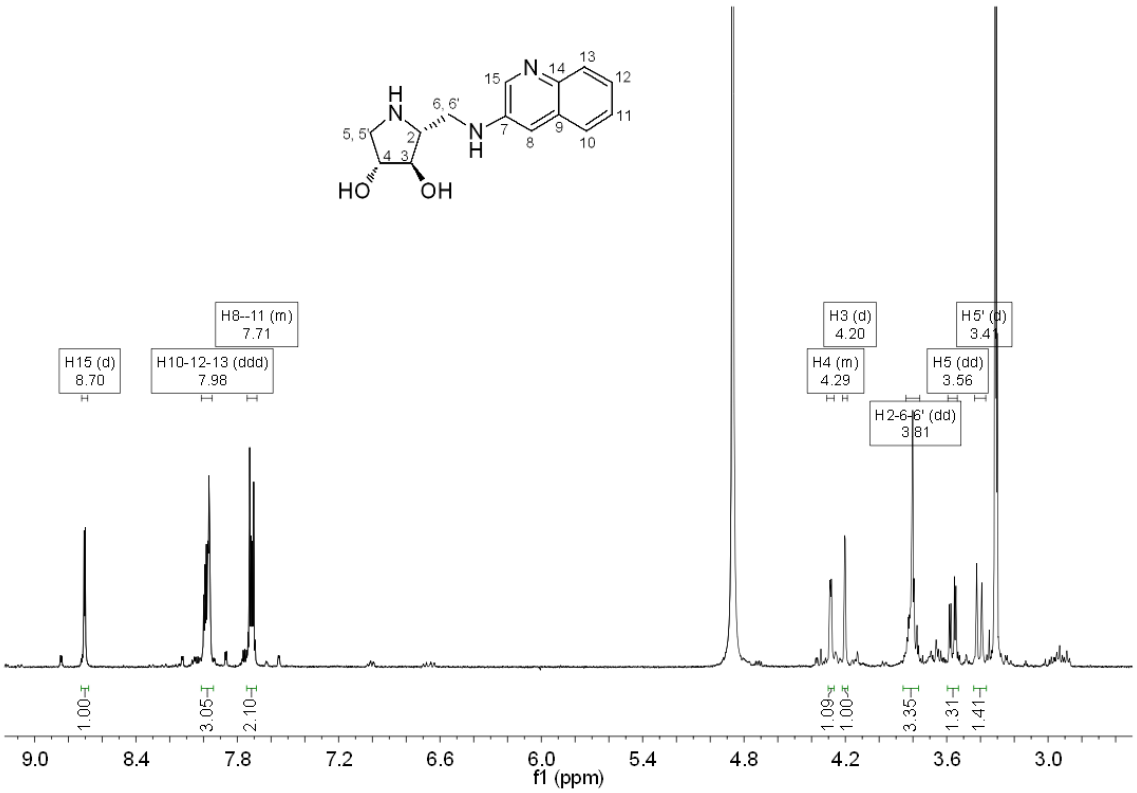

b)

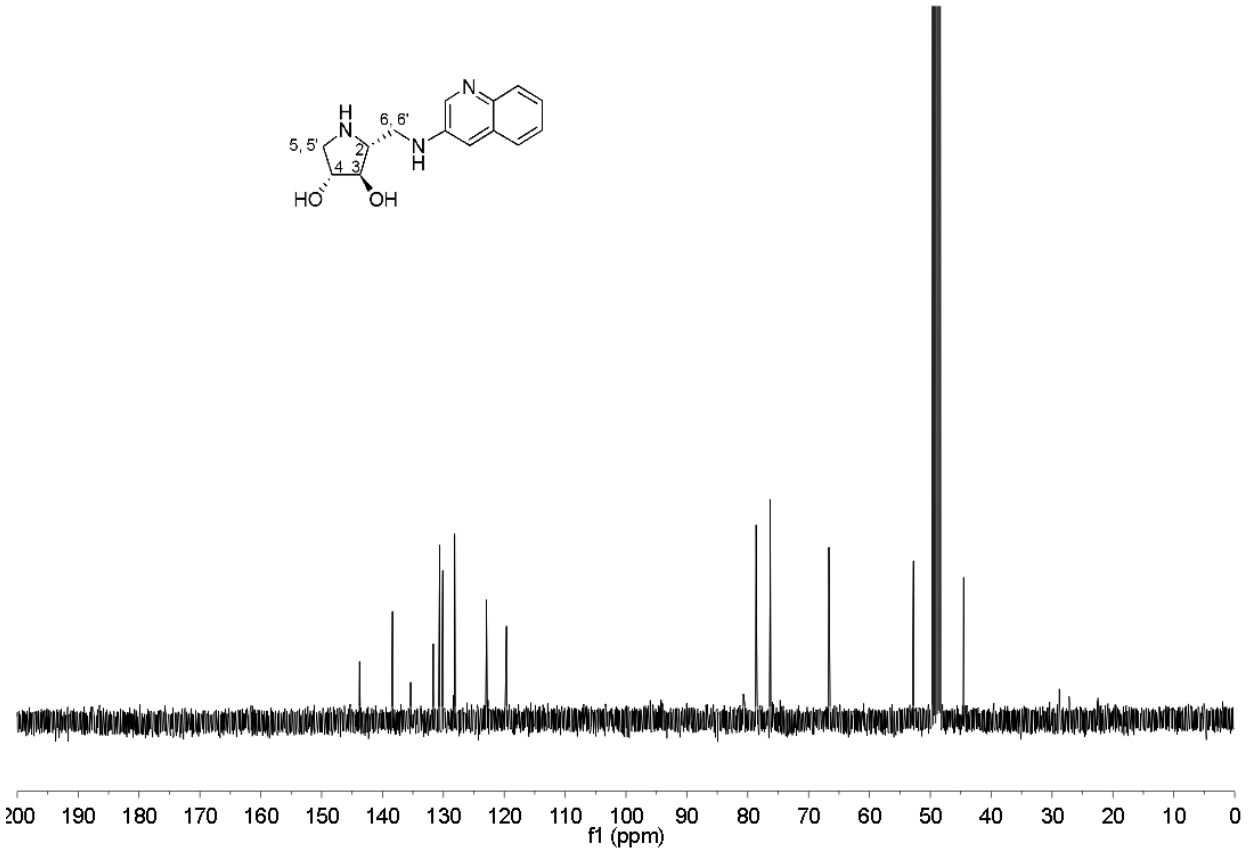
N
H
N
6, 6'
5, 5'
2
4
3
N
H
HO
OH
200 190 180 170 160 150 140 130 120 110 100 90 80 70 60 50 40 30 20 10 0
f1 (ppm)

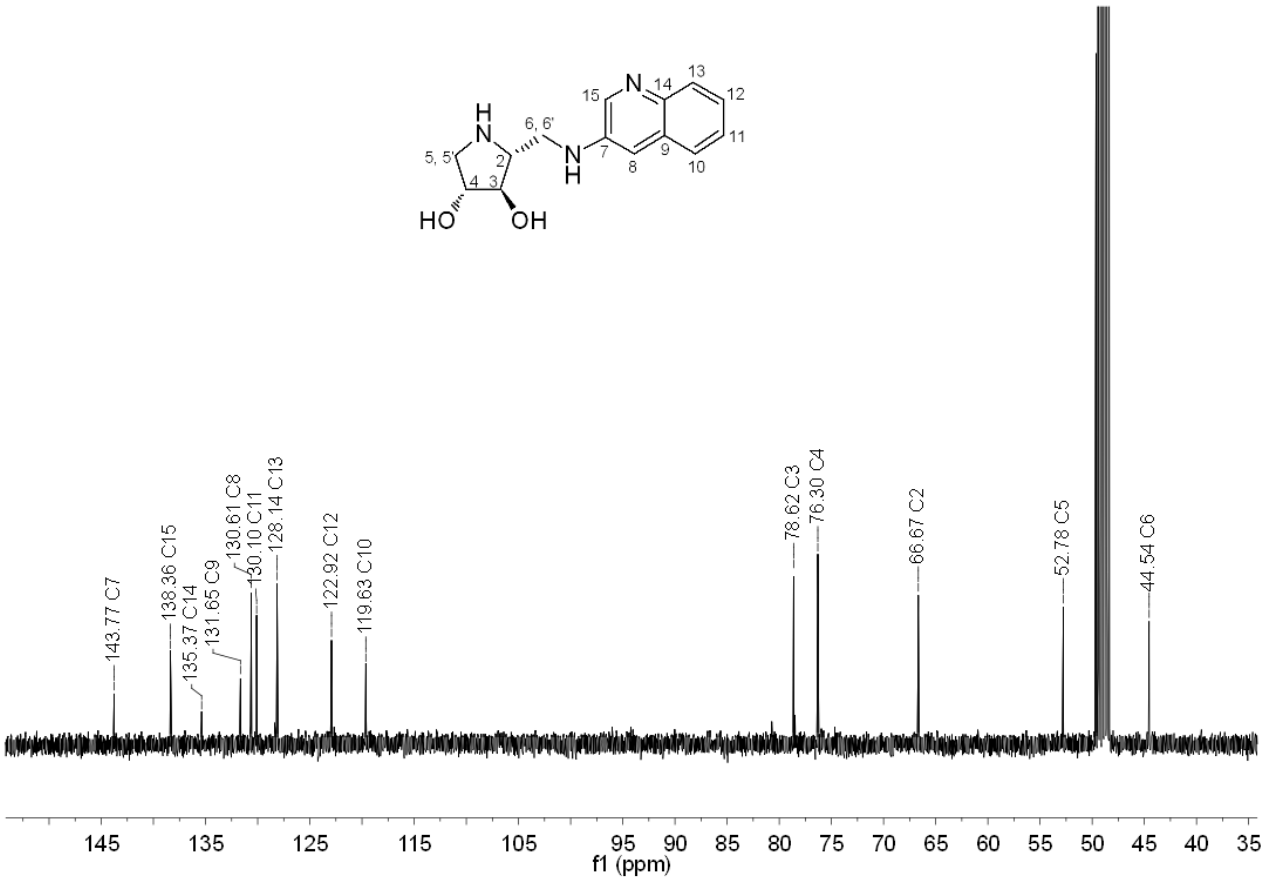
13
N
14
15
12
H
N
6, 6'
11
5, 5'
2
7
9
N
H
8
10
4
3
HO
OH
143.77 C7
138.36 C15
135.37 C14
131.65 C9
130.61 C8
130.10 C11
128.14 C13
122.92 C12
119.63 C10
78.62 C3
76.30 C4
66.67 C2
52.78 C5
44.54 C6
145 135 125 115 105 95 90 85 80 75 70 65 60 55 50 45 40 35
f1 (ppm)

c)

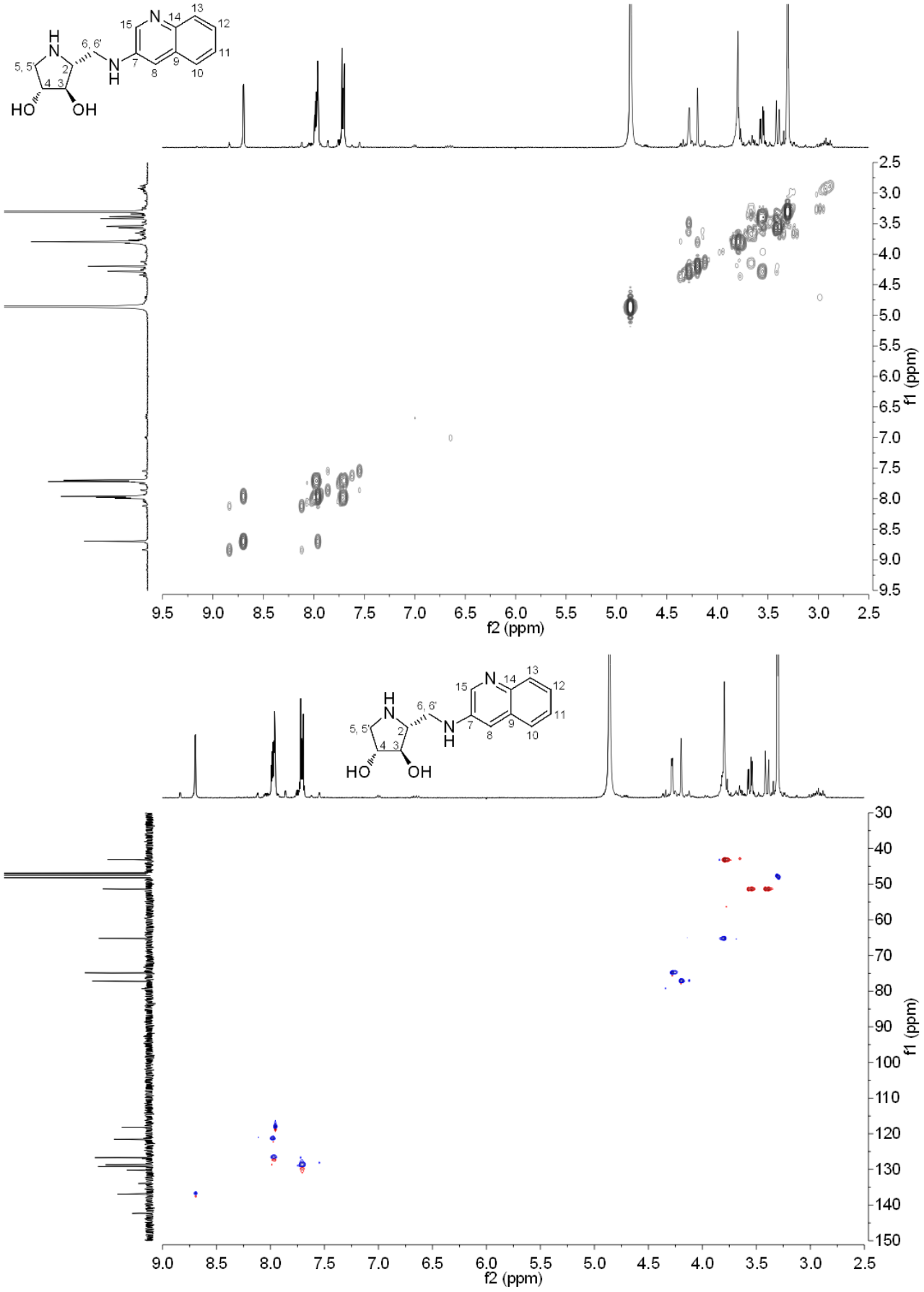

d)

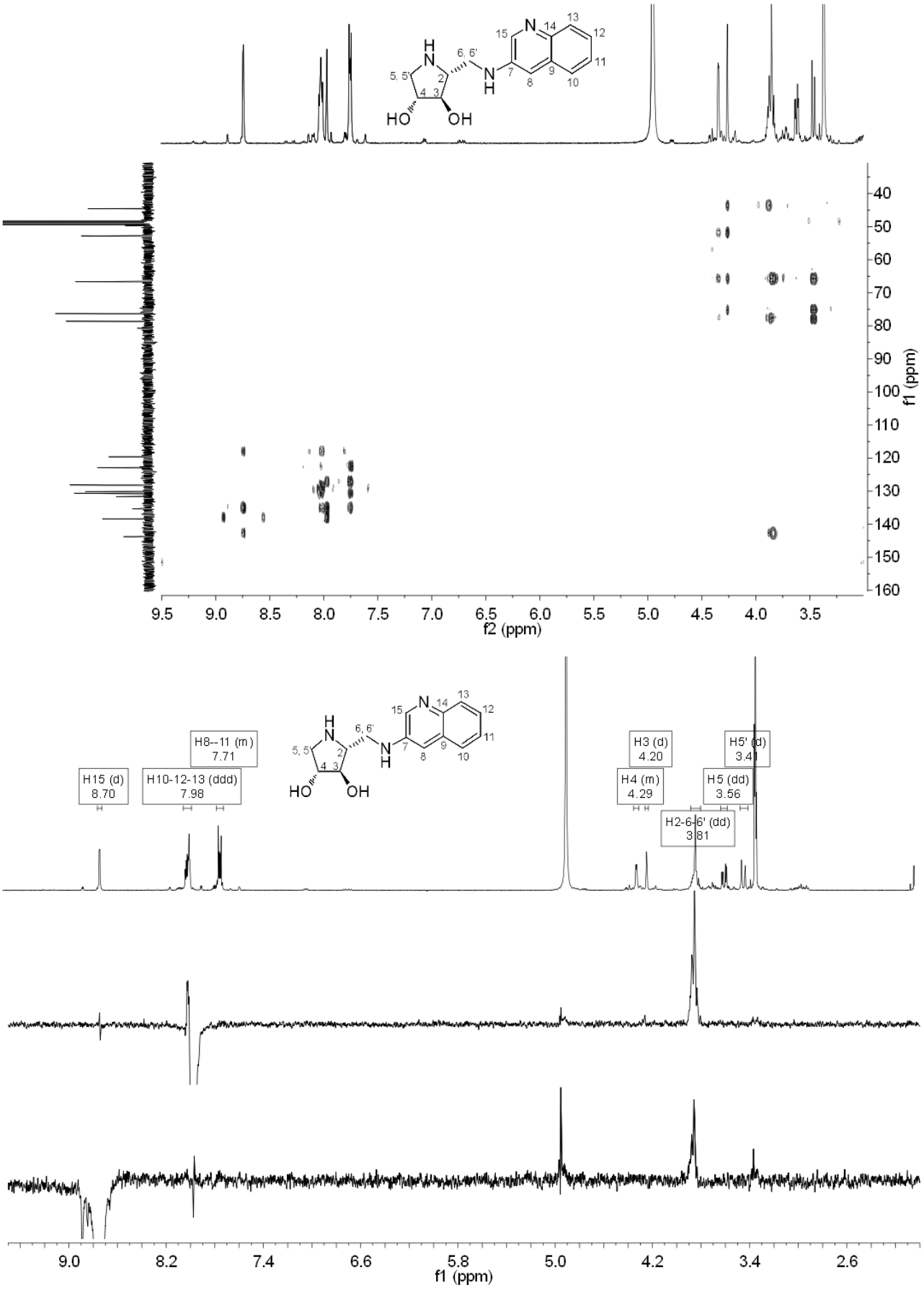
f2 (ppm)
f1 (ppm)
H15 (d) 8.70
H10-12-13 (ddd) 7.98
H8--11 (m) 7.71
H3 (d) 4.20
H4 (m) 4.29
H5 (dd) 3.56
H5' (d) 3.41
H2-6-6' (dd) 3.81
f1 (ppm)

Figure 8. Observed NMR spectra of **24d**: a) ^{1}H, b) ^{13}C, c) 2D ^{1}H-^{1}H COSY and 2D multiplicity-edited HSQC.

a)

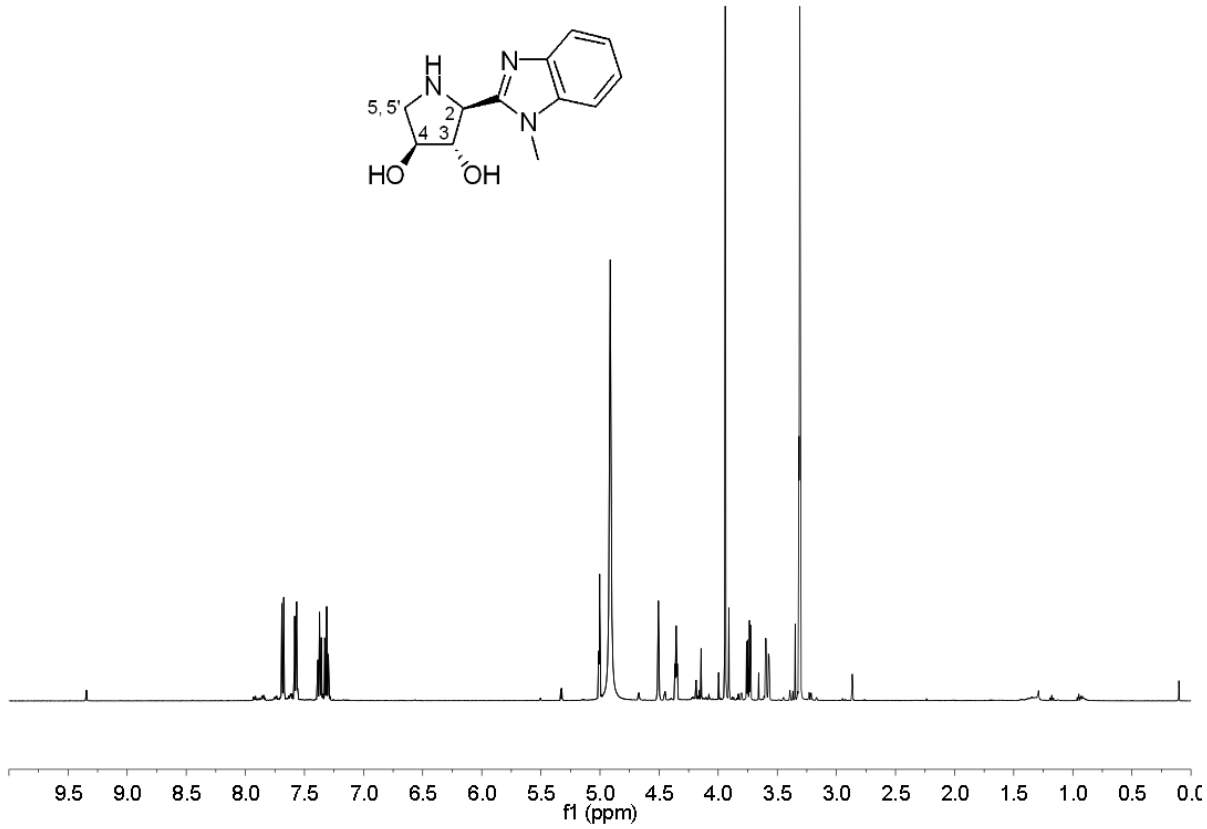

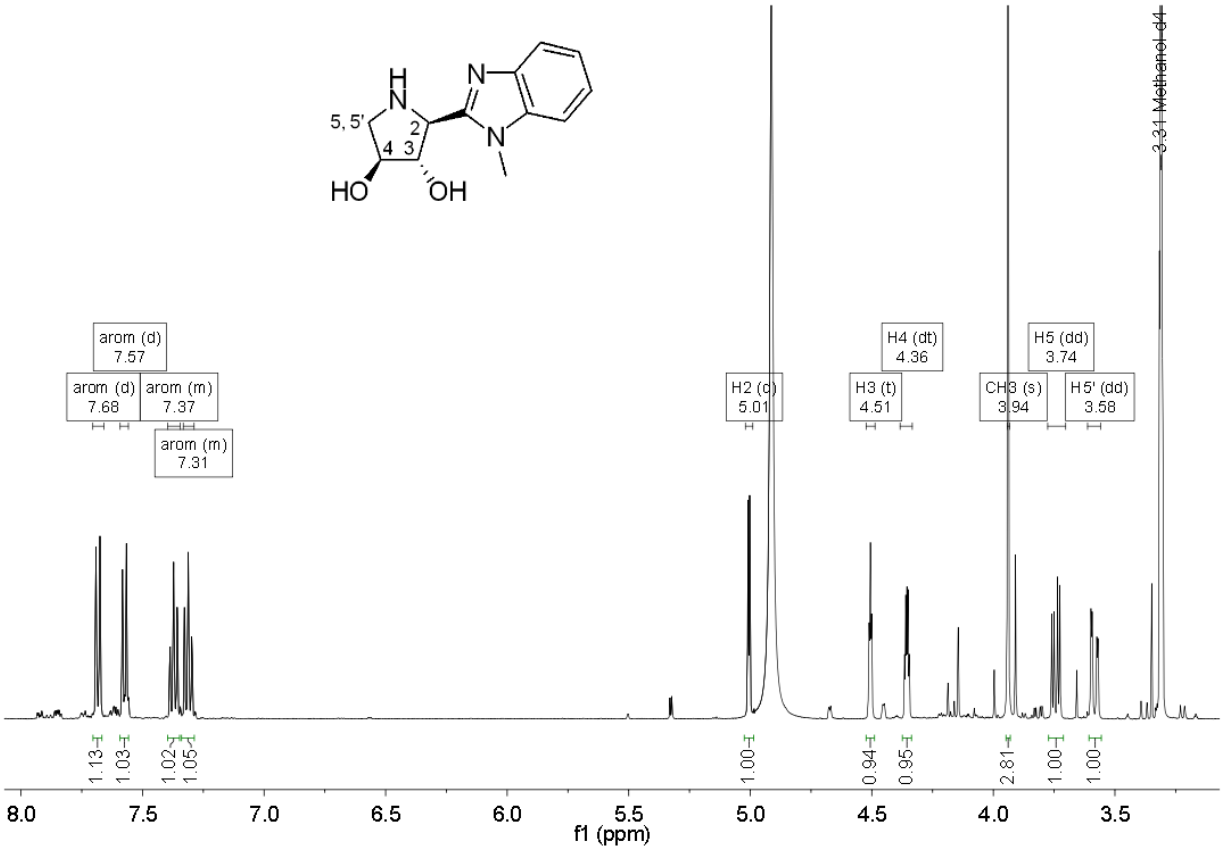

b)

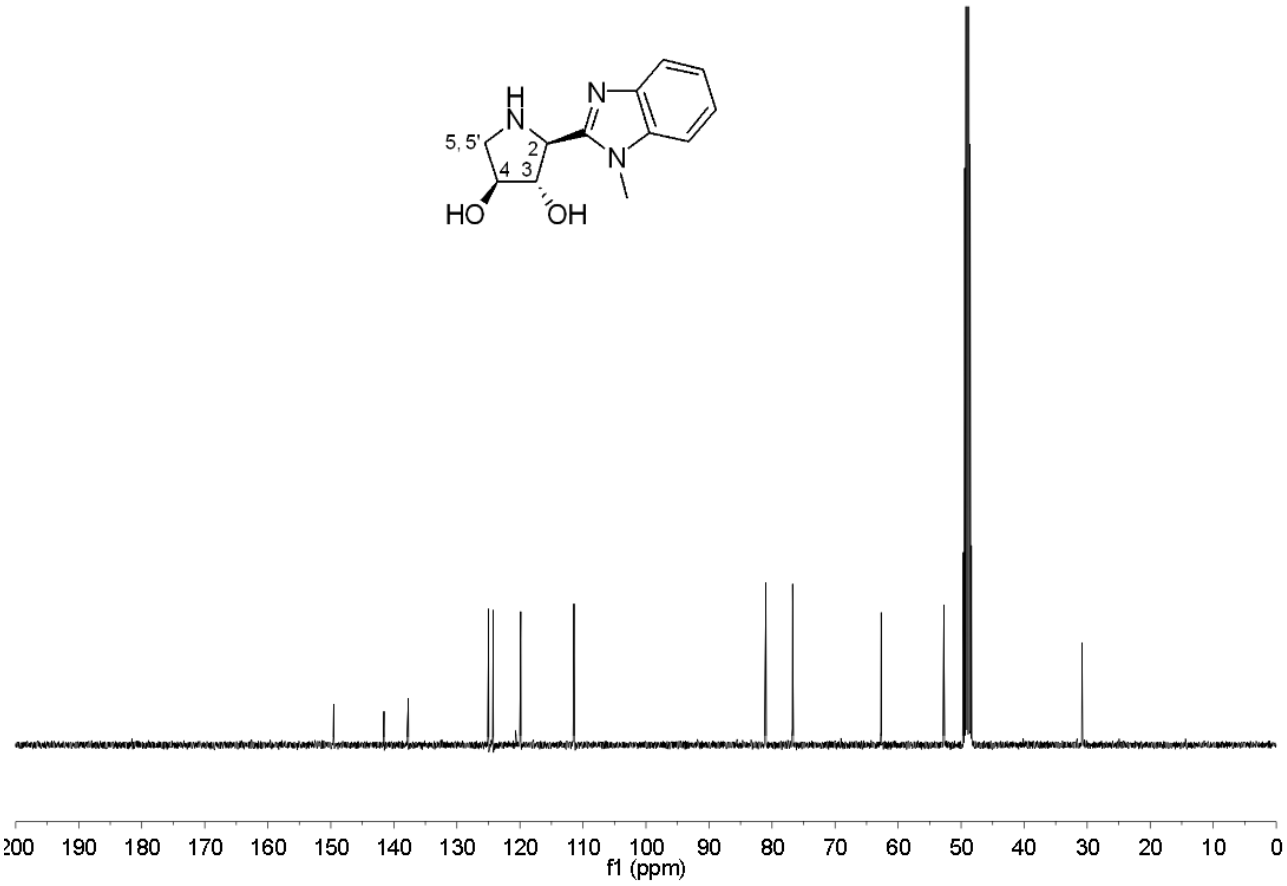

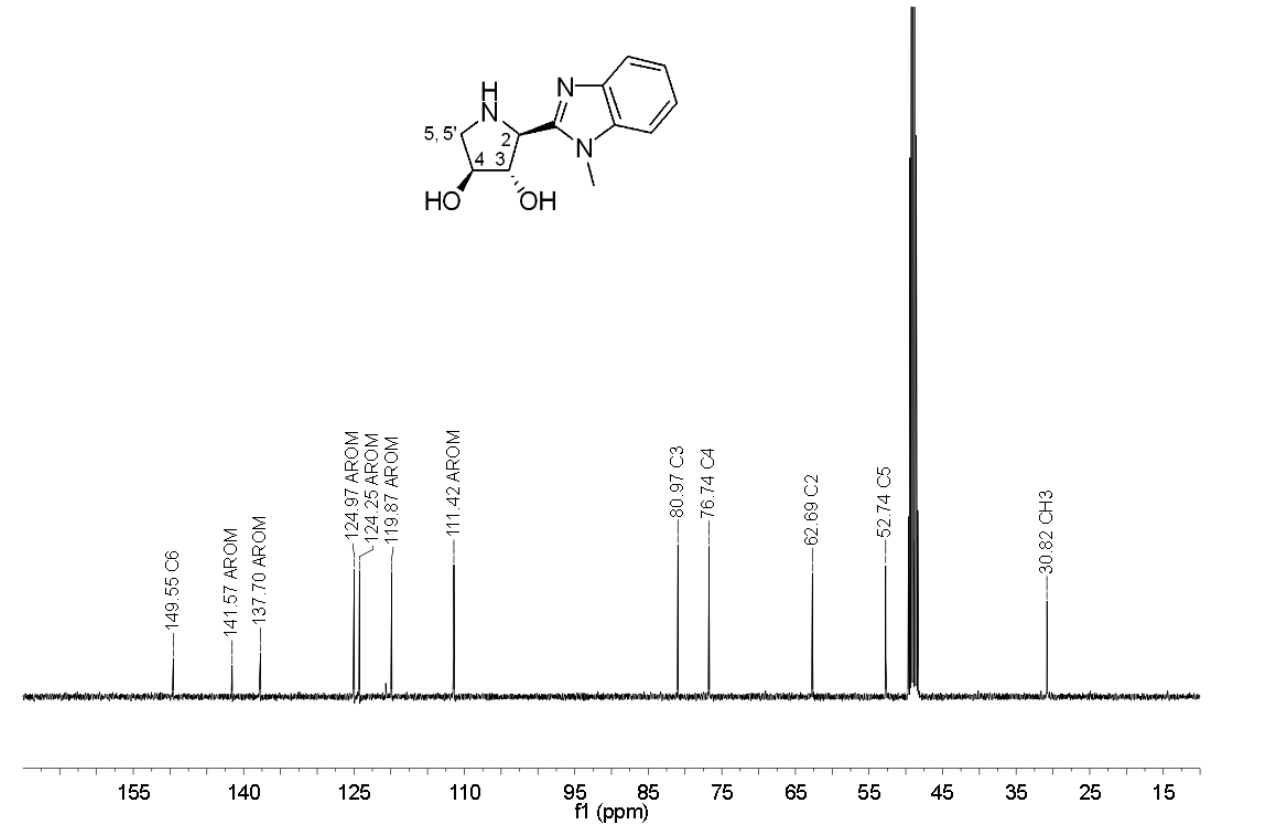

c)

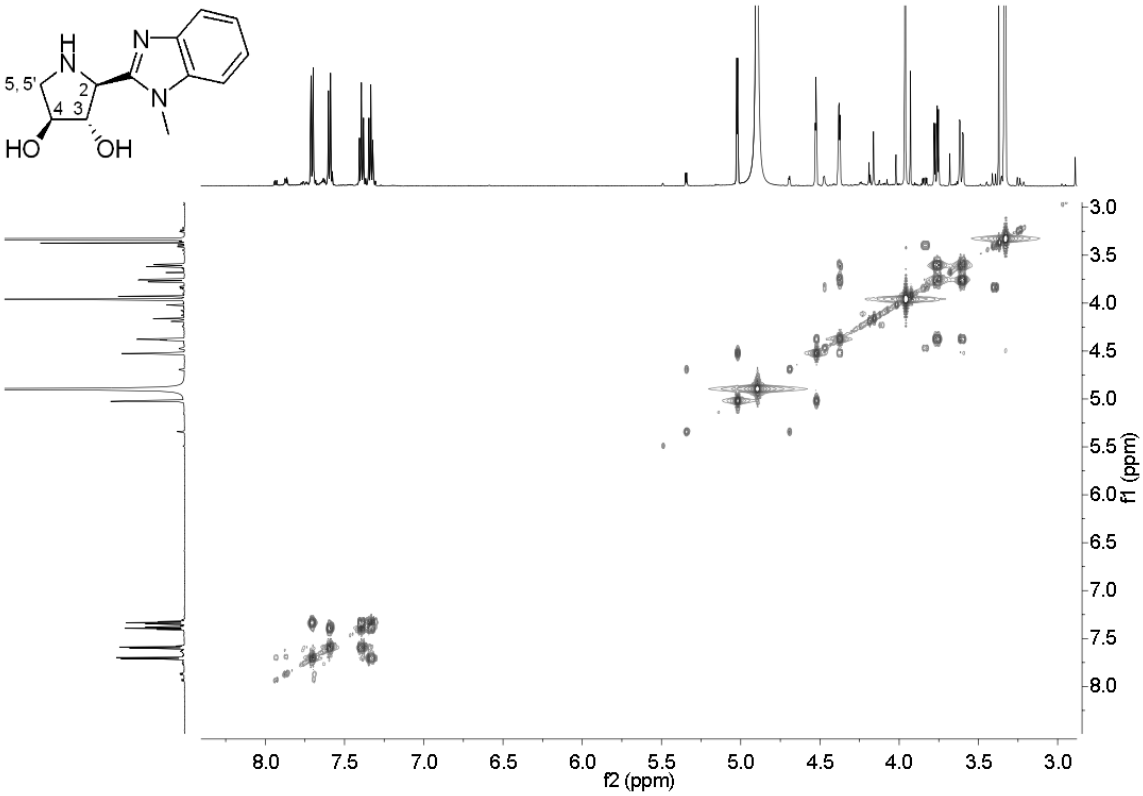

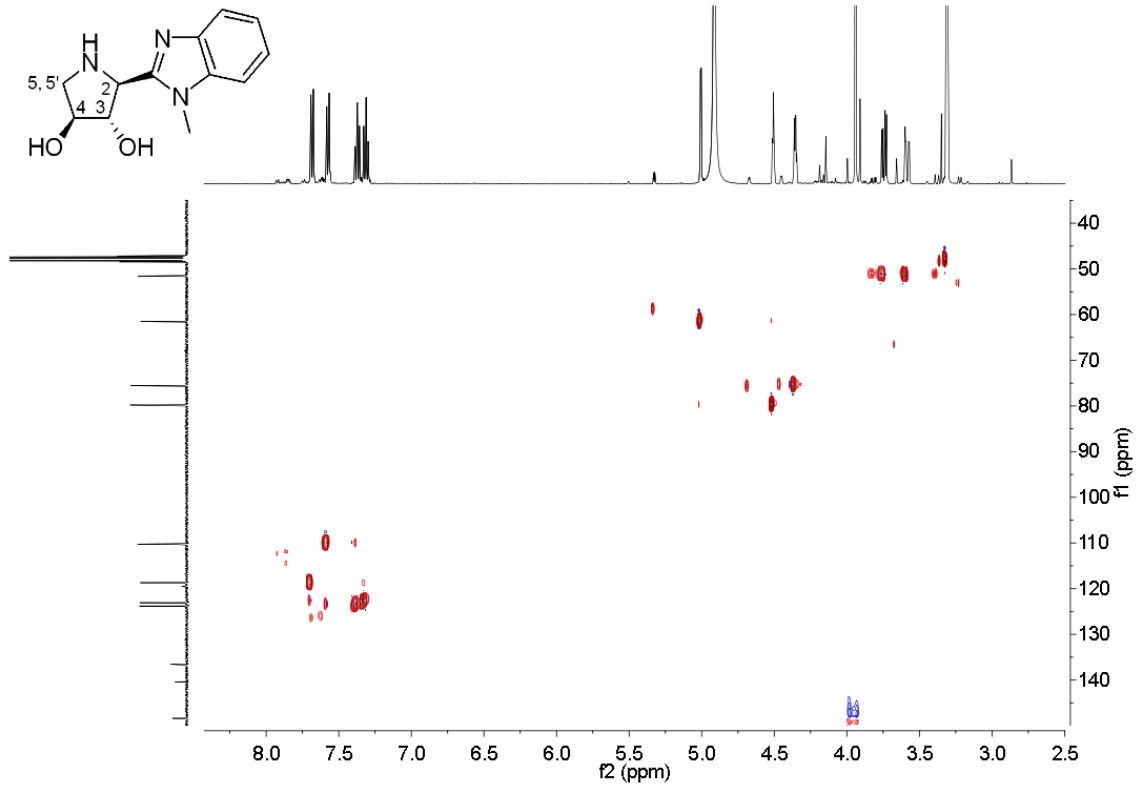

Figure 9. Observed NMR spectra of **23d** enantiomer of **24d**: a) ^{1}H and, b) ^{13}C.

a)

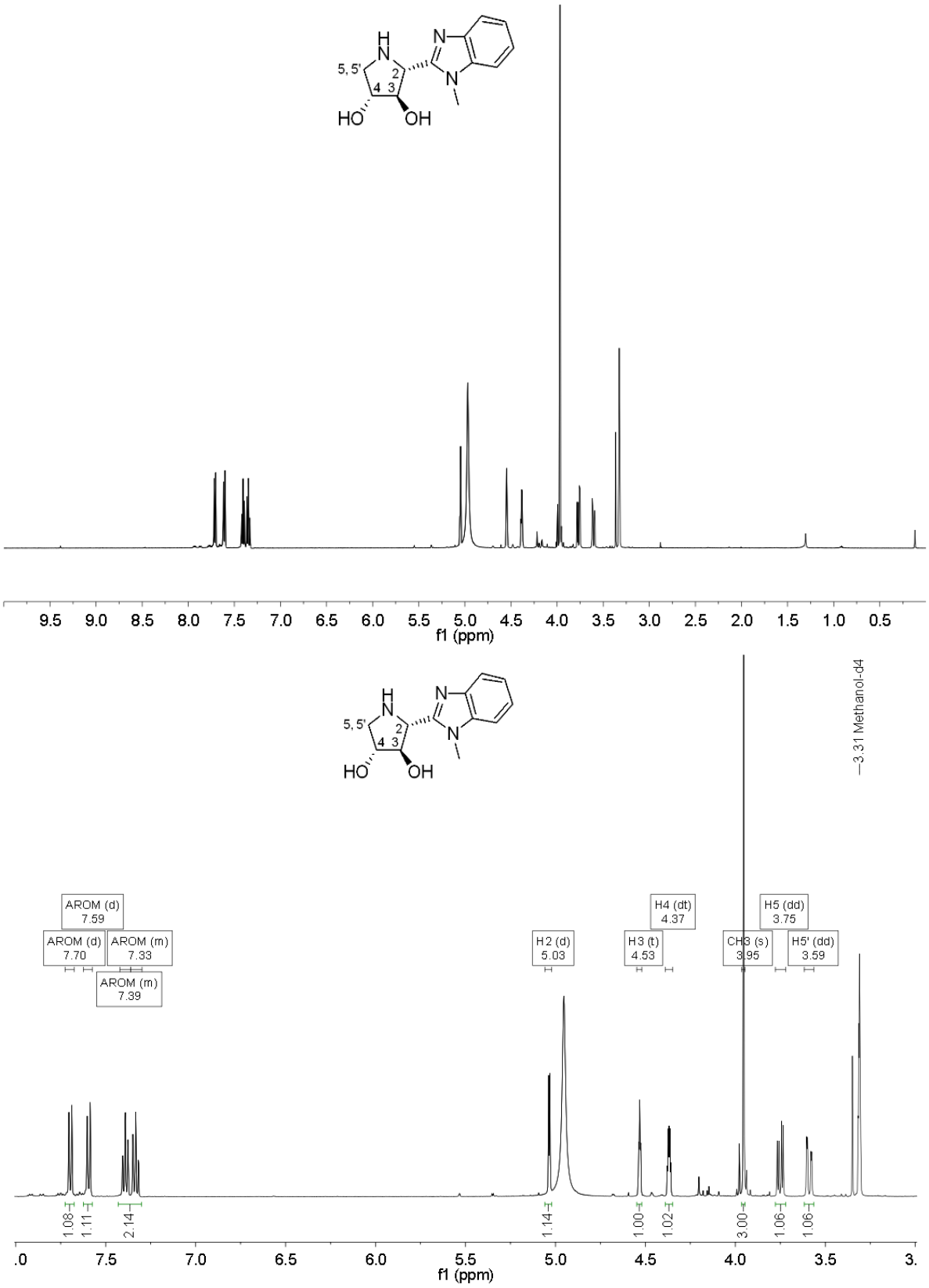

b)

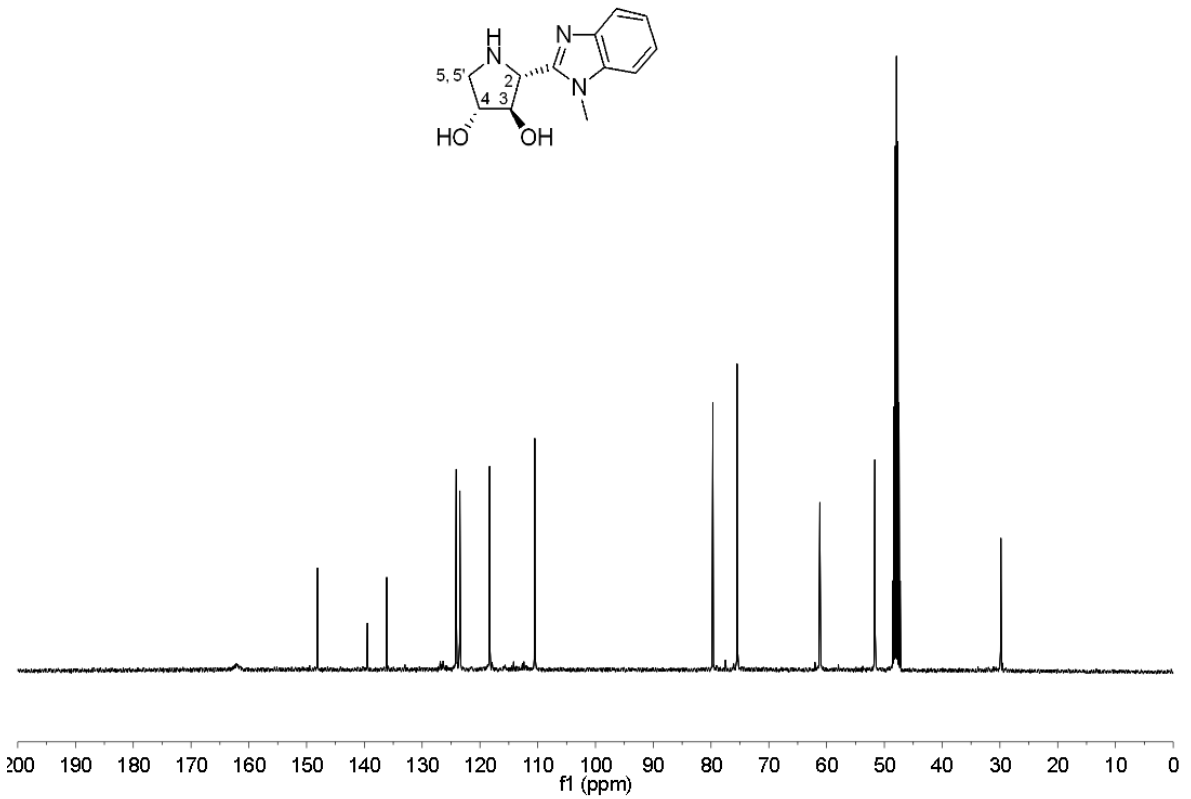

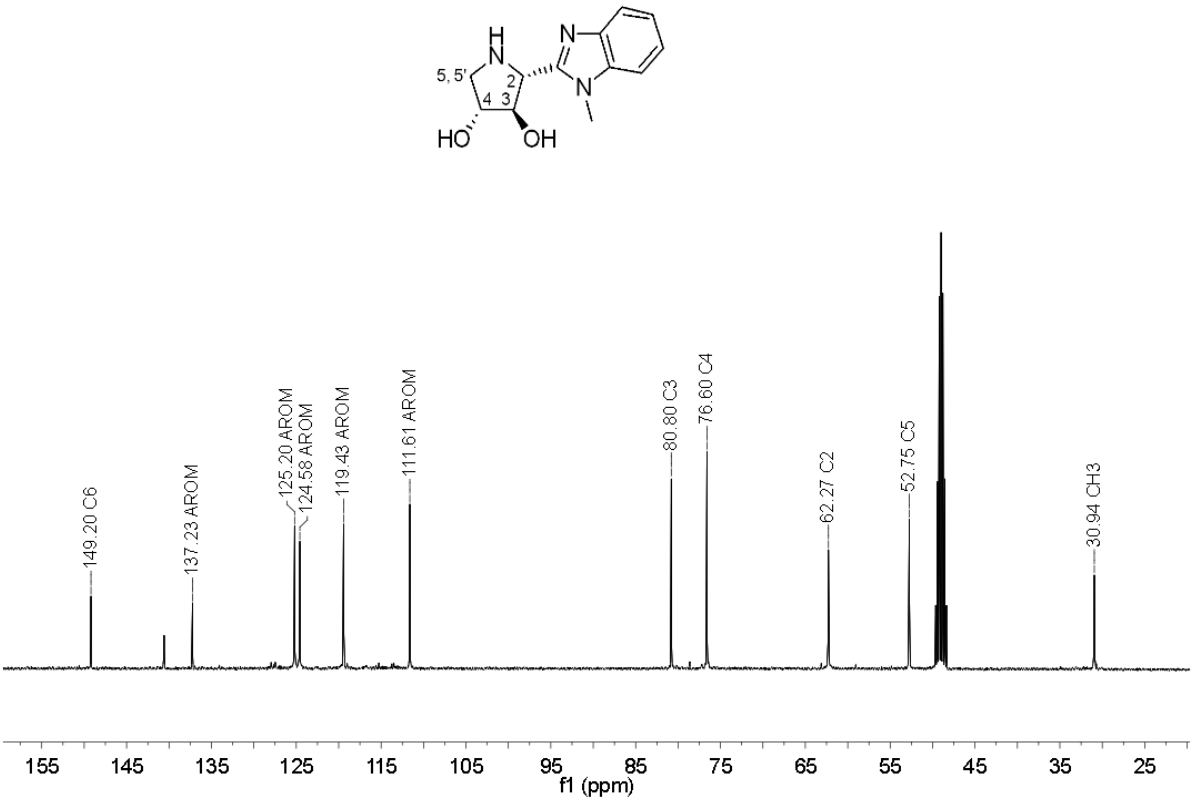

Figure 10. Observed NMR spectra of **23e** a) ^{1}H and, b) ^{13}C, c) 2D ^{1}H-^{1}H COSY and 2D multiplicity-edited HSQC and d) HMBC and selective NOE spectra.

a)

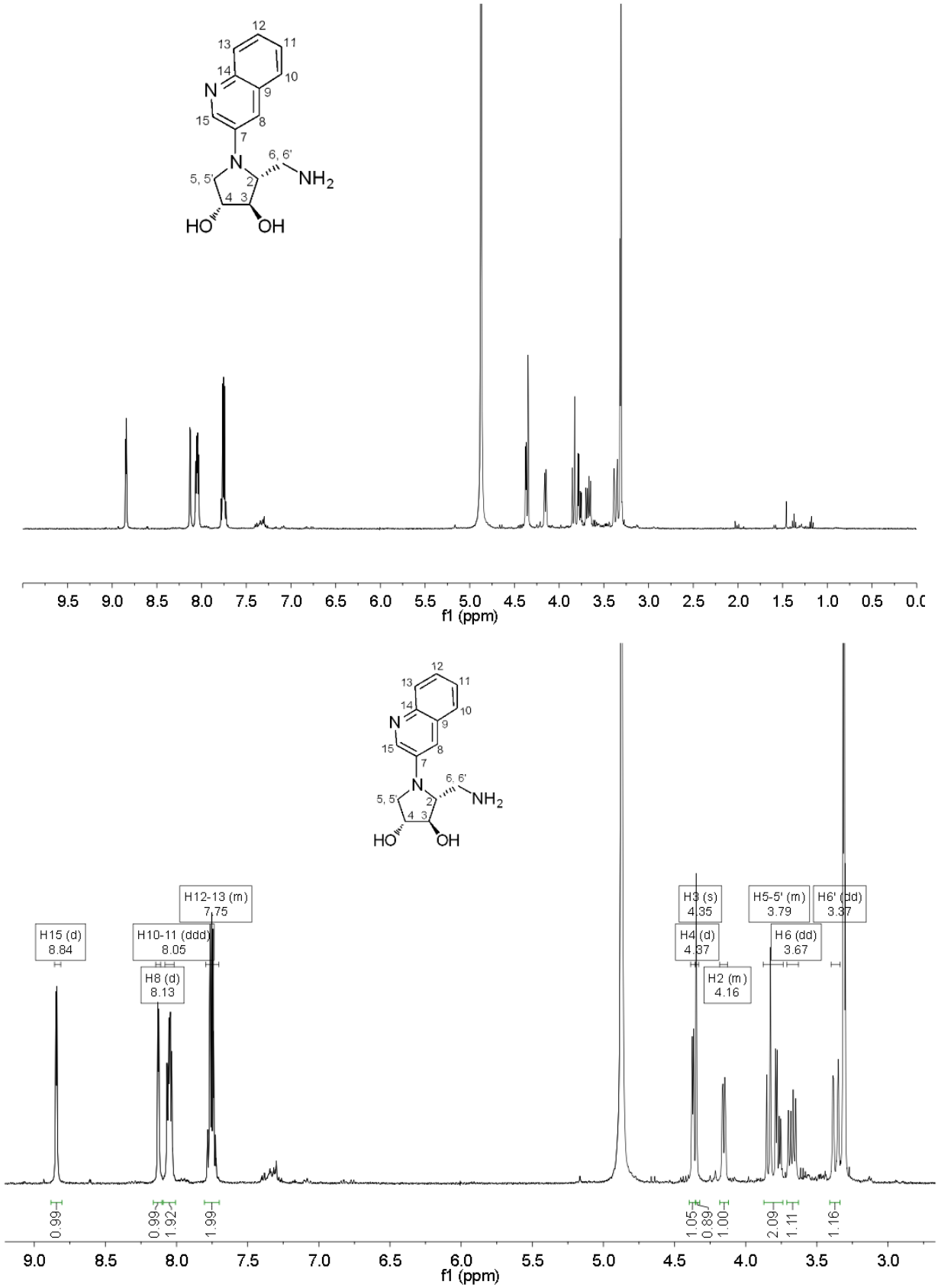

b)

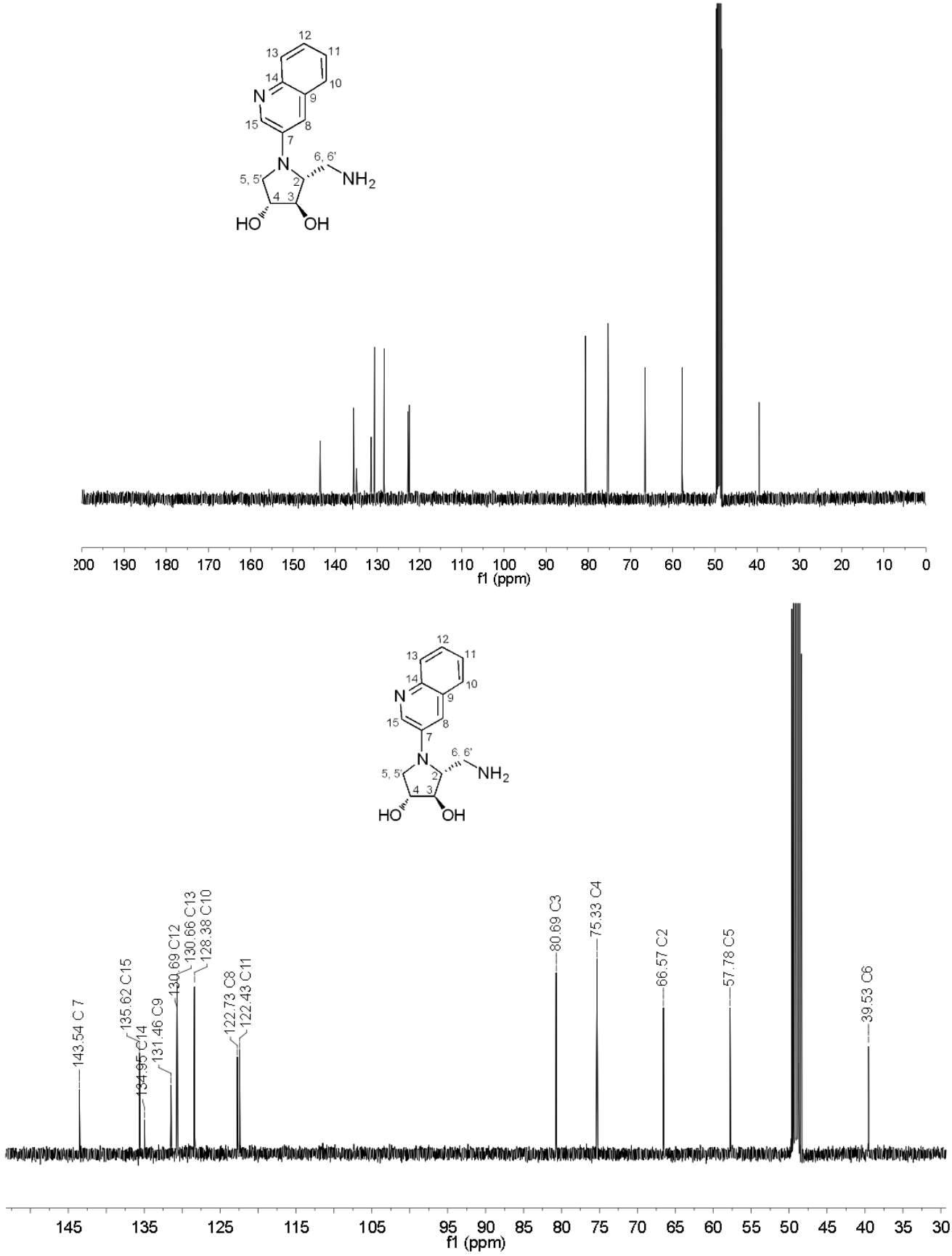

c)

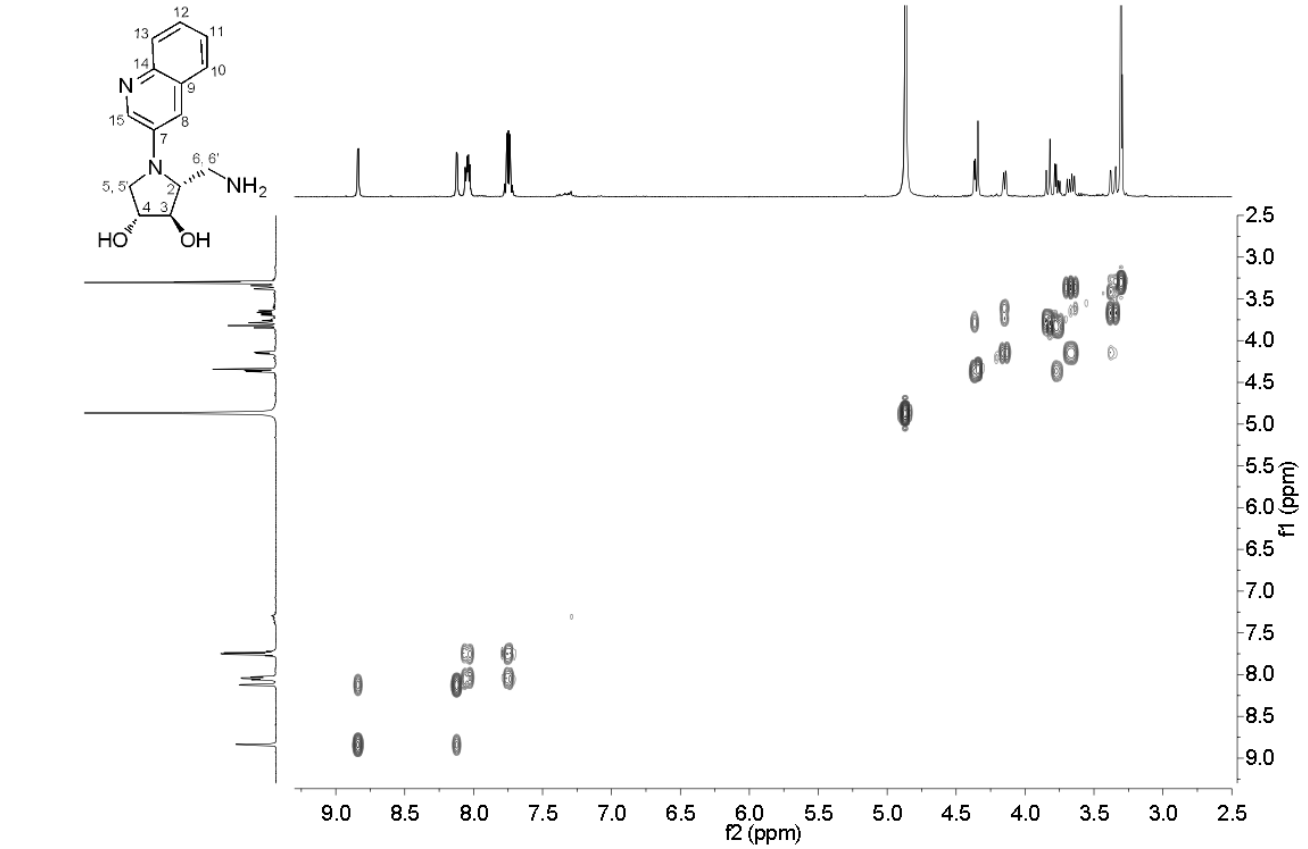

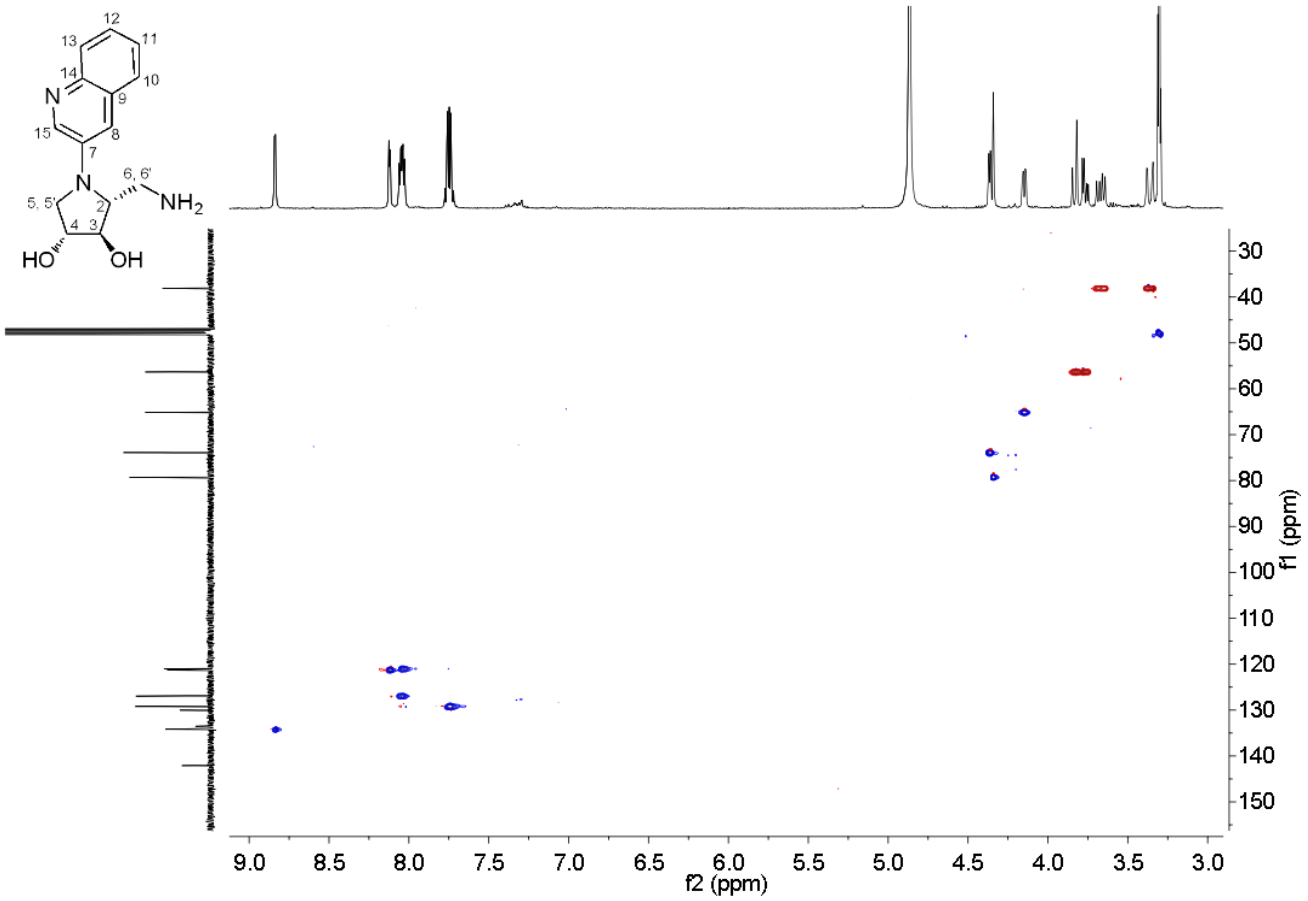

d)

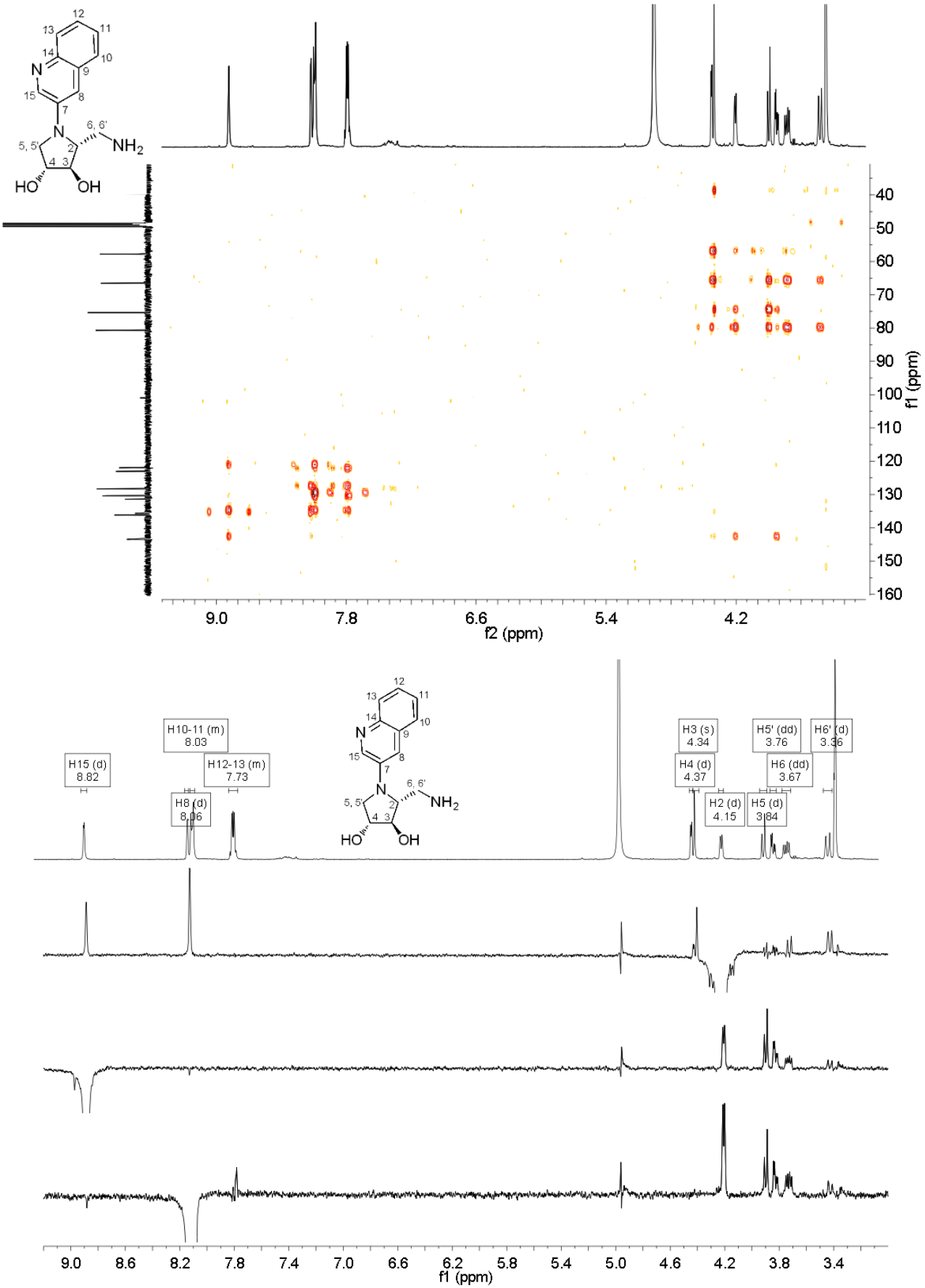

Figure 11. Observed NMR spectra of **24e** enantiomer of **23e** a) ^{1}H, b) ^{13}C.
a)

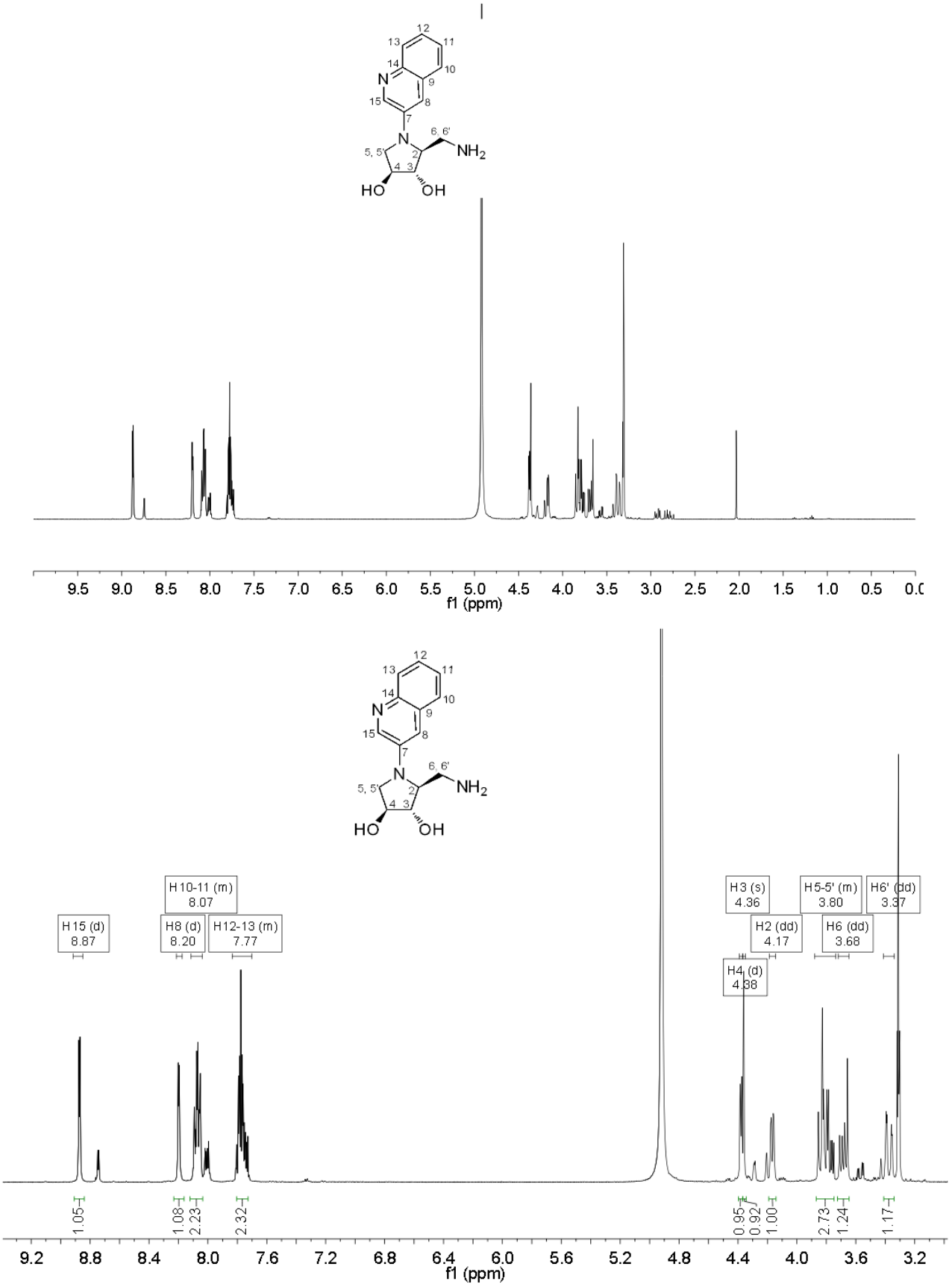

b)

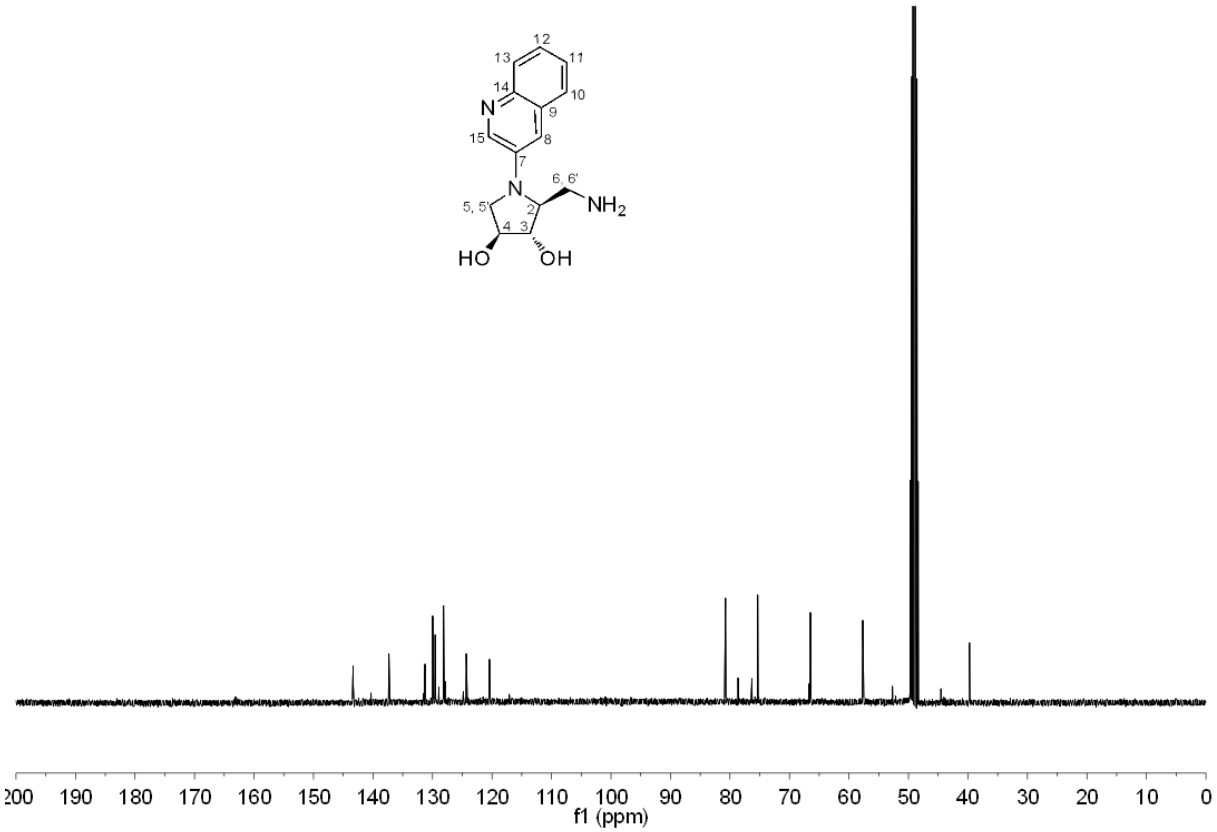

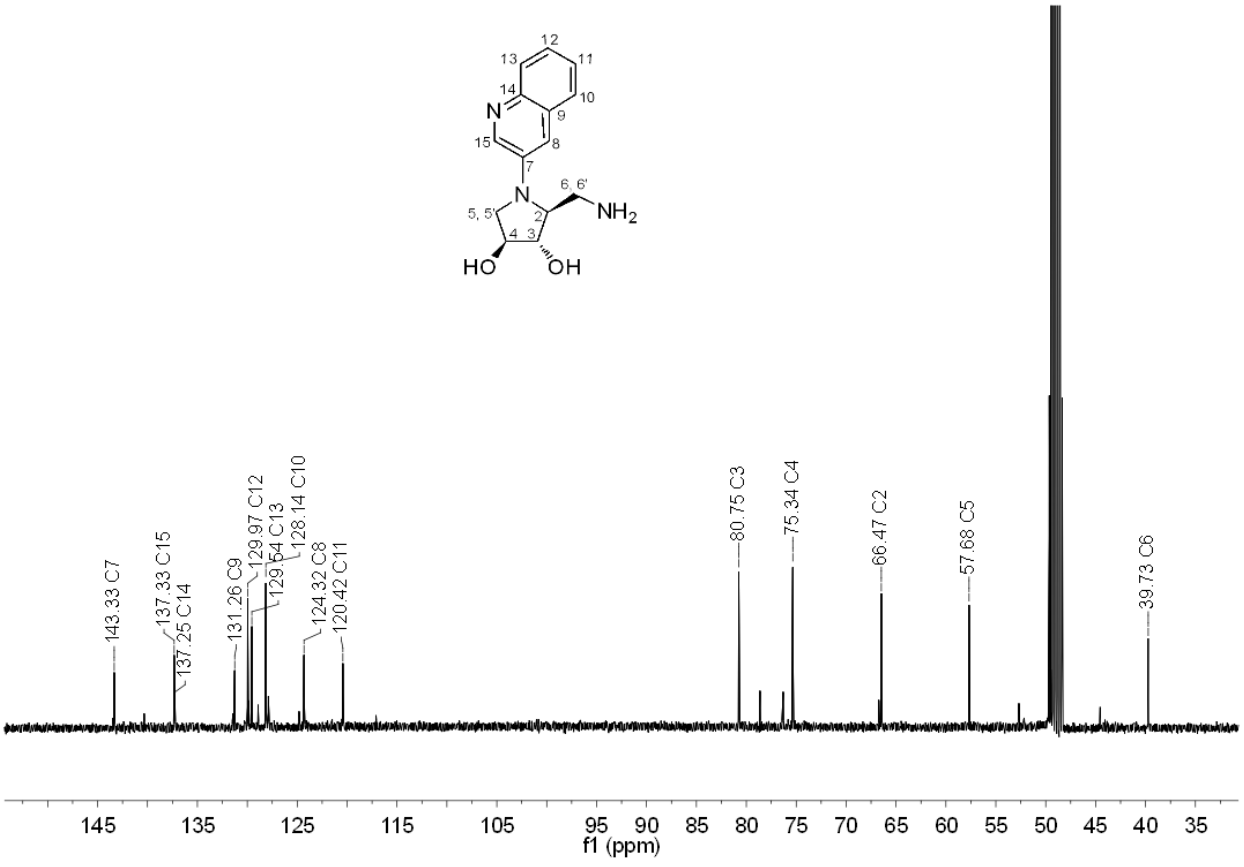

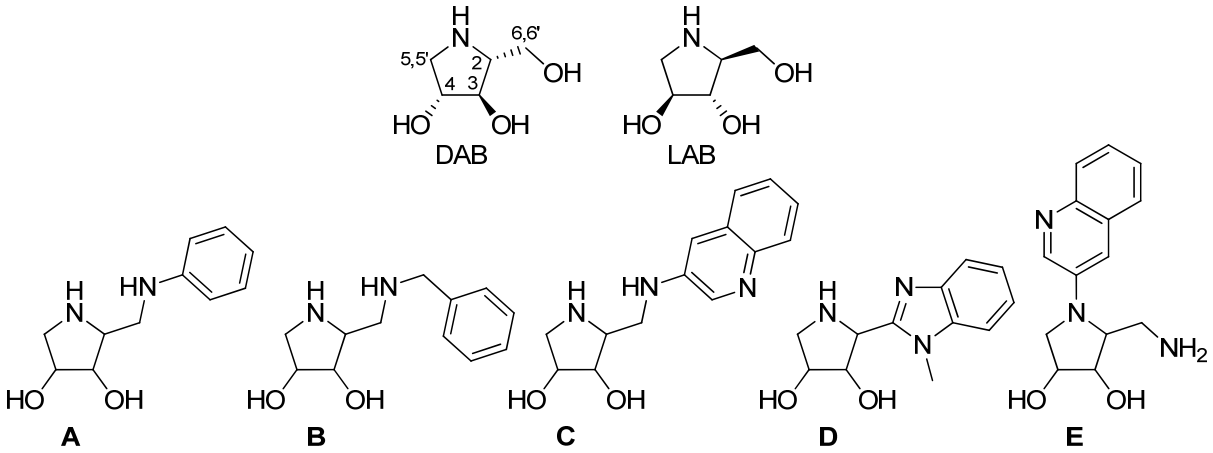

Product number	Config	H2 (C2)	H3 (C3)	H4 (C4)	H5, 5’ (C5)	H6, 6’ (C6)	$[\alpha]_D^{20}$	MS (oa-TOF) *m/z* [M + H]+
	DAB/LAB	3.63 (69.3)	4.11 (78.4)	4.35 (77.0)	3.59, 3.37 (52.7)	3.97, 3.85 (61.7)	-	-
23a	**DAB**	3.72 (67.24)	4.11 (78.47)	4.24 (76.24)	3.48, 3.34 (52.21)	3.58, 3.53 (45.02)	+ 46.4 (*c* = 1.4 in MeOH)	209.1276
24a	**LAB**	3.72 (67.32)	4.11 (78.50)	4.24 (76.28)	3.48, 3.34 (52.26)	3.58, 3.53 (45.07)	– 41.5 (*c* = 1.1 in MeOH)	209.1267
23b	**DAB**	3.82 (64.85)	4.21 (79.27)	4.25 (75.85)	3.58, 3.41 (53.14)	3.58 (48.48)	+ 14.25 (*c* = 1.0 in MeOH)	223.1431
24b	**LAB**	3.82 (64.62)	4.20 (79.27)	4.24 (75.72)	3.57, 3.40 (53.04)	3.57 (48.36)	– 14.36 (*c* = 1.3 in MeOH)	223.1440
23c	**DAB**	3.81 (66.67)	4.20 (78.62)	4.29 (76.30)	3.56, 3.41 (52.78)	3.81 (44.54)	+22.6 (*c* = 0.5 in MeOH)	260.1381
23e	**DAB**	4.16 (66.57)	4.35 (80.69)	4.37 (75.33)	3.79 (57.78)	3.37, 3.67 (39.53)	– 28.0 (*c* = 0.5 in MeOH)	260.1389
24c	**LAB**	3.82 (66.46)	4.21 (78.62)	4.29 (76.27)	3.57, 3.42 (52.62)	3.82 (44.47)	– 35.0 (*c* = 1.0 in MeOH)	260.1404
24e	**LAB**	4.17 (66.47)	4.36 (80.75)	4.38 (75.34)	3.80 (57.68)	3.37 , 3.68 (39.73)	+ 17.7 (*c* = 0.7 in MeOH	260.1390
23d	**DAB**	5.03 (62.27)	4.53 (80.80)	4.37 (76.60)	3.75, 3.59 (52.75)	(149.20)	+ 2.4 (*c* = 1.0 in MeOH)	234.1235
24d	**LAB**	5.01 (62.69)	4.51 (80.97)	4.36 (76.74)	3.74, 3.58 (52.74)	(149.55)	– 2.6 (*c* = 0.9 in MeOH)	234.1230

Figure 12. Observed NMR spectra of **25a**: a) ^{1}H, b) ^{13}C, c) 2D ^{1}H-^{1}H COSY and 2D multiplicity-edited HSQC.

a)

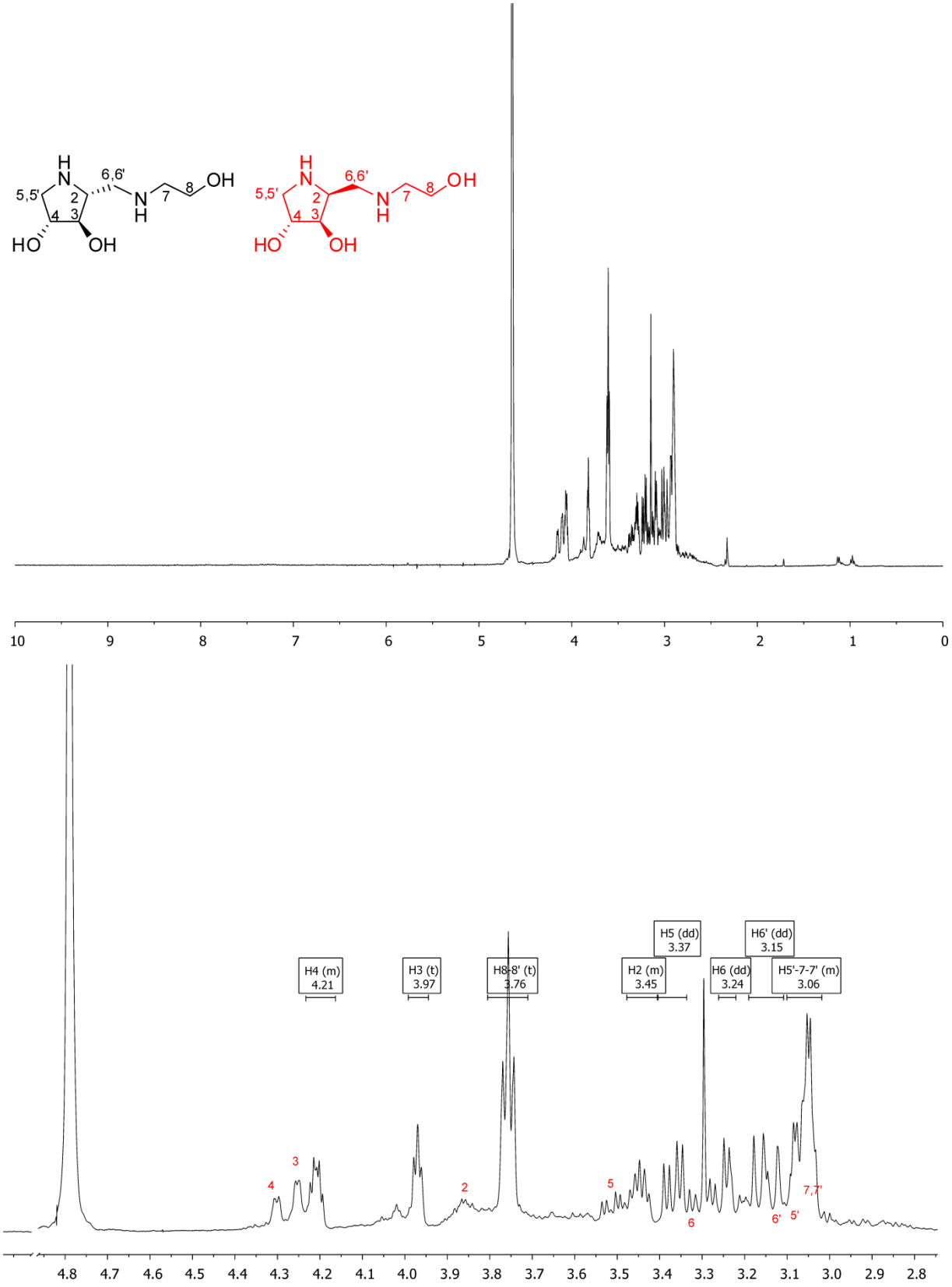

b)

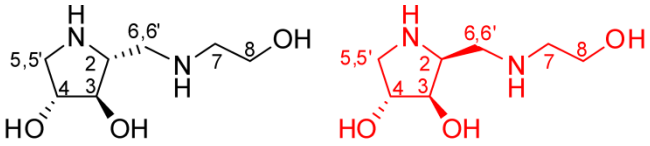

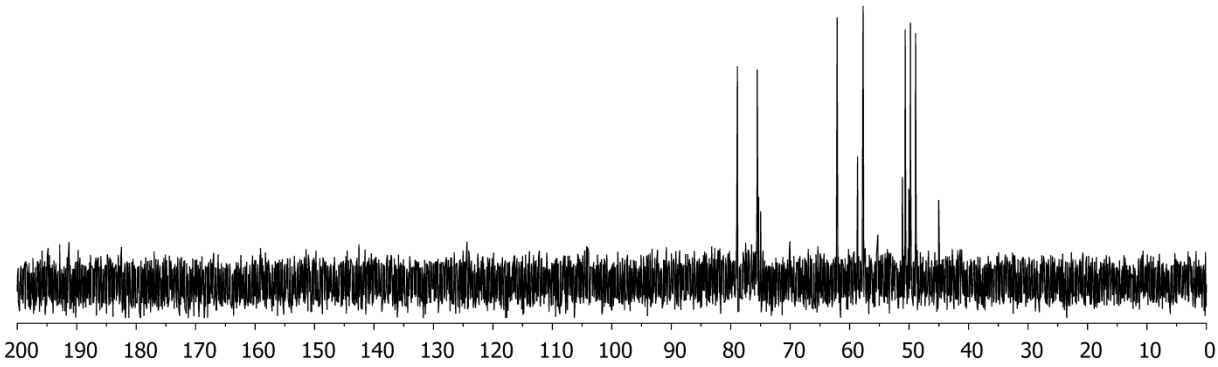

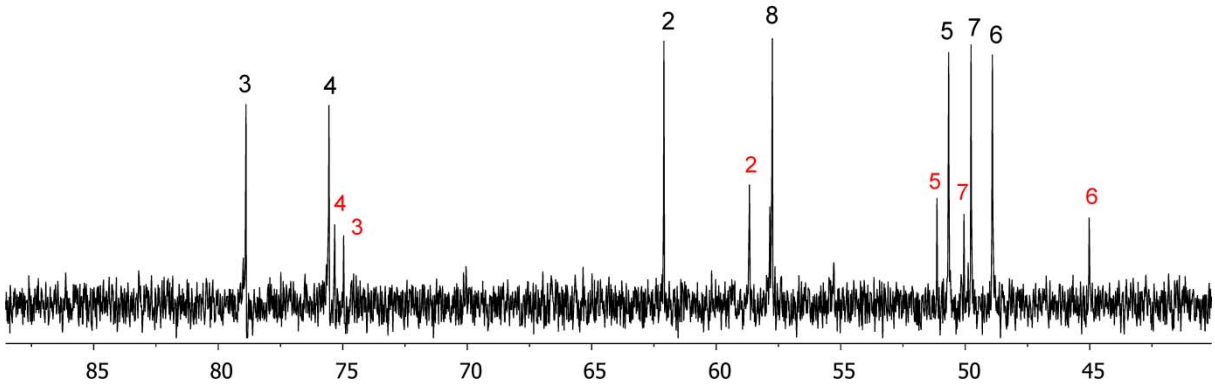

c)

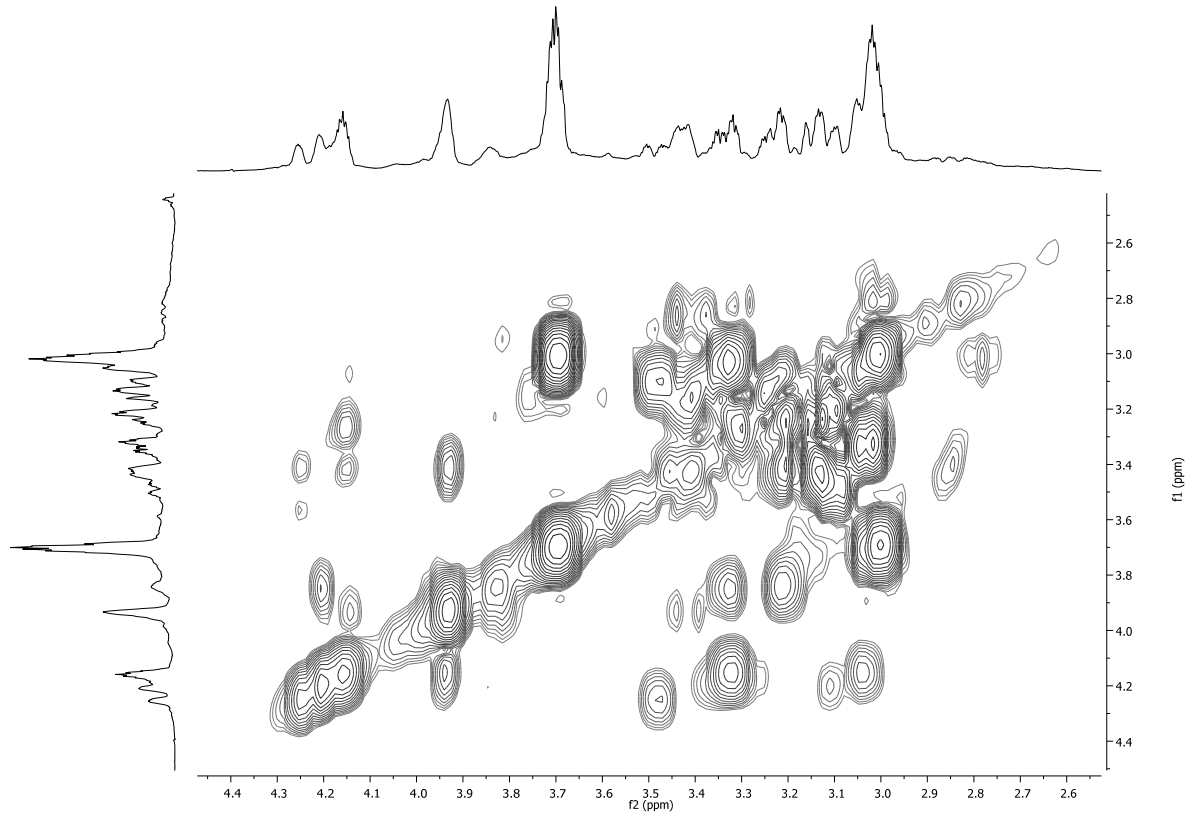

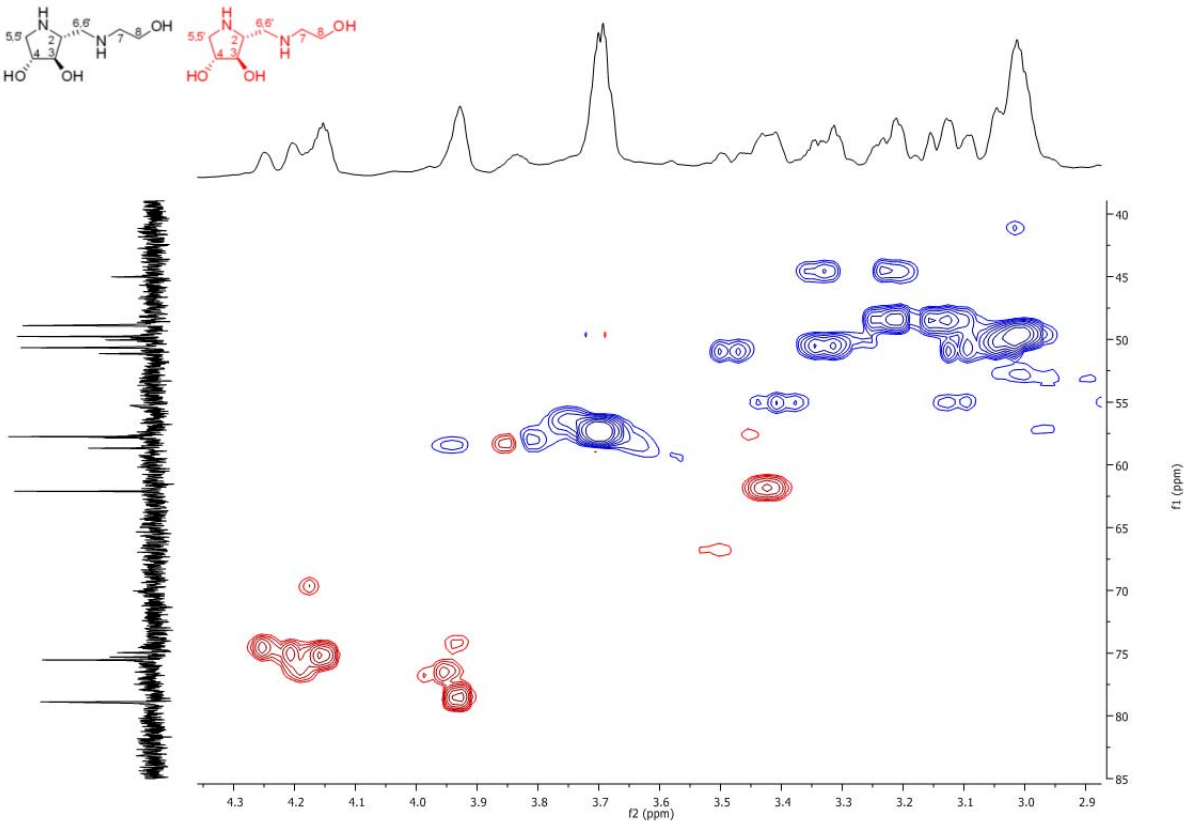

Figure 13. Observed NMR spectra of **25f**: a) ^{1}H, b) ^{13}C, c) 2D ^{1}H-^{1}H COSY and 2D multiplicity-edited HSQC.

a)

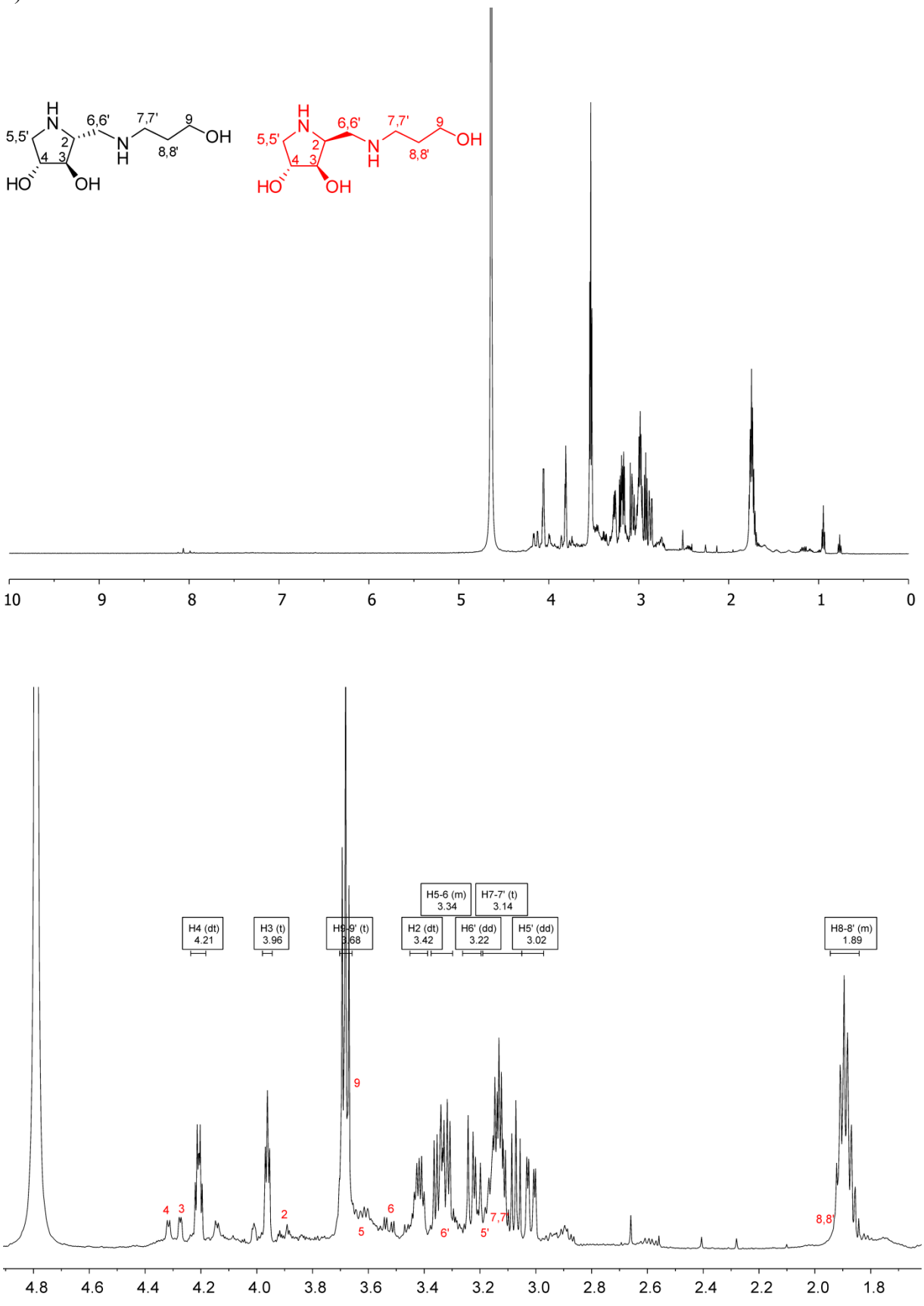

b)

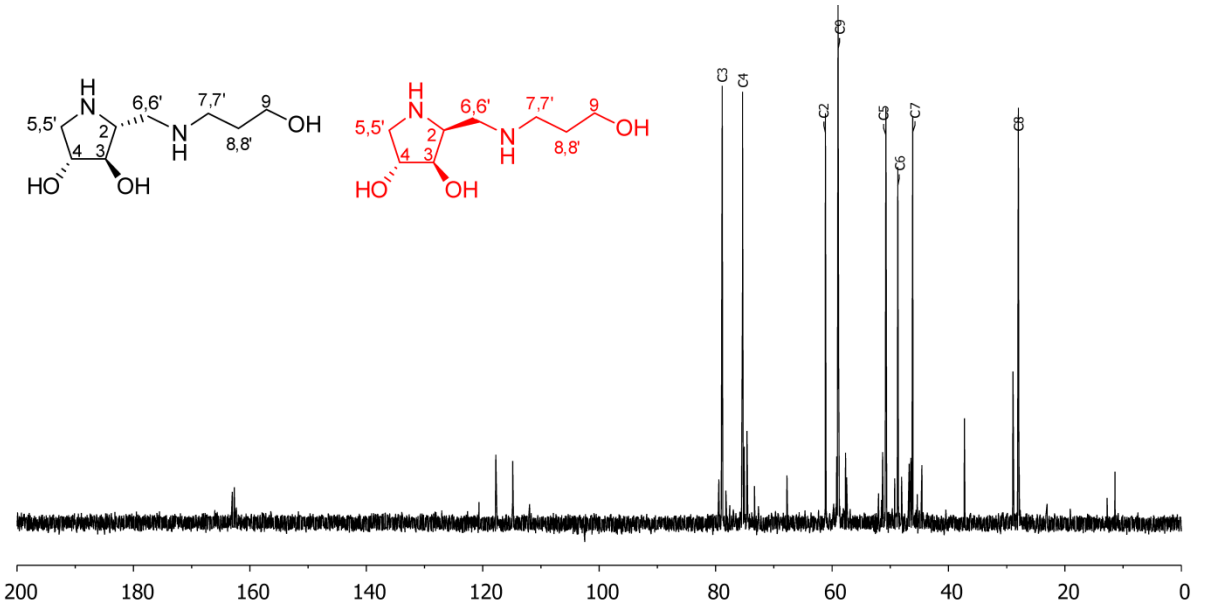

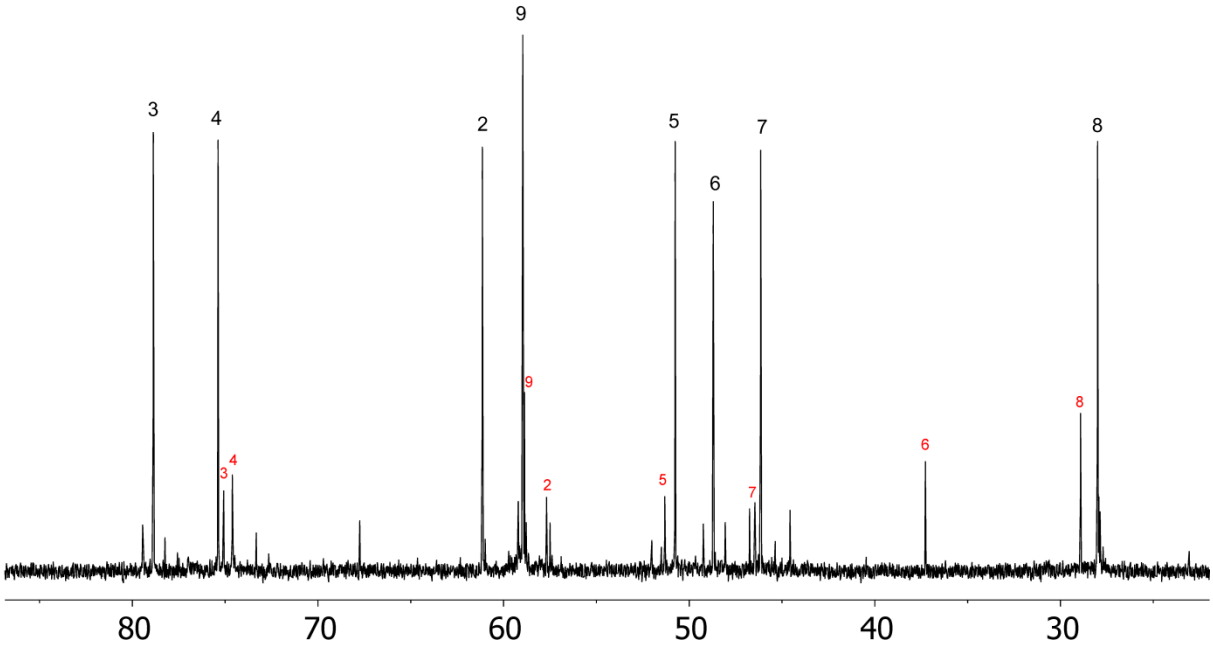

c)

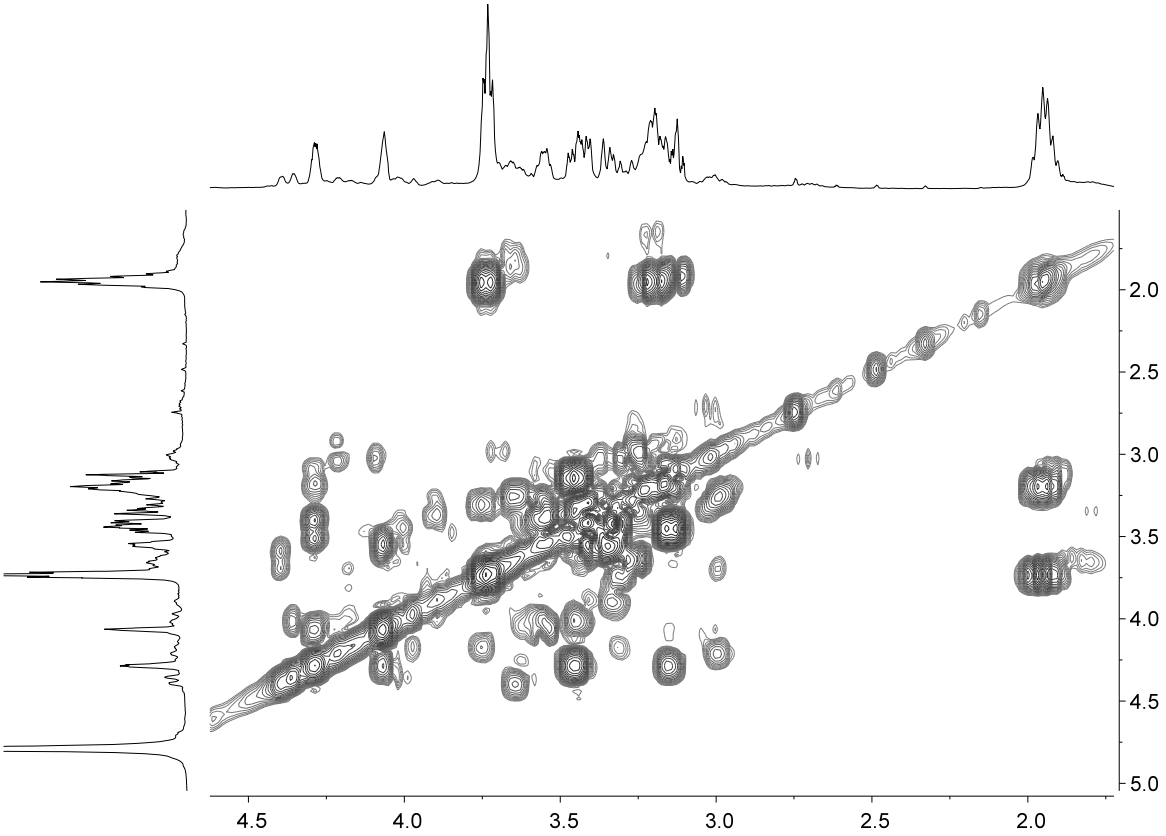

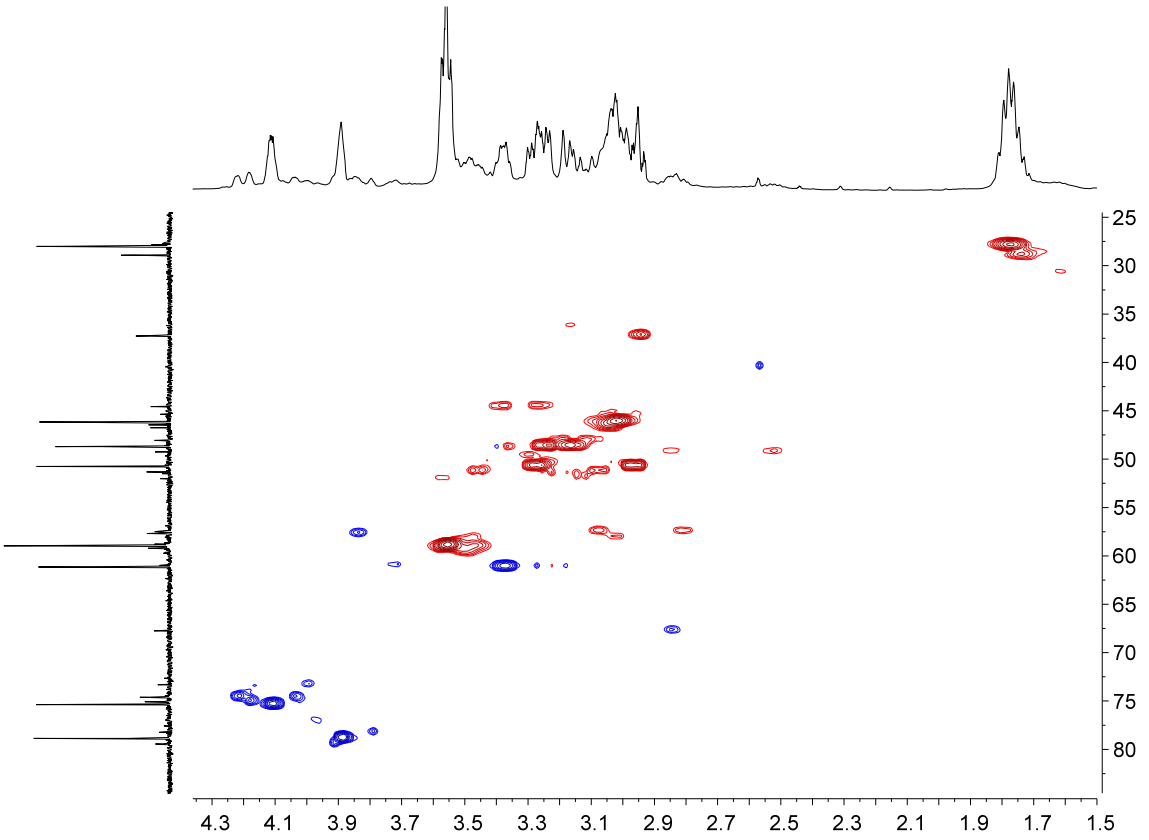

Figure 14. Observed NMR spectra of **25g**: a) ^{1}H, b) ^{13}C, c) 2D ^{1}H-^{1}H COSY and 2D multiplicity-edited HSQC.

a)

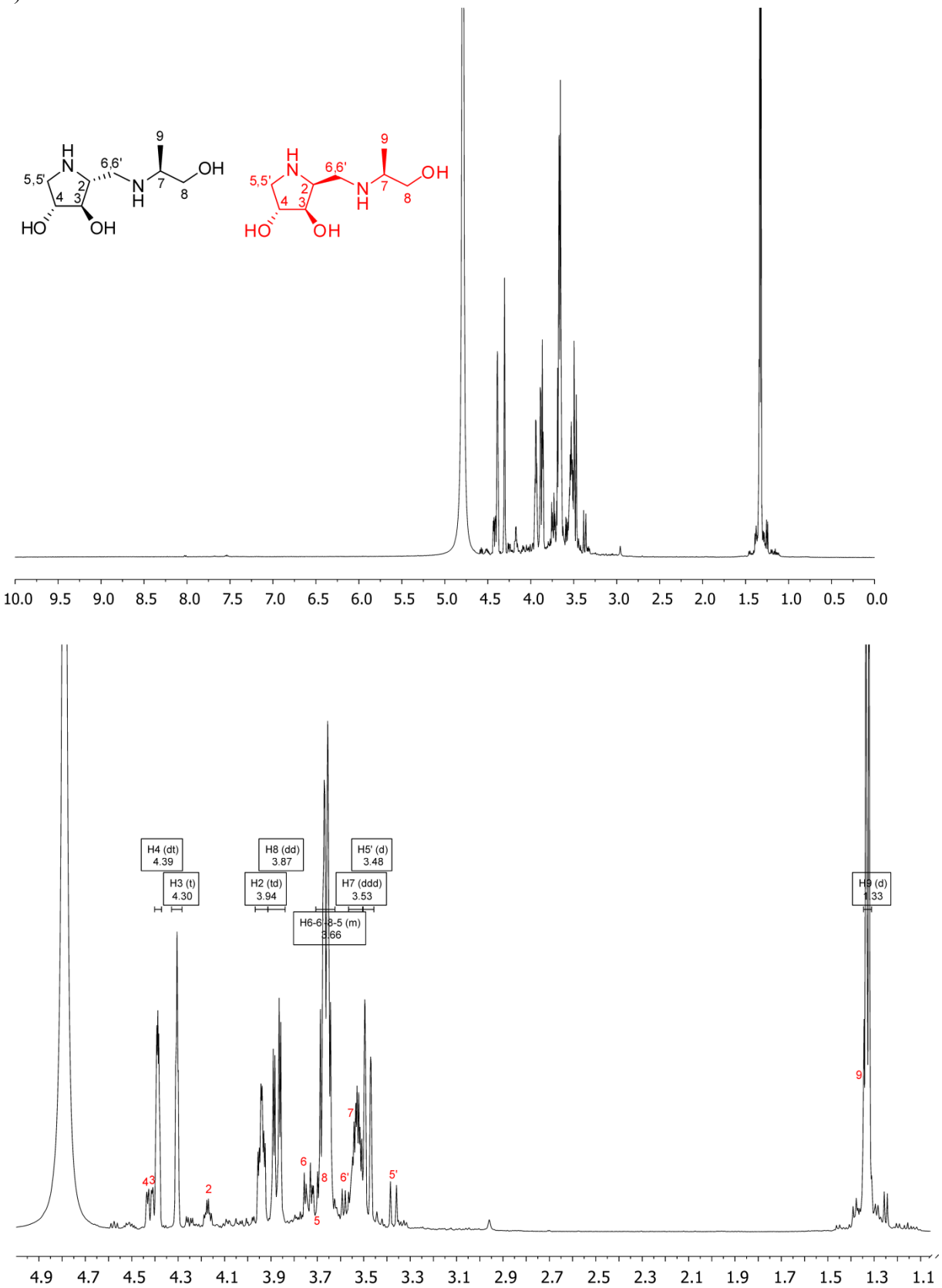

b)

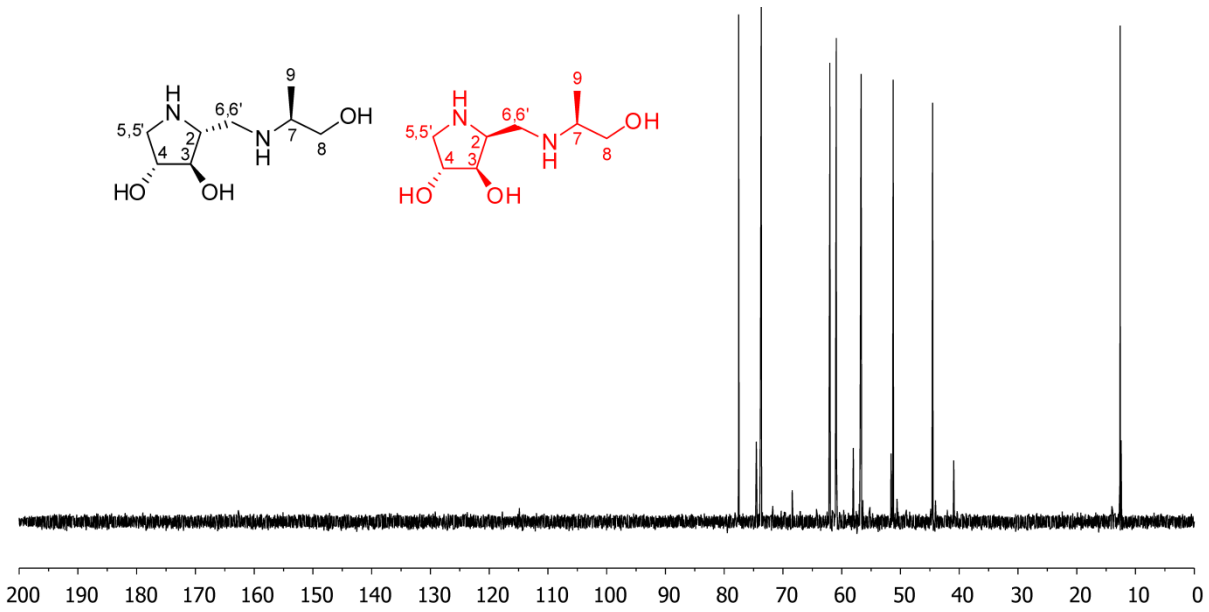

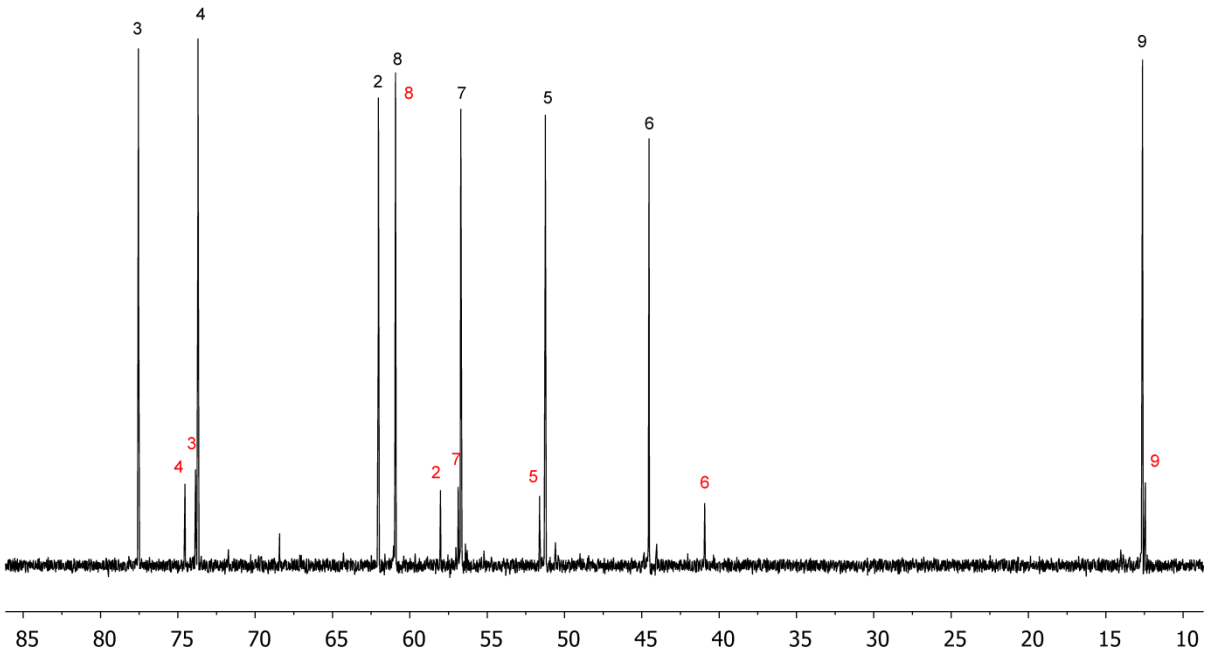

c)

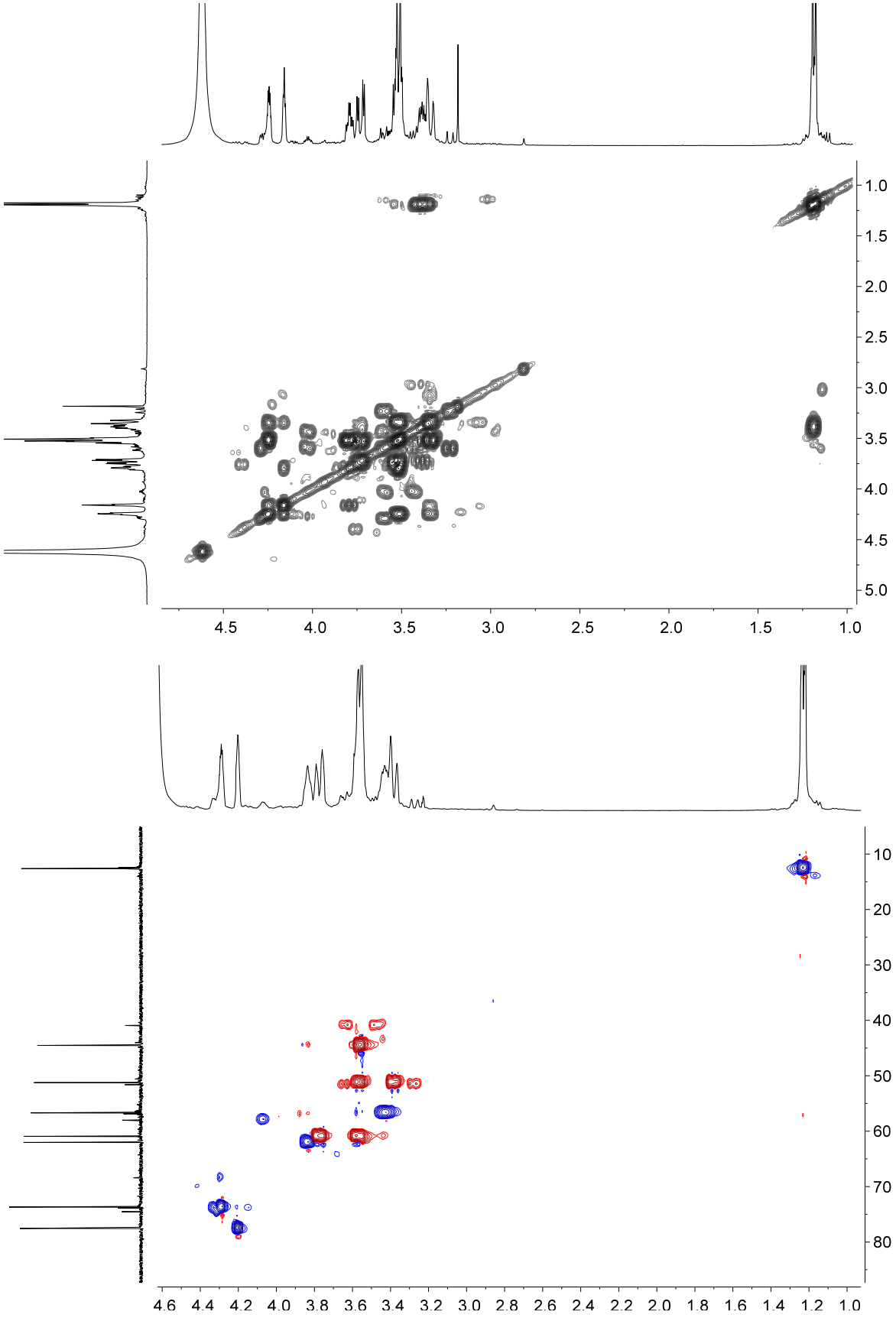
1.0
1.5
2.0
2.5
3.0
3.5
4.0
4.5
5.0
4.5
4.0
3.5
3.0
2.5
2.0
1.5
1.0
10
20
30
40
50
60
70
80
4.6
4.4
4.2
4.0
3.8
3.6
3.4
3.2
3.0
2.8
2.6
2.4
2.2
2.0
1.8
1.6
1.4
1.2
1.0

Figure 14(bis). Observed NMR spectra of purified **25g**: a) ^{1}H, b) ^{13}C, c) 2D ^{1}H-^{1}H COSY and 2D multiplicity-edited HSQC.

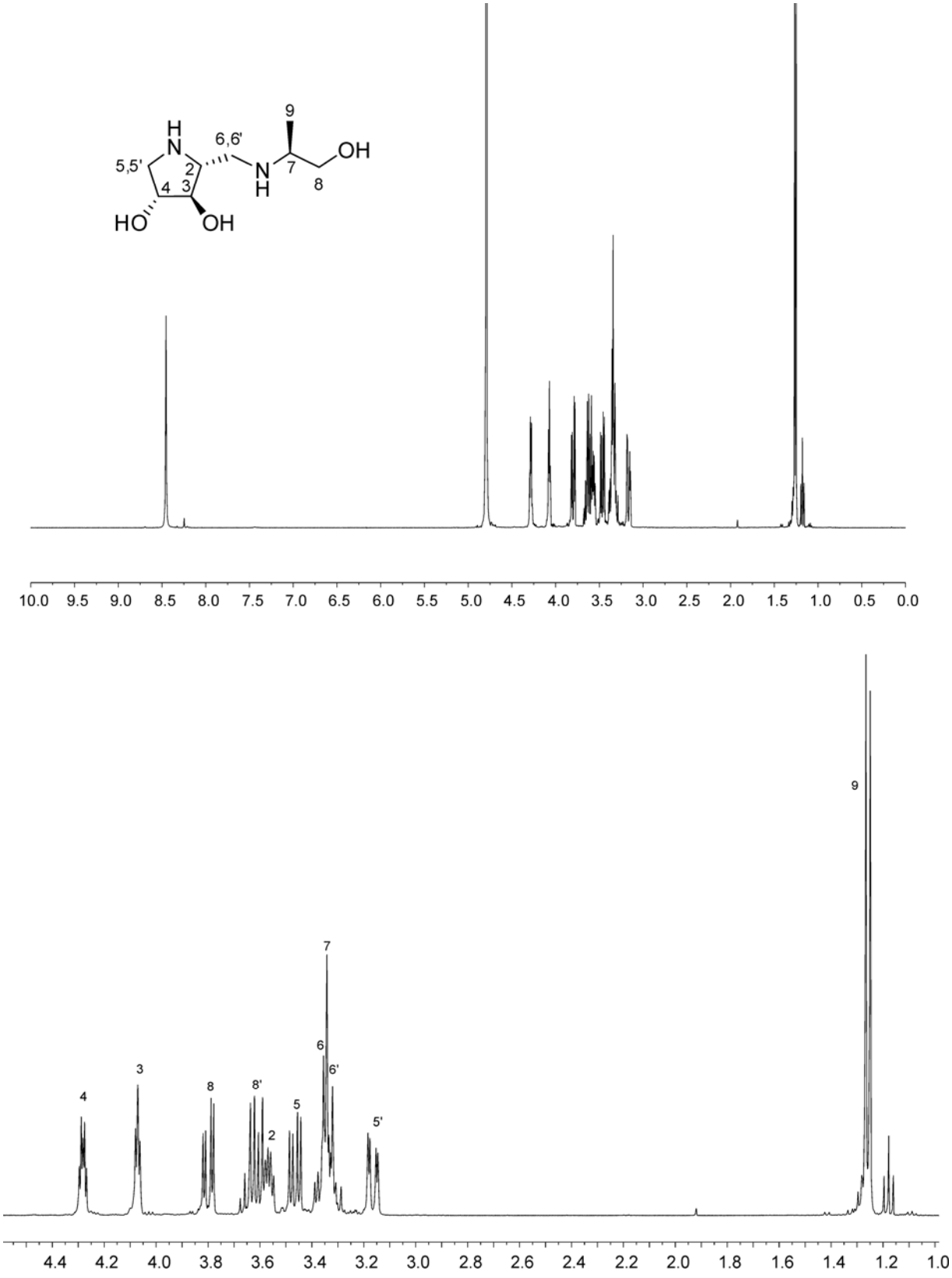

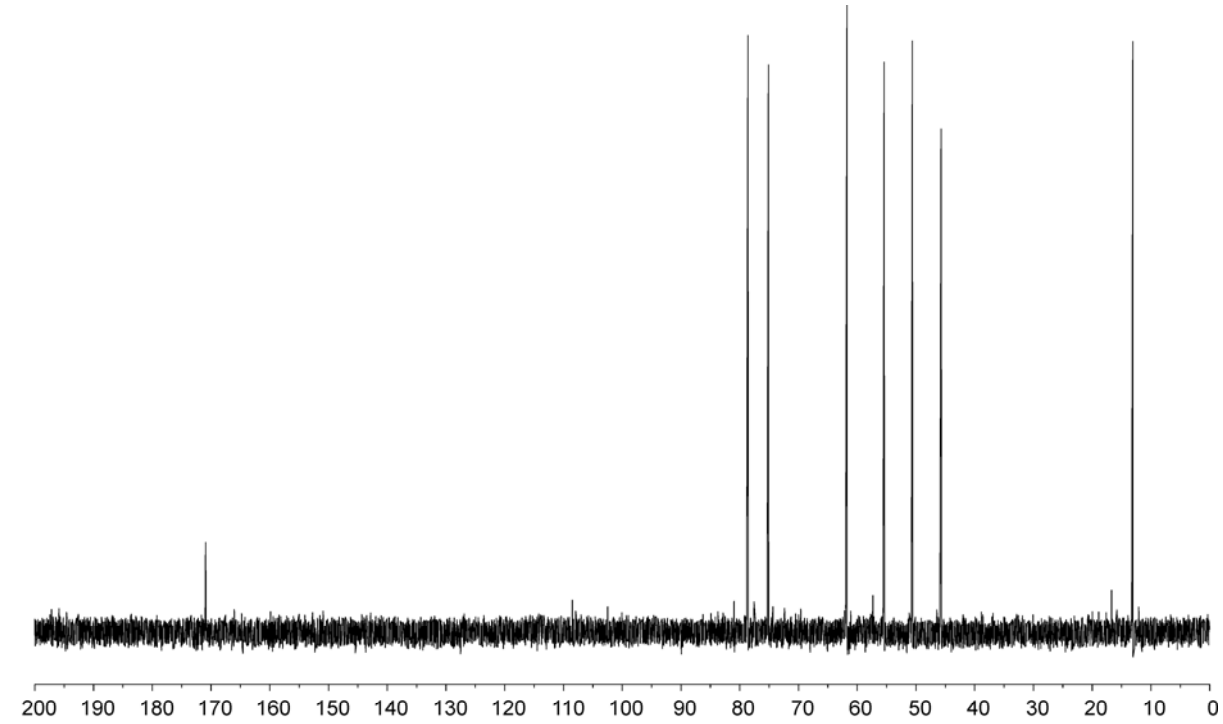

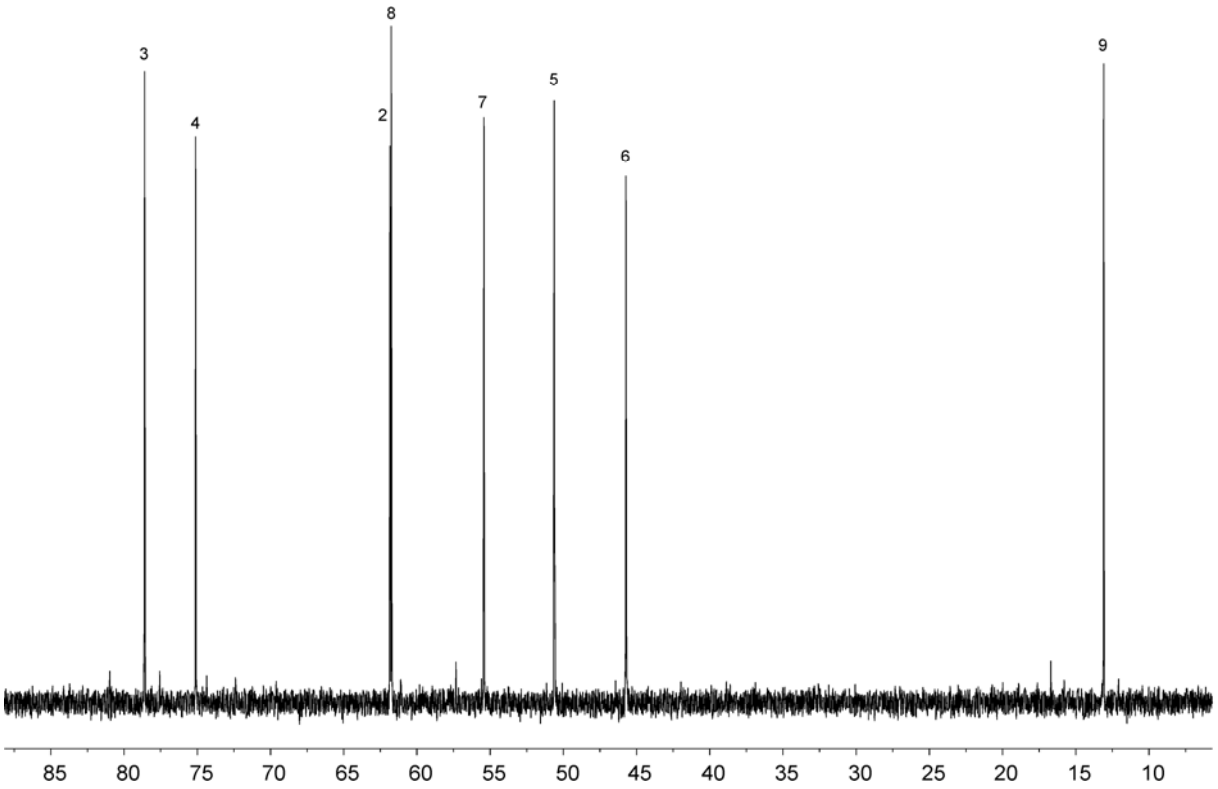

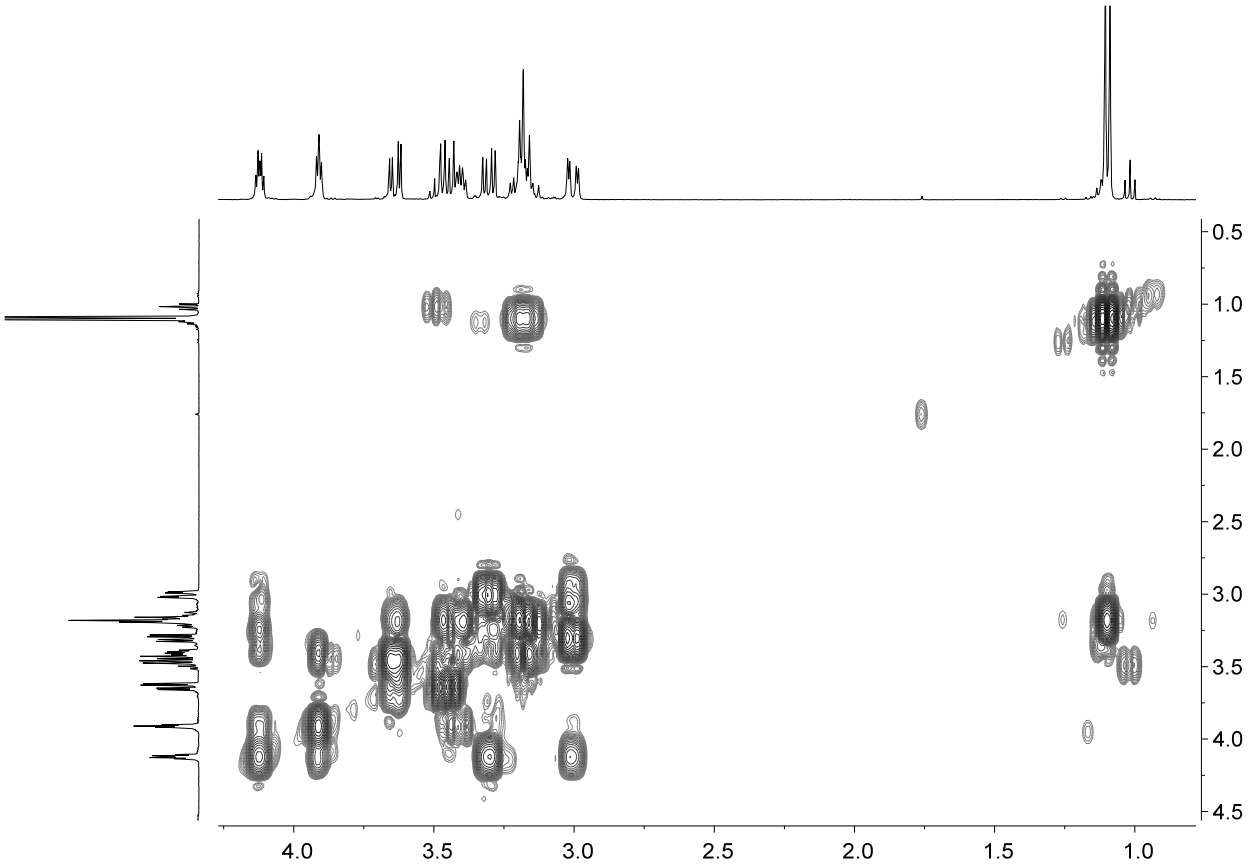

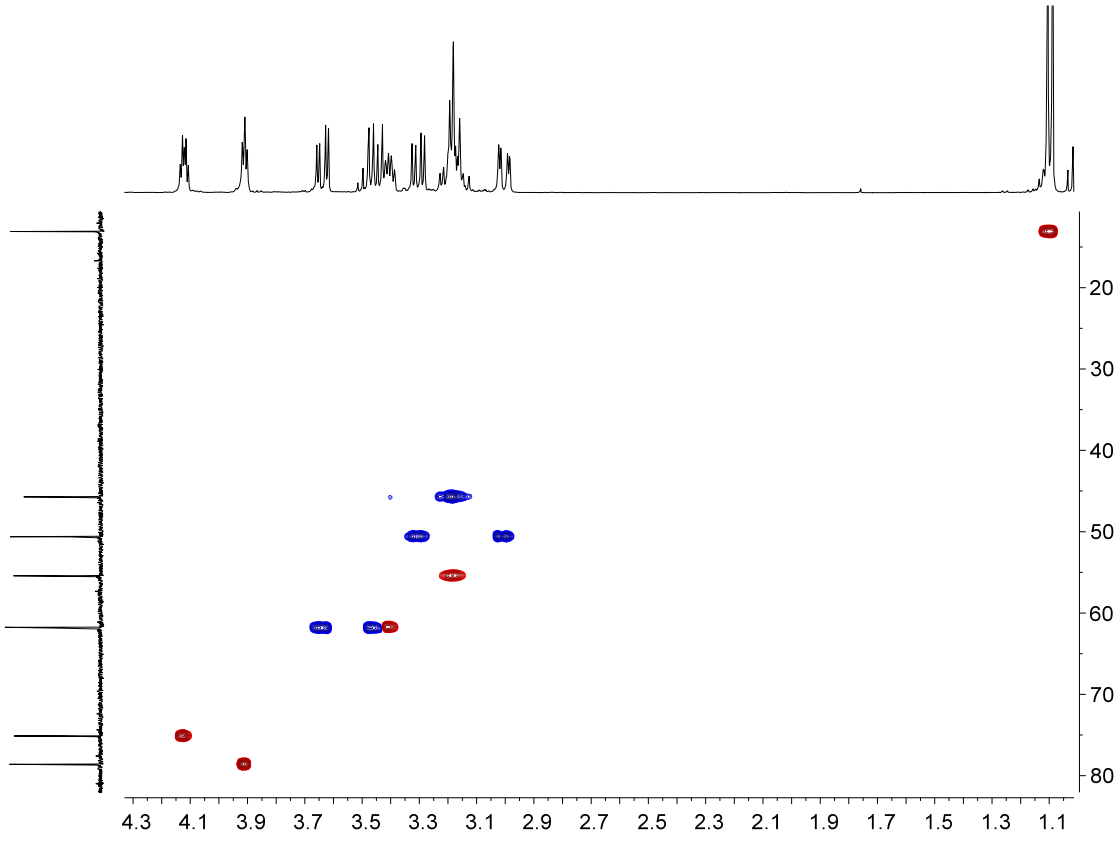

Figure 15. Observed NMR spectra of **25h**: a) ^{1}H, b) ^{13}C, c) 2D ^{1}H-^{1}H COSY and 2D multiplicity-edited HSQC.

a)

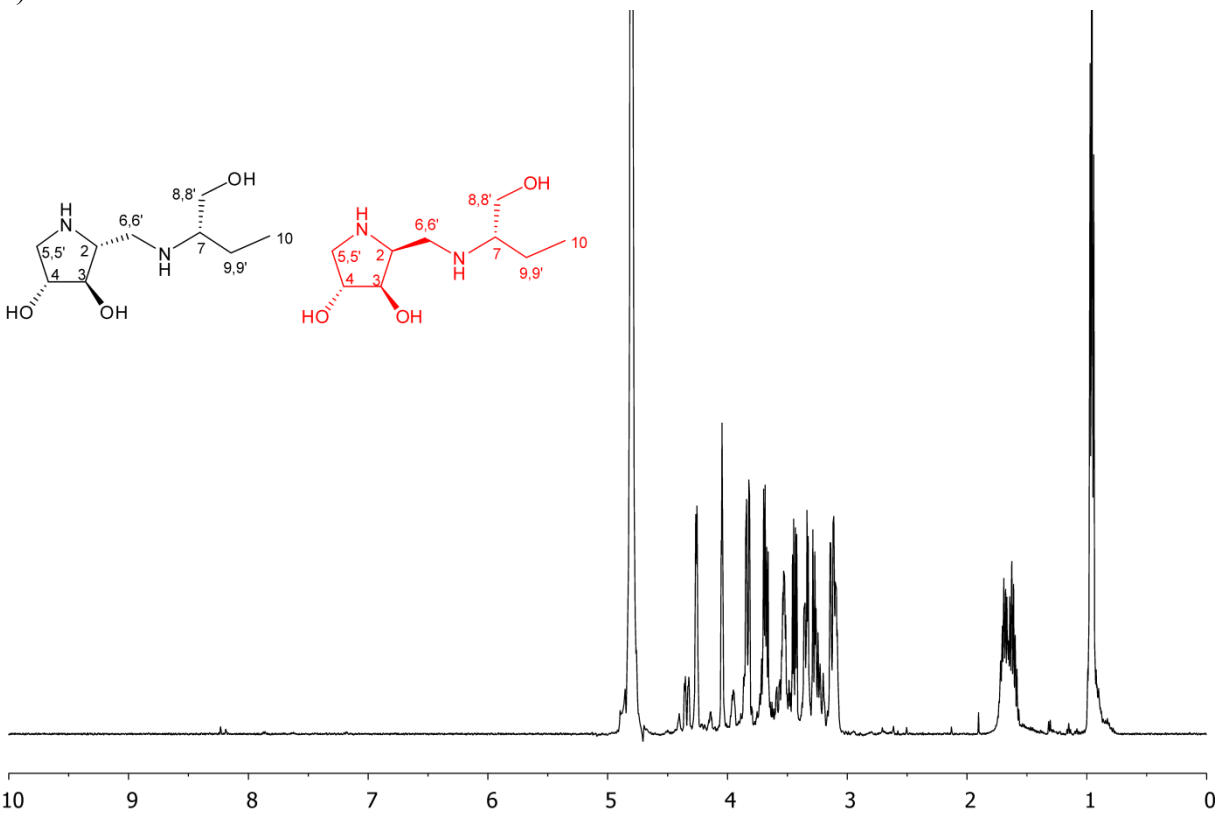

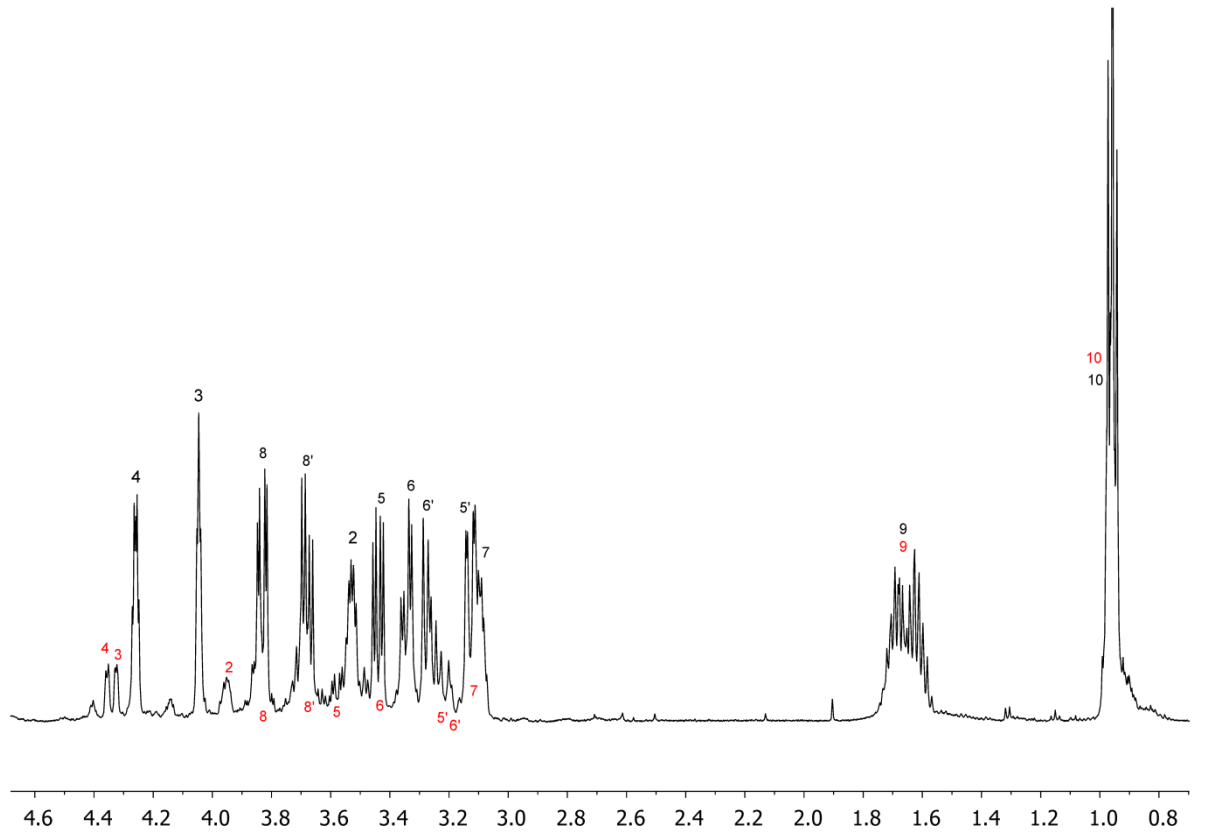

b)

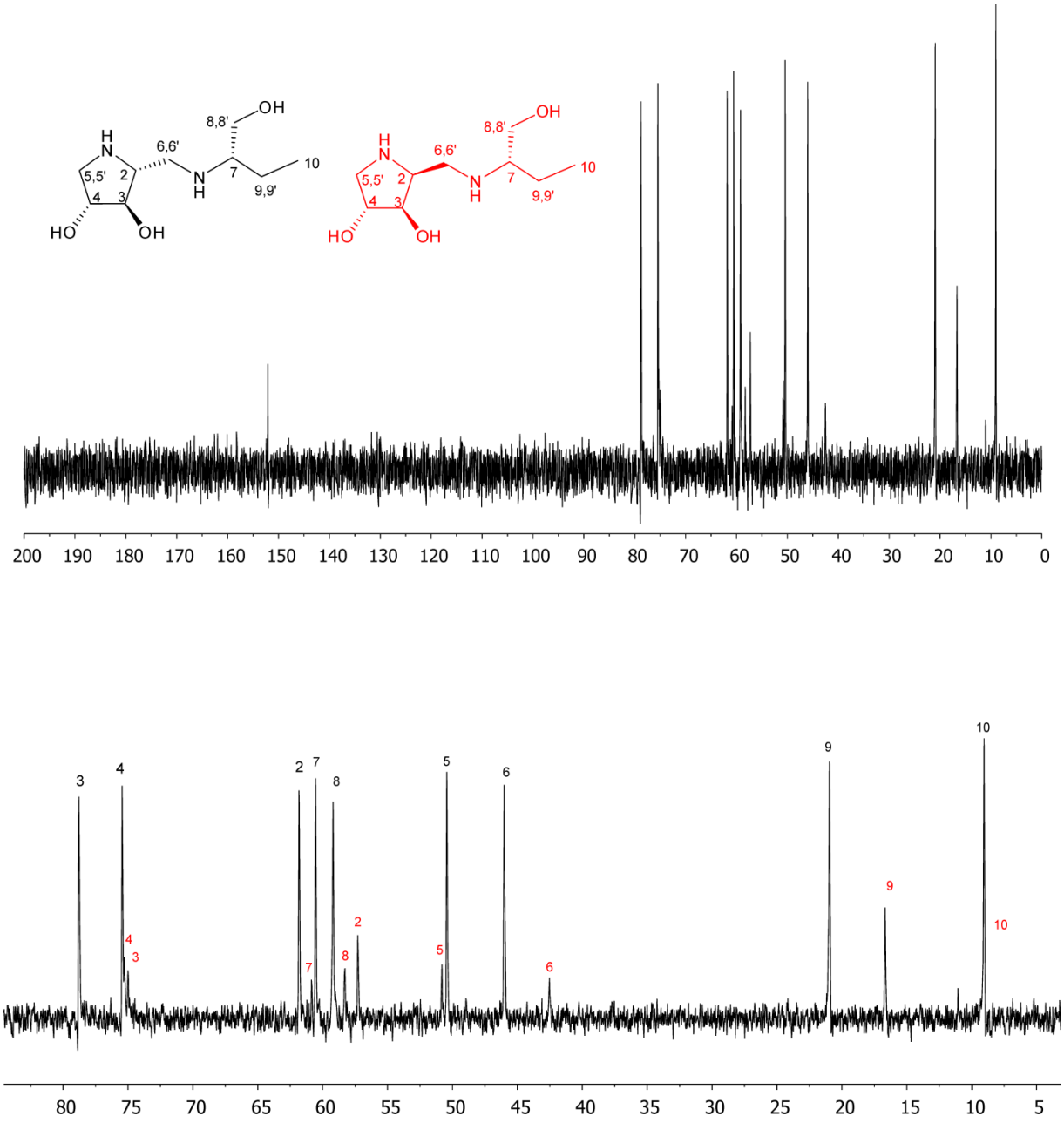

c)

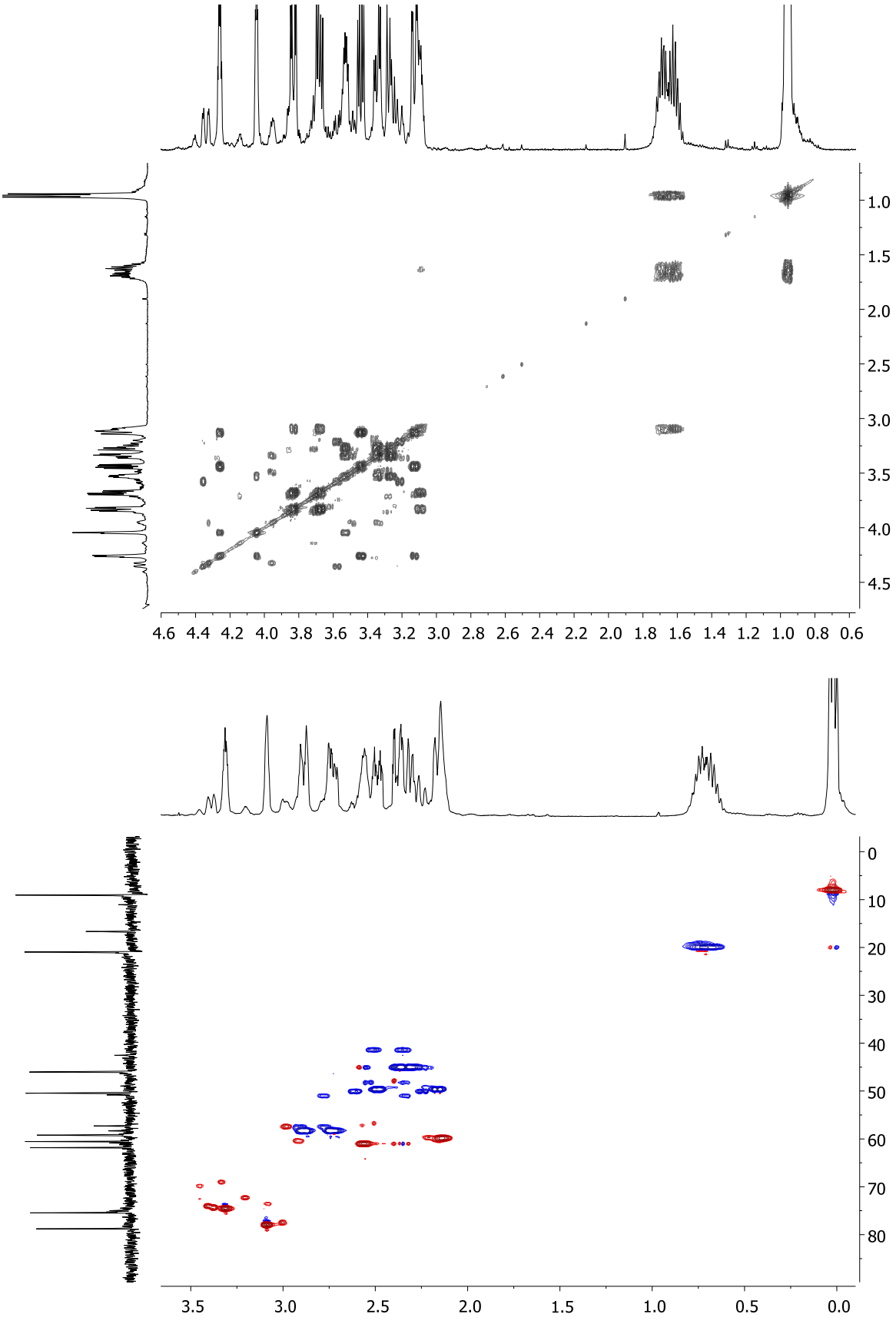
1.0
1.5
2.0
2.5
3.0
3.5
4.0
4.5
4.6 4.4 4.2 4.0 3.8 3.6 3.4 3.2 3.0 2.8 2.6 2.4 2.2 2.0 1.8 1.6 1.4 1.2 1.0 0.8 0.6
0
10
20
30
40
50
60
70
80
3.5 3.0 2.5 2.0 1.5 1.0 0.5 0.0

Figure 16. Observed NMR spectra of **25i**: a) ^{1}H, b) ^{13}C, c) 2D ^{1}H-^{1}H COSY and 2D multiplicity-edited HSQC.

a)

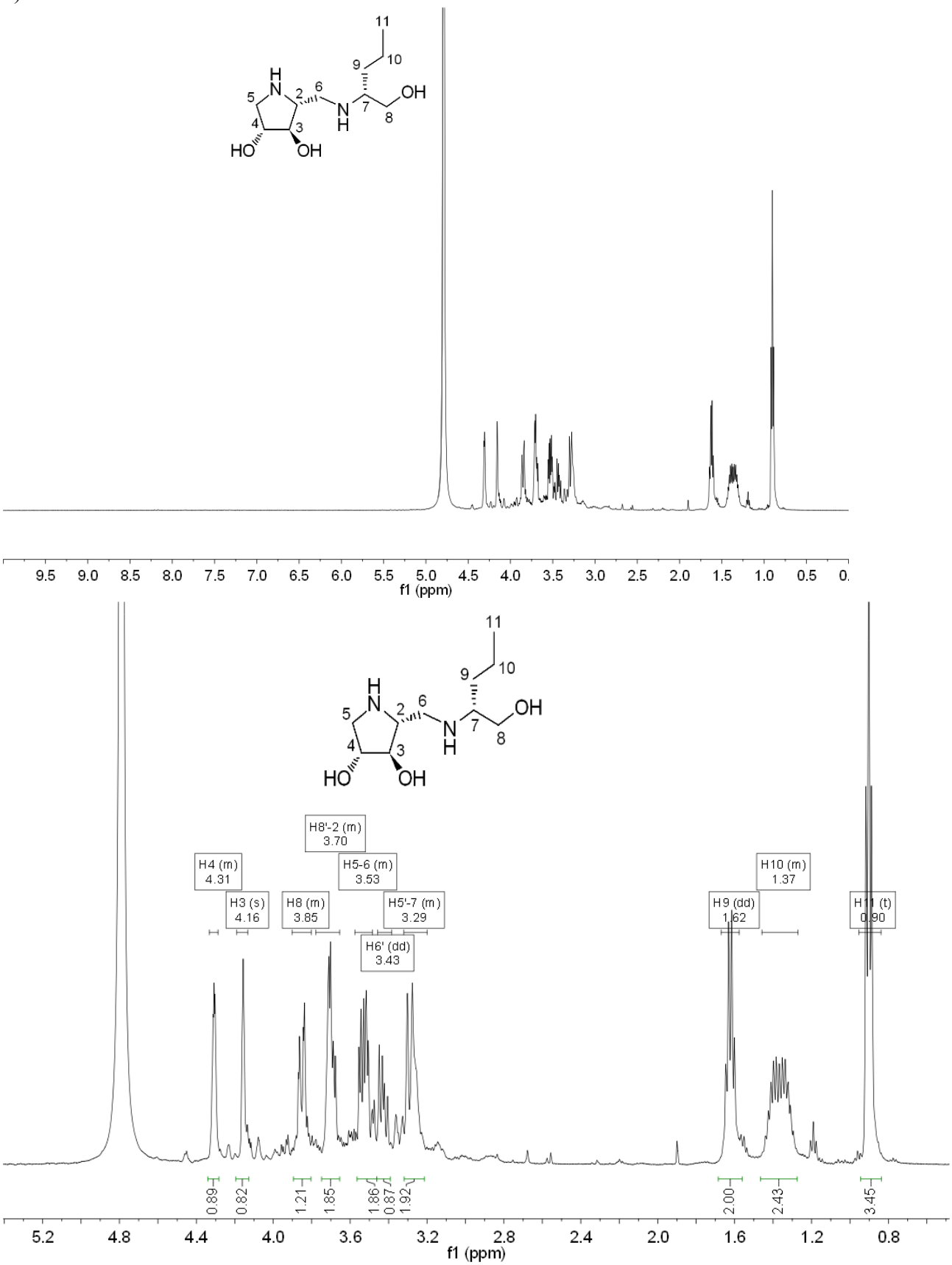

b)

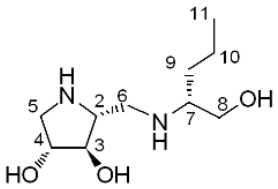

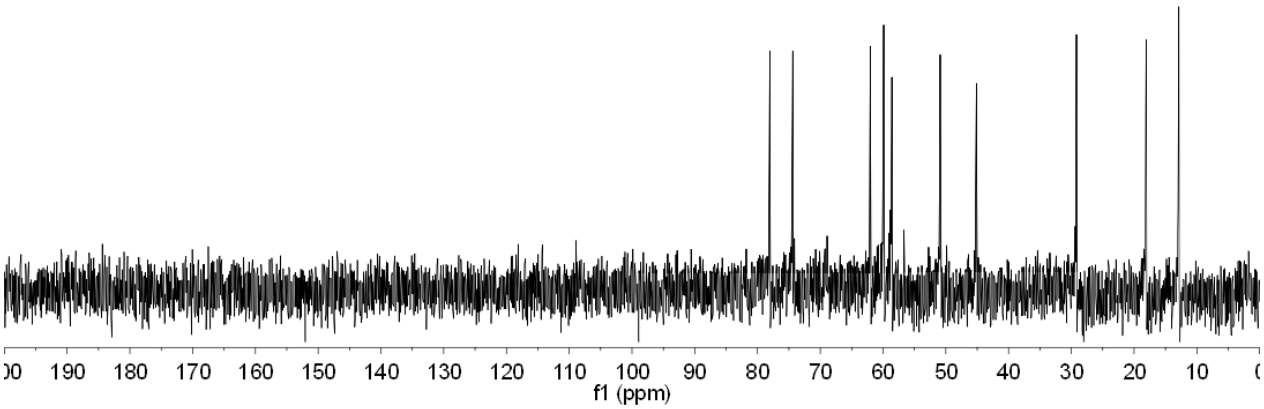

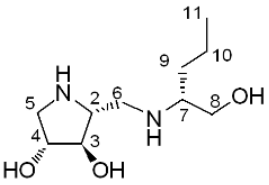

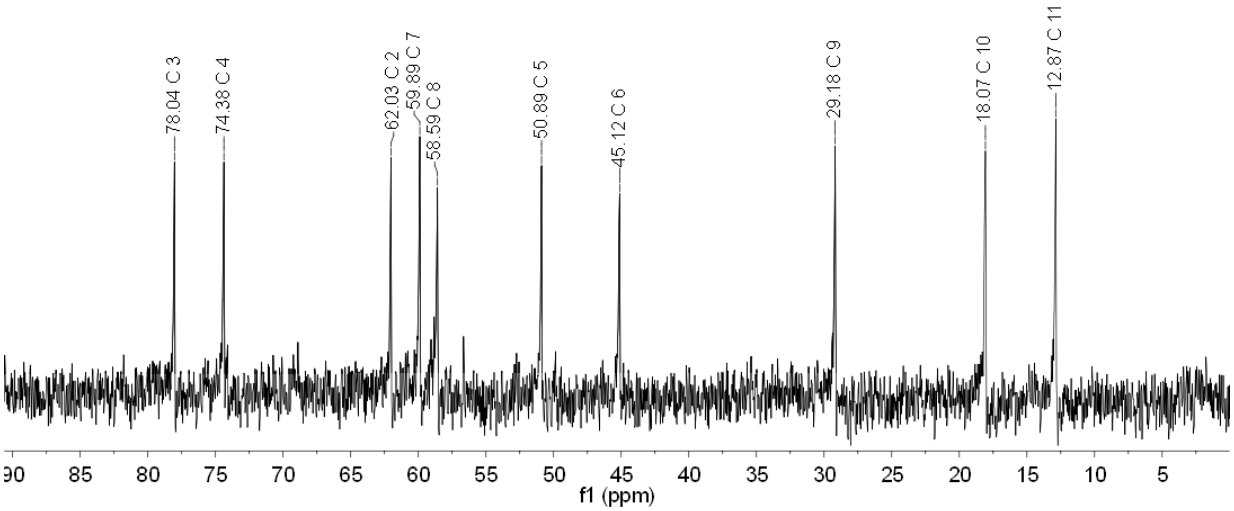

c)

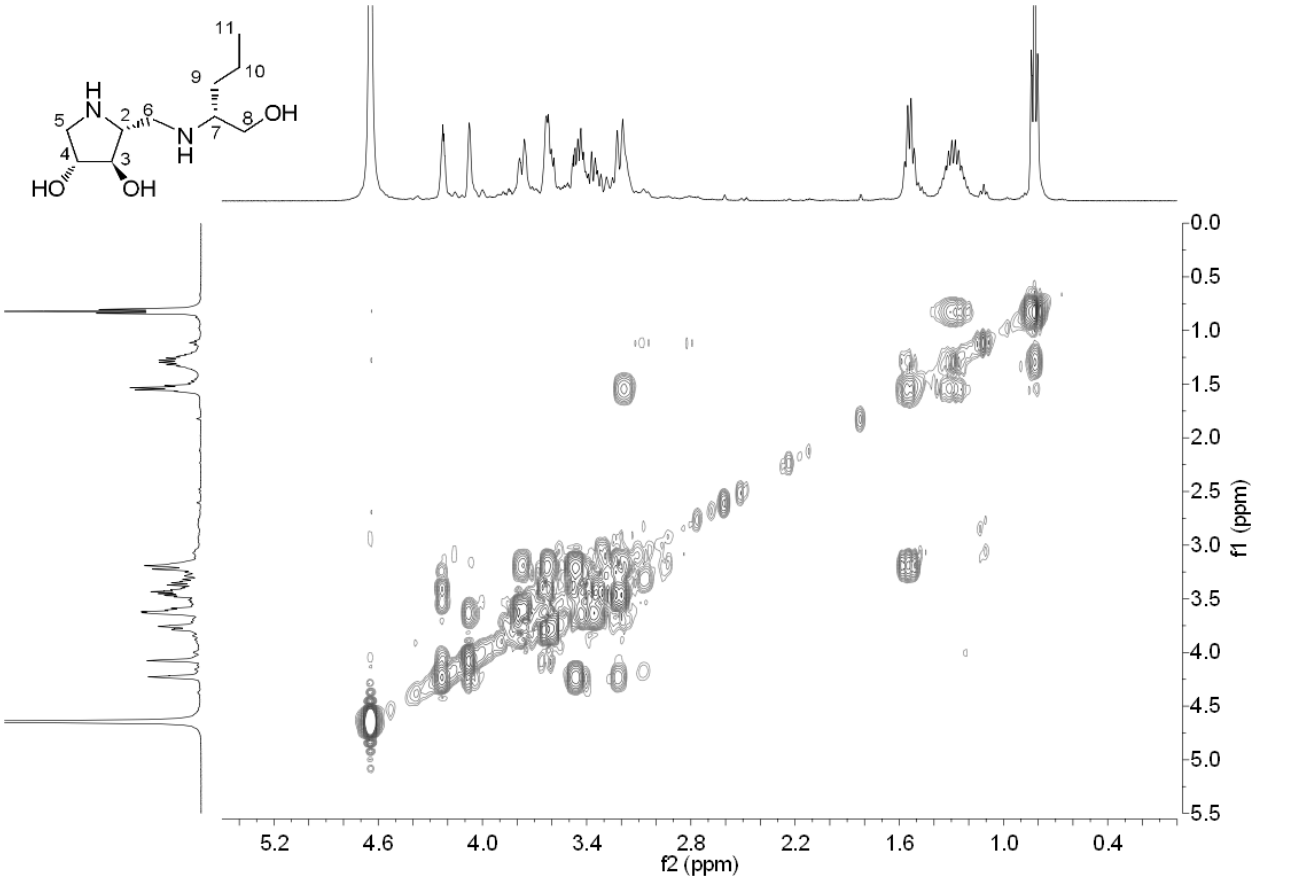

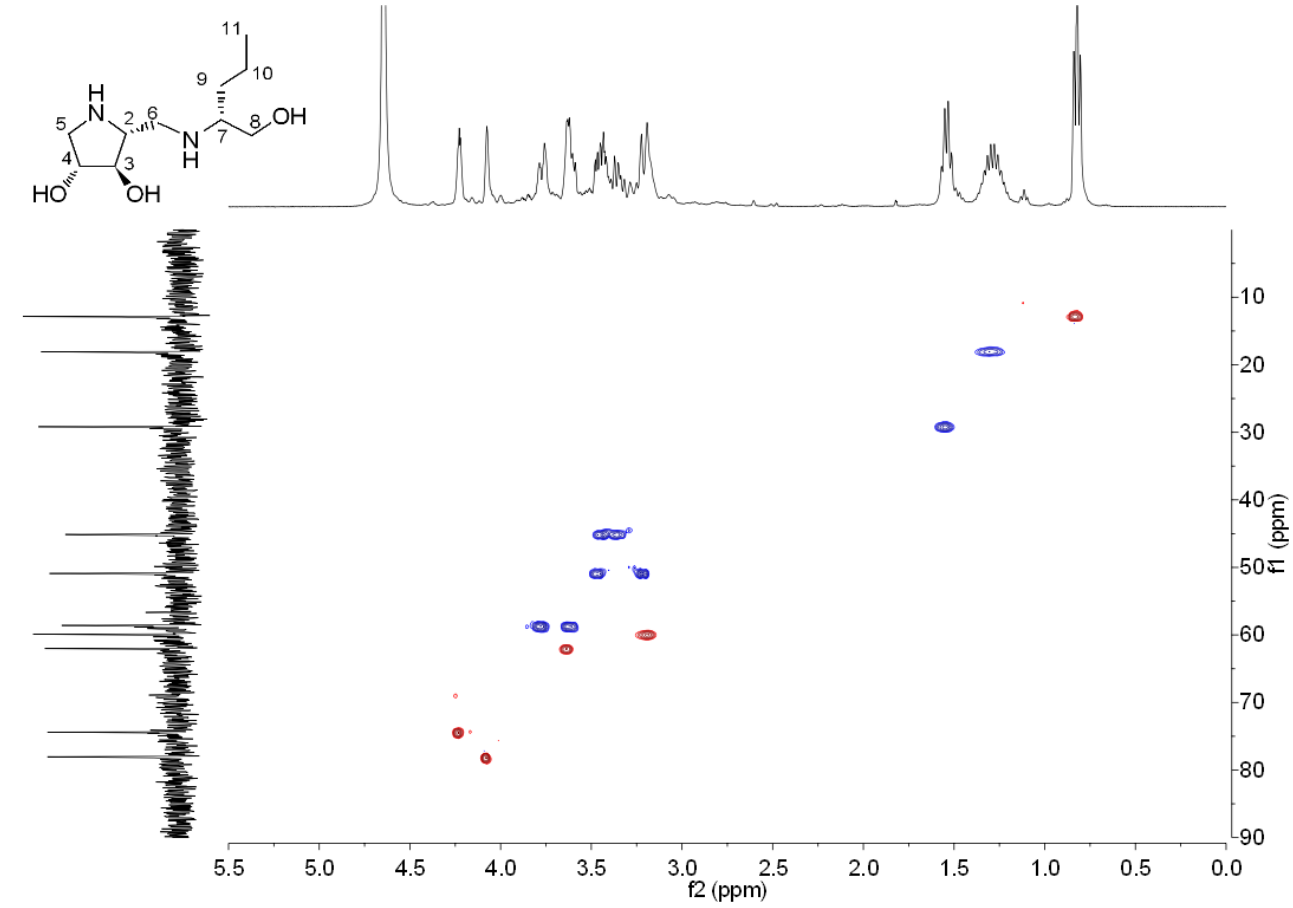

Figure 17. Observed NMR spectra of **25j**: a) ^{1}H, b) ^{13}C, c) 2D ^{1}H-^{1}H COSY and 2D multiplicity-edited HSQC.

a)

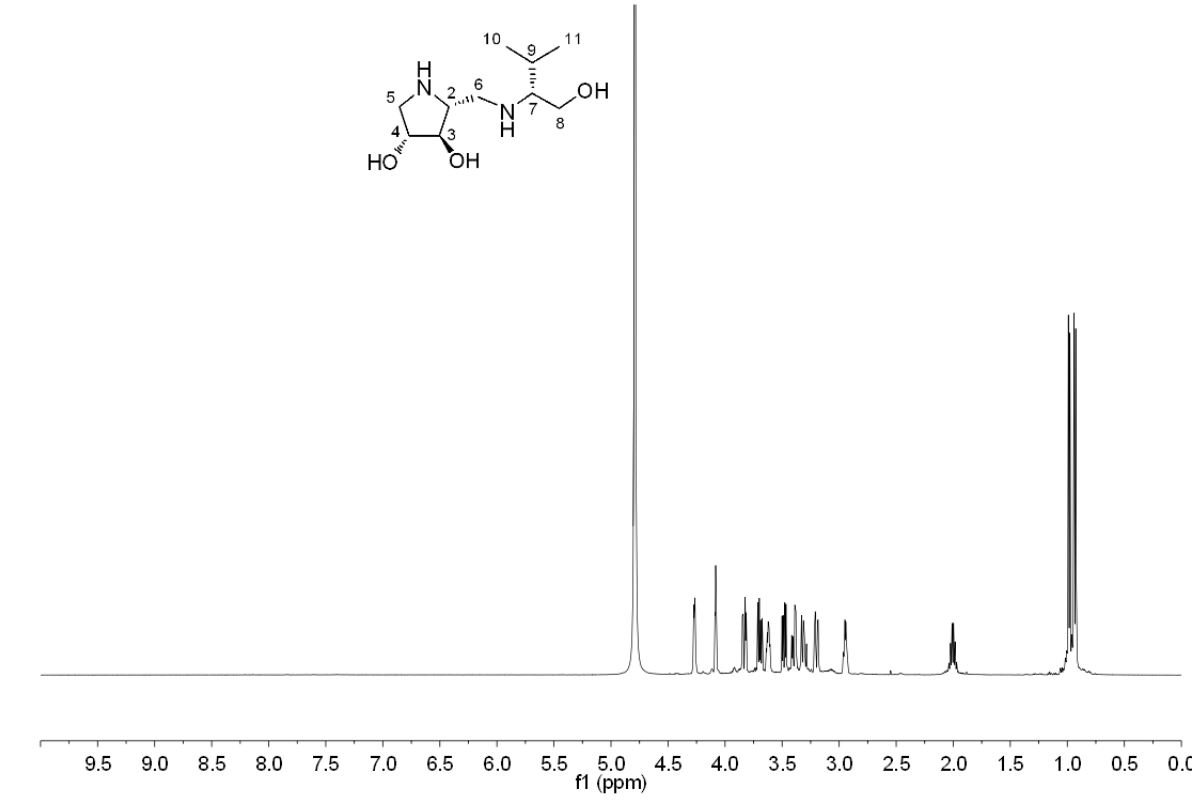

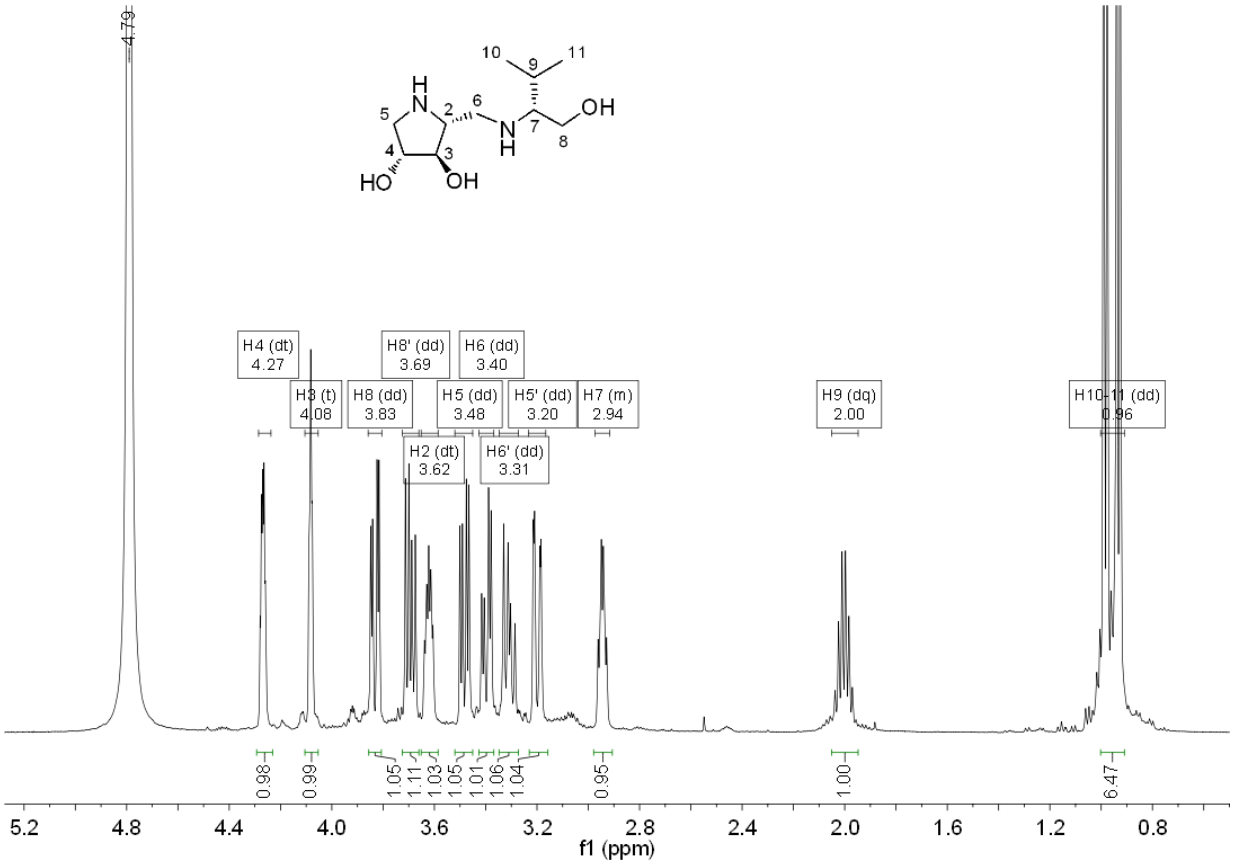

b)

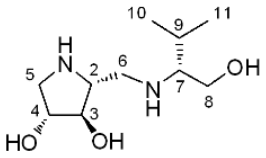

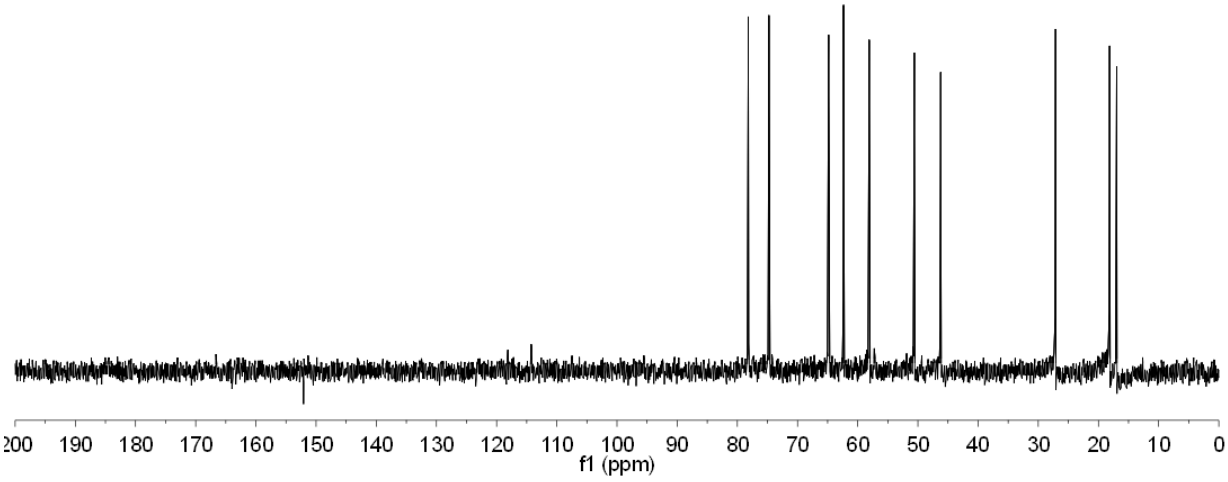

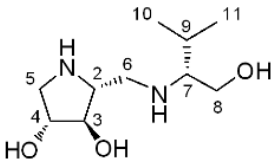

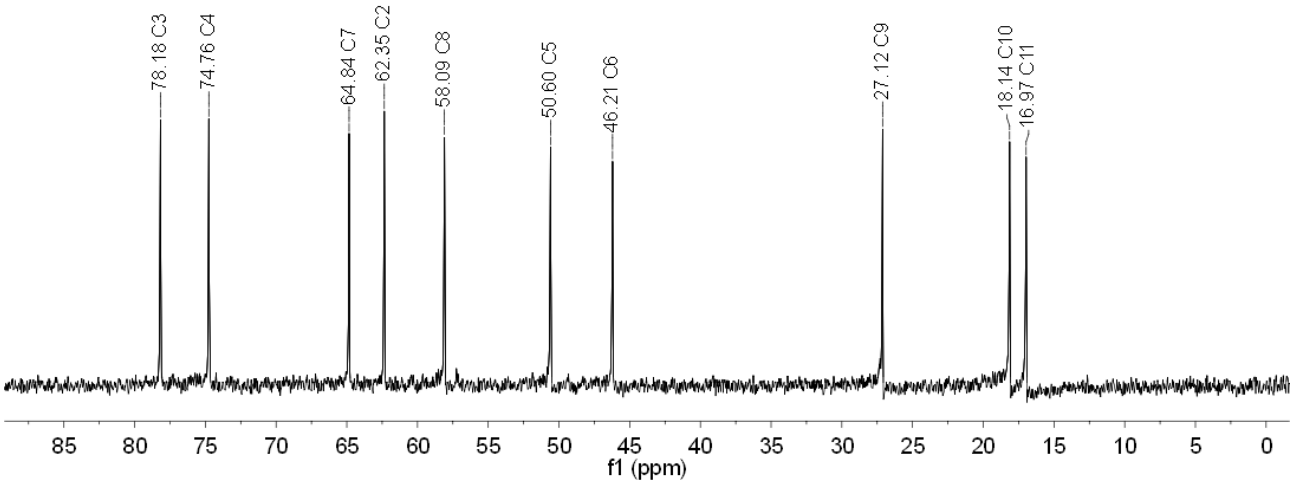

c)

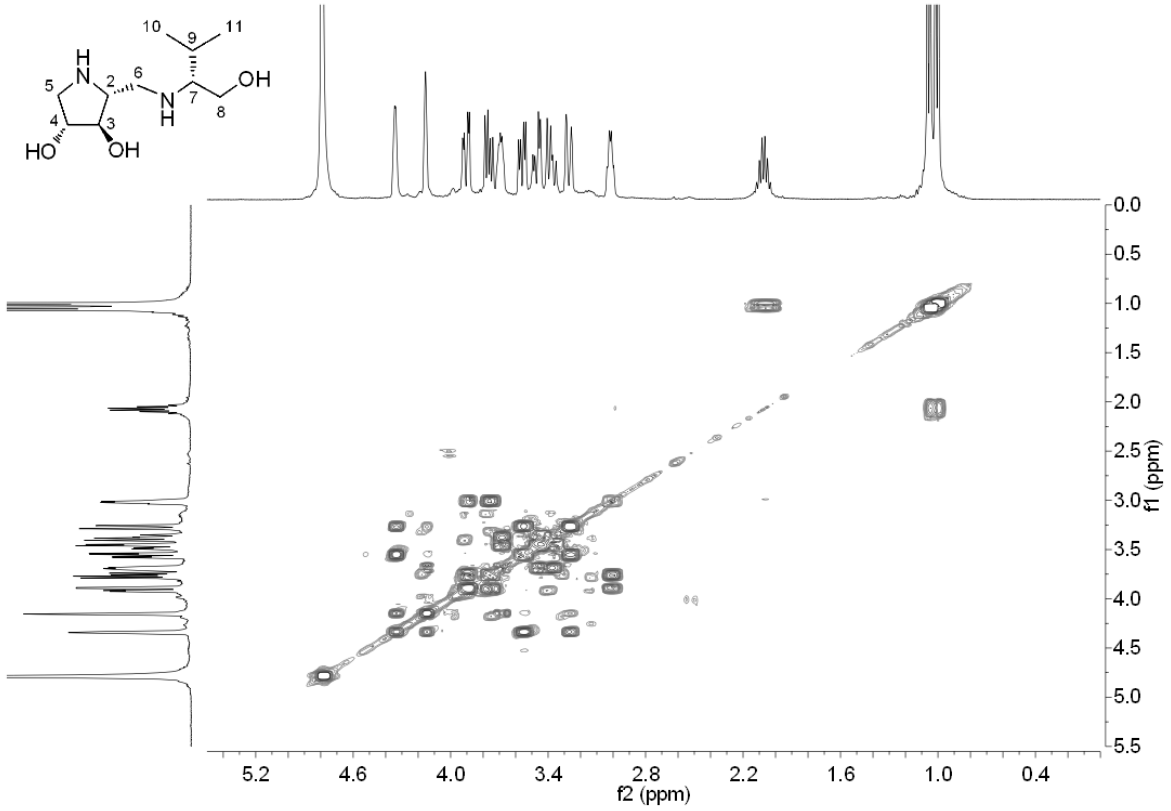

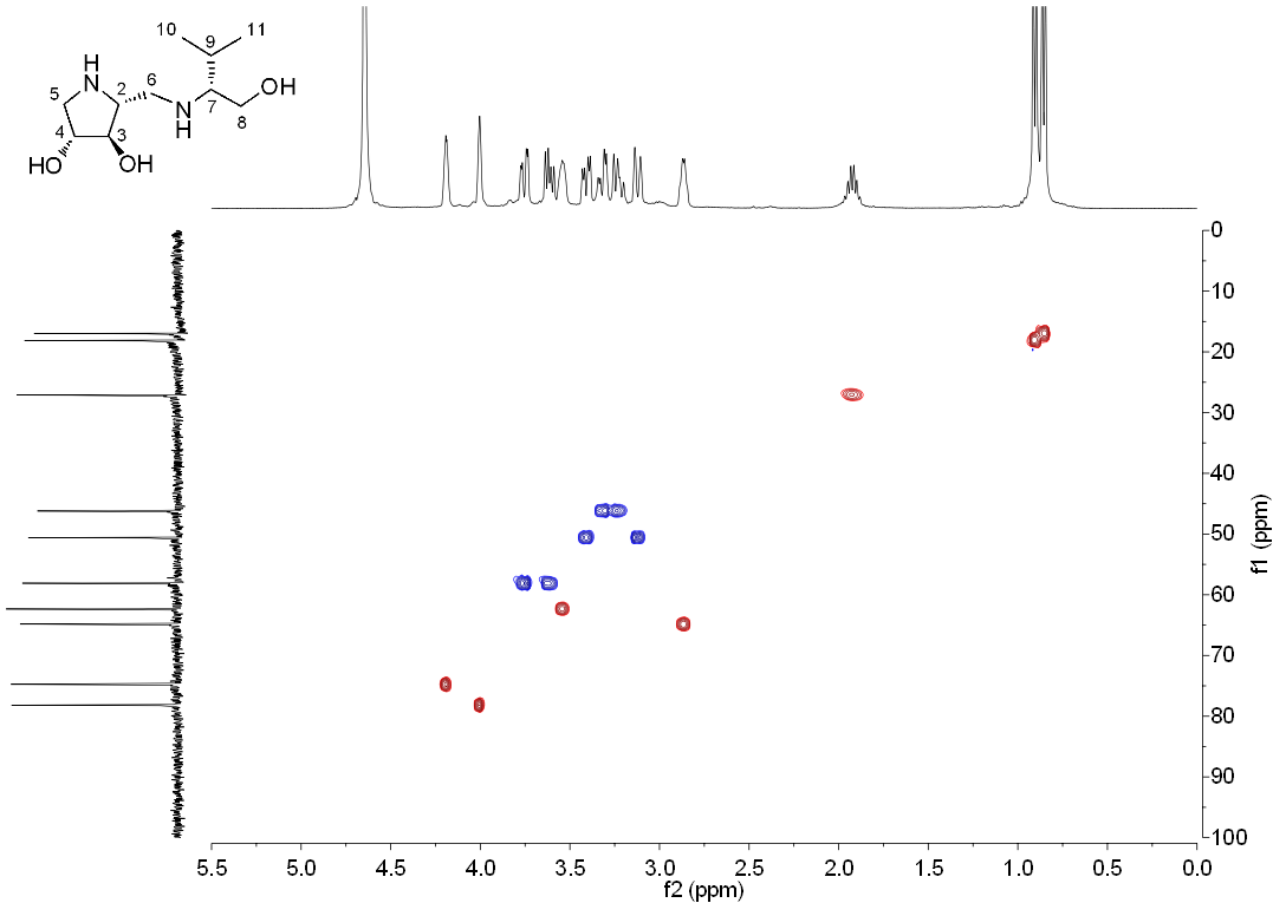

Figure 16. Observed NMR spectra of **25k**: a) ^{1}H, b) ^{13}C, c) 2D ^{1}H-^{1}H COSY and 2D multiplicity-edited HSQC.

a)

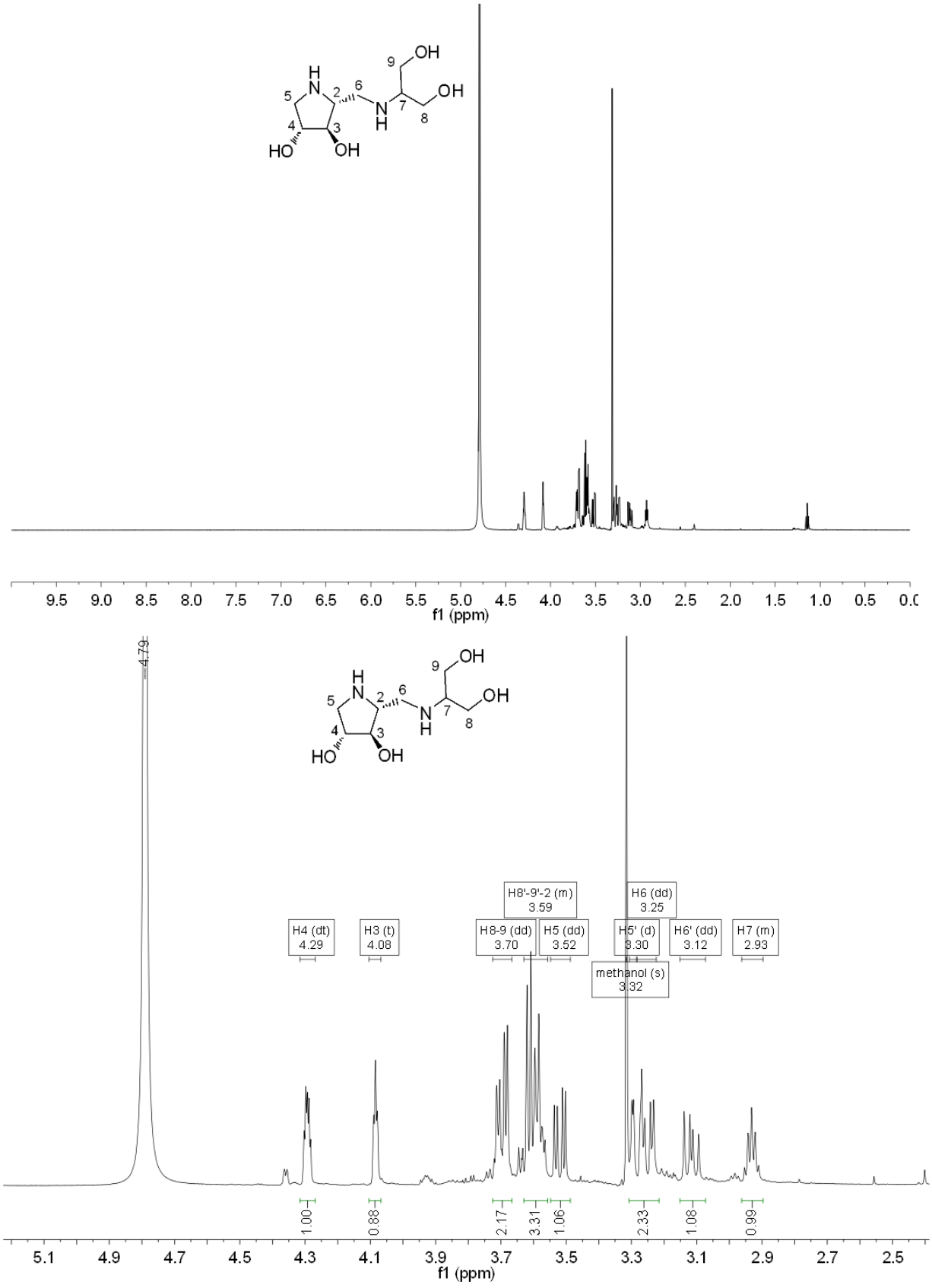

b)

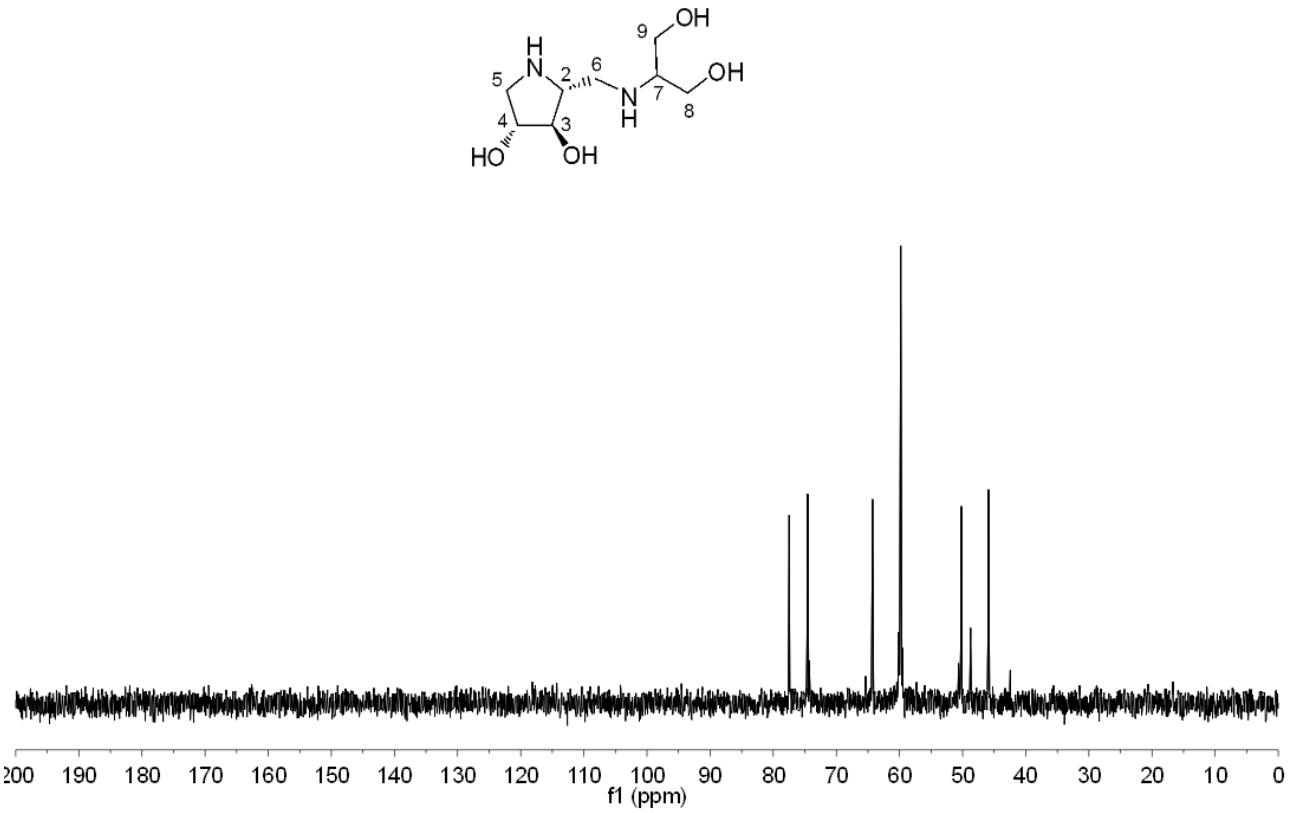

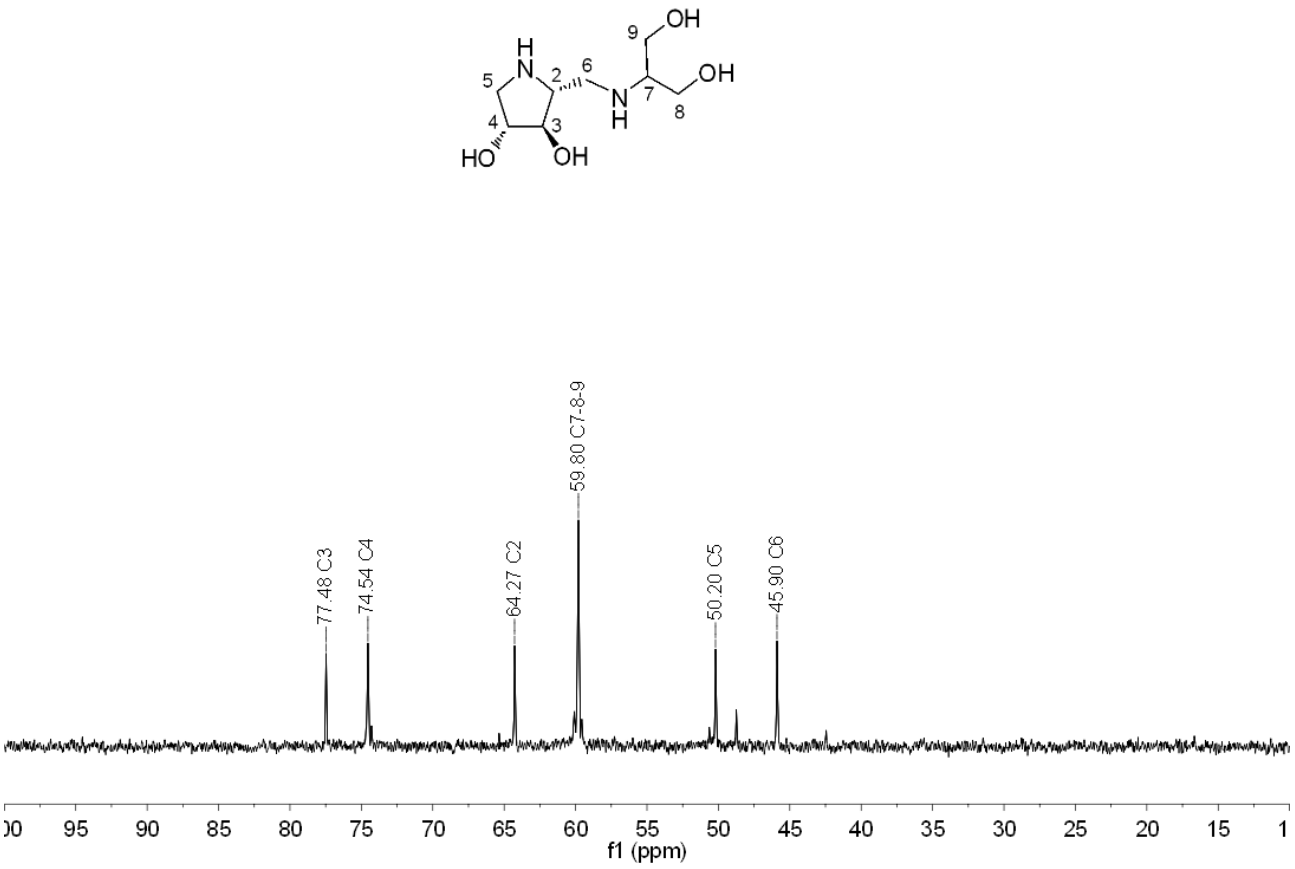

c)

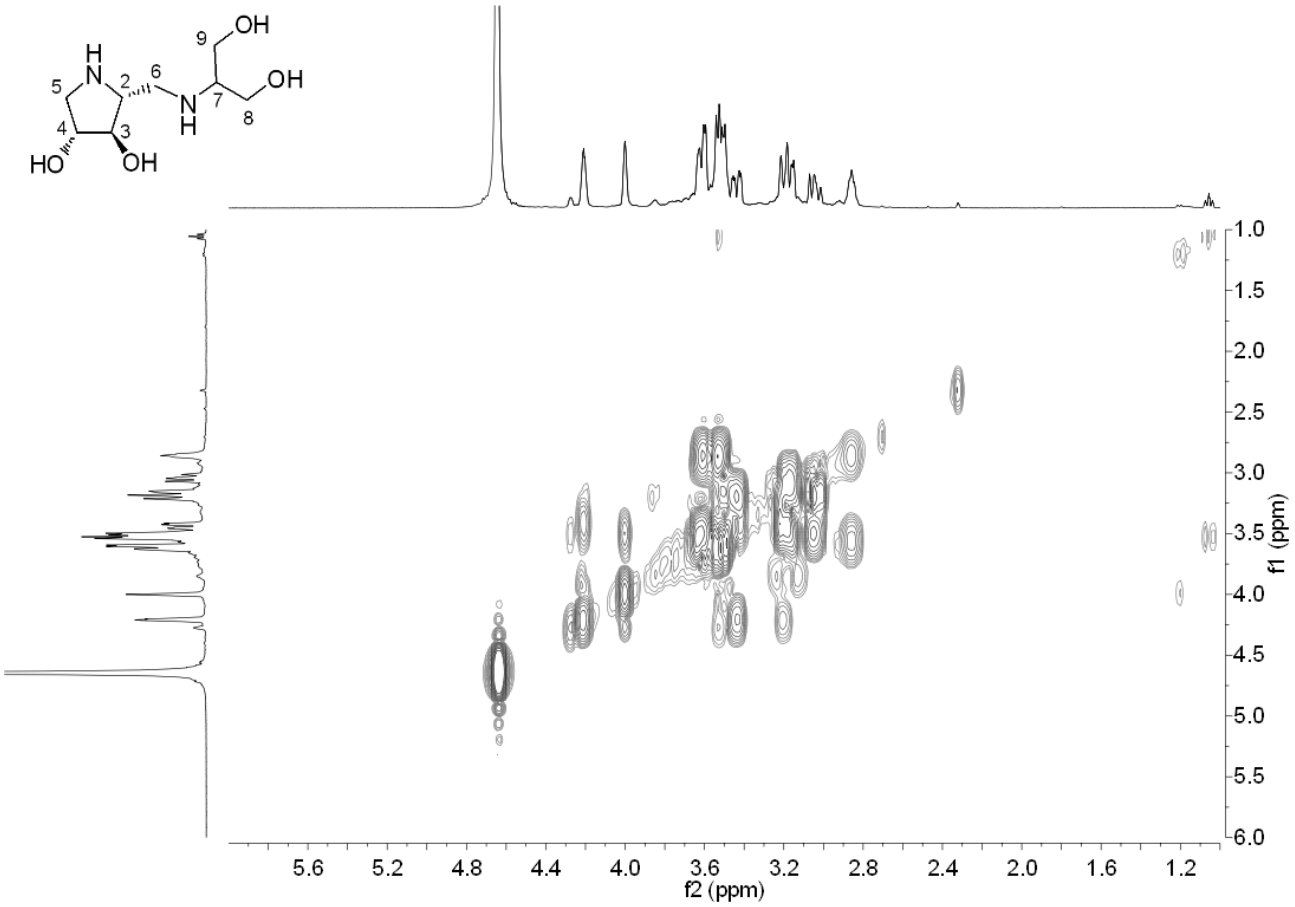

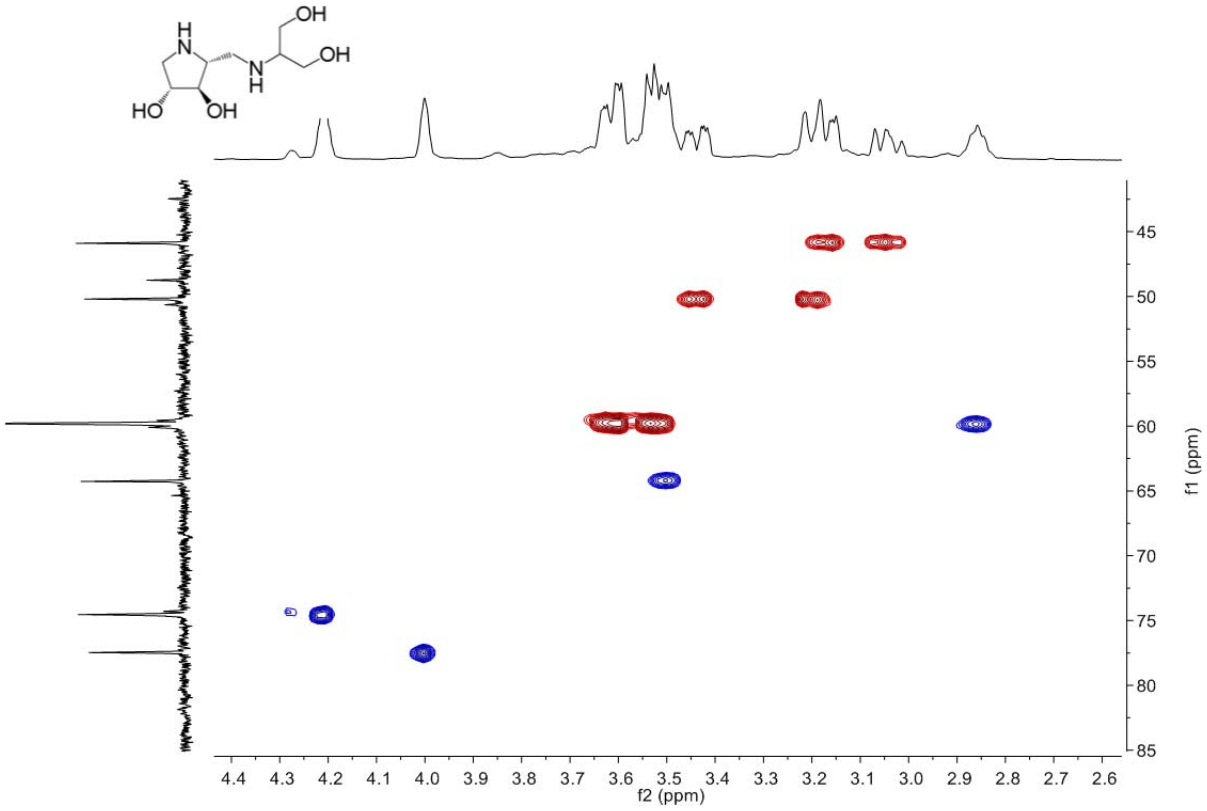

Figure 17. Observed NMR spectra of **25l**: a) ^{1}H, b) ^{13}C, c) 2D ^{1}H-^{1}H COSY and 2D multiplicity-edited HSQC.

a)

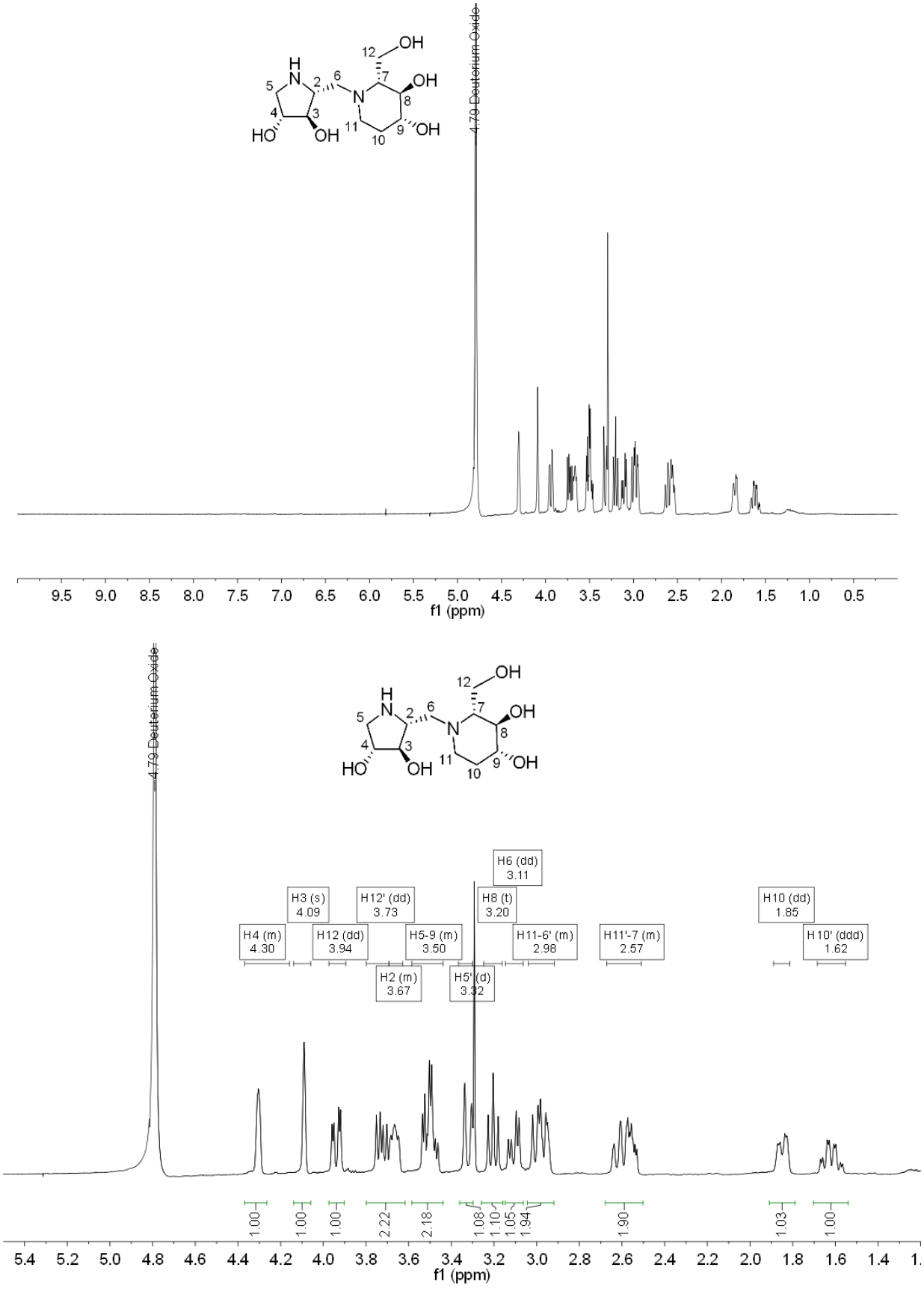

b)

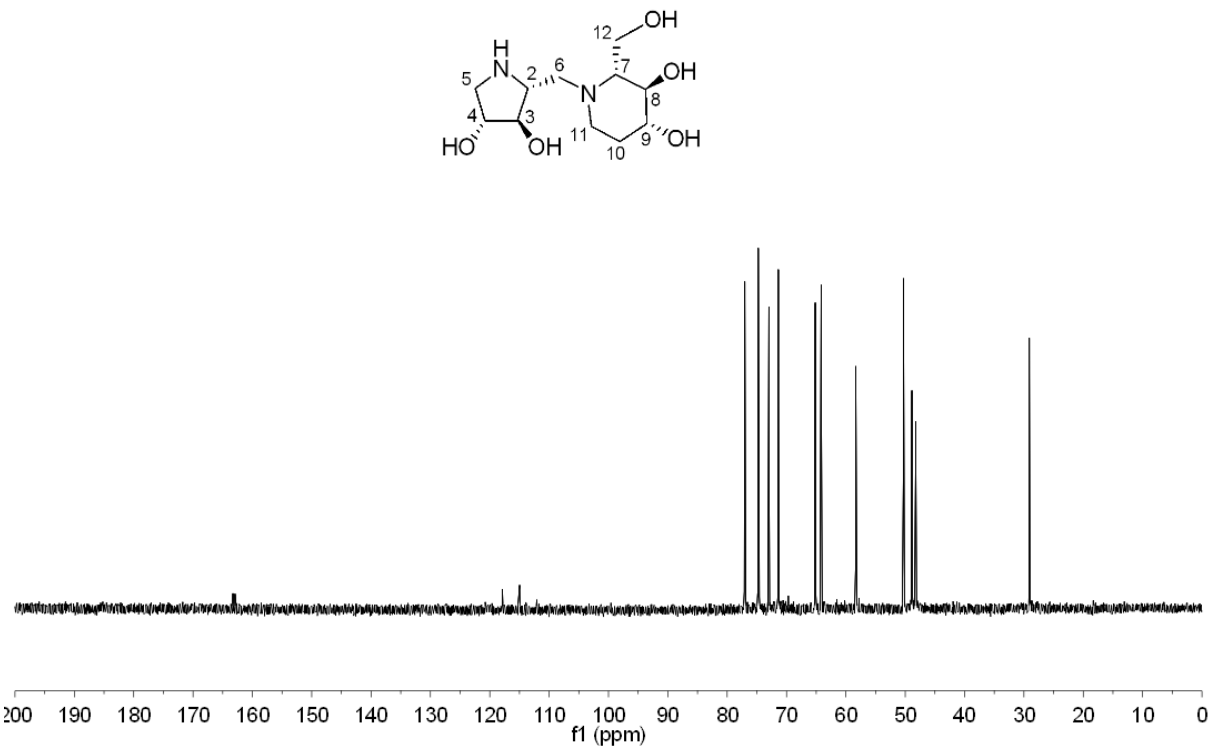

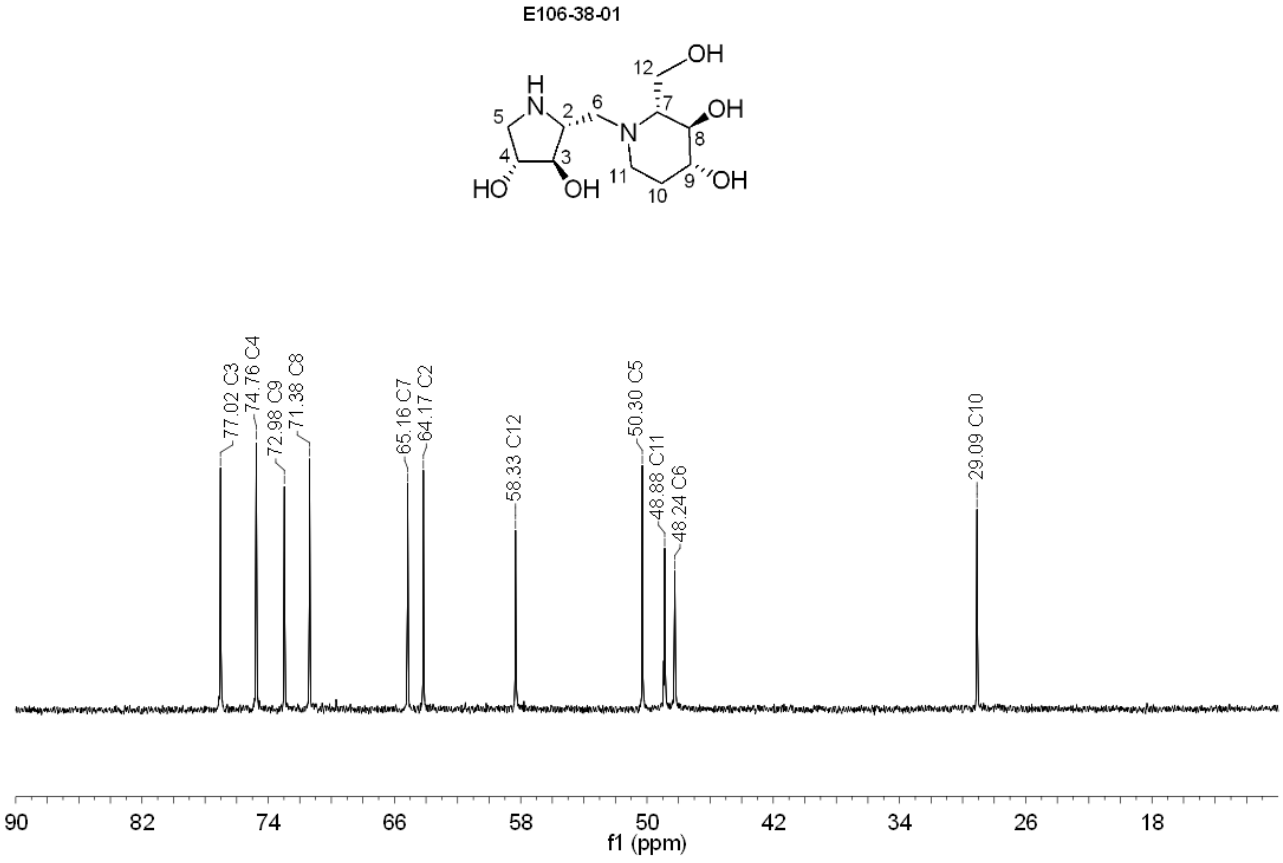

c)

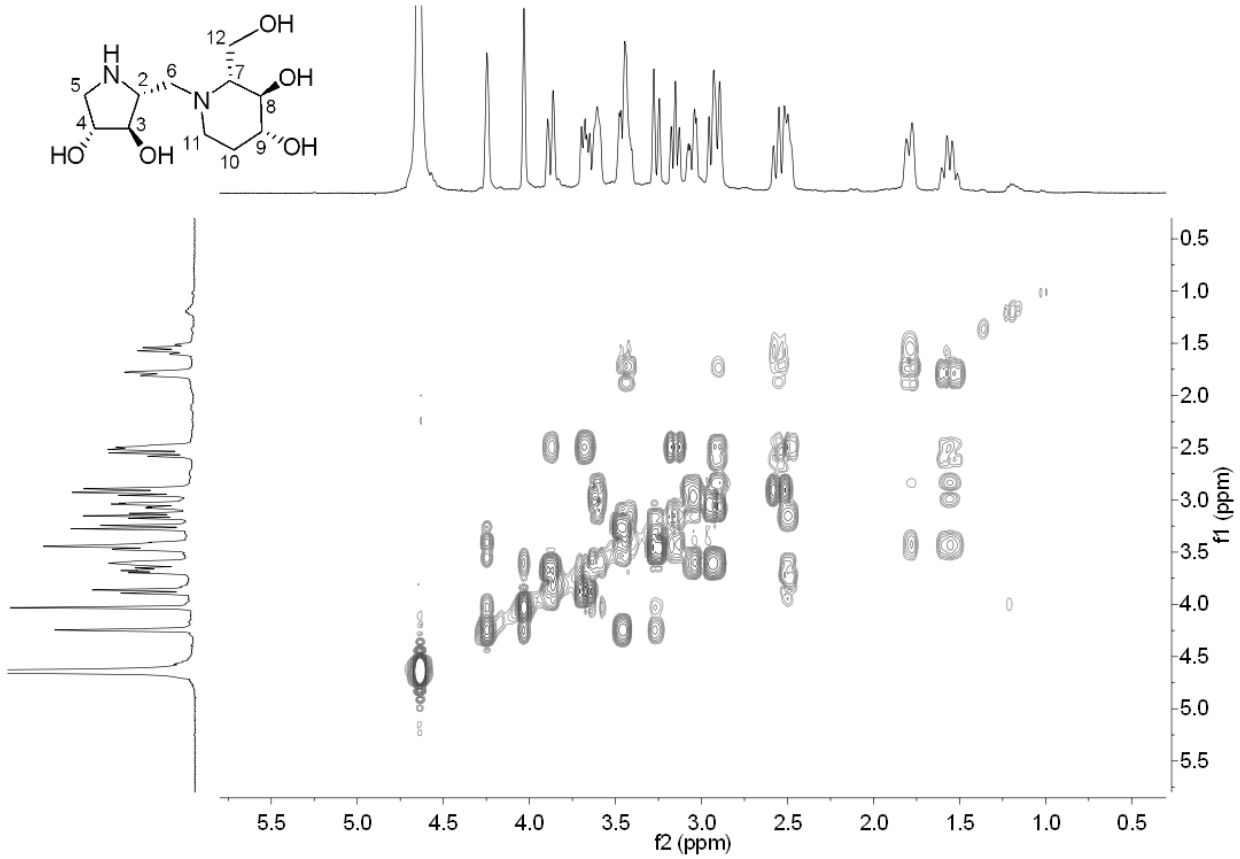

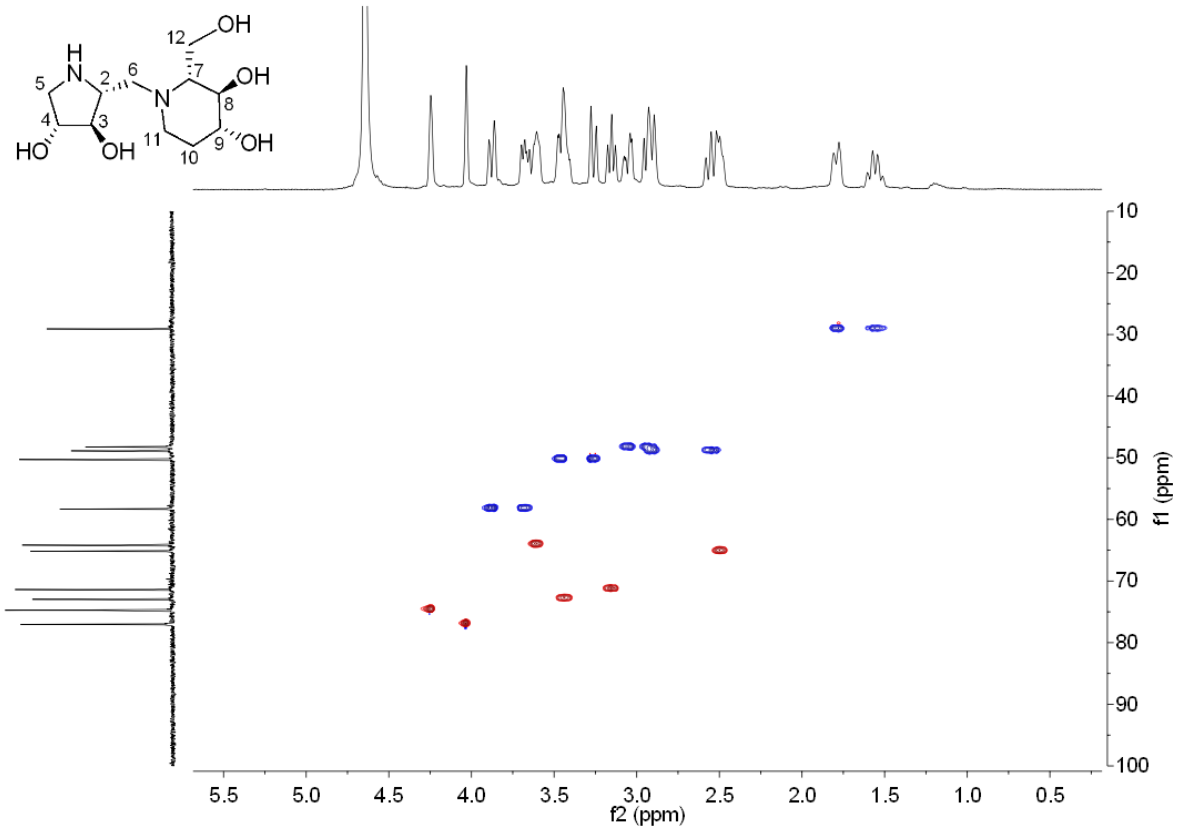

Table 3

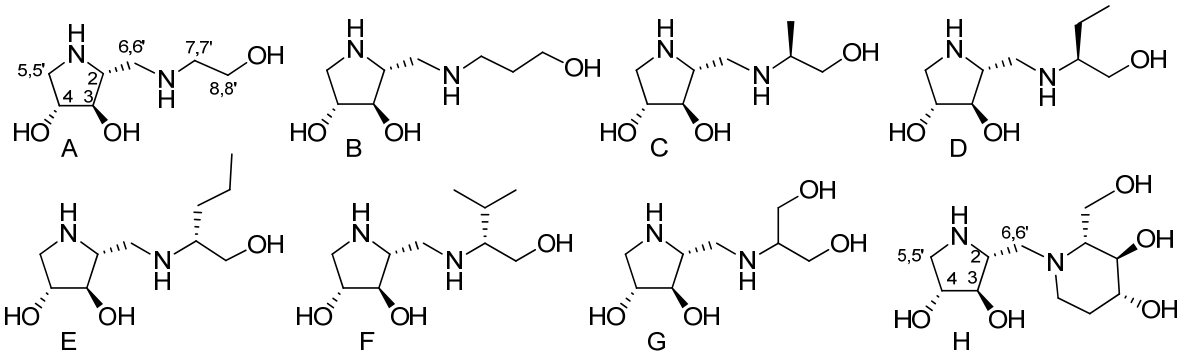

Product	Structure	H2 (C2)	H3 (C3)	H4 (C4)	H5, 5' (C5)	H6, 6' (C6)	H7 (C7)	$[\alpha]_D^{20}$	MS (oa-TOF) *m/z* [M + H]+
25e	**A**	3.56 (62.10)	4.07 (78.88)	4.30 (75.55)	3.46, 3.13 (50.66)	3.35, 3.27 (48.90)	3.13 (49.76)	+ 4.7 (*c* = 1.0 in MeOH)	177.1226
25f	**B**	3.42 (61.03)	3.96 (78.78)	4.21 (75.31)	3.34, 3.02 (50.64)	3.34, 3.22(48.68)	3.12 (46.05)	+ 6.7 (*c* = 0.9 in MeOH)	191.1375
25g	**C**	3.94 (62.03)	4.30 (77.55)	4.39 (73.70)	3.66, 3.48 (51.24)	3.66 (44.53)	3.53 (56.70)	+ 14.0 (*c* = 1.5 in MeOH)	191.1375
25h	**D**	3.44 (61.83)	3.98 (78.78)	4.21, (75.46)	3.38, 3.04 (50.44)	3.26, 3.17 (46.02)	3.04 (60.55)	+ 16.1 (*c* = 1.0 in MeOH)	205.1547
25i	**E**	3.70 (62.03)	4.16 (78.04)	4.31 (74.38)	3.53, 3.29 (50.89)	3.53, 3.43 (45.12)	3.29 (59.89)	+ 1.05 (*c* = 0.9 in MeOH)	219.1691
25j	**F**	3.62 (62.35)	4.08 (78.18)	4.27 (74.76)	3.48, 3.20 (50.60)	3.40, 3.31 (46.21)	2.94 (64.84)	+ 18.3 (*c* = 0.9 in MeOH)	219.1693
25k	**G**	3.59 (64.27)	4.08 (77.48)	4.29 (74.54)	3.52, 3.30 (50.20)	3.25, 3.12(45.90)	2.93 (59.80)	+ 15.2 (*c* = 1.2 in MeOH)	207.1333
25l	**H**	3.67 (64.17)	4.09 (77.02)	4.30 (74.76)	3.50, 3.32 (50.30)	3.11, 2.98 (48.24)		+ 35.4 (*c* = 0.9 in MeOH)	263.1592

Figure 18. Observed NMR spectra of **28m**: a) ^{1}H, b) ^{13}C, c) 2D ^{1}H-^{1}H COSY and 2D multiplicity-edited HSQC.

a)

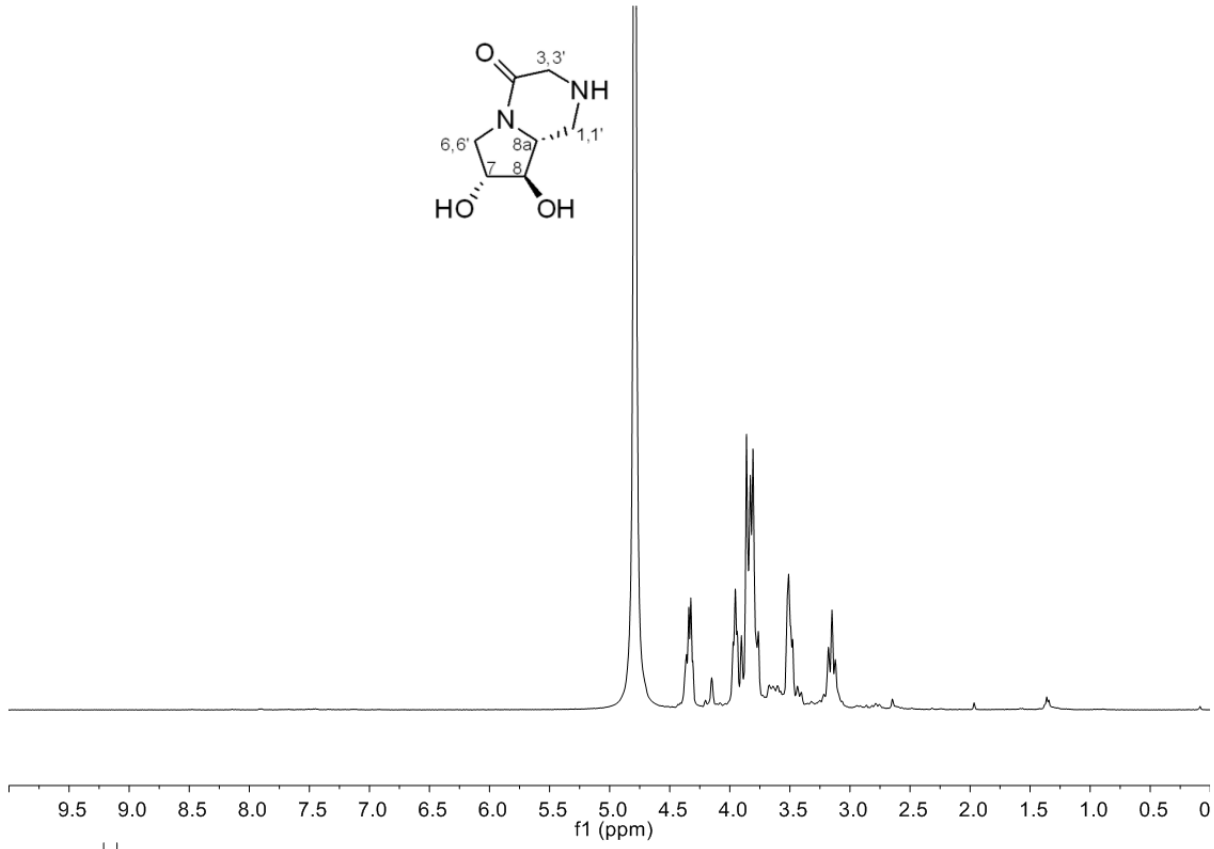

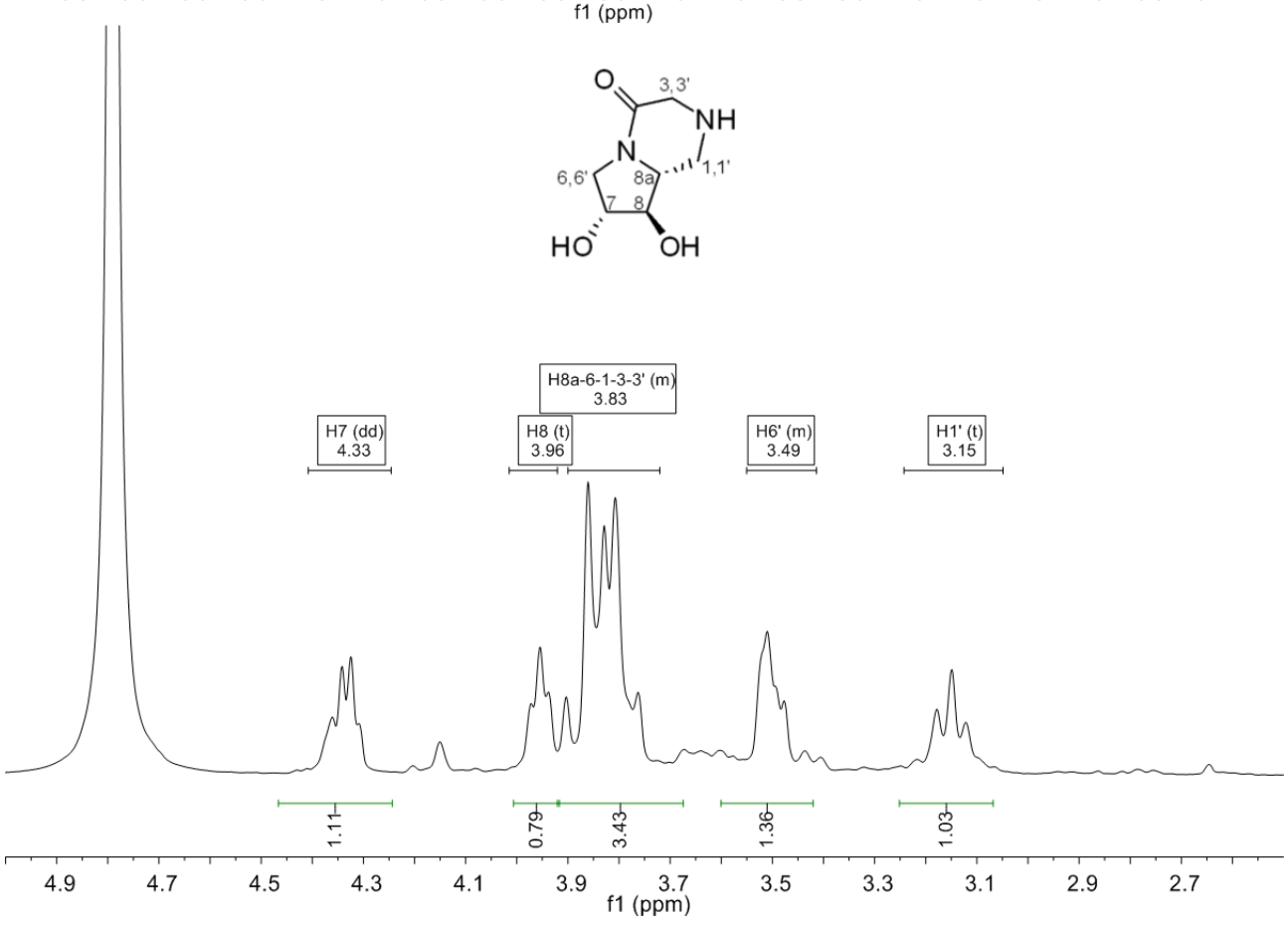

b)

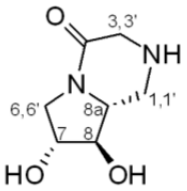

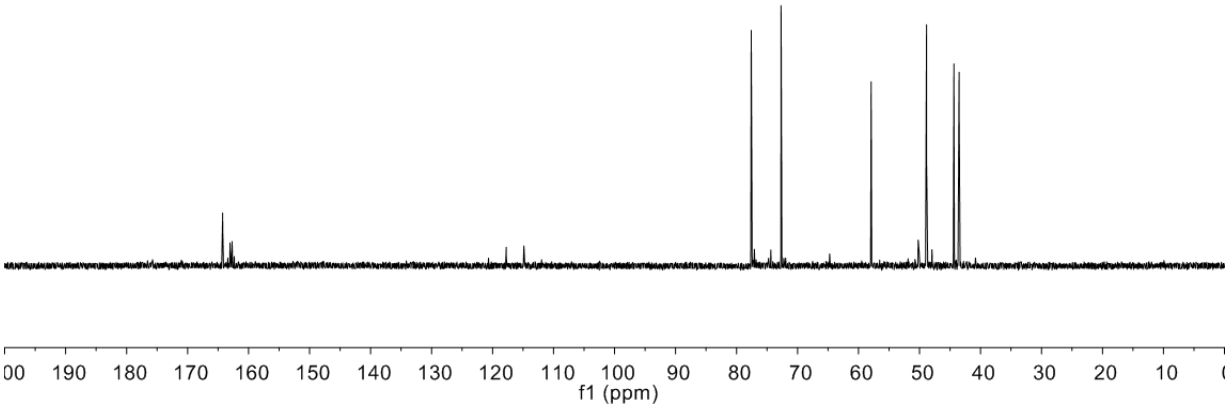

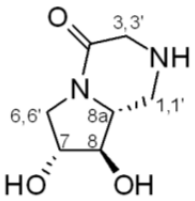

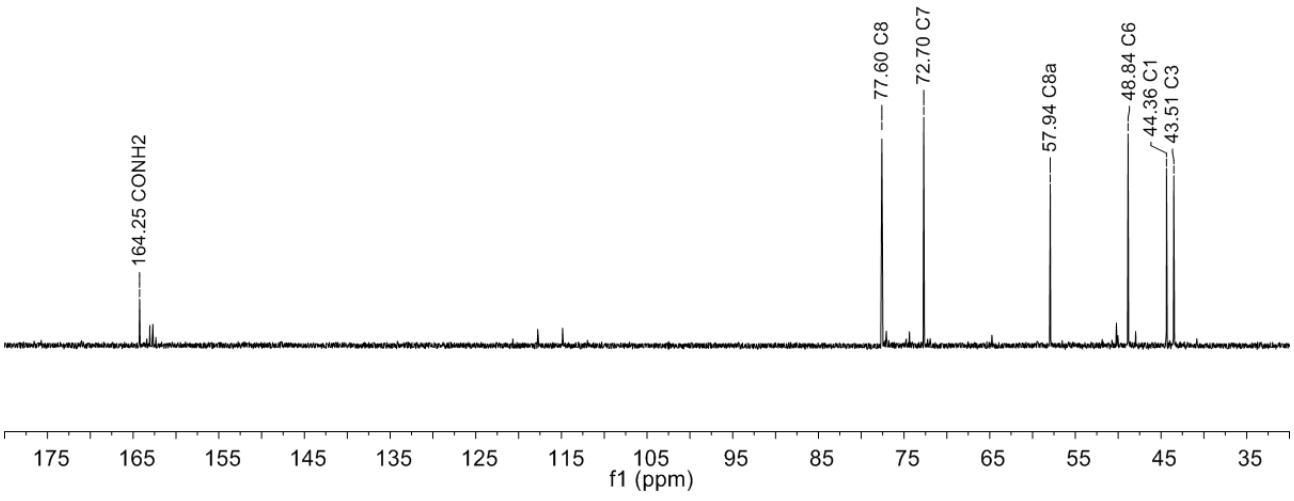

c)

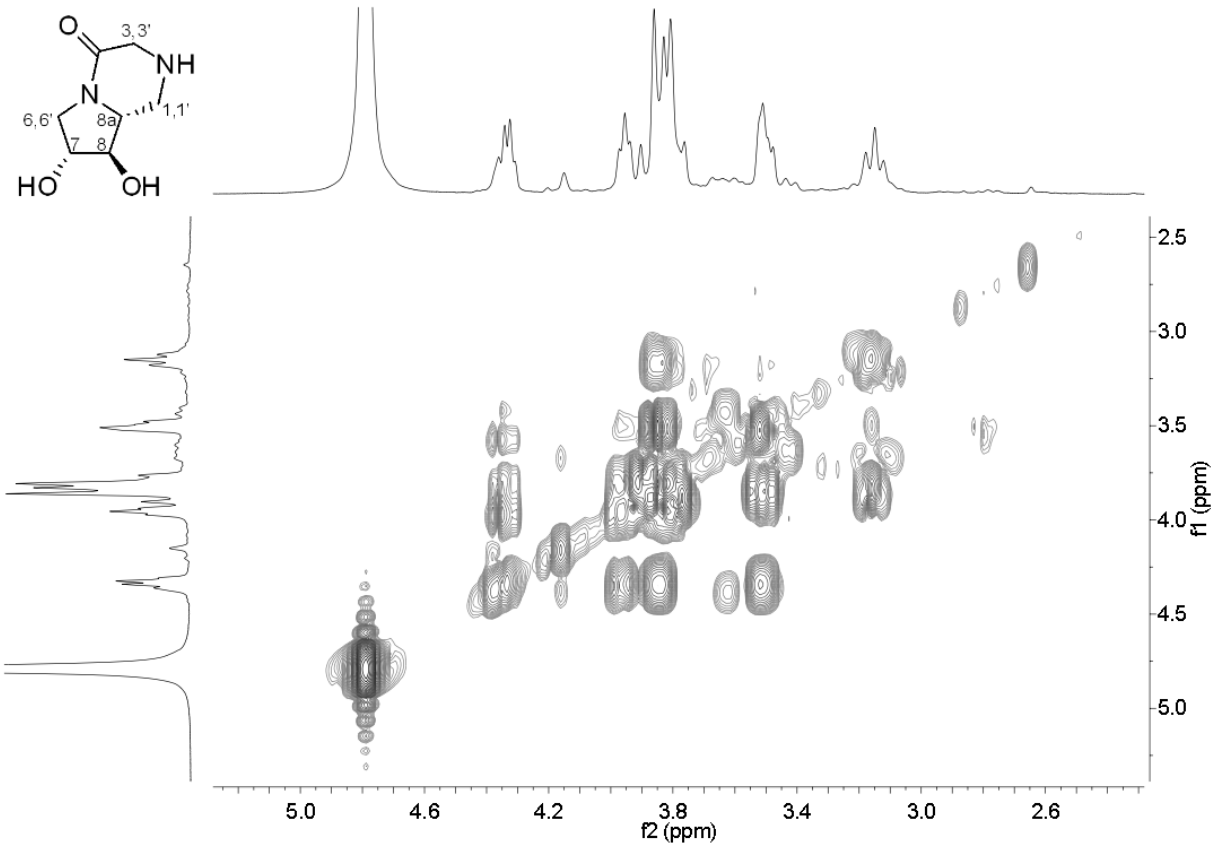

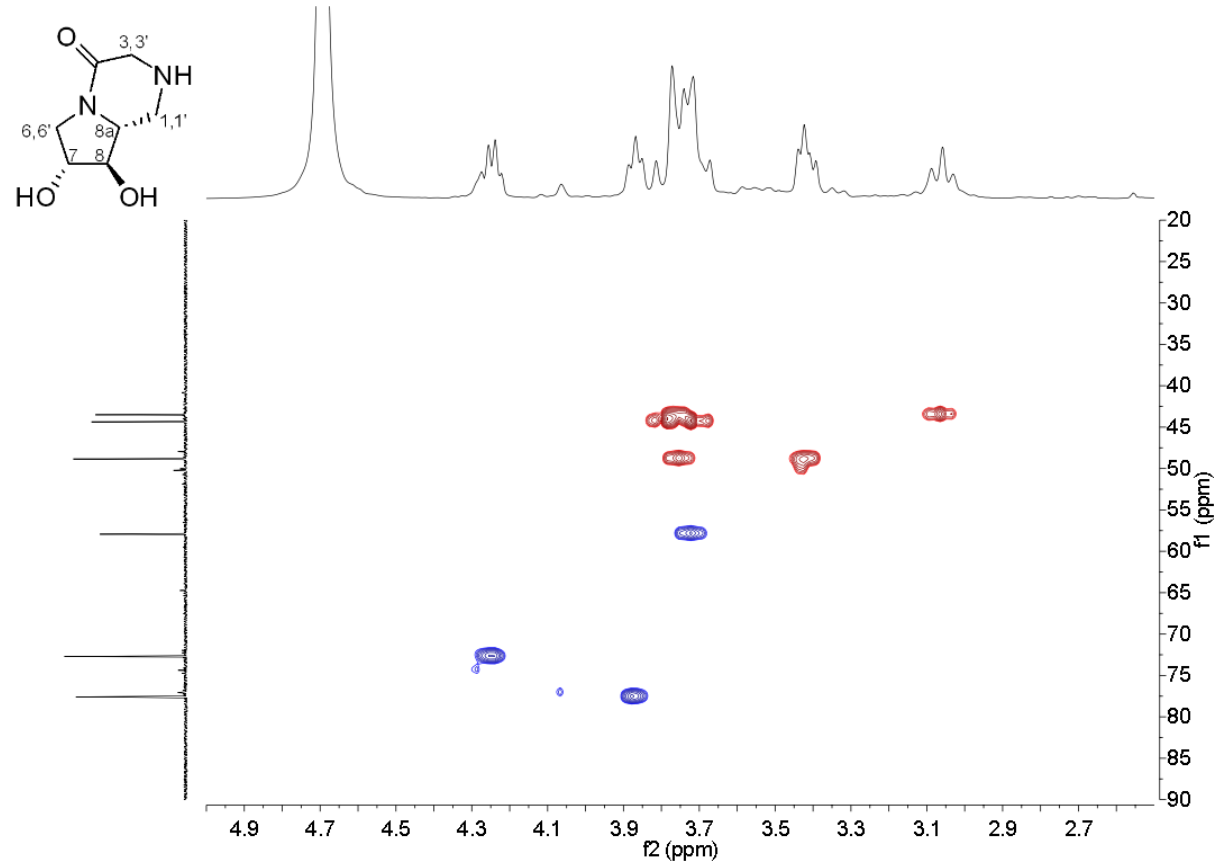

Figure 19. Observed NMR spectra of **28n**: a) ^{1}H, b) ^{13}C, c) 2D ^{1}H-^{1}H COSY and 2D multiplicity-edited HSQC and d) magnitude-mode ge-2D HMBC.

a)

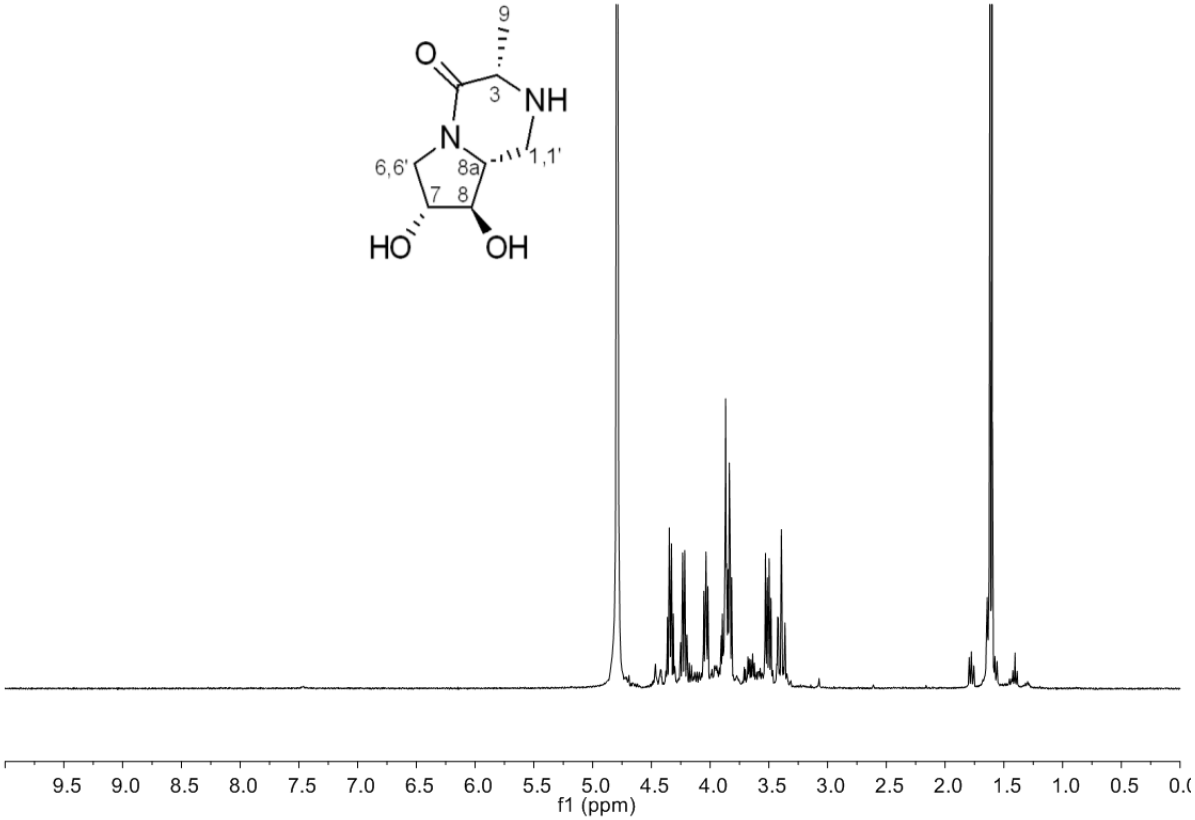

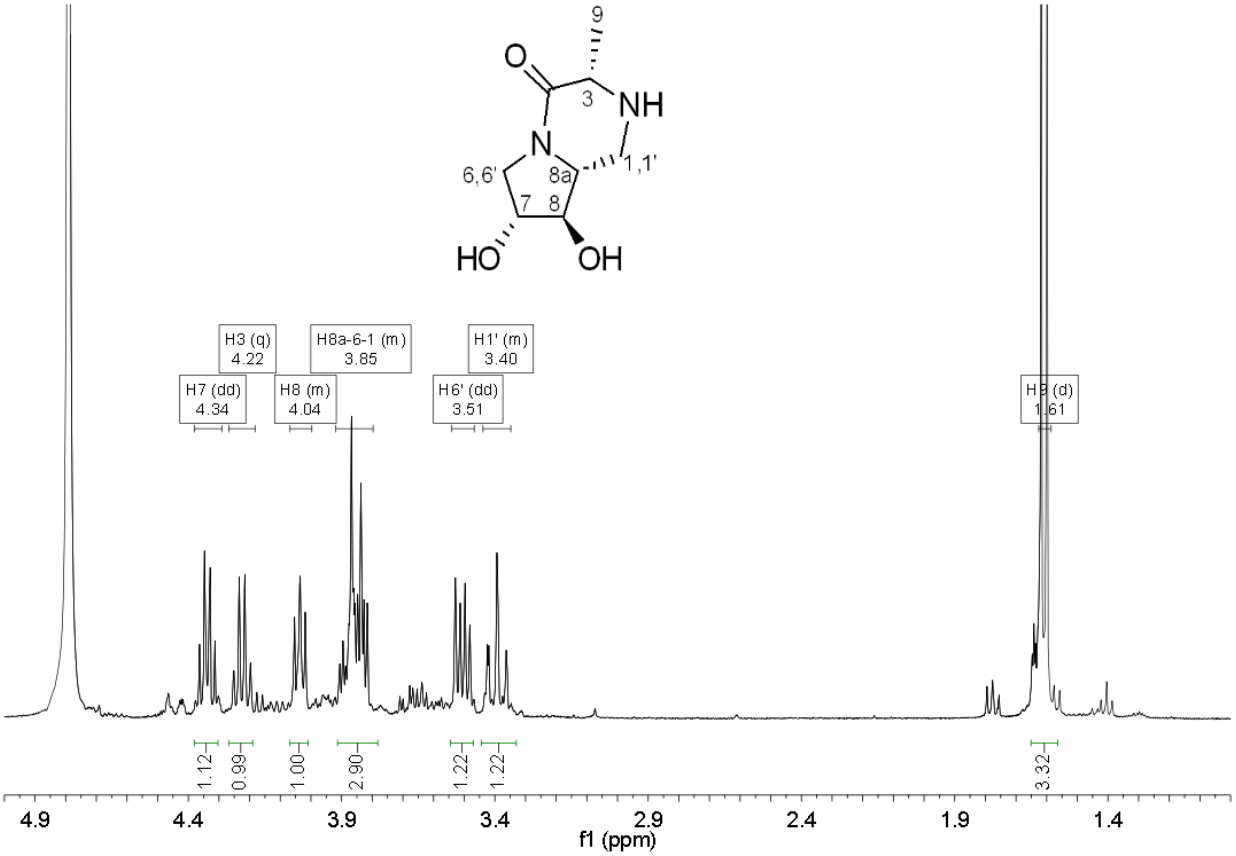

b)

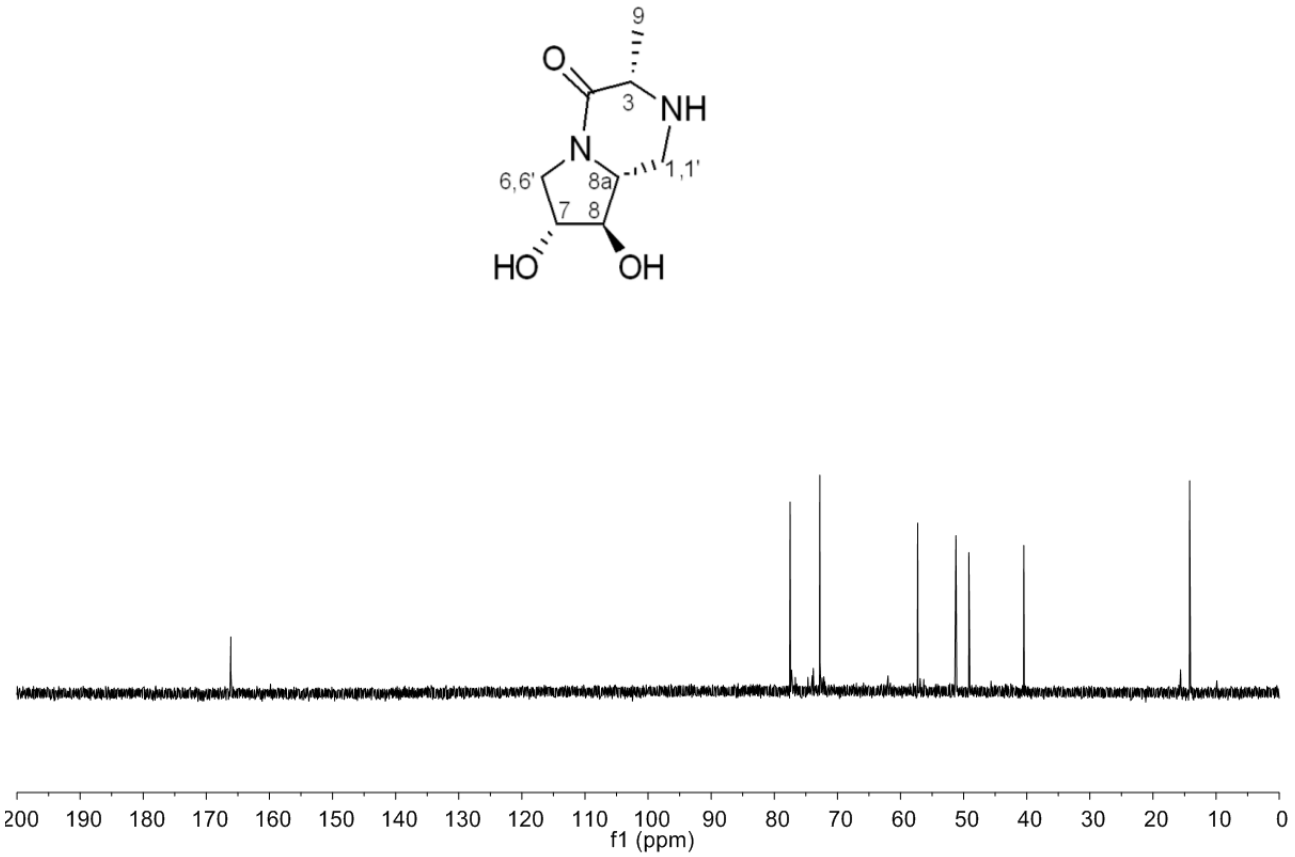

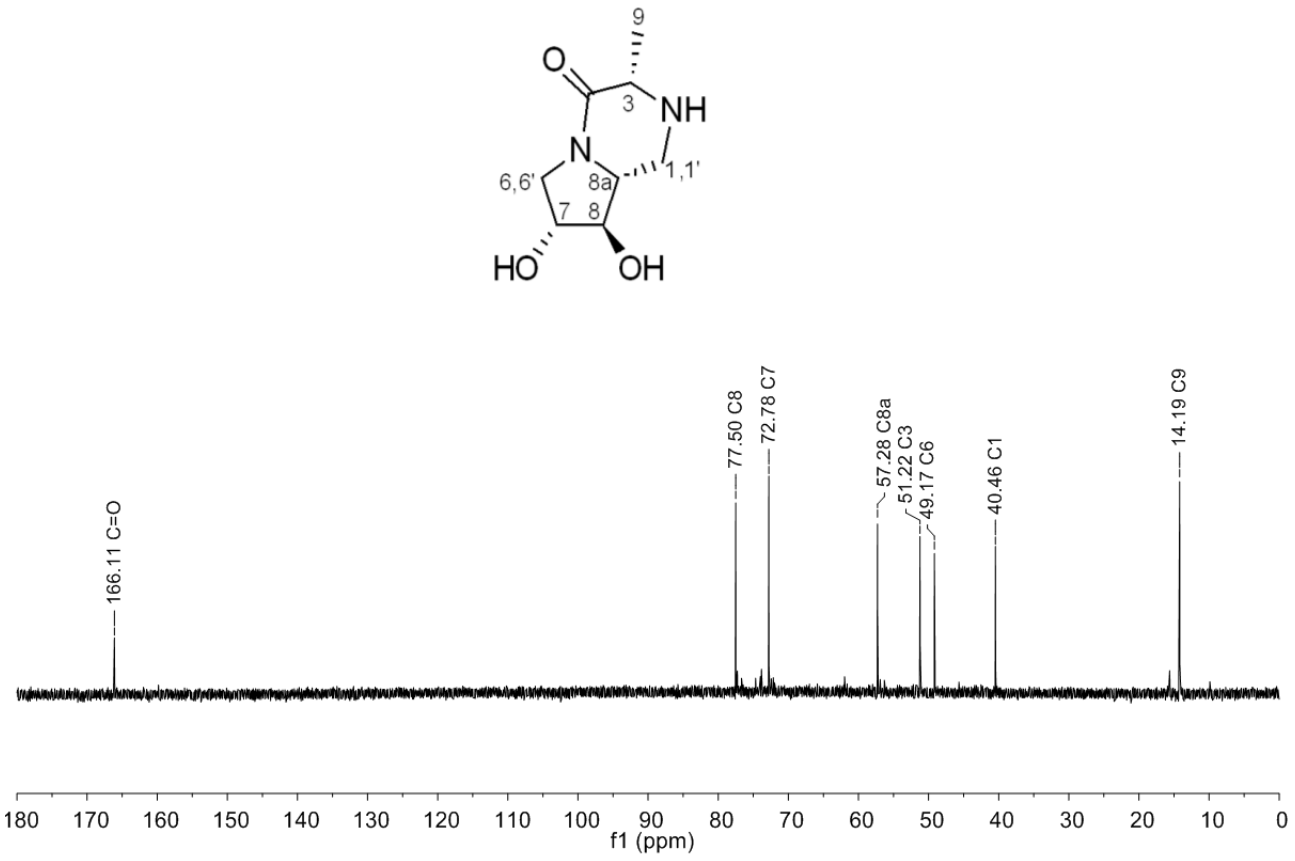

c)

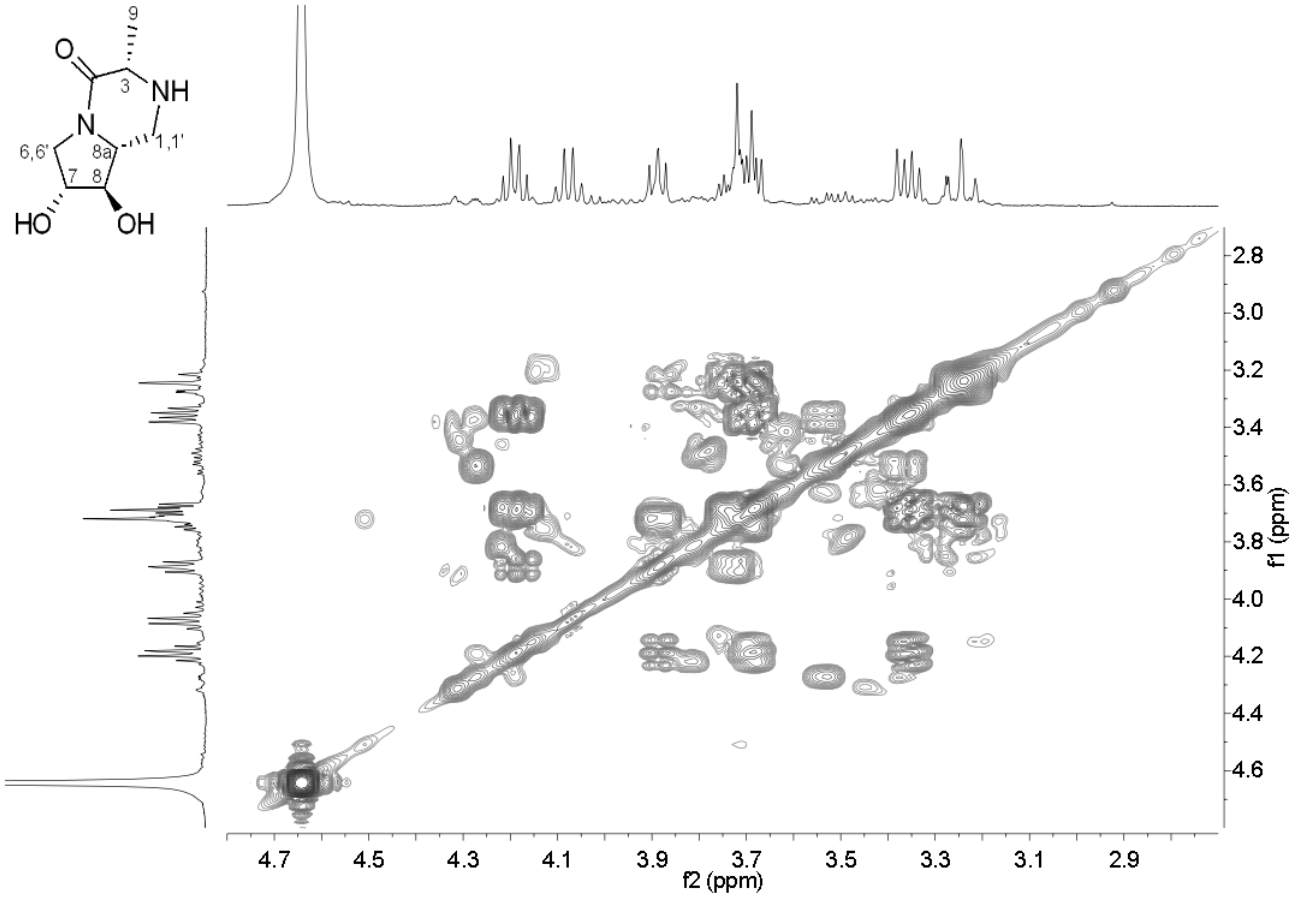

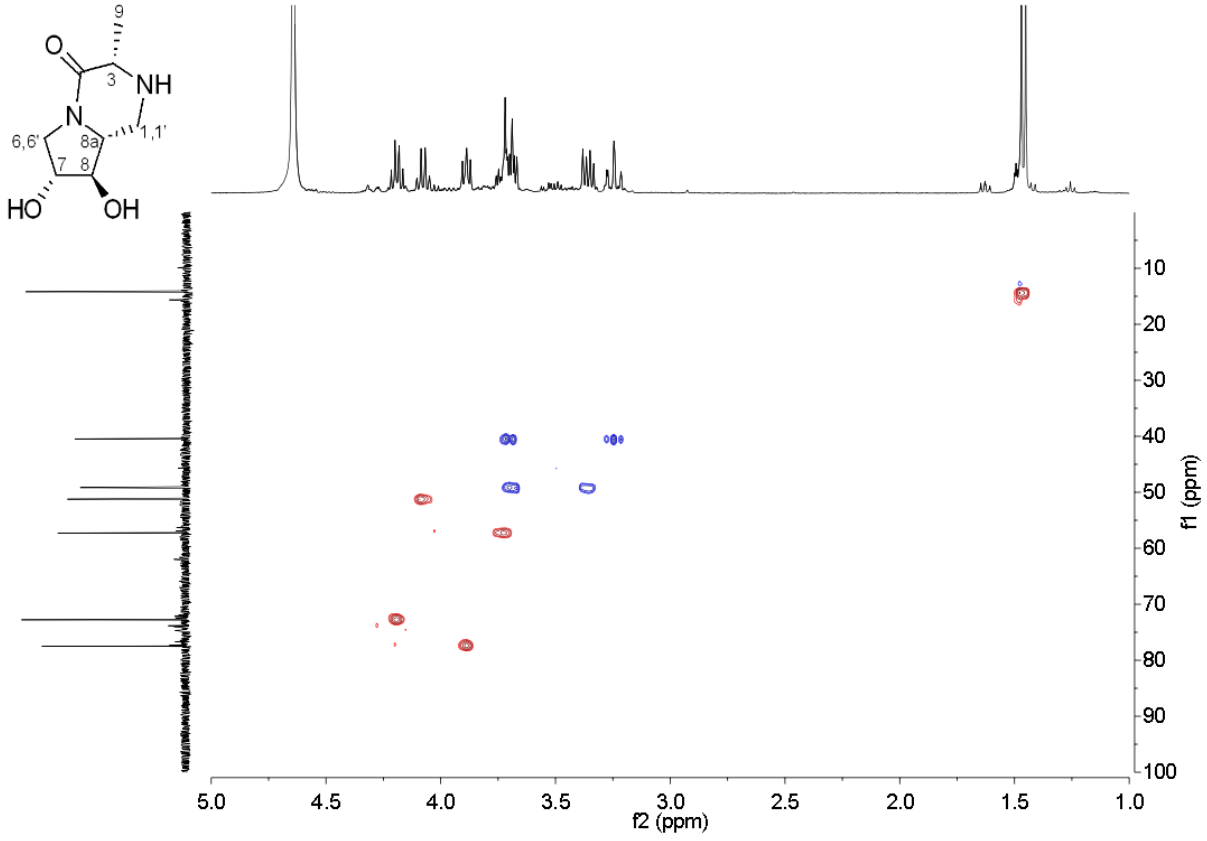

d)

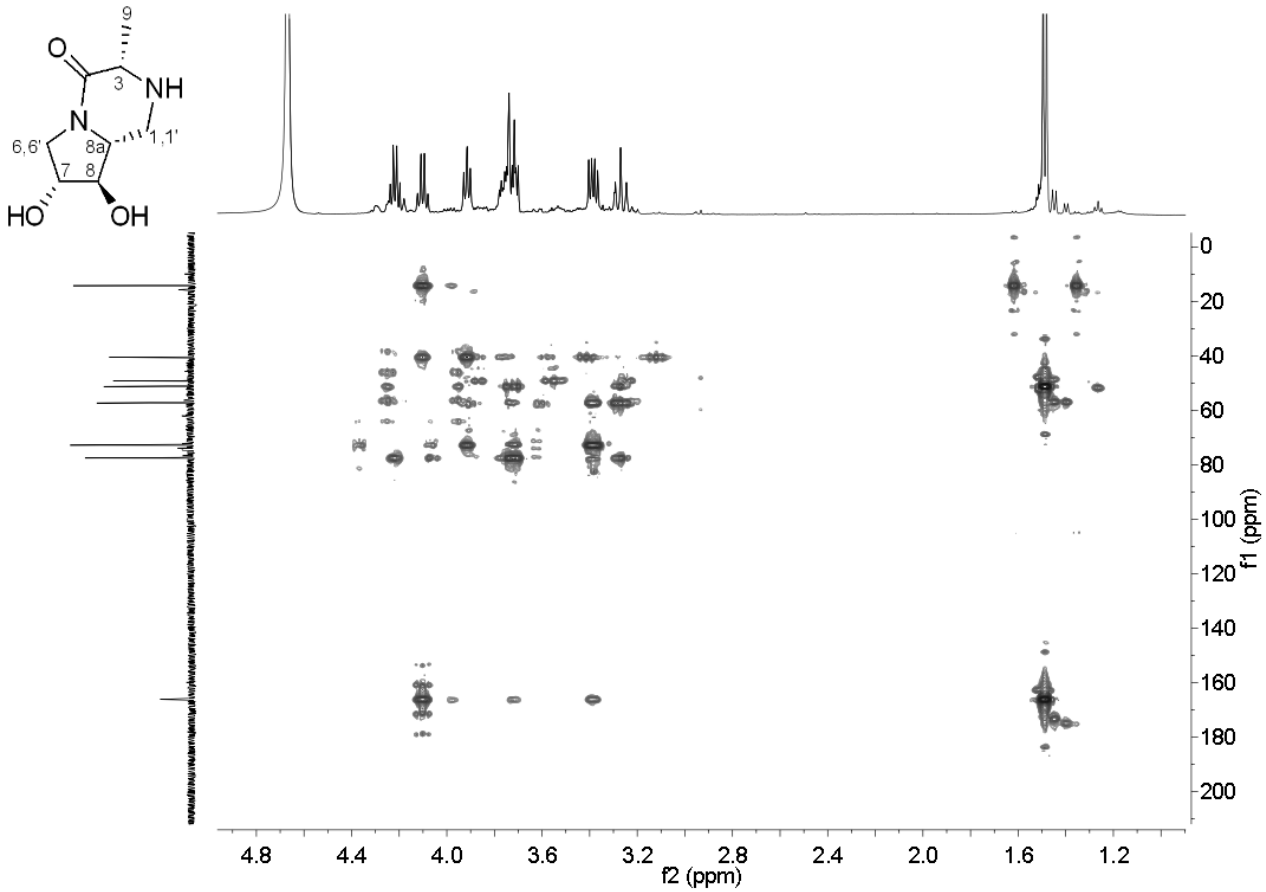

Figure 20. Observed NMR spectra of **28p**: a) ^{1}H, b) ^{13}C, c) 2D ^{1}H-^{1}H COSY and 2D multiplicity-edited HSQC.

a)

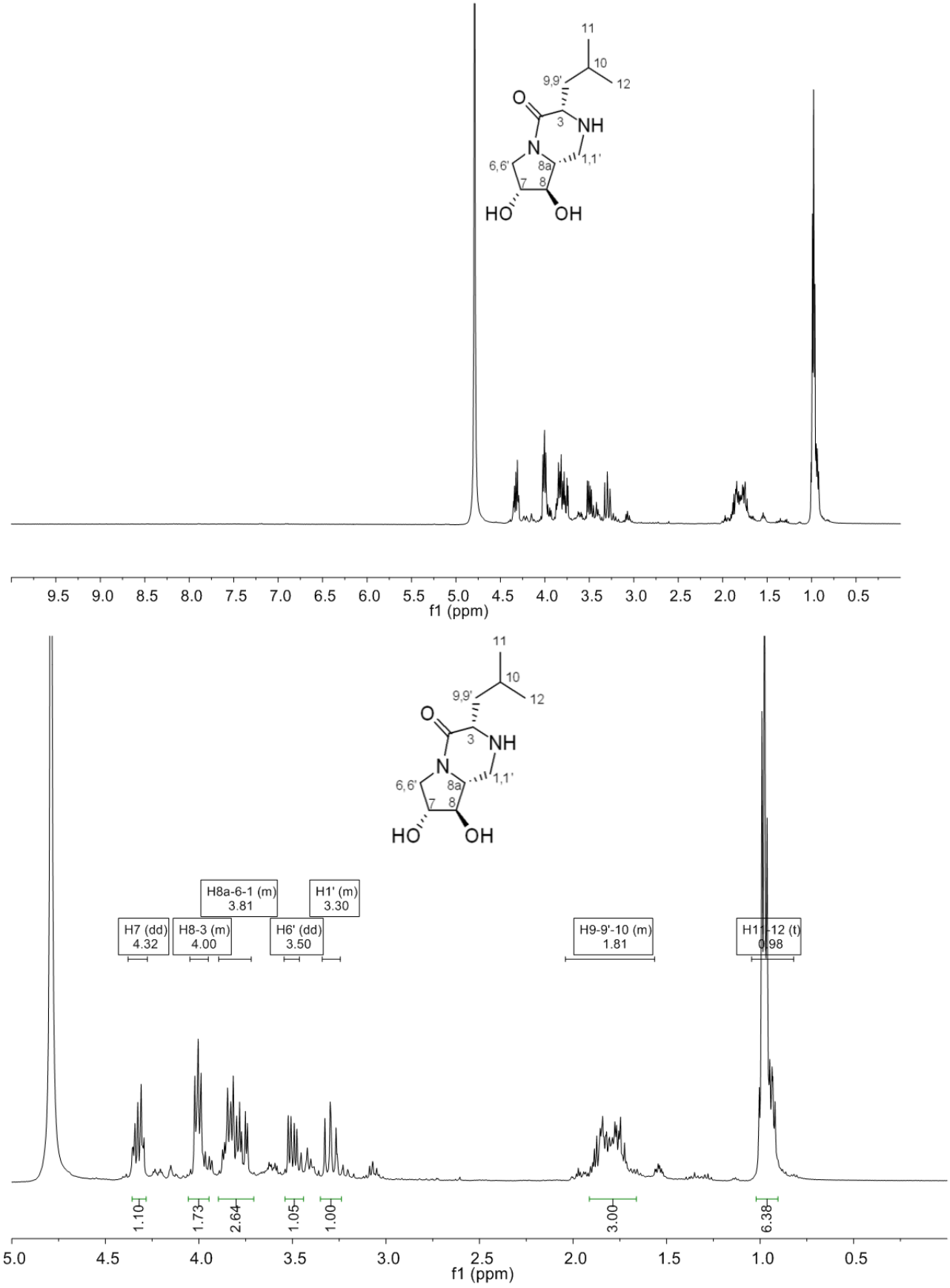

b)

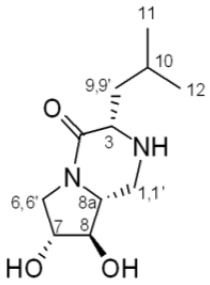

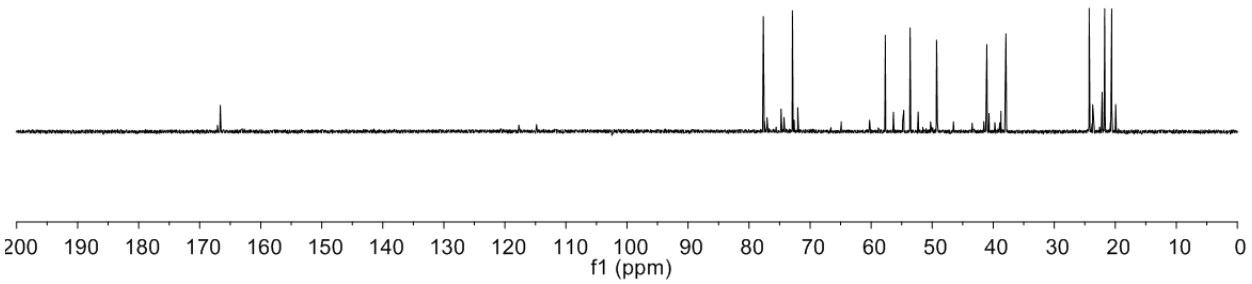

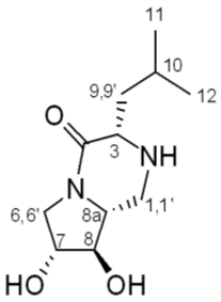

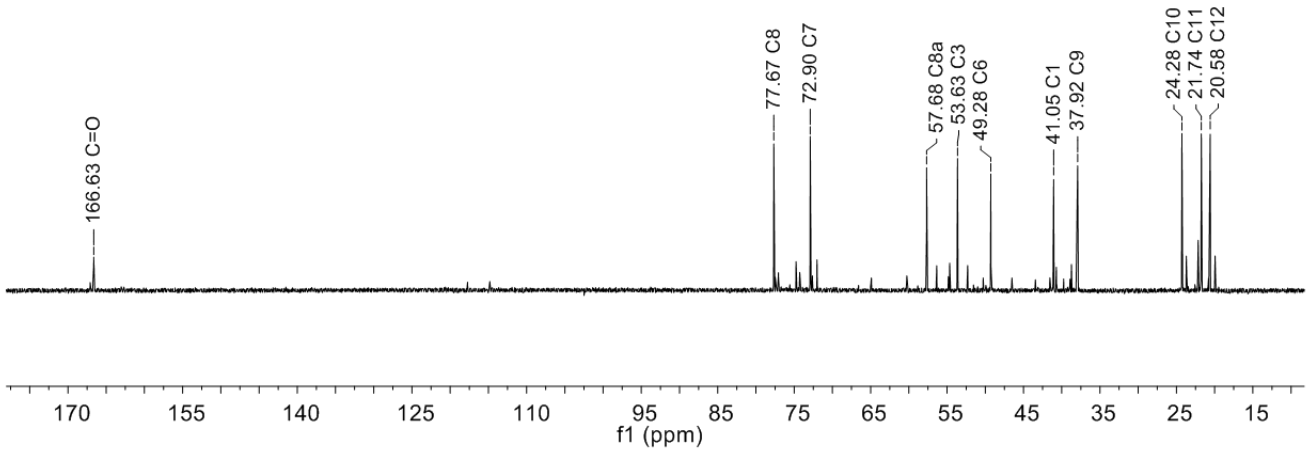

c)

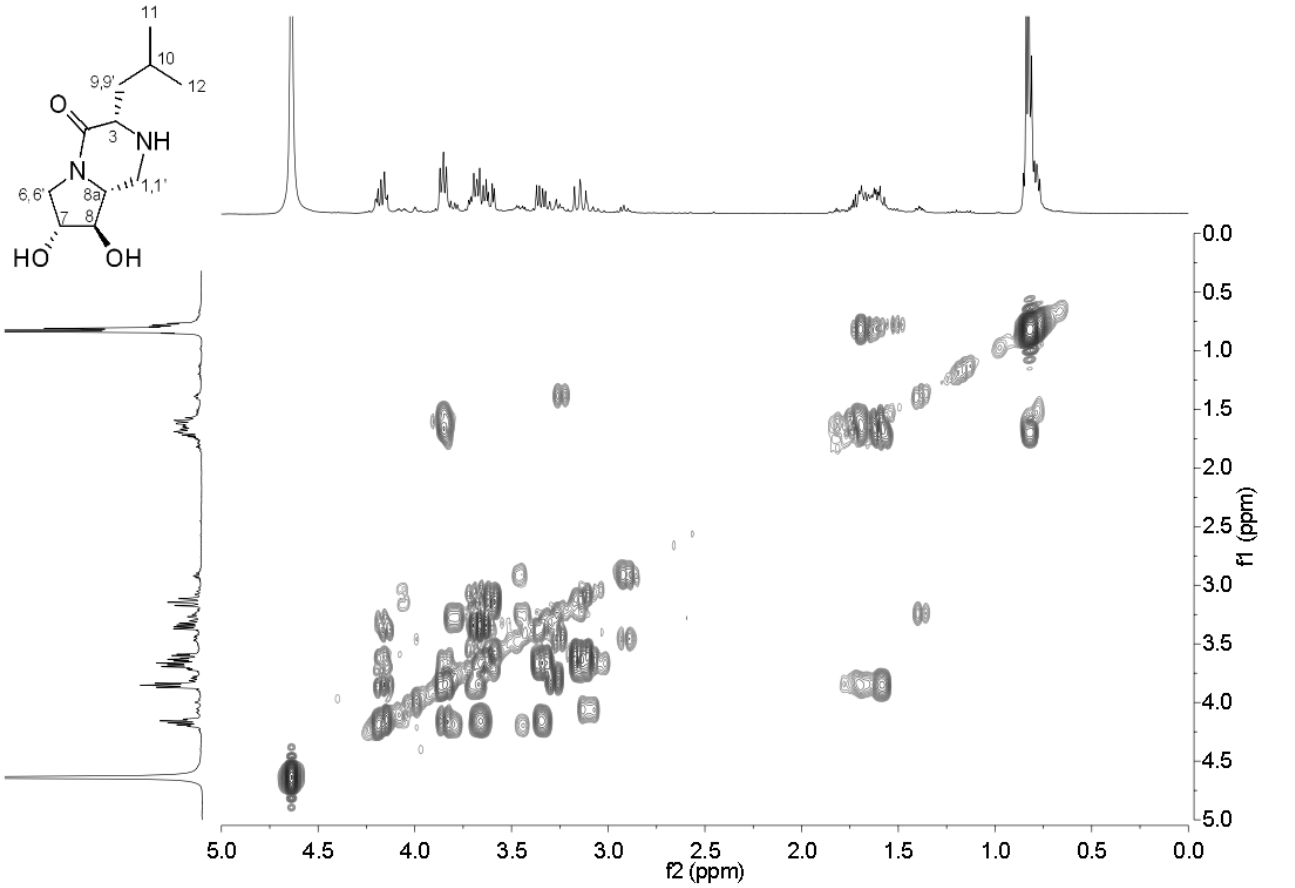

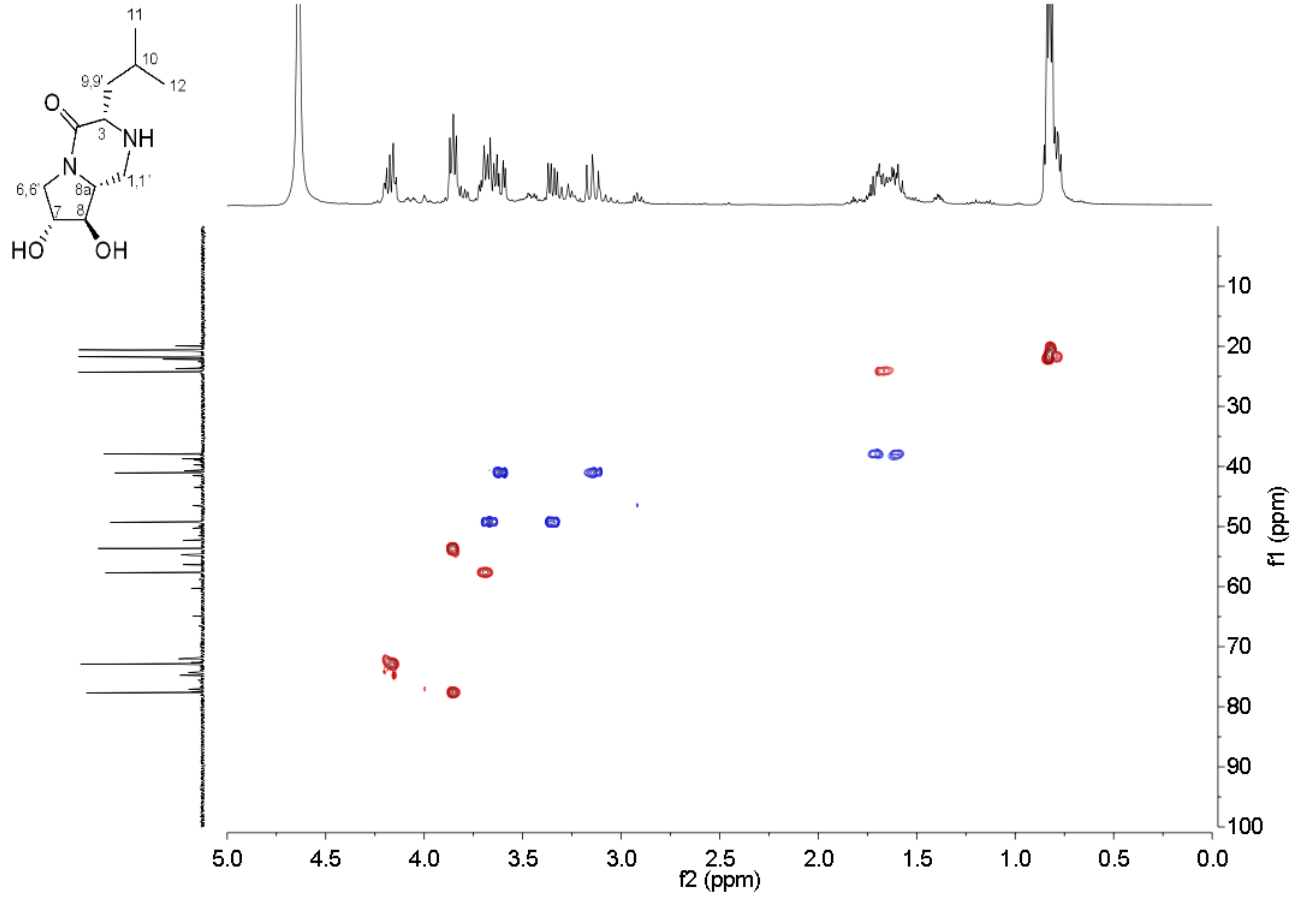

Figure 21. Observed NMR spectra of **28q**: a) ^{1}H, b) ^{13}C, c) 2D ^{1}H-^{1}H COSY and 2D multiplicity-edited HSQC and d).magnitude-mode ge-2D HMBC.

a)

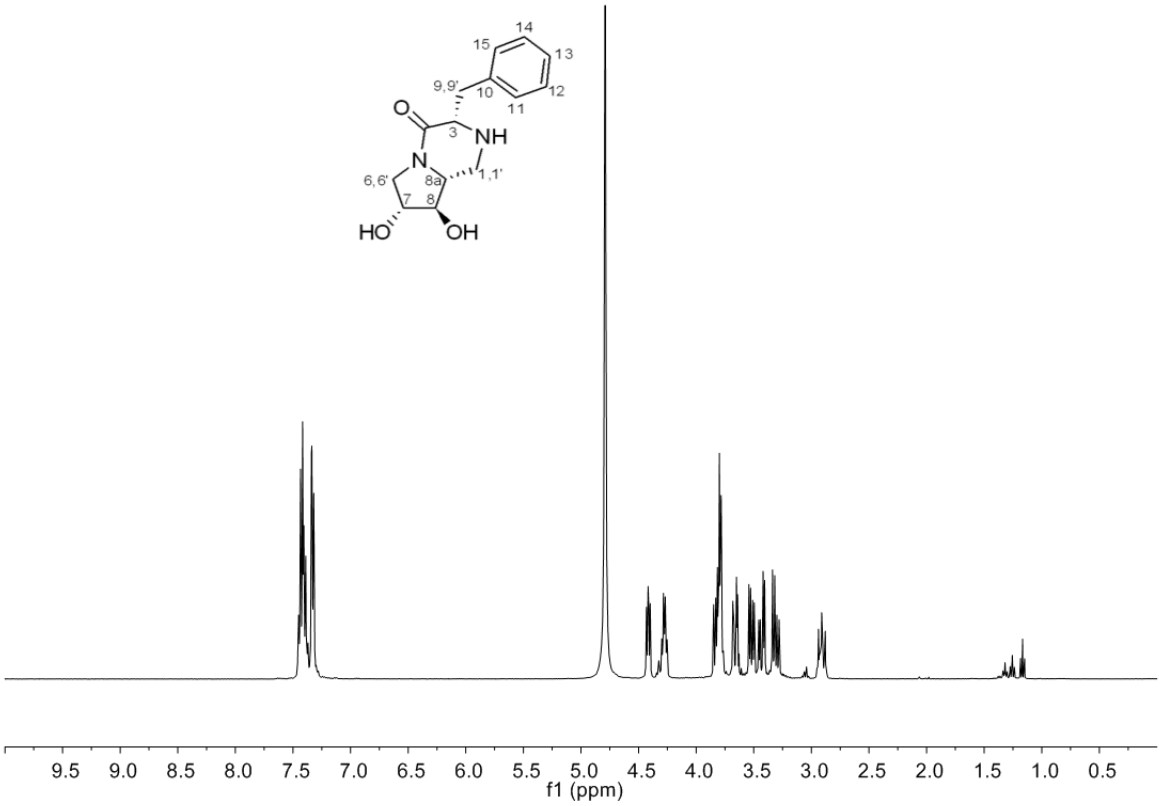

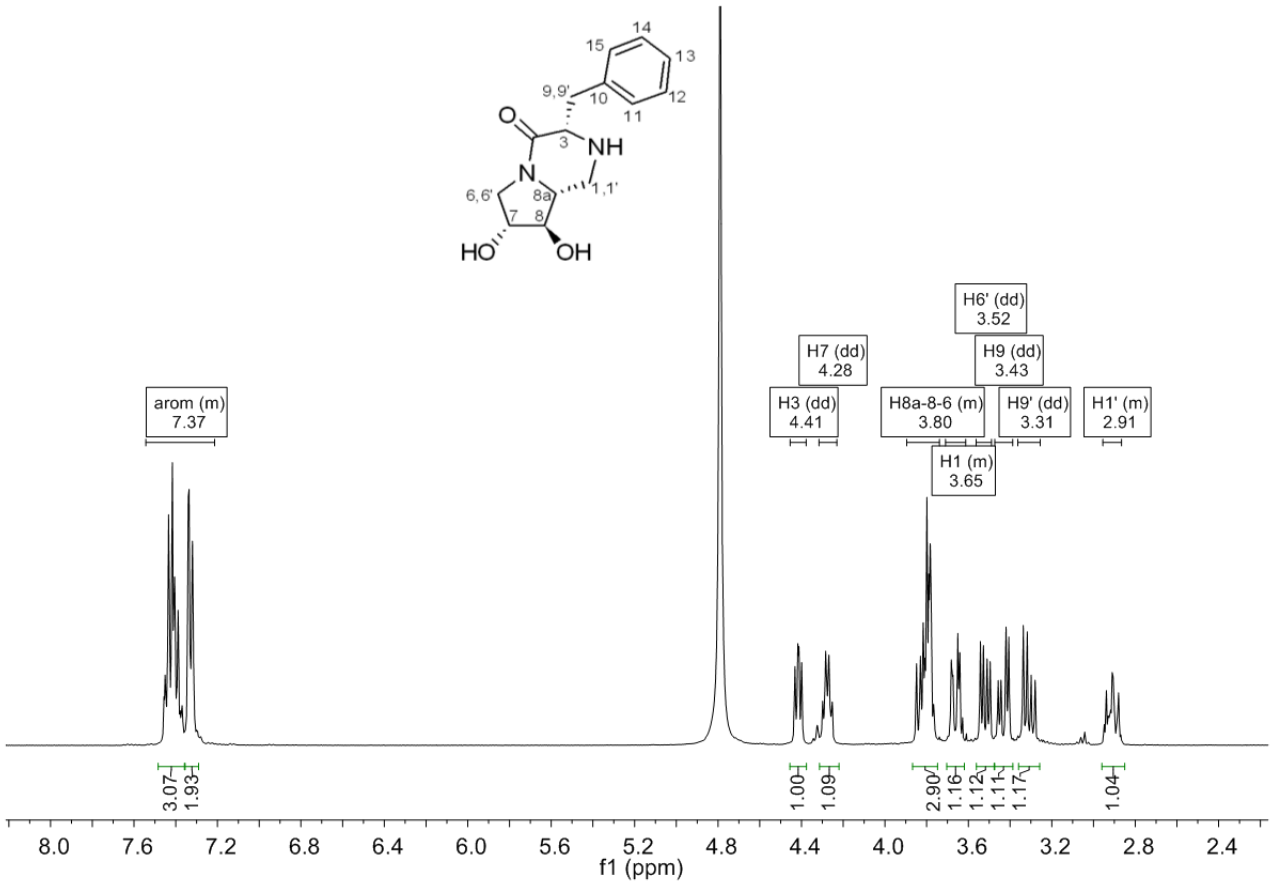

b)

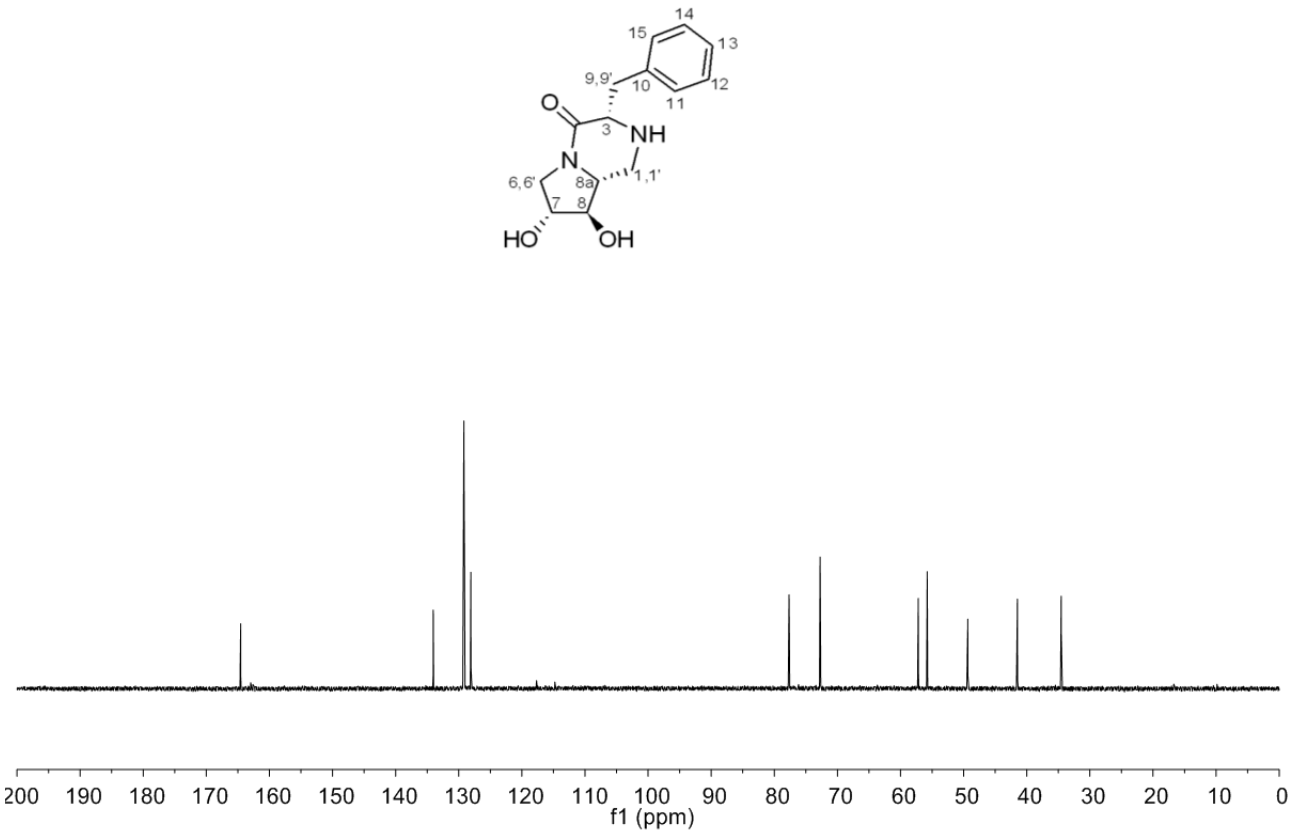

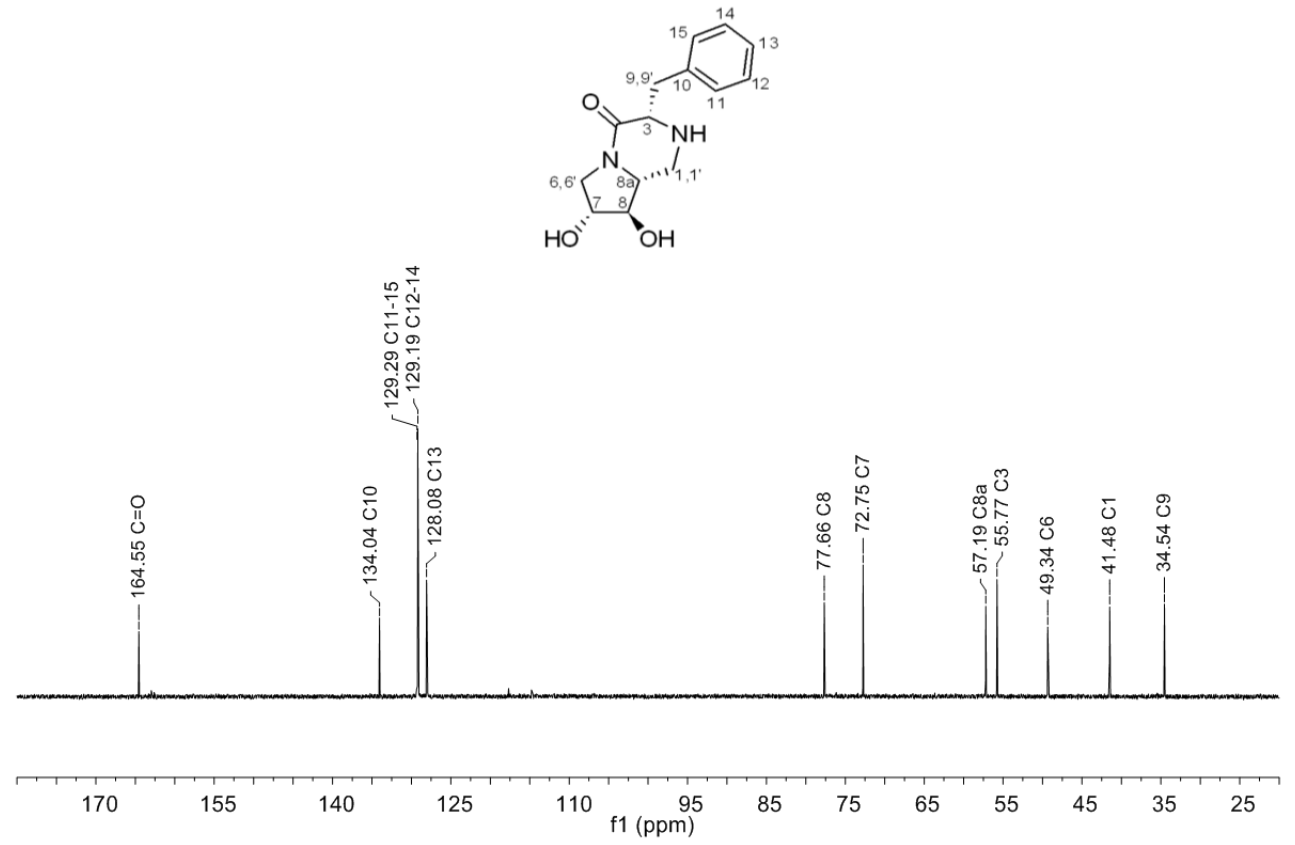

c)

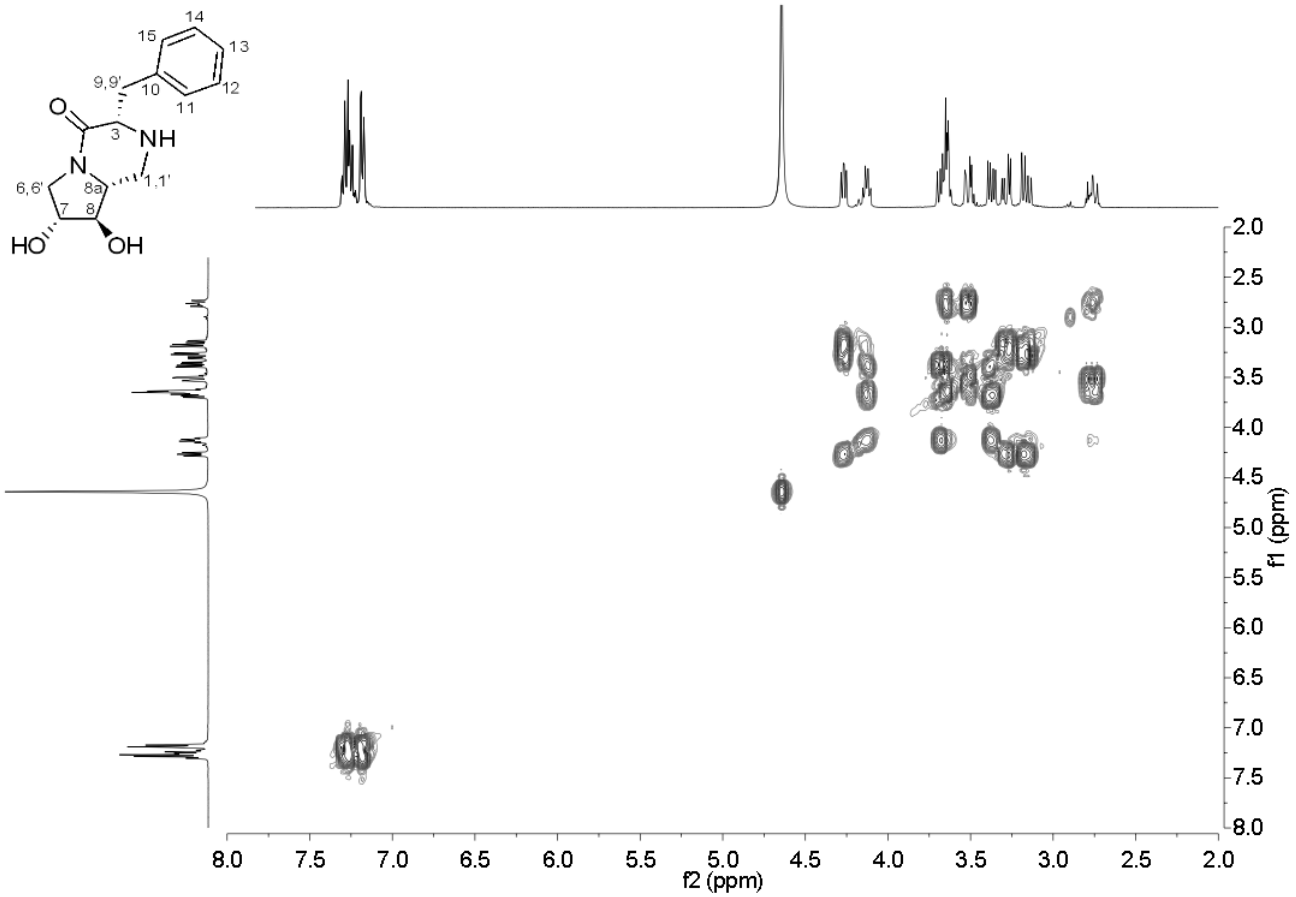

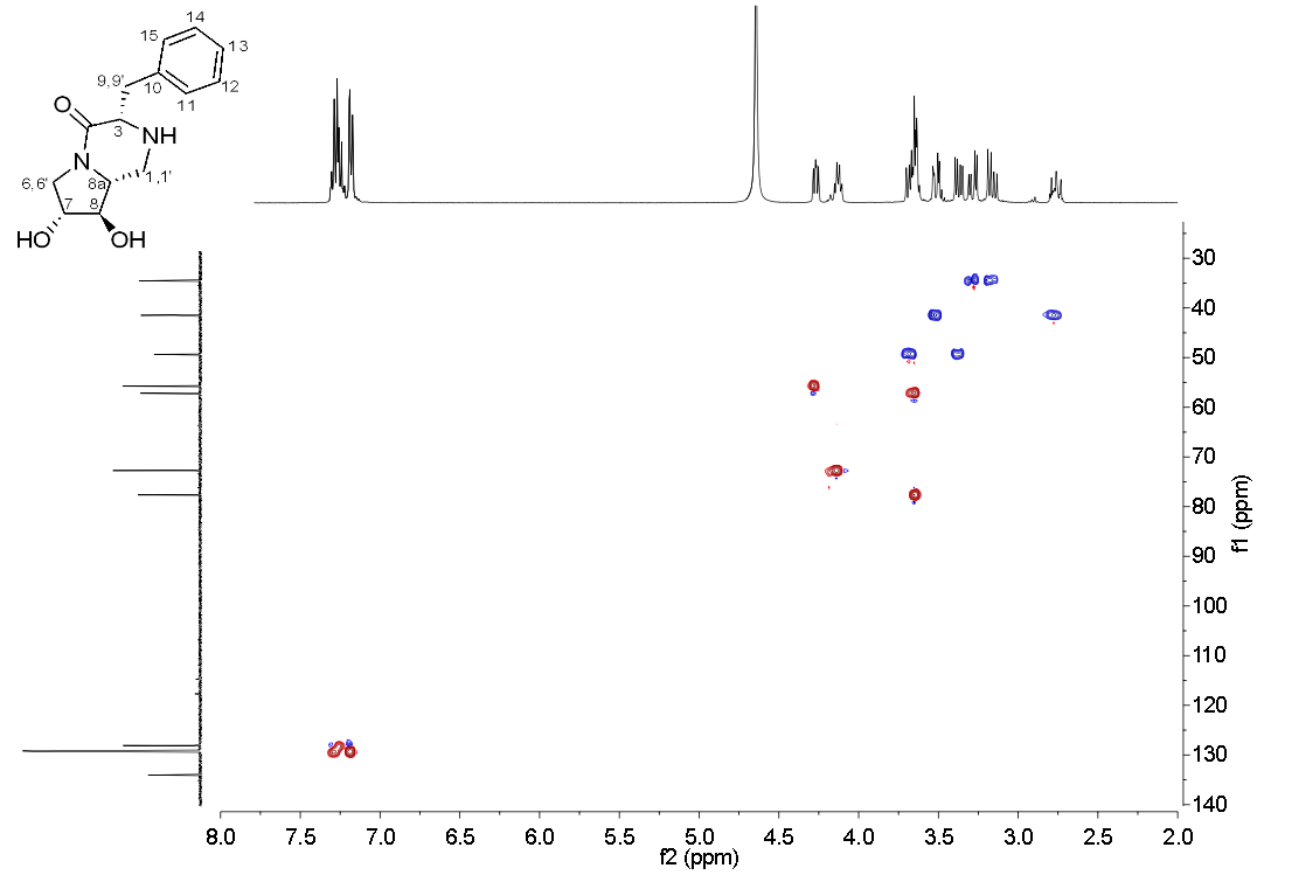

d)

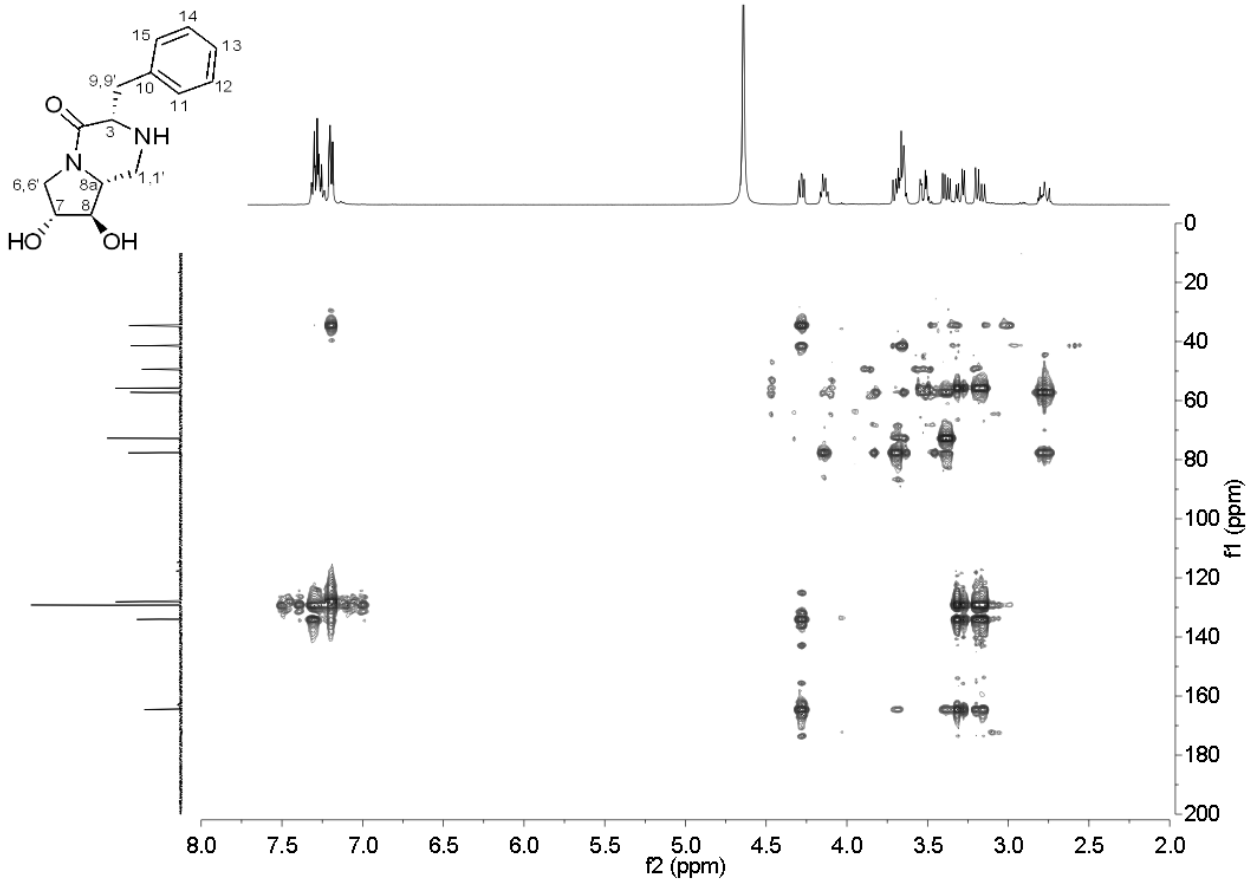

Figure 22. Observed NMR spectra of **28u**: a) ^{1}H, b) ^{13}C, c) 2D ^{1}H-^{1}H COSY and 2D multiplicity-edited HSQC and d).magnitude-mode ge-2D HMBC.

a)

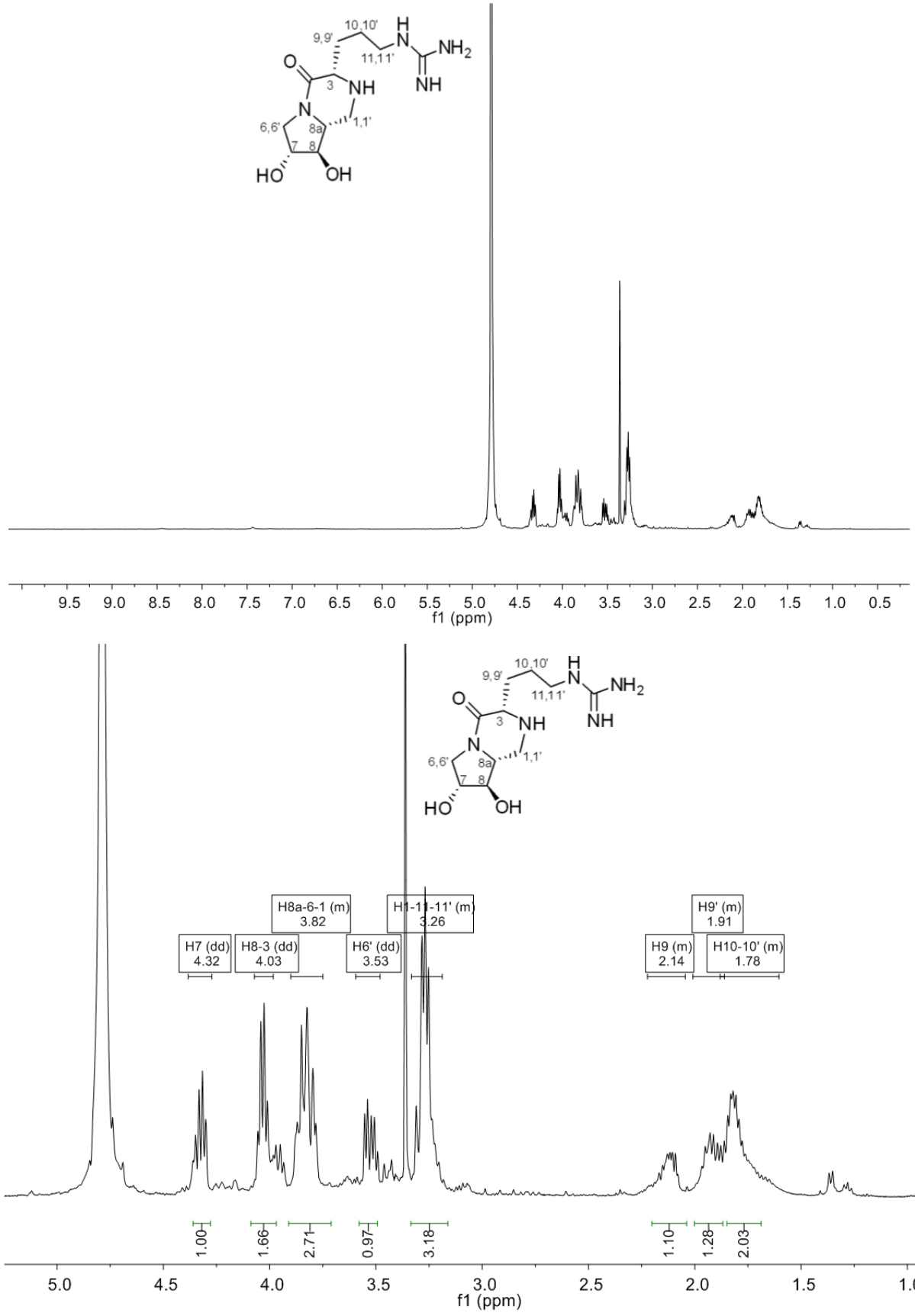

b)

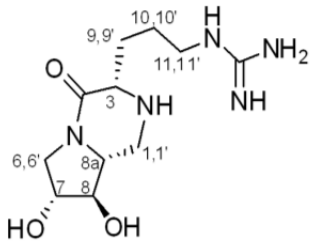

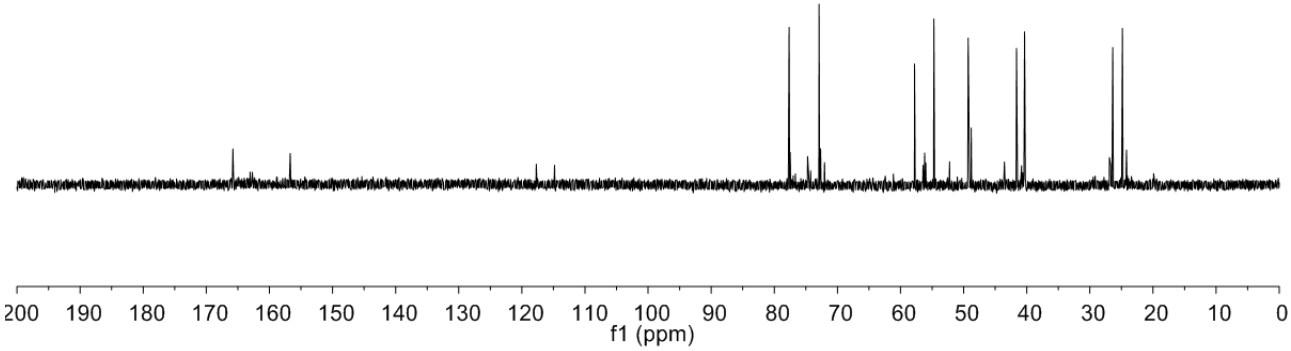

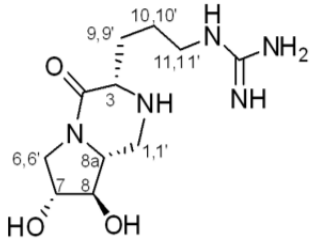

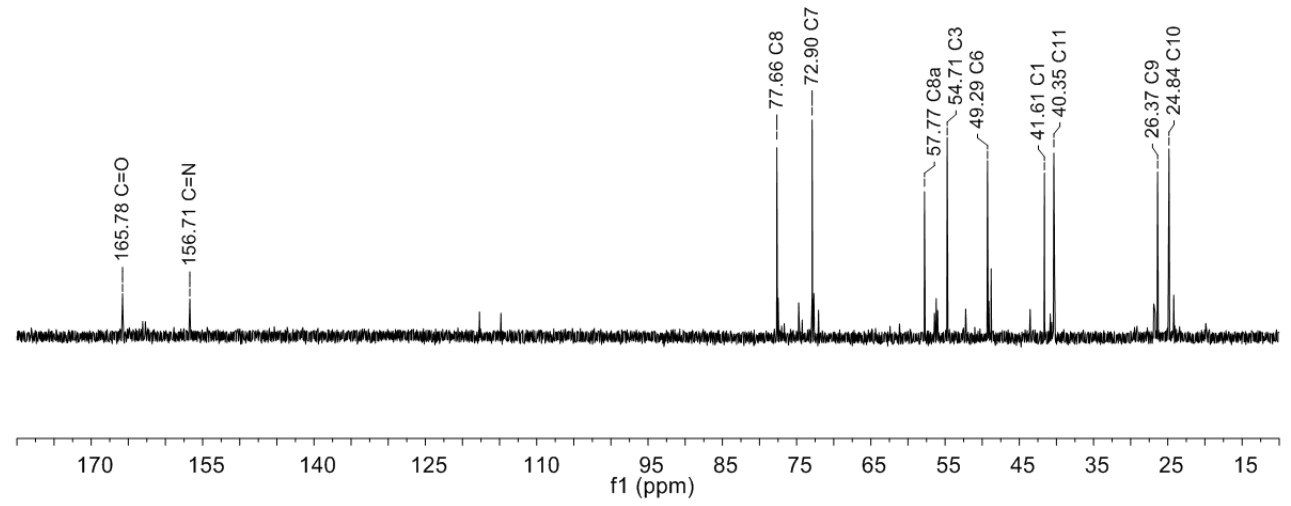

c)

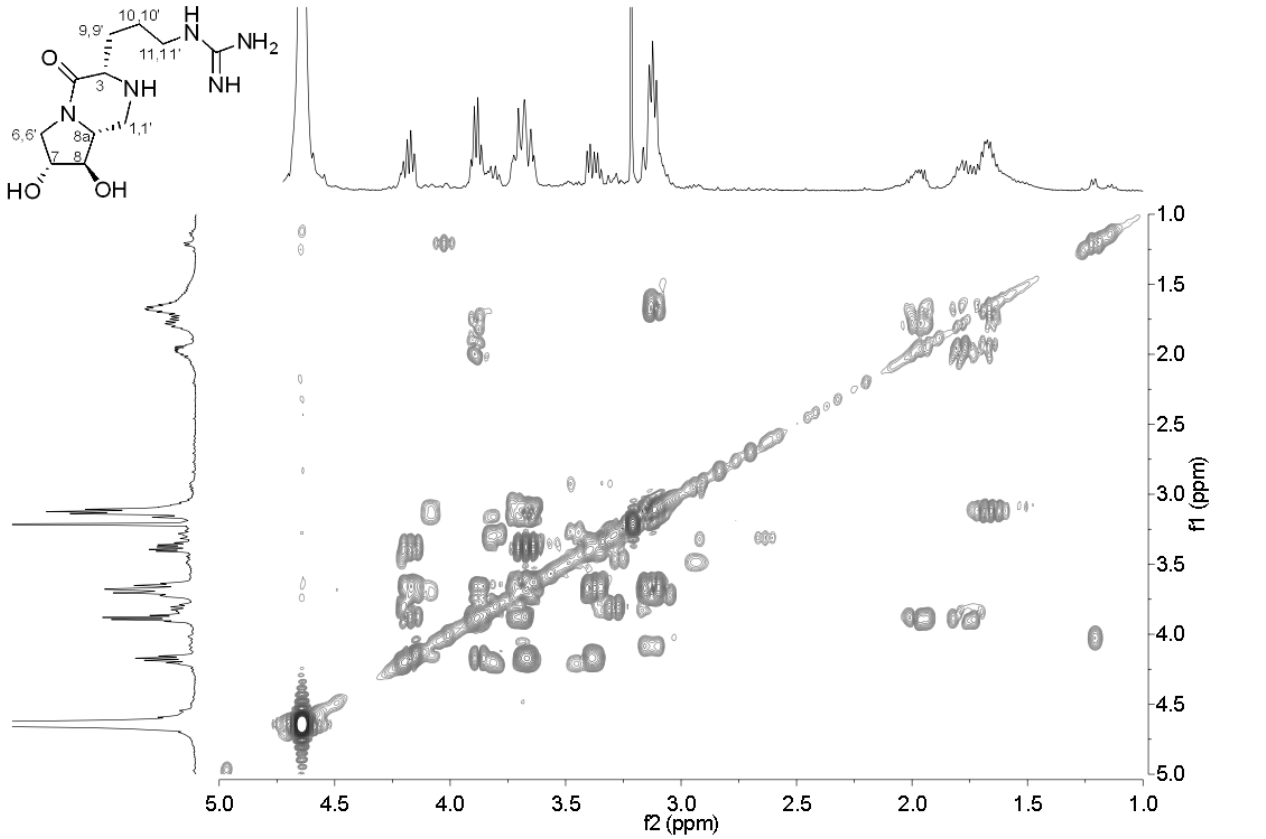

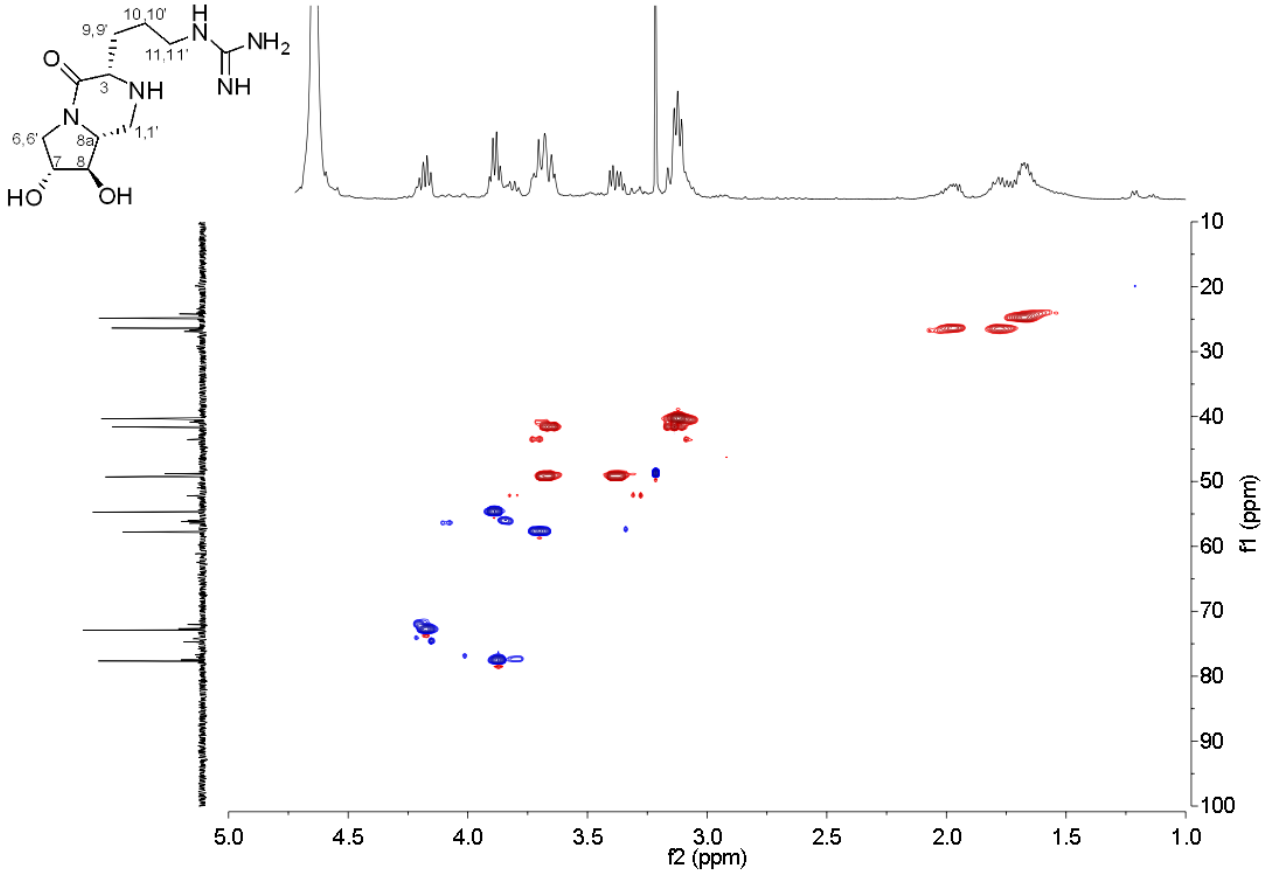

d)

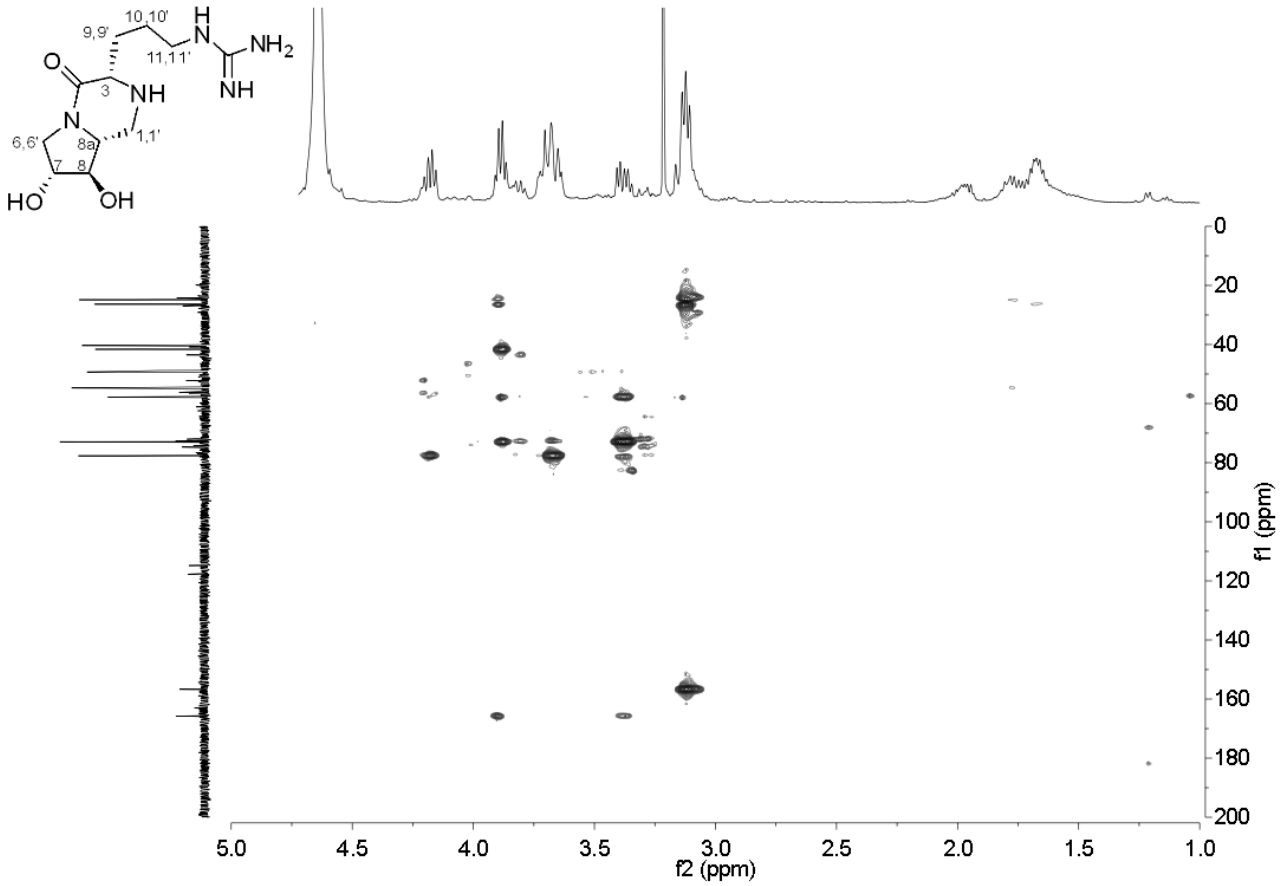

Figure 23. Caracterization of the proline derivative (**26v**) after purification. Coexistence of 3 species: two fused tricyclic species (**28v**), corresponding to the inversion of the nitrogen bridgehead, and one DAB-proline amide conjugate, (*S*)-1-(((2*R*,3*R*,4*R*)-3,4-dihydroxypyrrolidin-2-yl)methyl)pyrrolidine-2-carboxamide.

a)

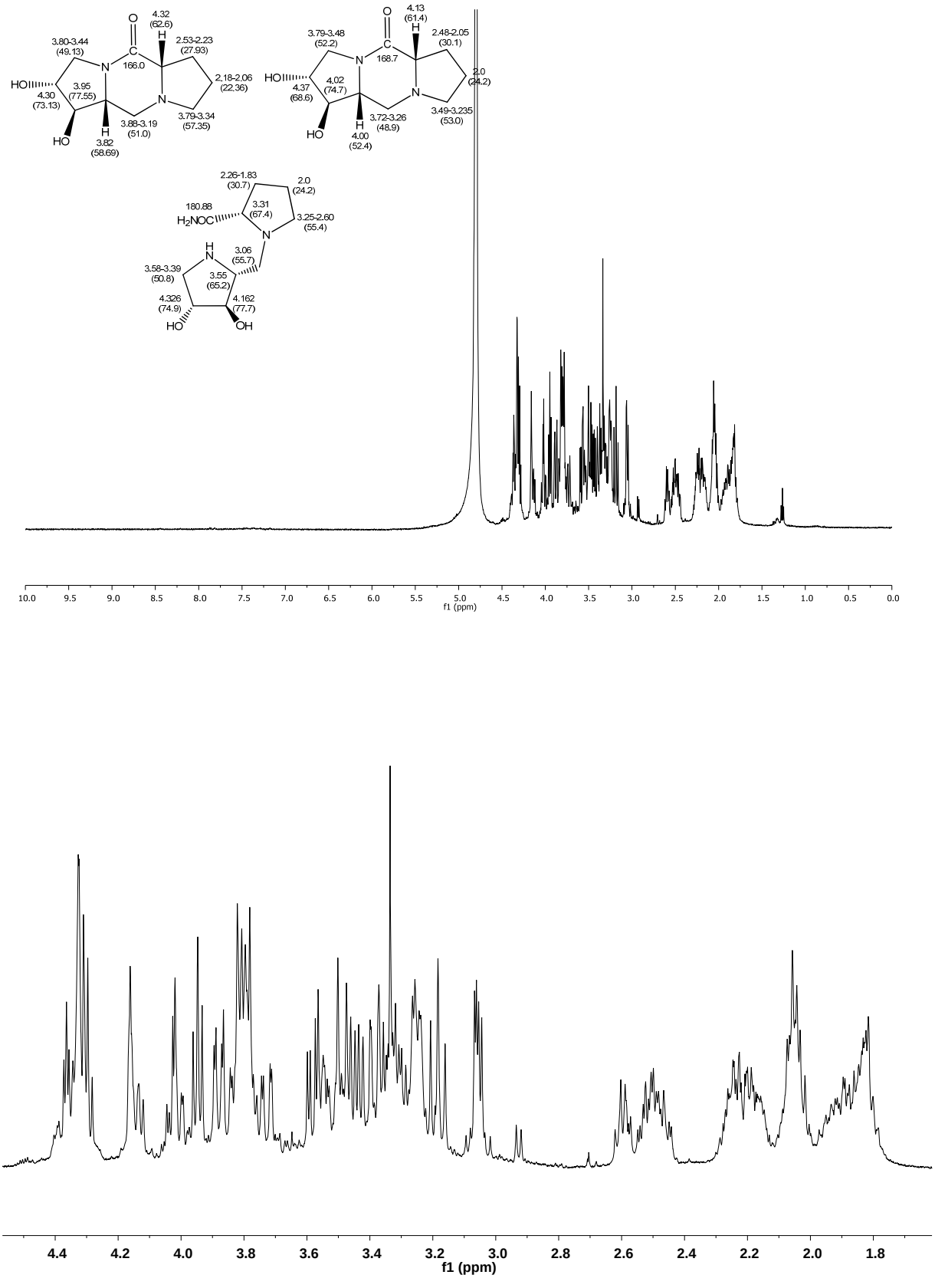

b)

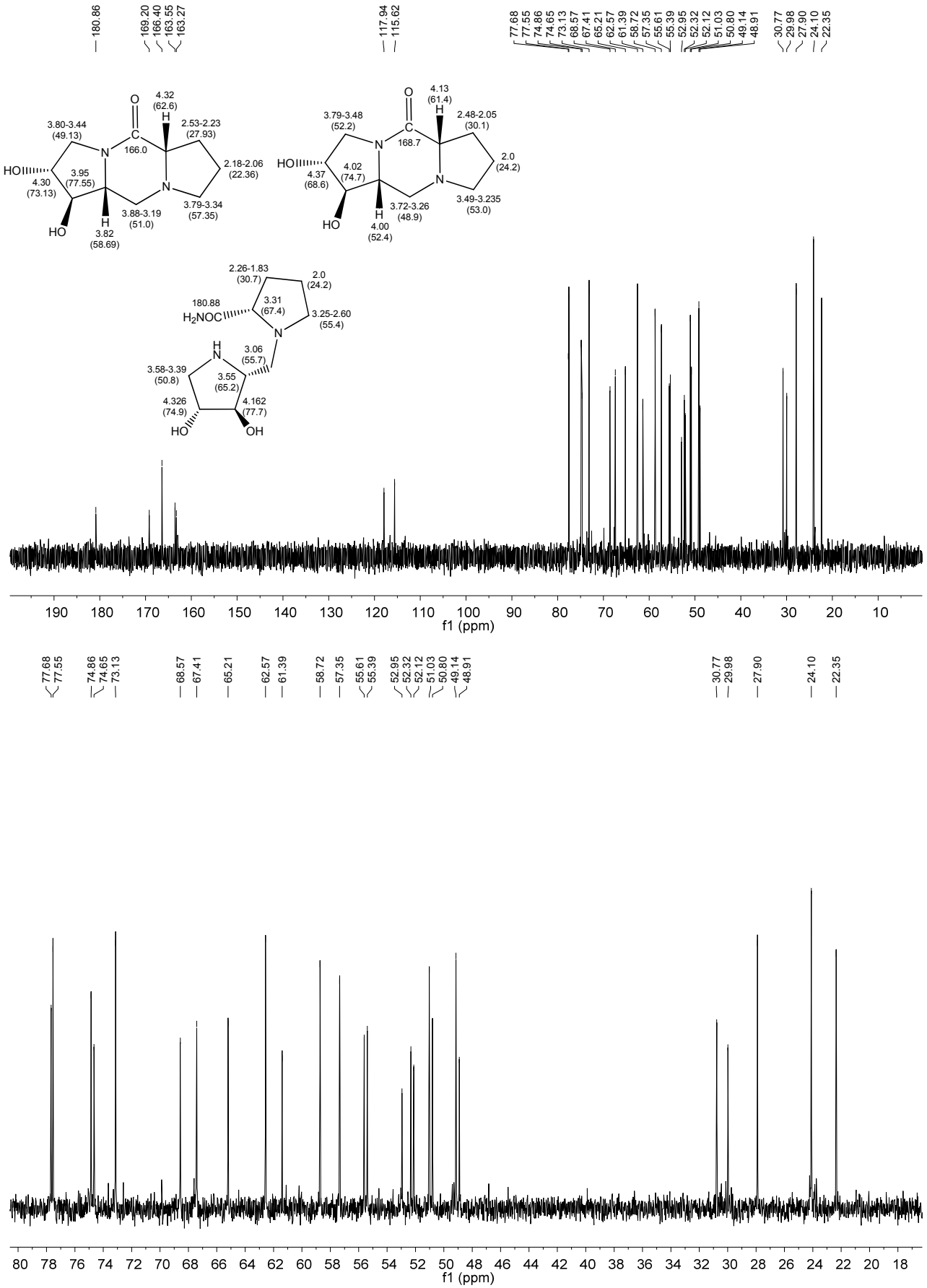
180.86
169.20
166.40
163.55
163.27
117.94
115.62
77.68
77.55
74.86
74.65
73.13
68.57
67.41
65.21
62.57
61.39
58.72
57.35
55.61
55.39
52.95
52.32
52.12
51.03
50.80
49.14
48.91
30.77
29.98
27.90
24.10
22.35
f1 (ppm)

c)

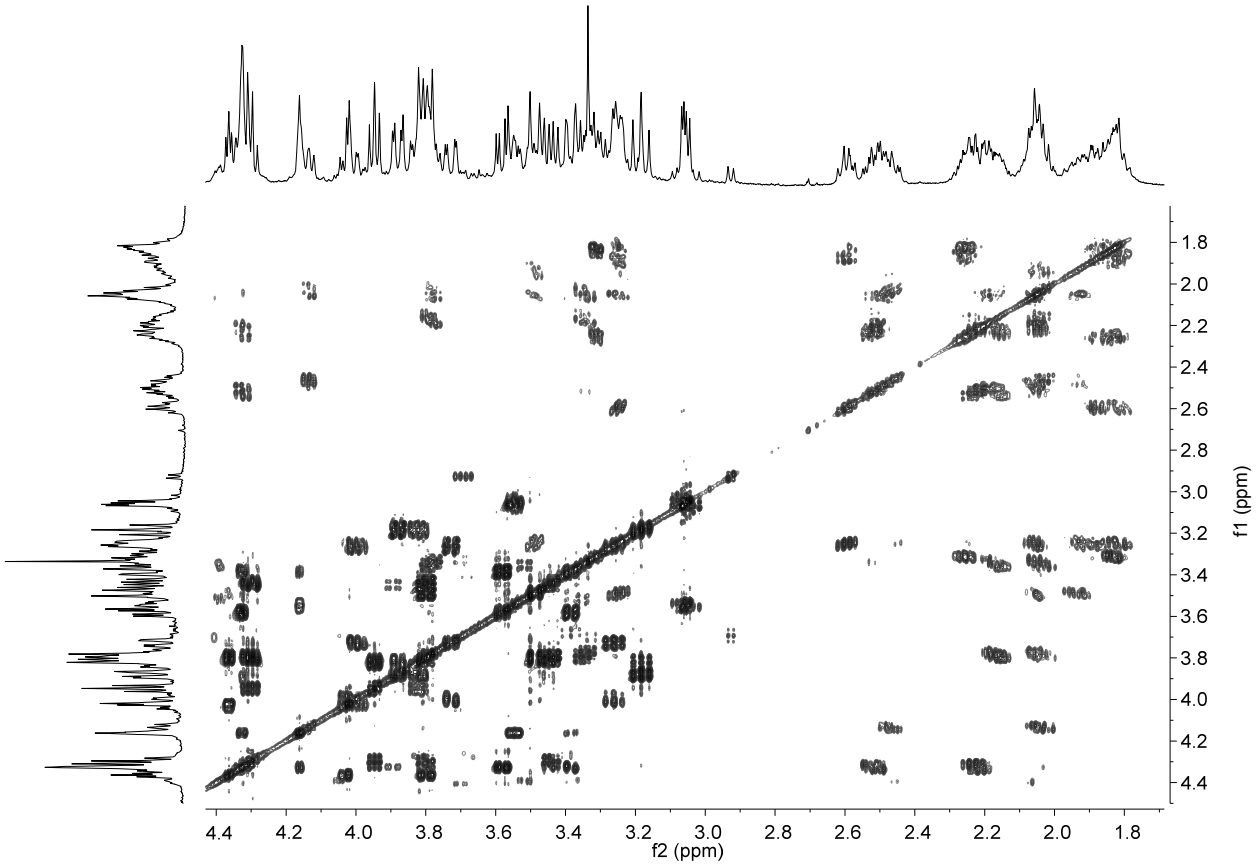

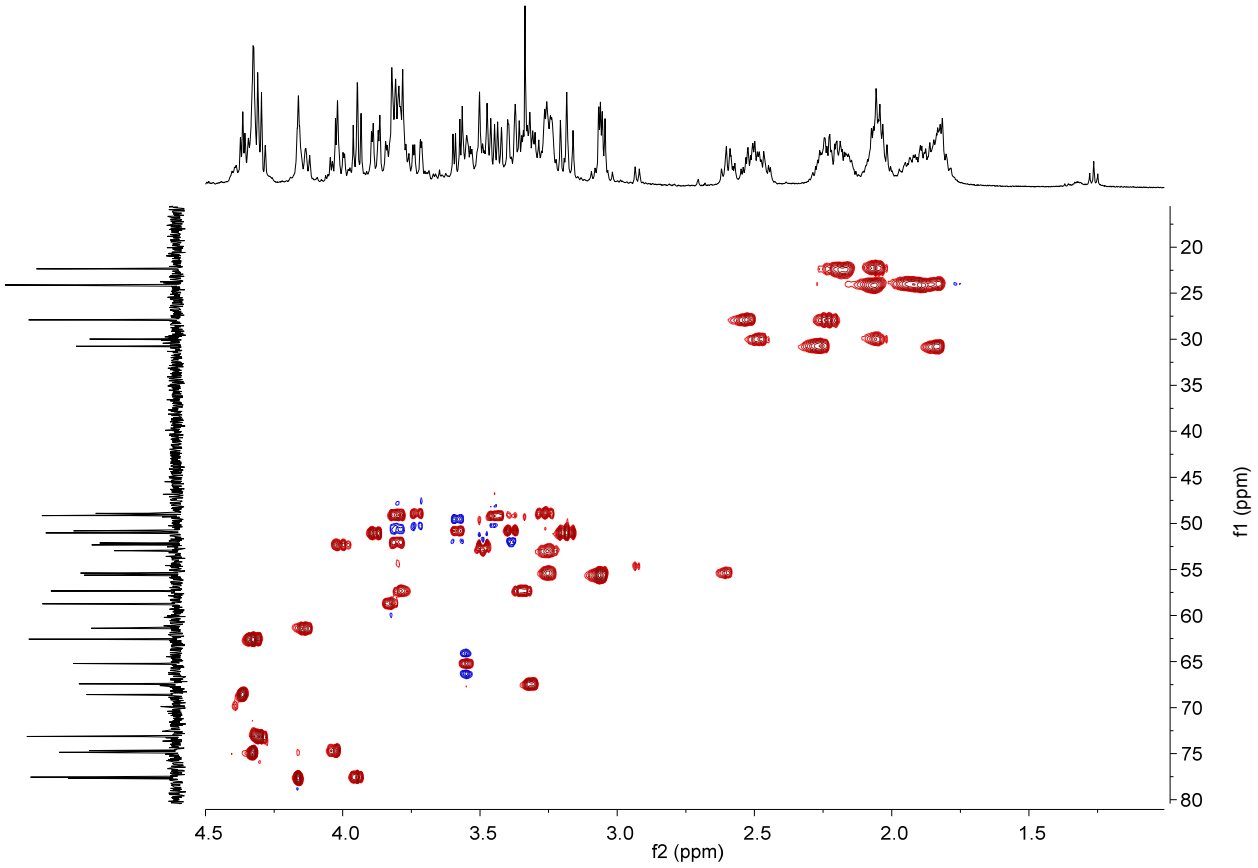

d)

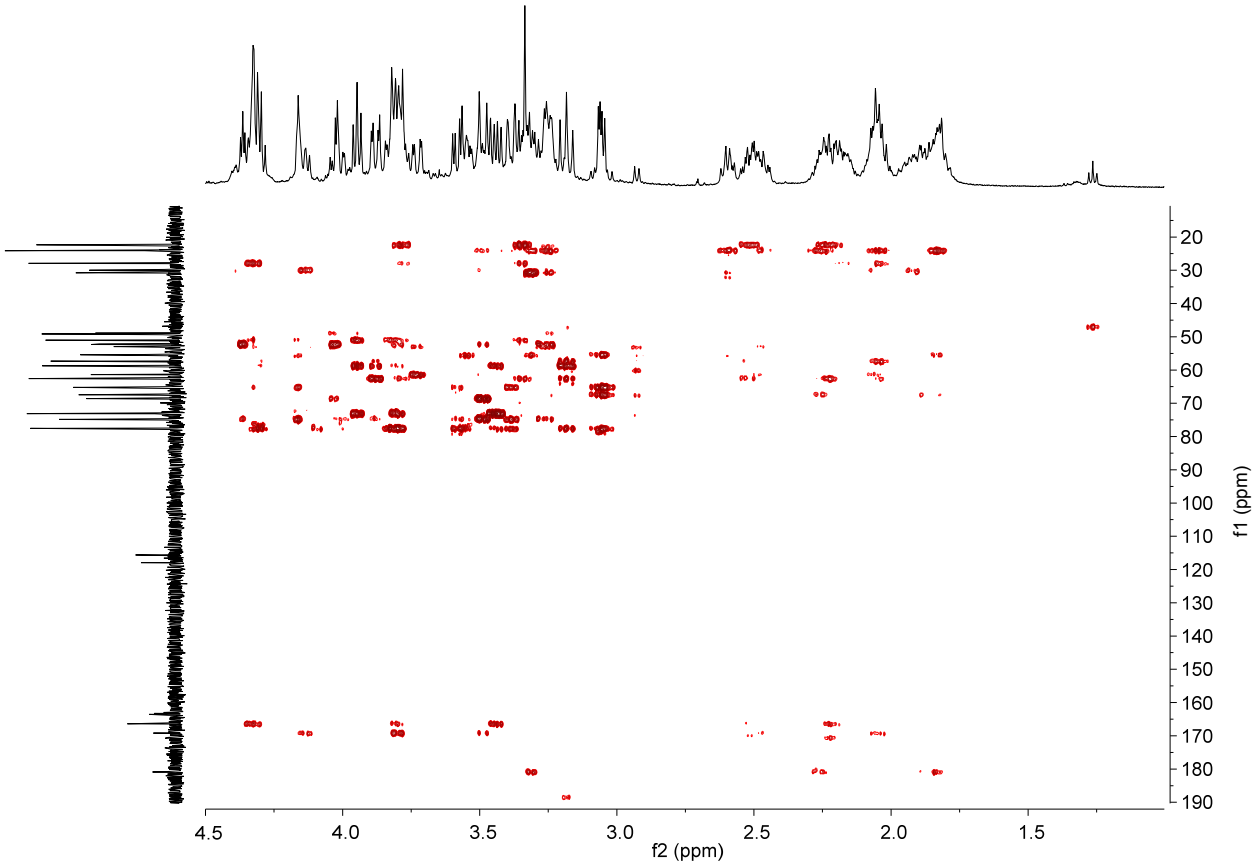
20
30
40
50
60
70
80
90
100
110
120
130
140
150
160
170
180
190
f1 (ppm)
4.5
4.0
3.5
3.0
2.5
2.0
1.5
f2 (ppm)

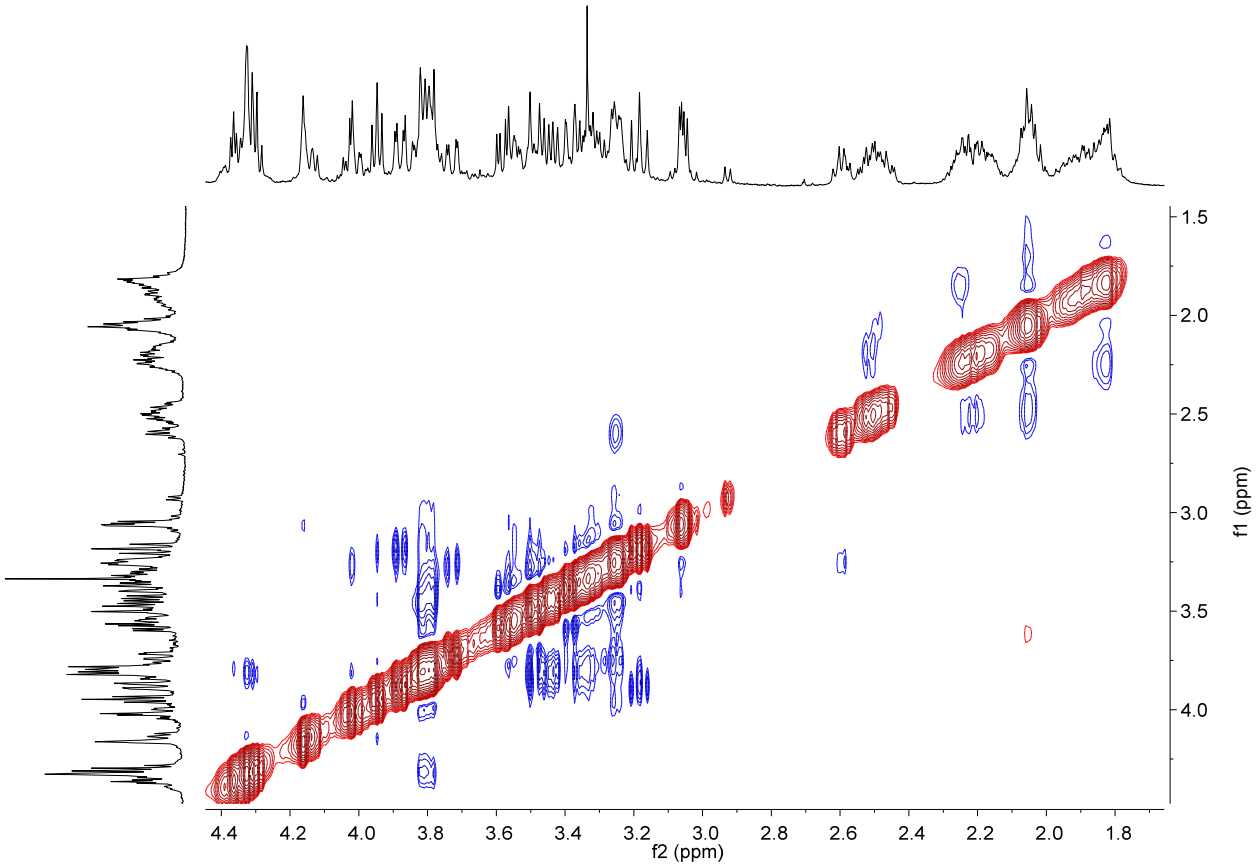
1.5
2.0
2.5
3.0
3.5
4.0
f1 (ppm)
4.4
4.2
4.0
3.8
3.6
3.4
3.2
3.0
2.8
2.6
2.4
2.2
2.0
1.8
f2 (ppm)

Figure 24. Observed NMR spectra of **28v**: a) ^{1}H, b) ^{13}C, c) 2D ^{1}H-^{1}H COSY and 2D multiplicity-edited HSQC and d).magnitude-mode ge-2D HMBC.

a)

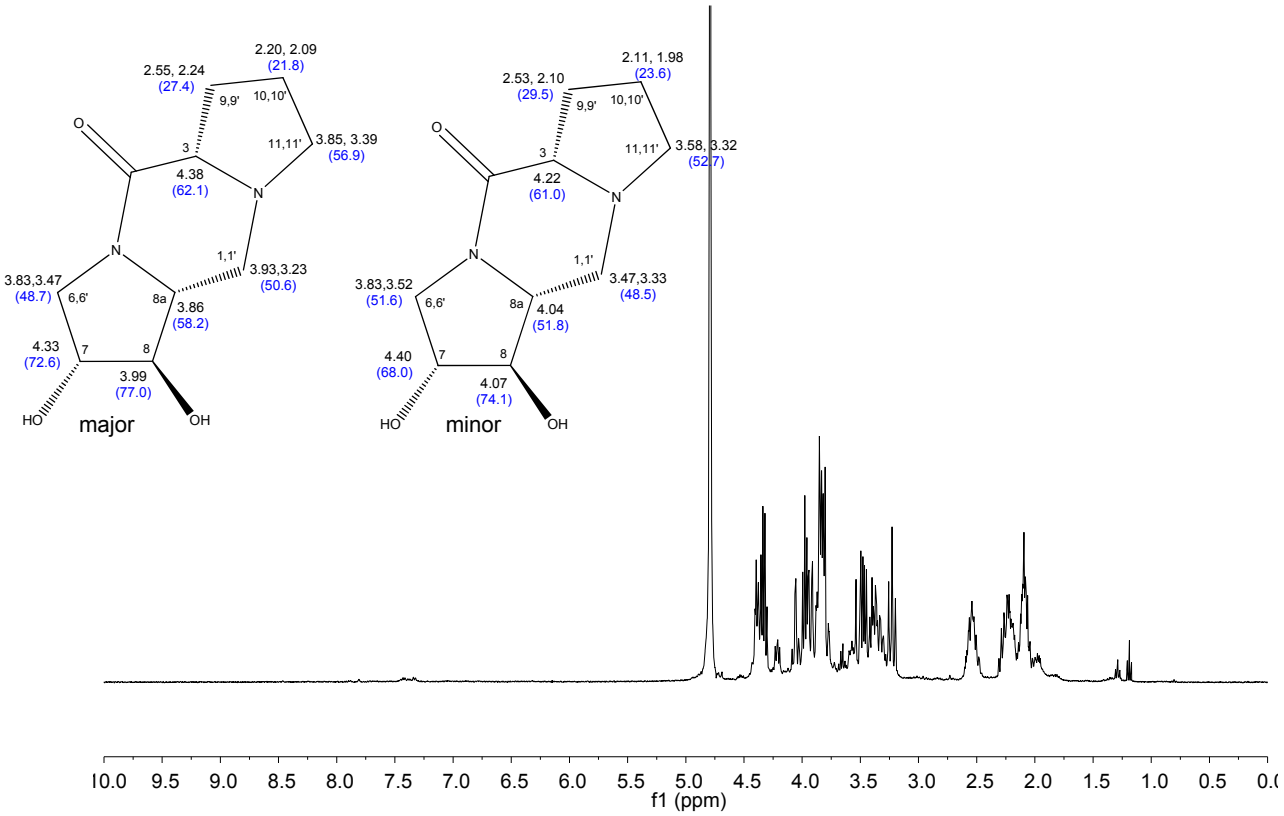

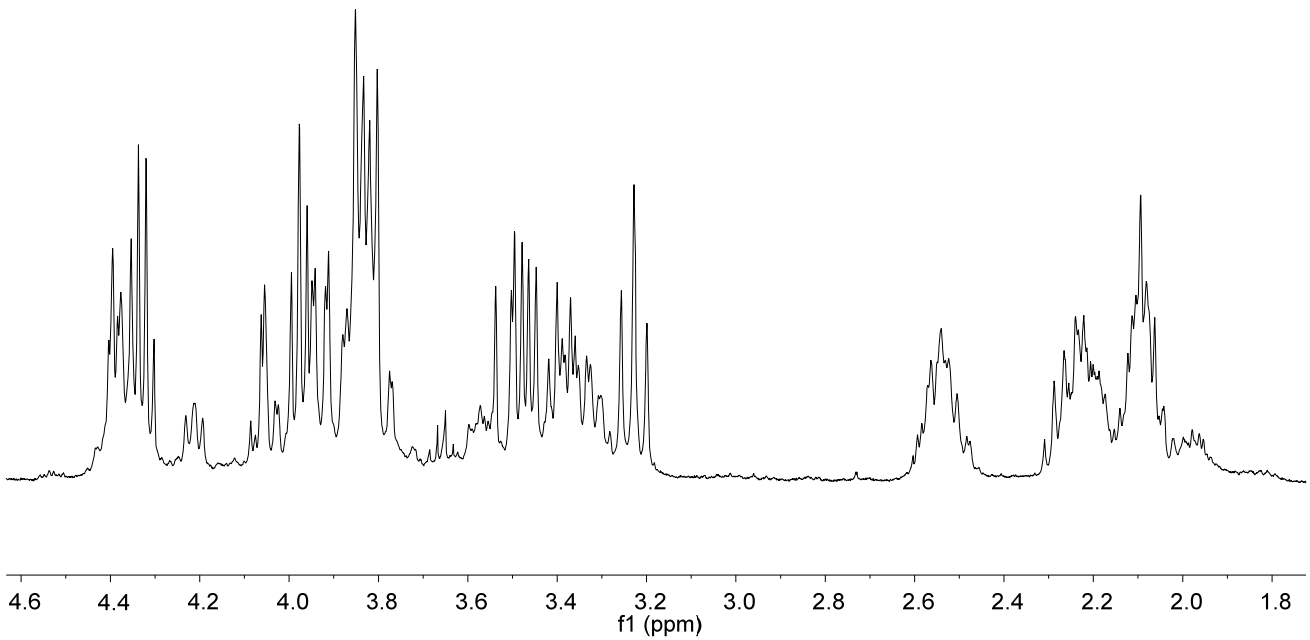

b)

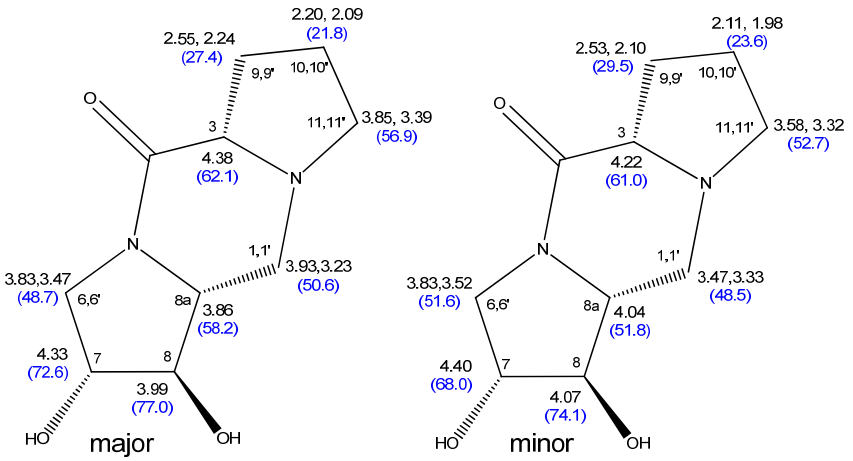

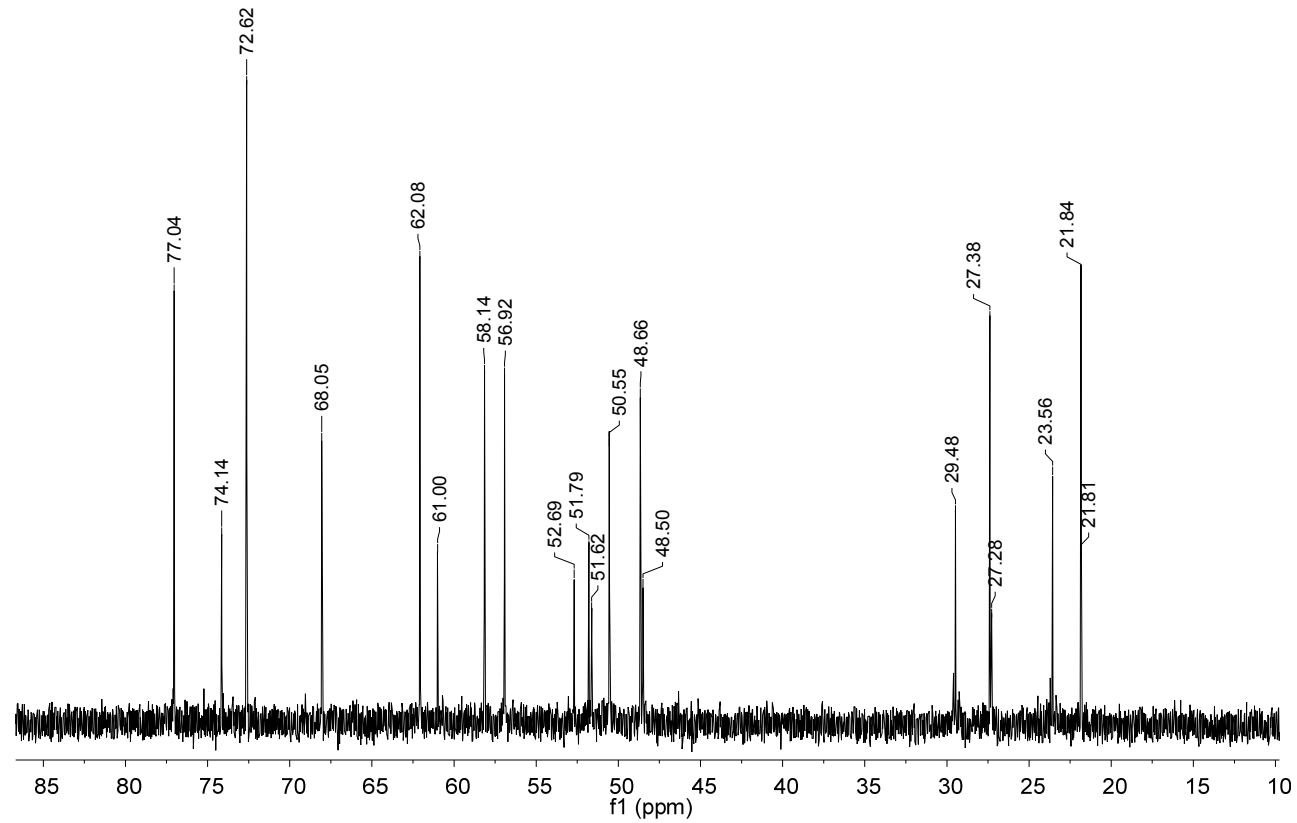

c)

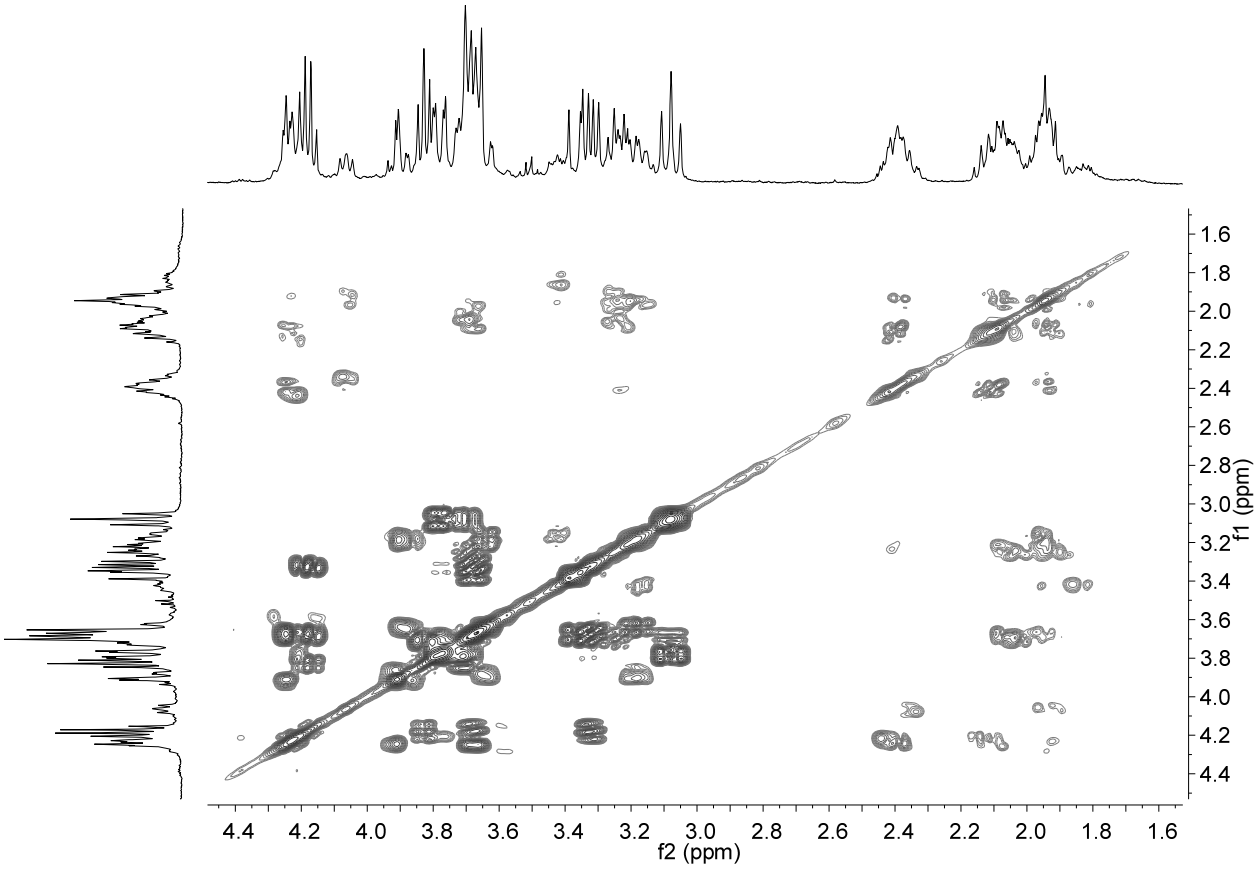

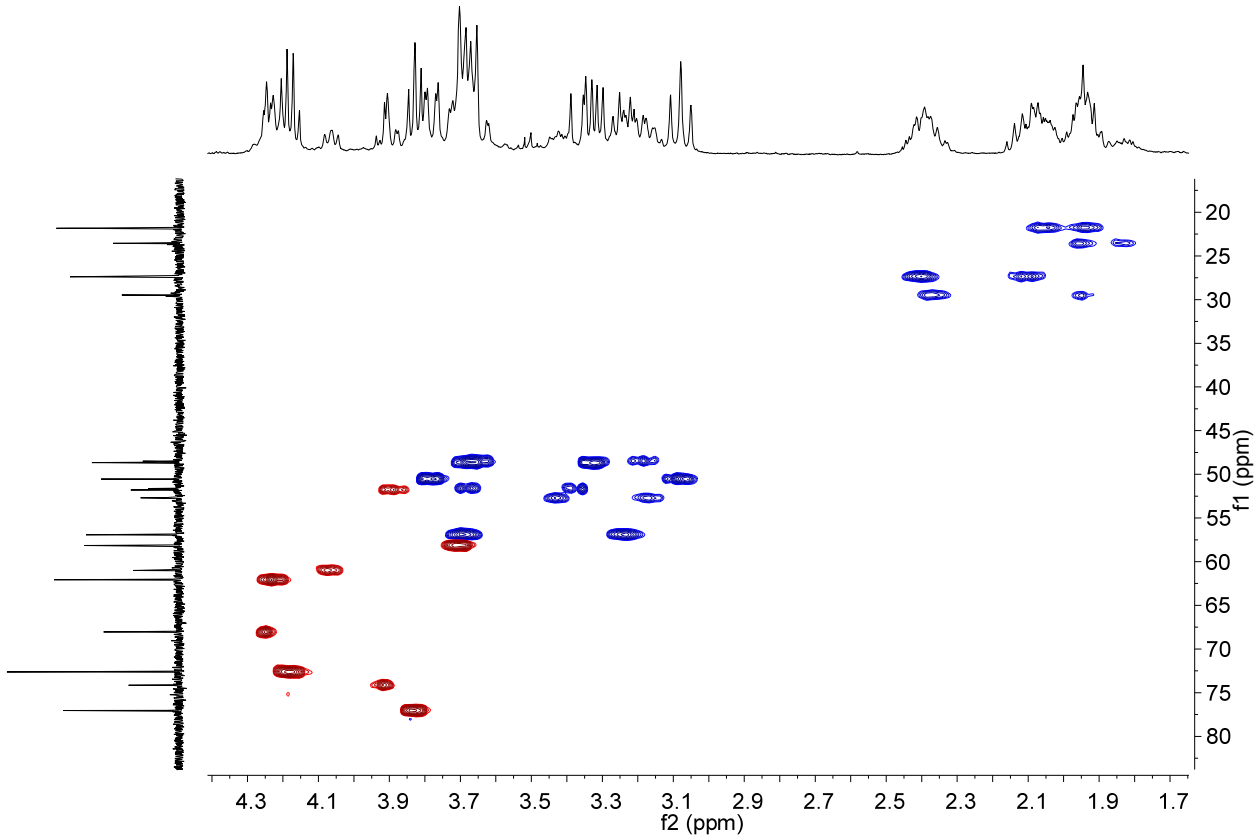

Figure 25. Observed NMR spectra of **30o**: a) ^{1}H, b) ^{13}C, c) 2D ^{1}H-^{1}H COSY and 2D multiplicity-edited HSQC.

a)

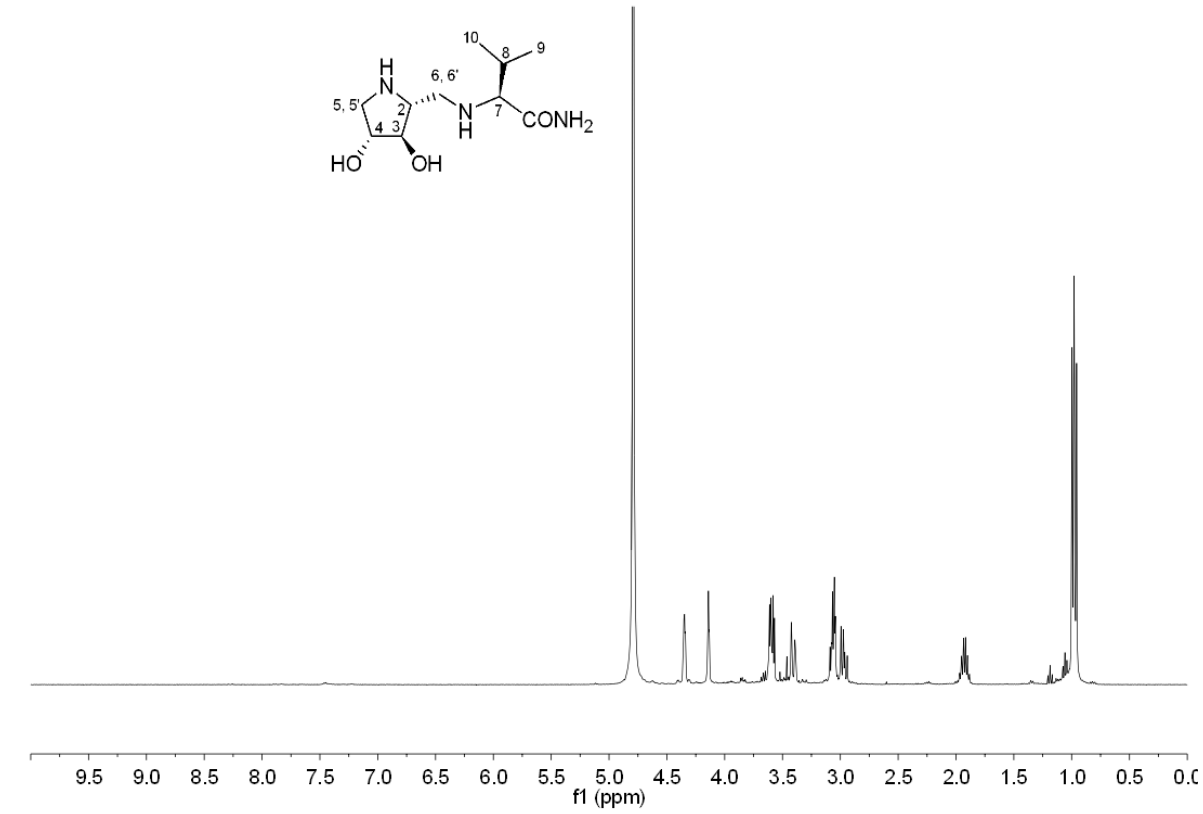

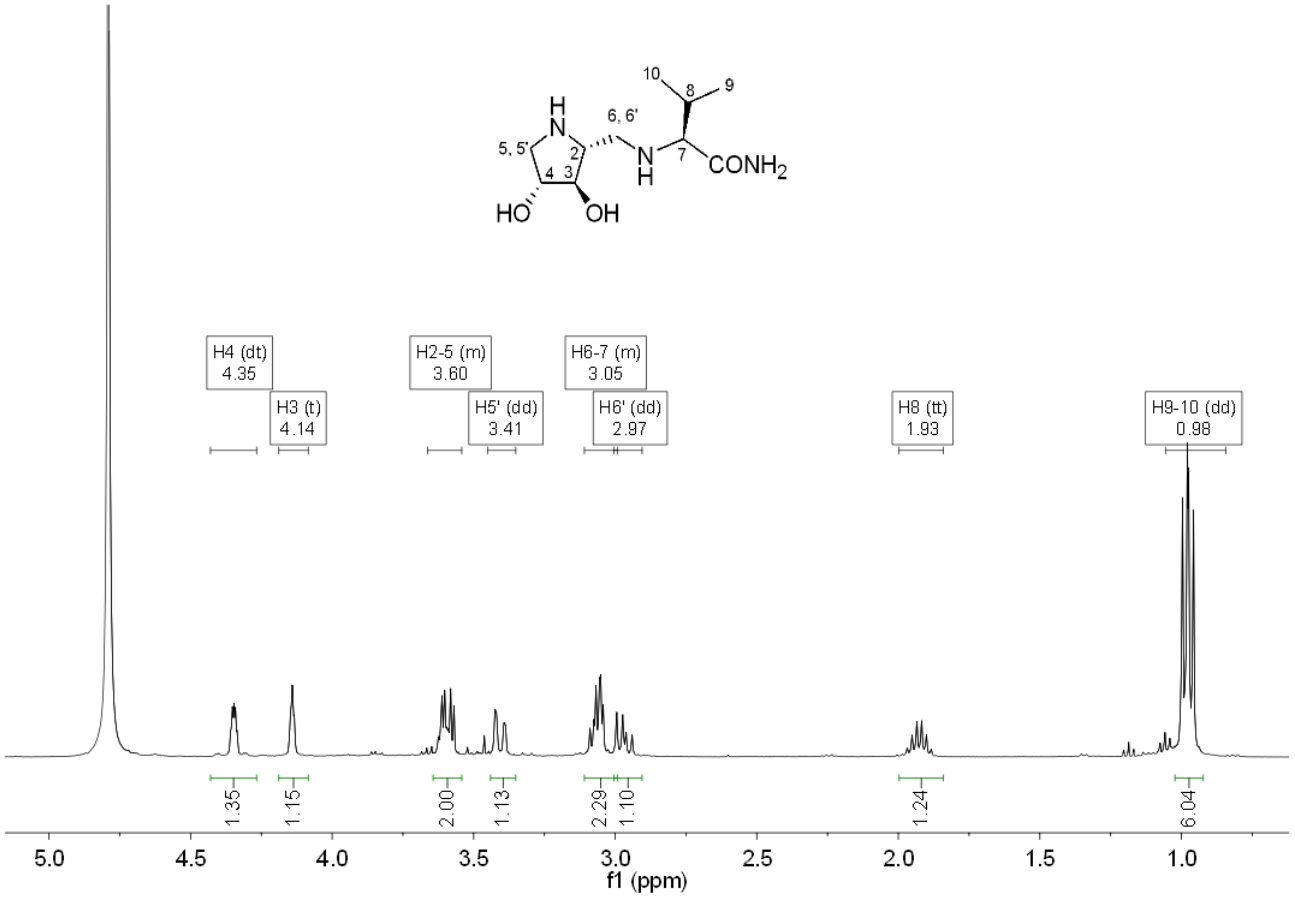

b)

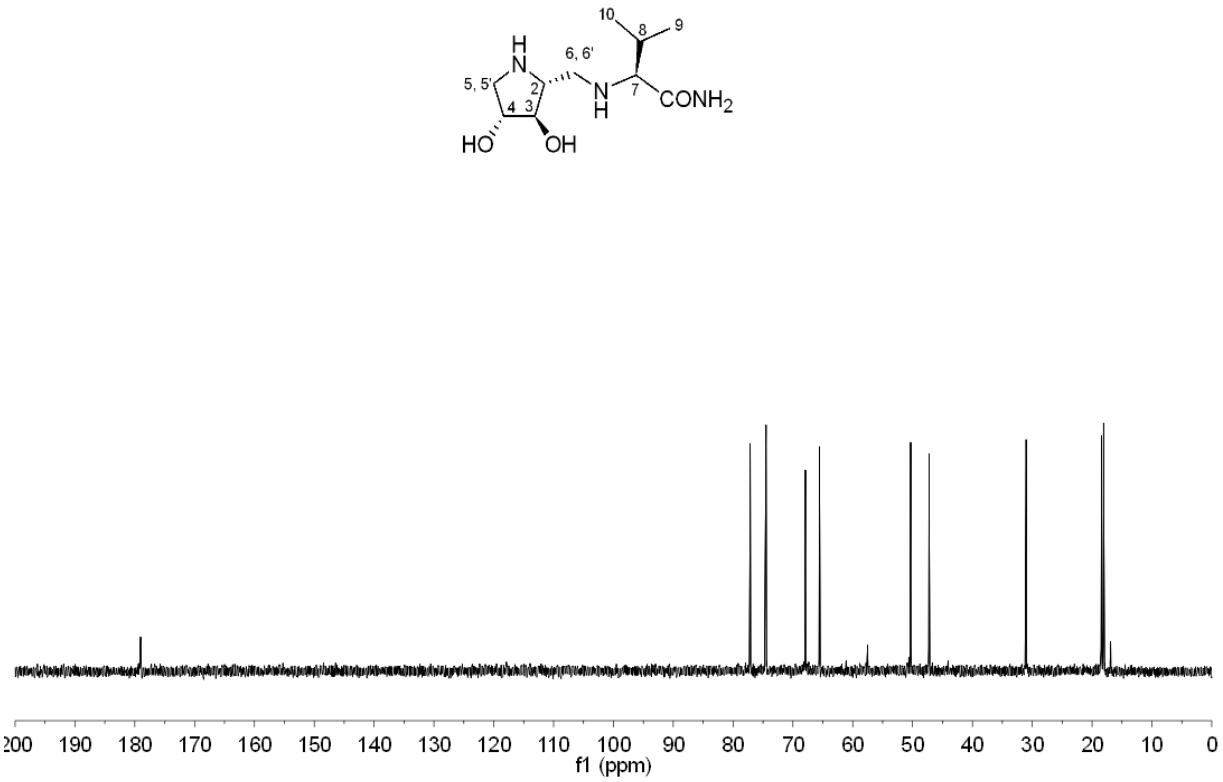

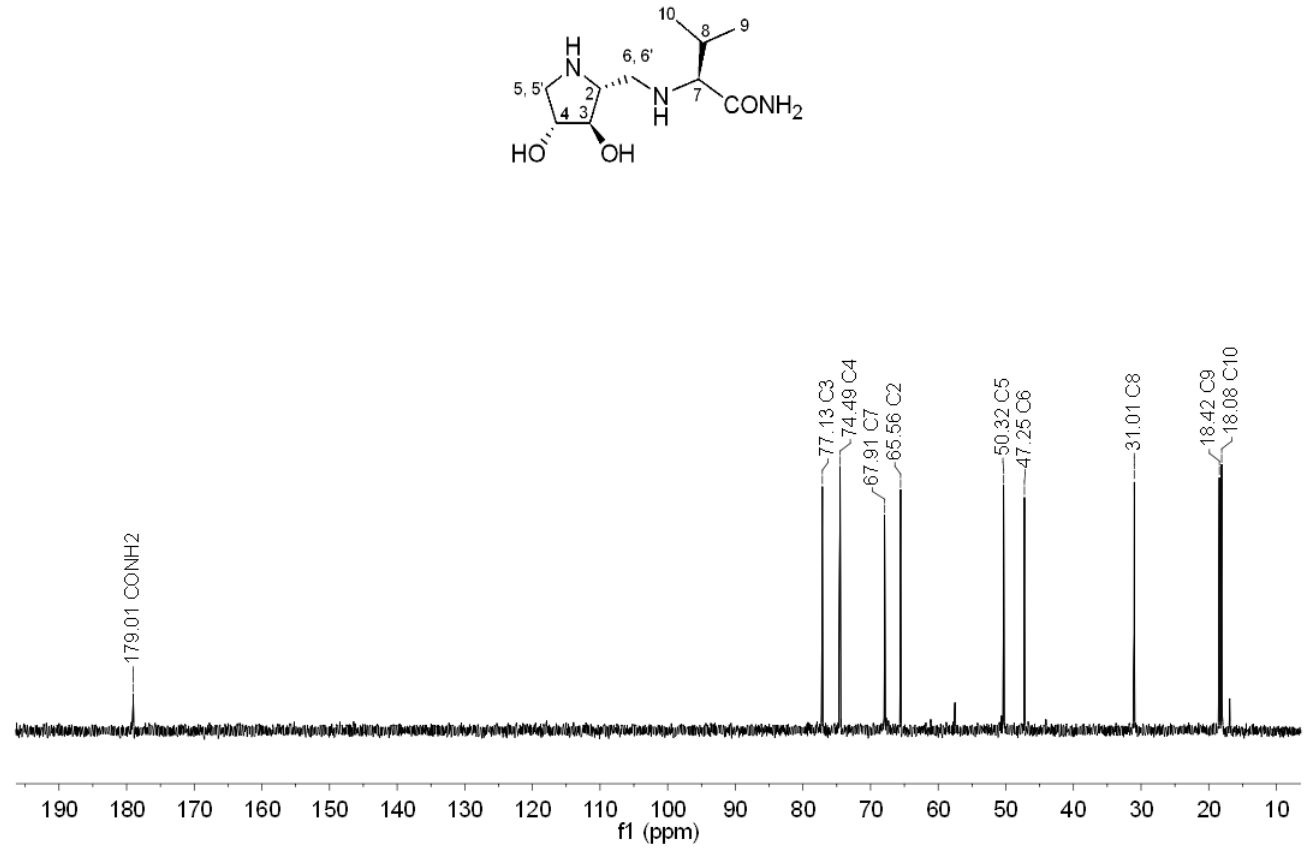

c)

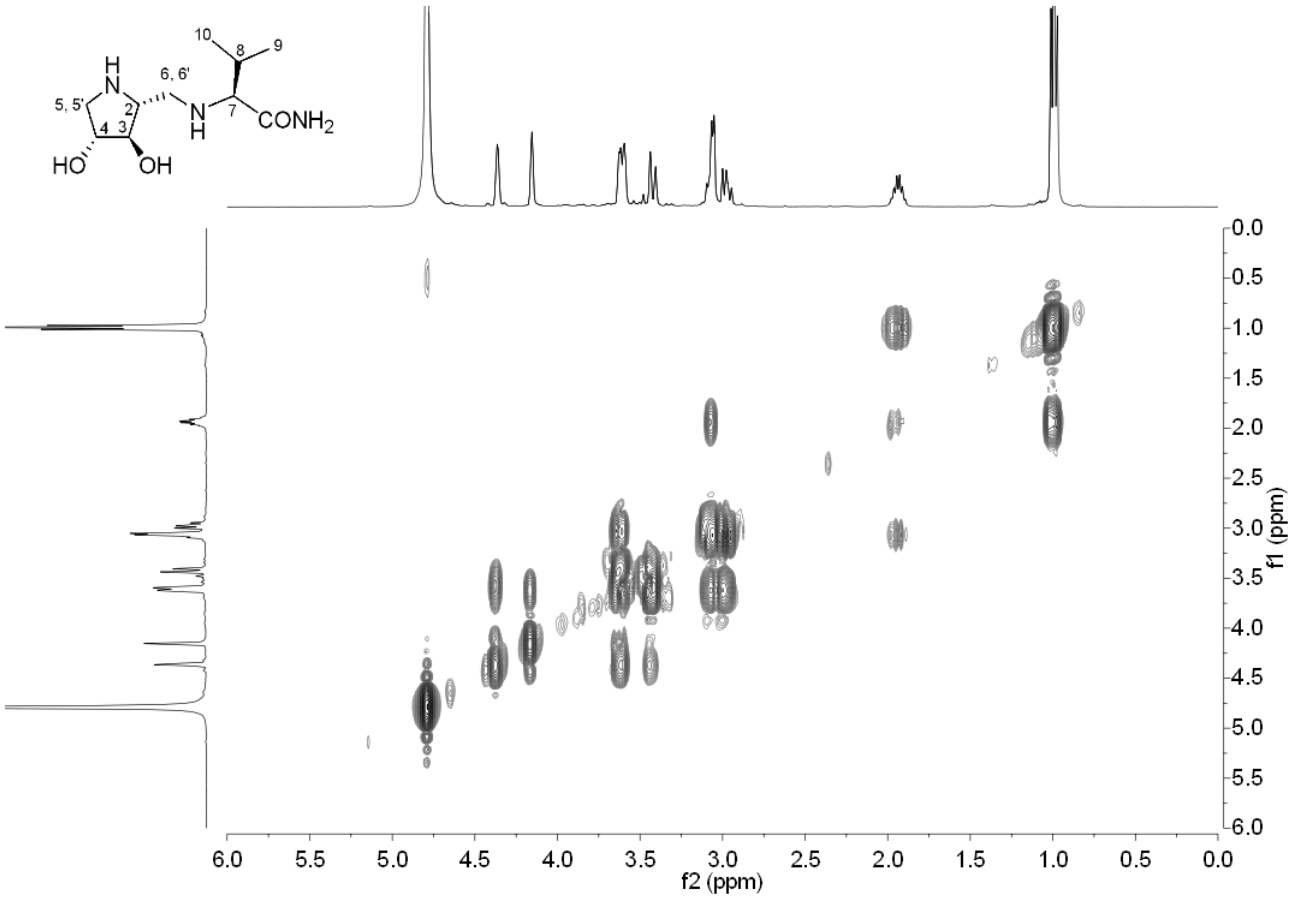

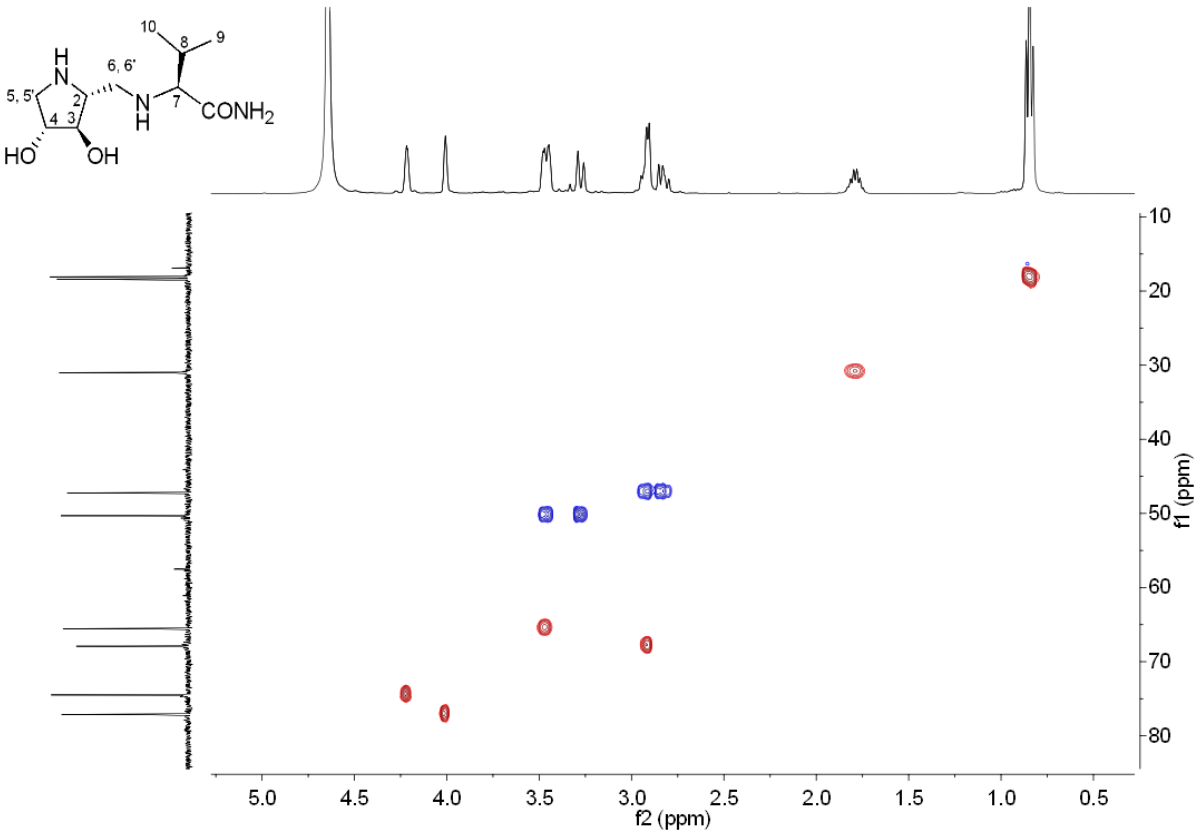

Figure 26. Observed NMR spectra of **30t** a) ^{1}H, b) ^{13}C, c) 2D ^{1}H-^{1}H COSY and 2D multiplicity-edited HSQC and d).magnitude-mode ge-2D HMBC.

a)

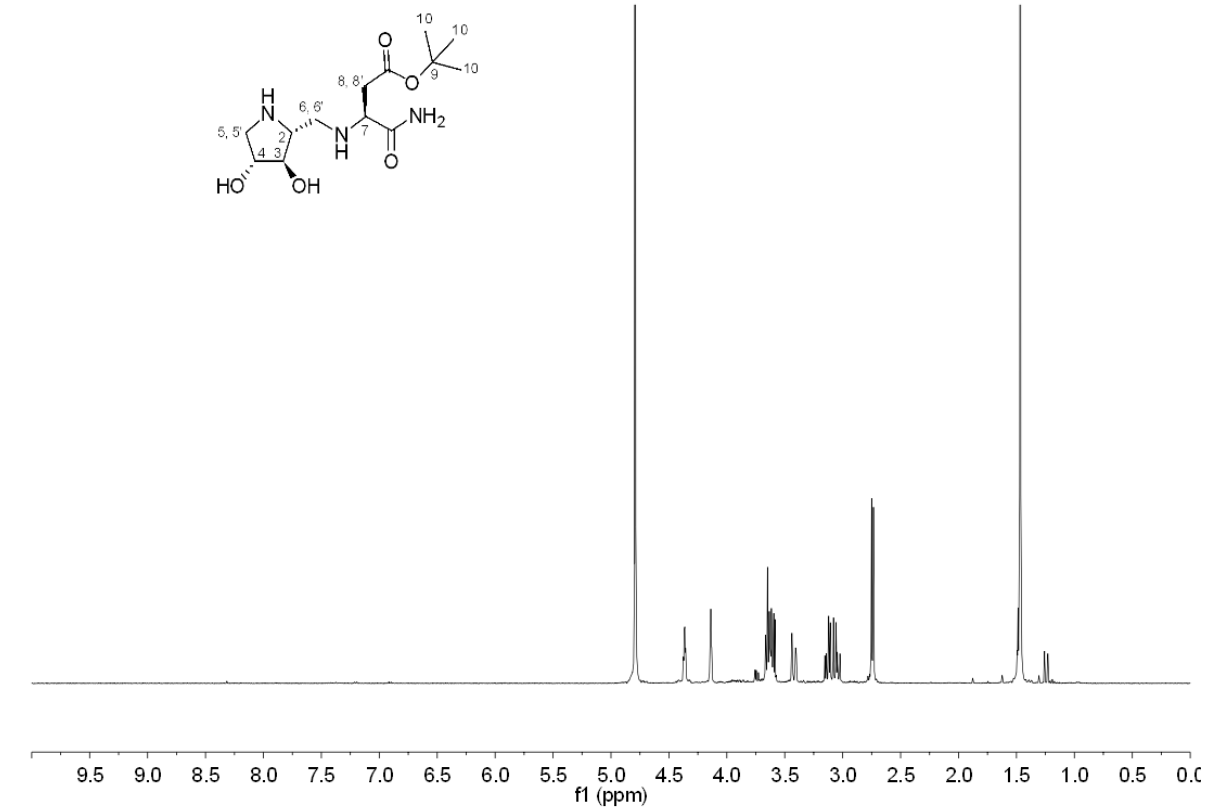

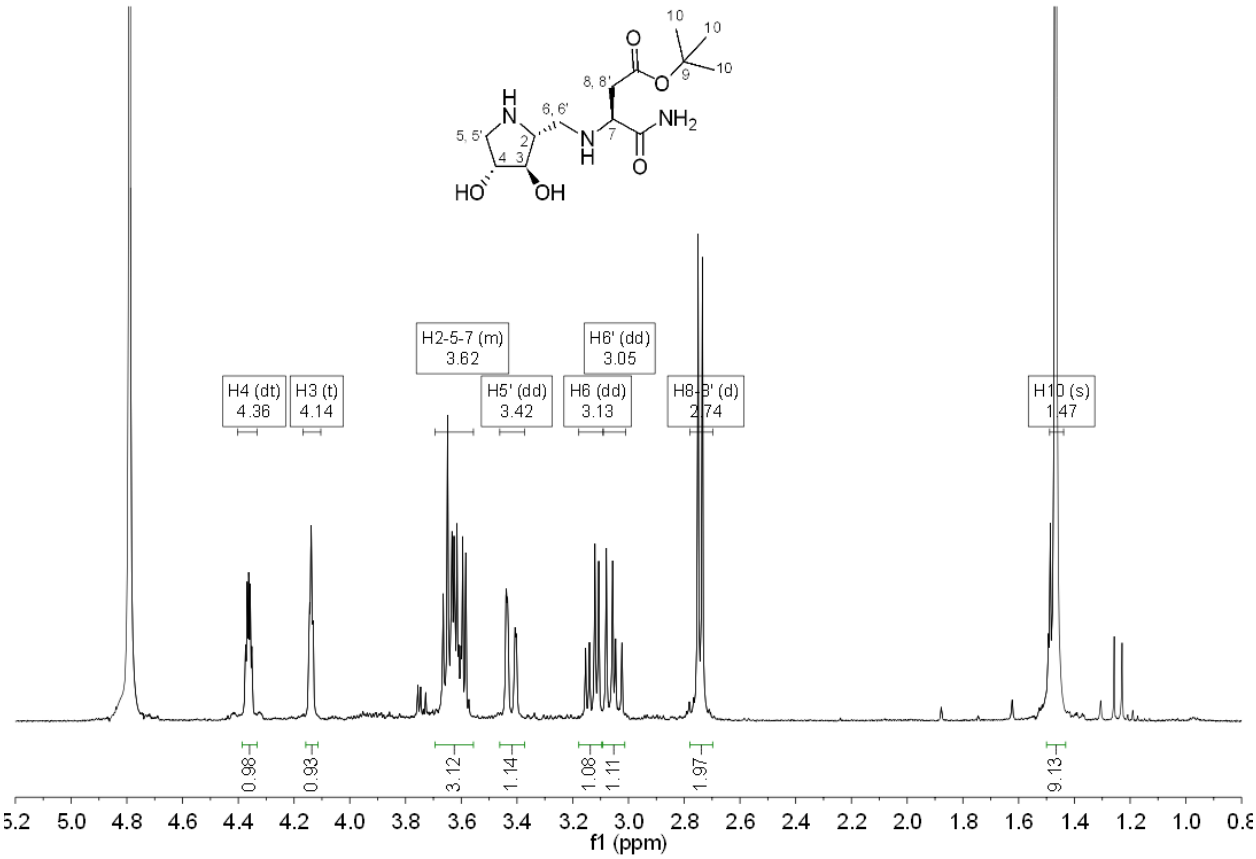

b)

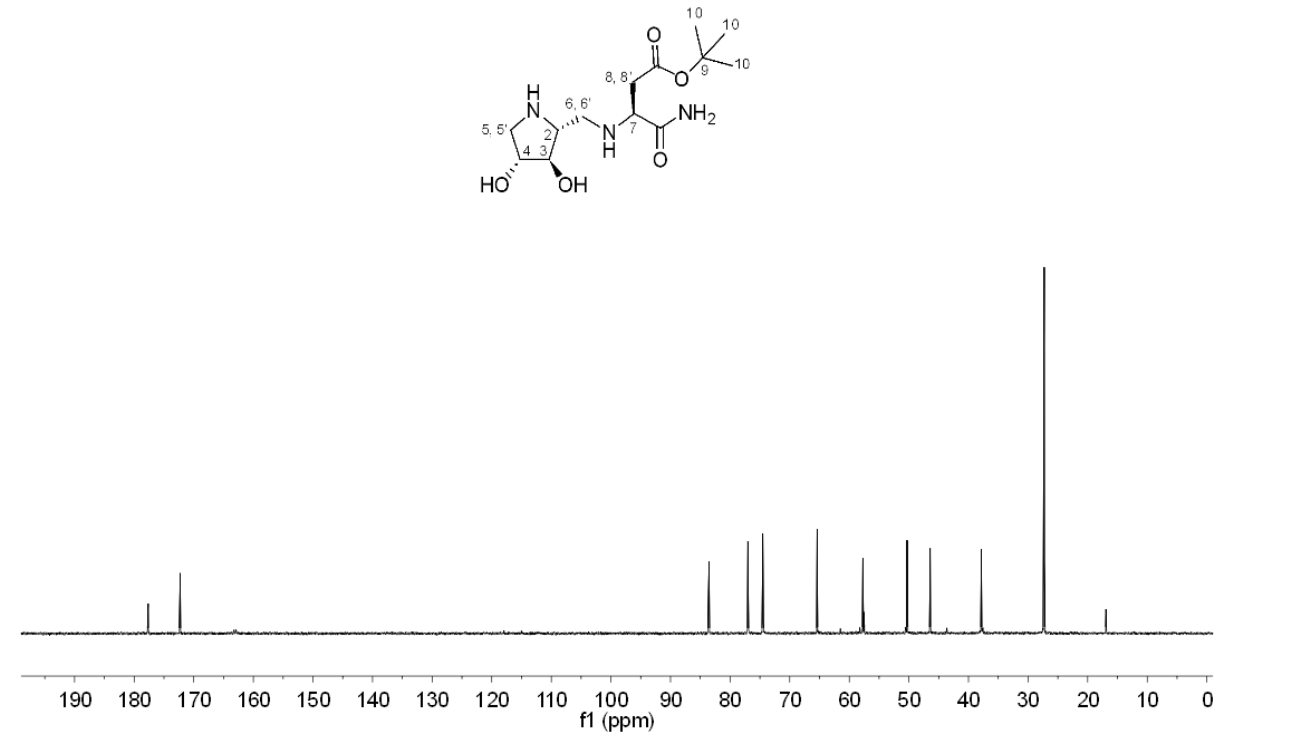

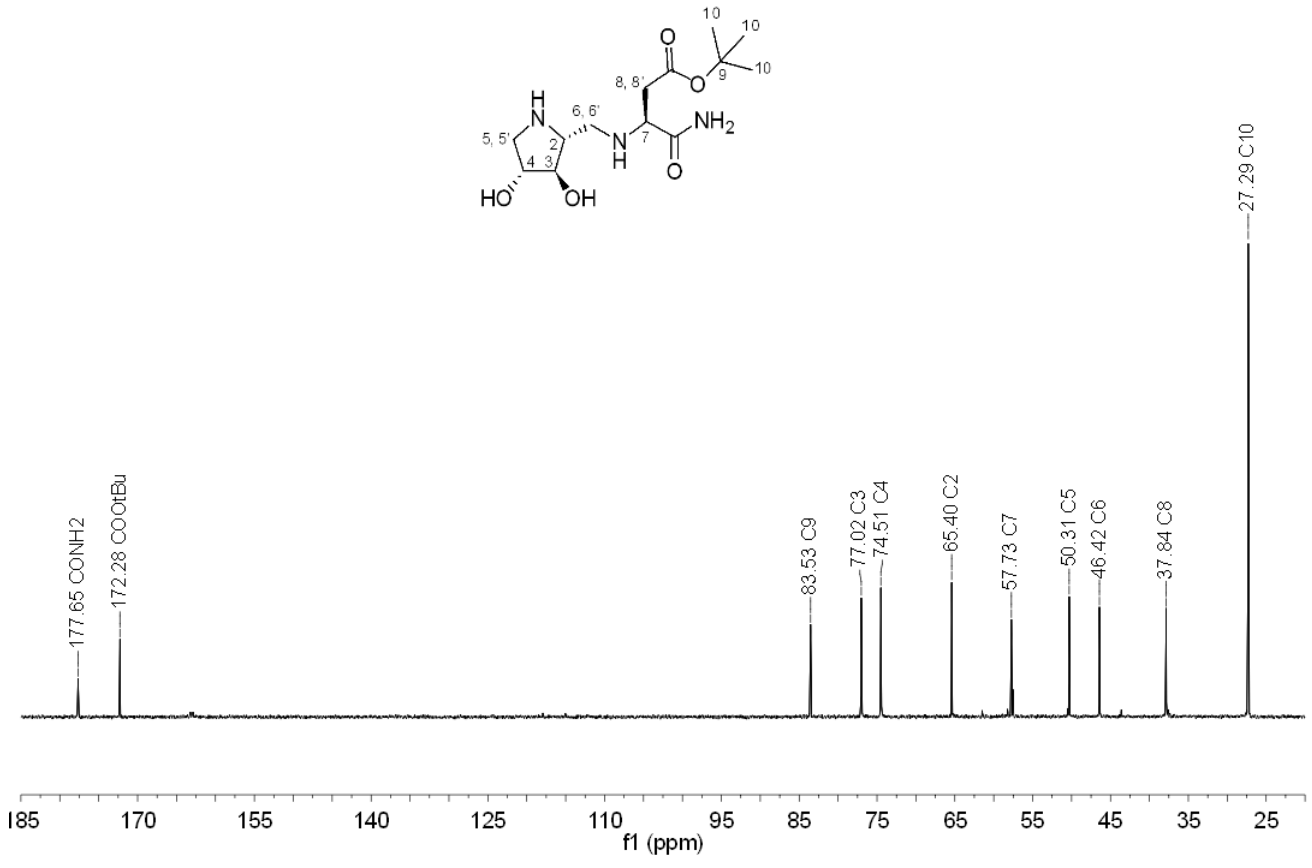

b)

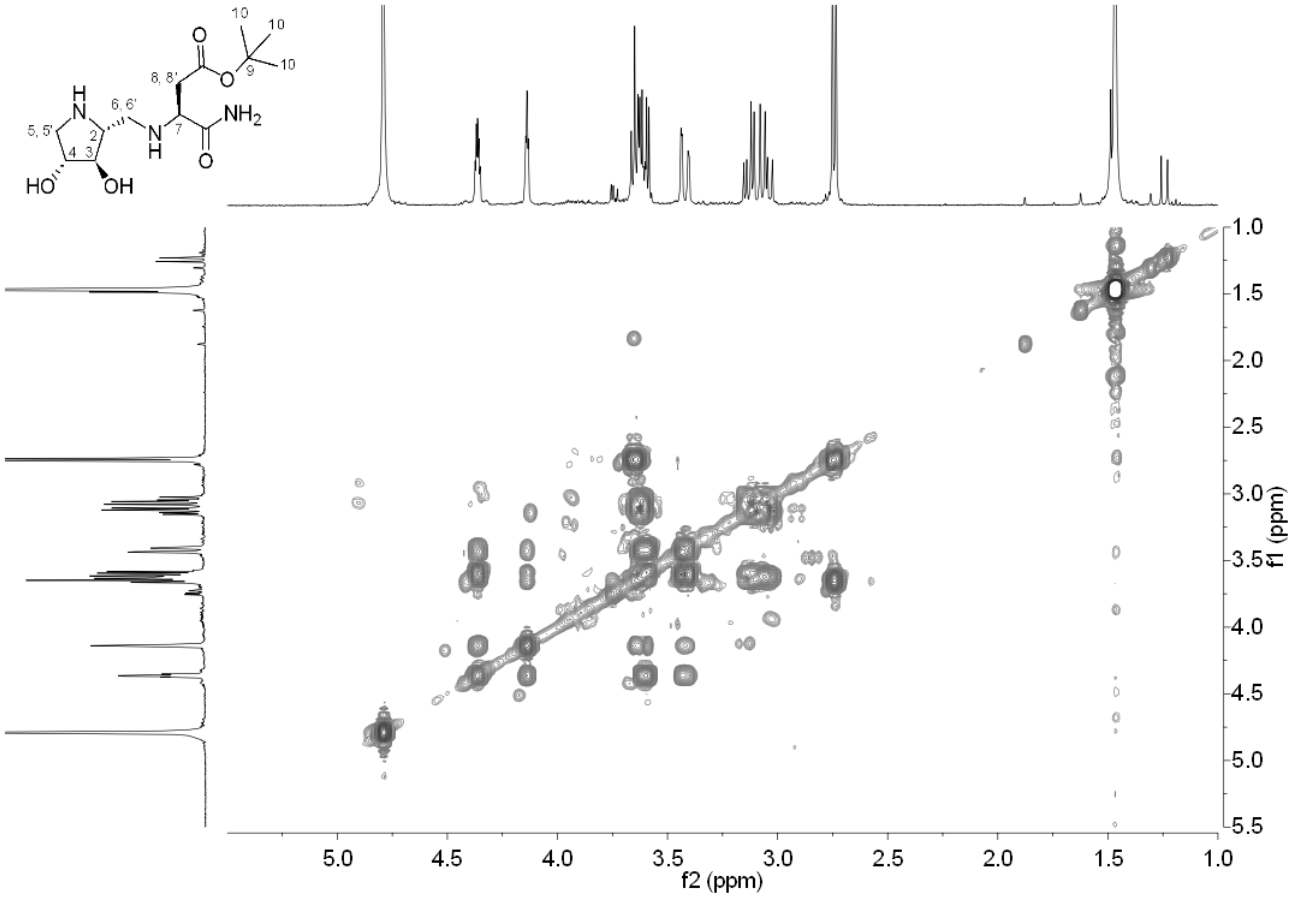

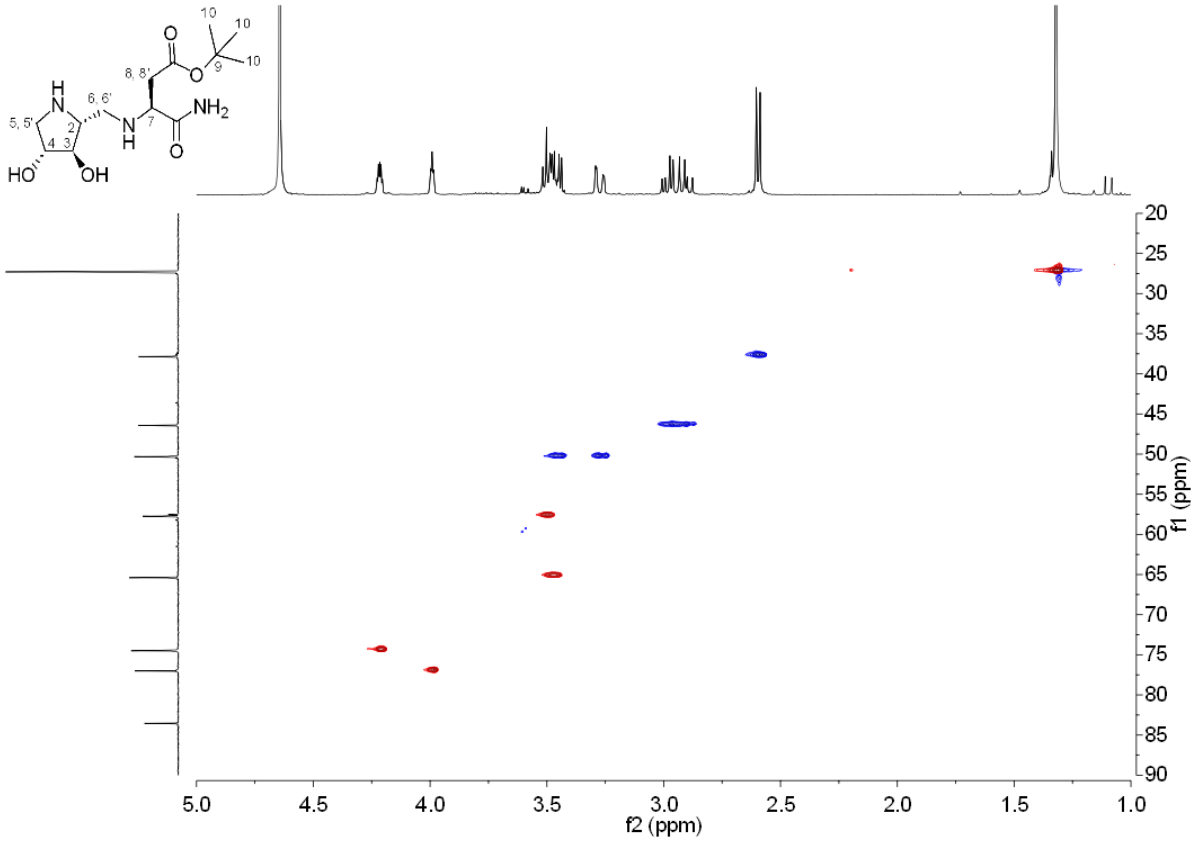

Figure 27. Observed NMR spectra of **29m**: a) ^{1}H, b) ^{13}C, c) 2D ^{1}H-^{1}H COSY and 2D multiplicity-edited HSQC and d).magnitude-mode ge-2D HMBC.

a)

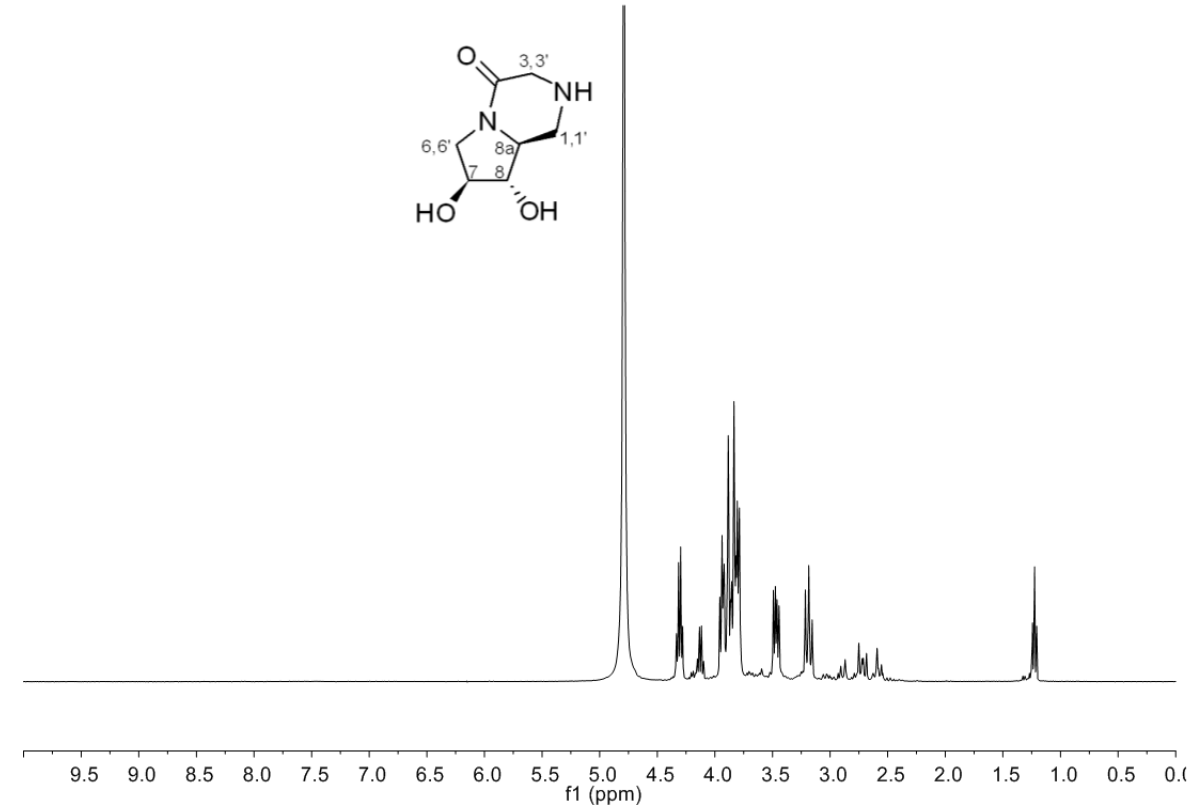

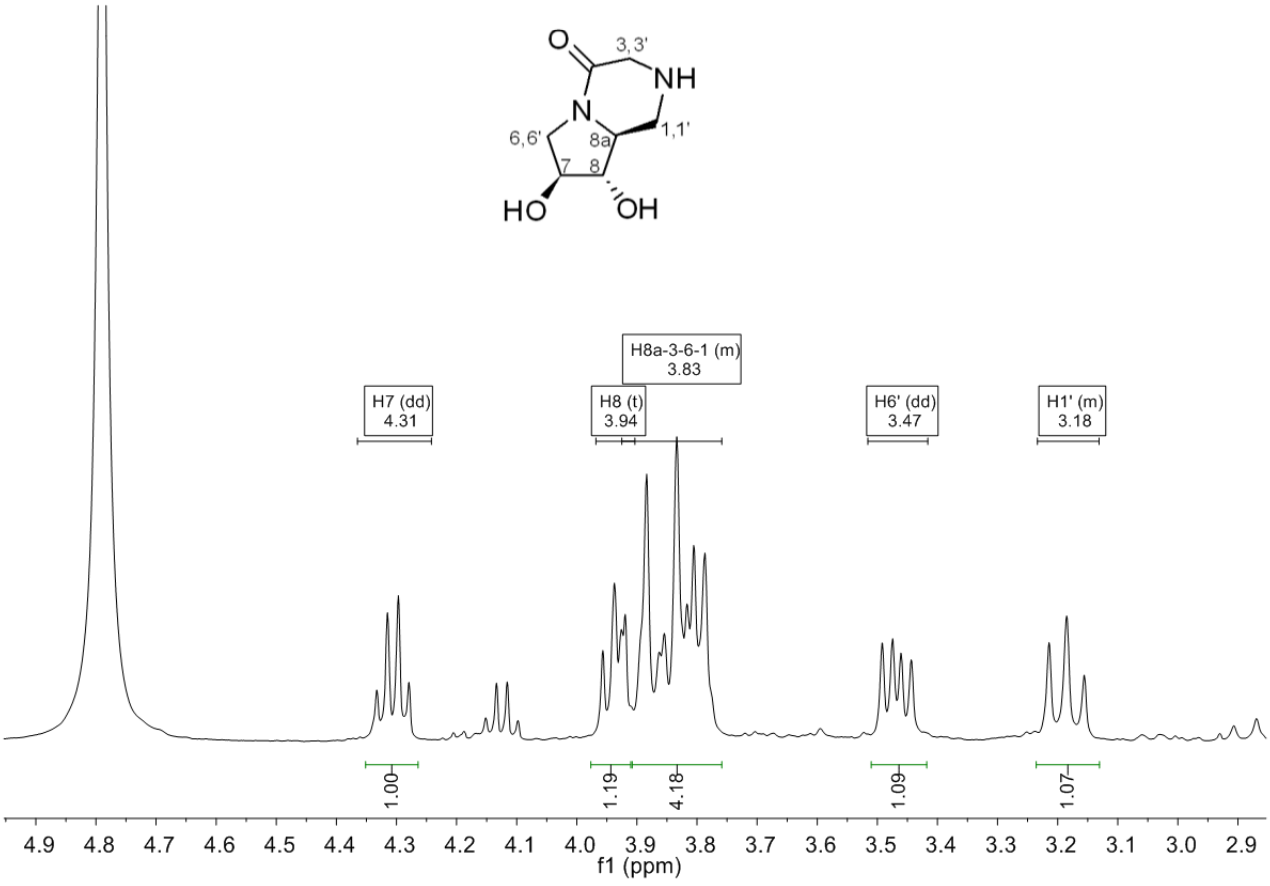

b)

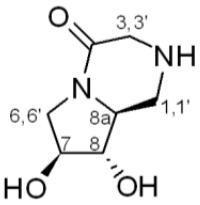

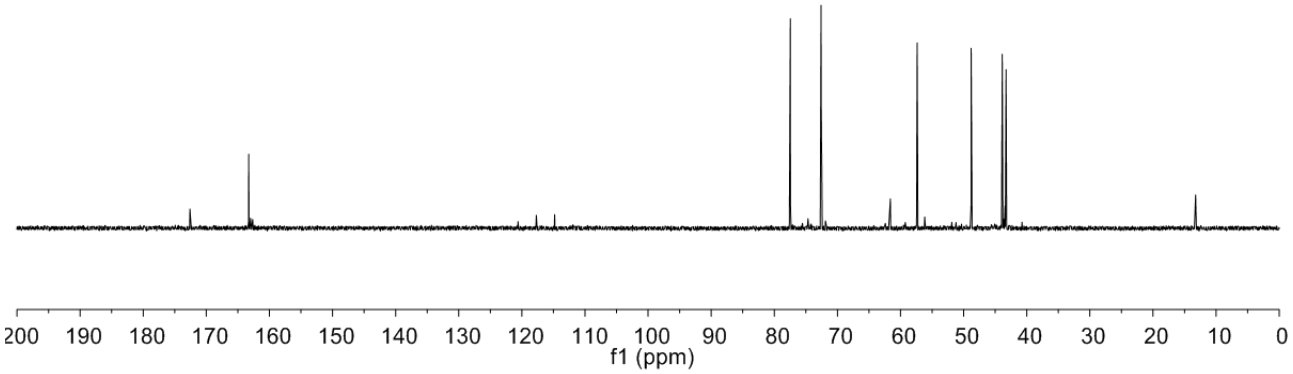

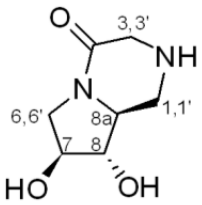

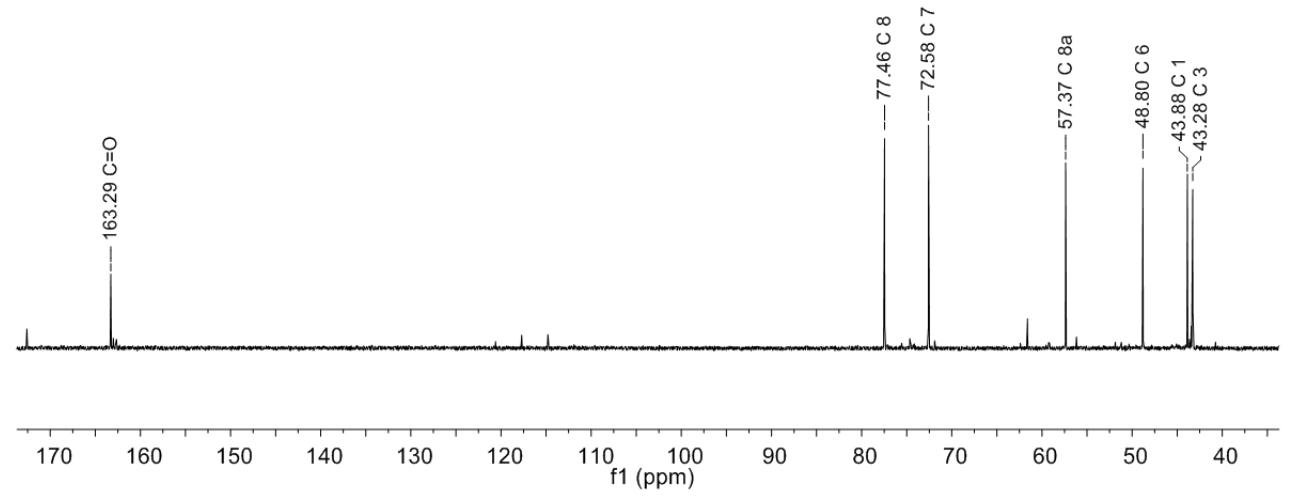

c)

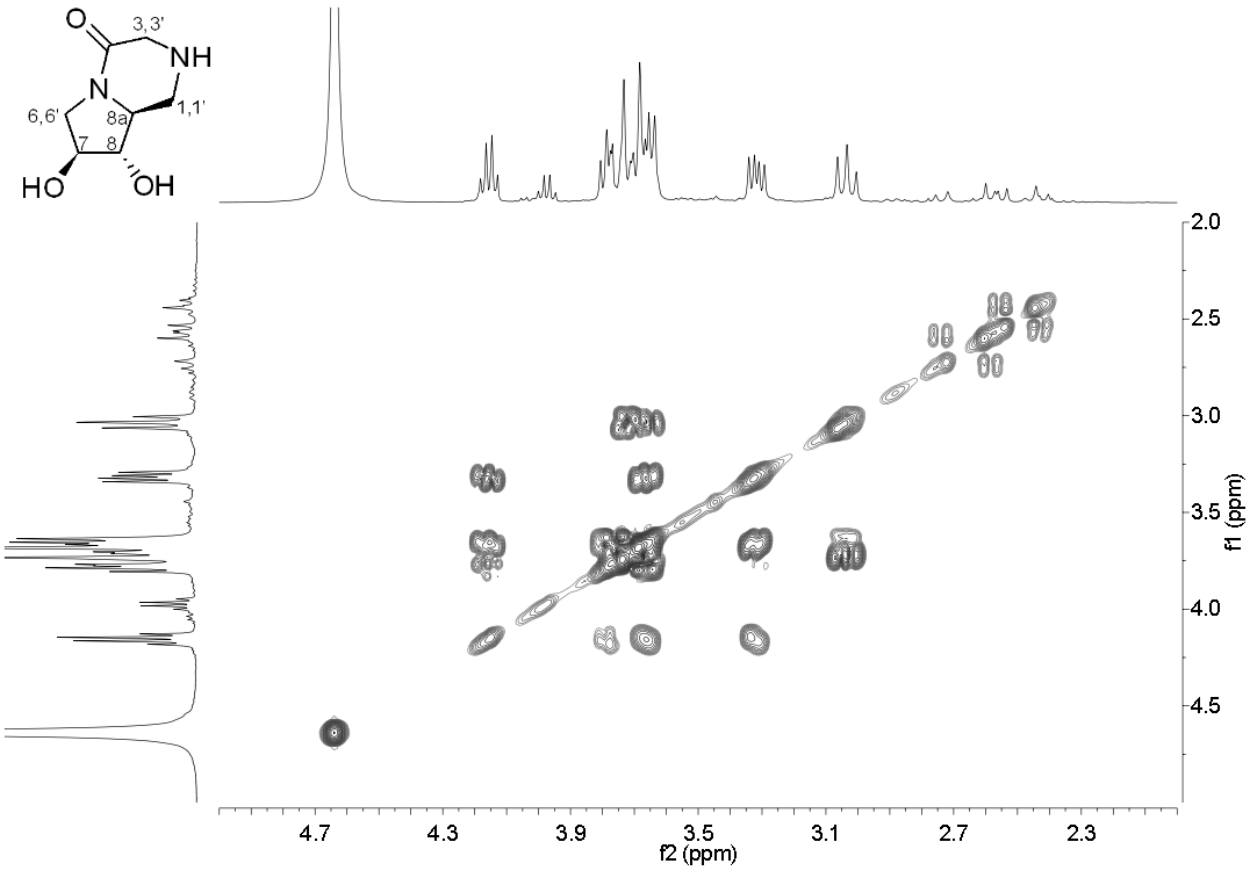

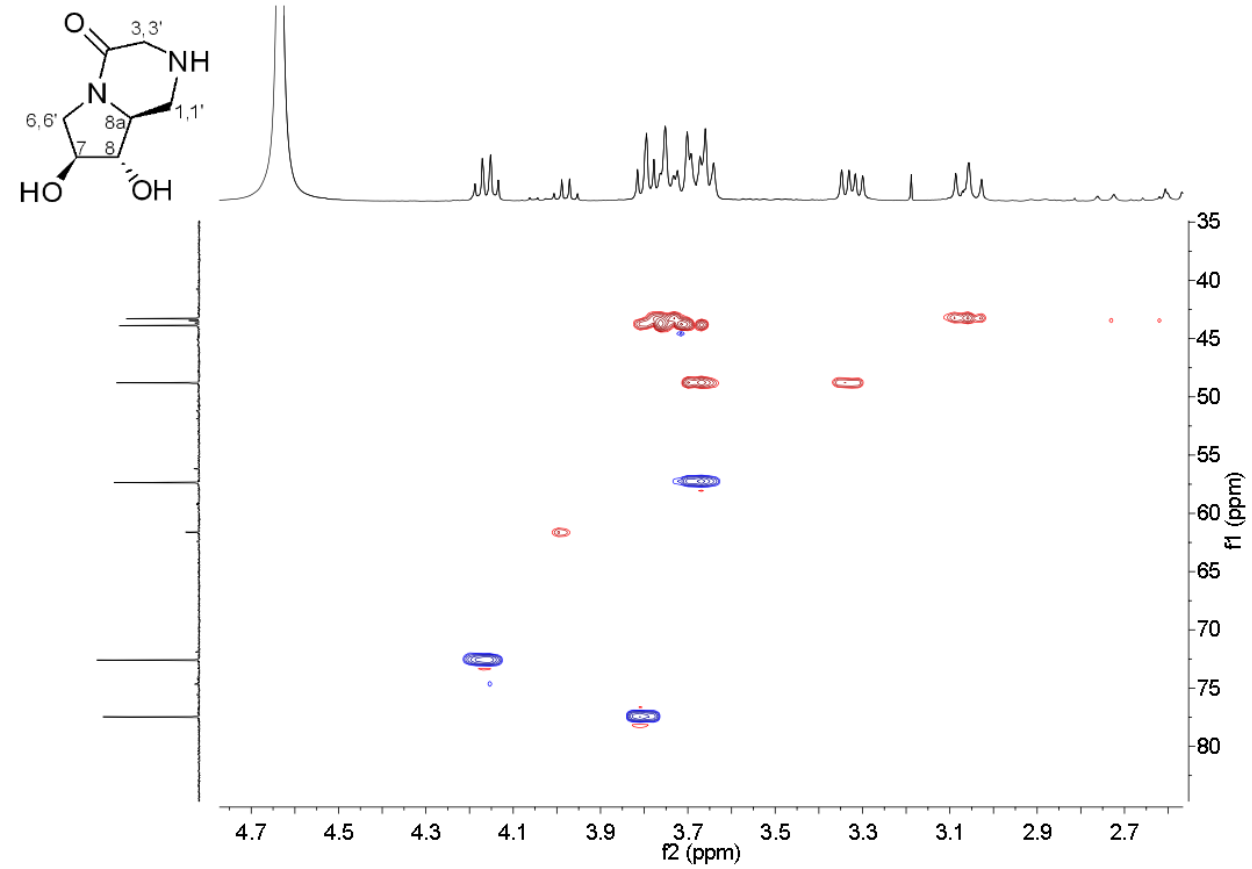

d)

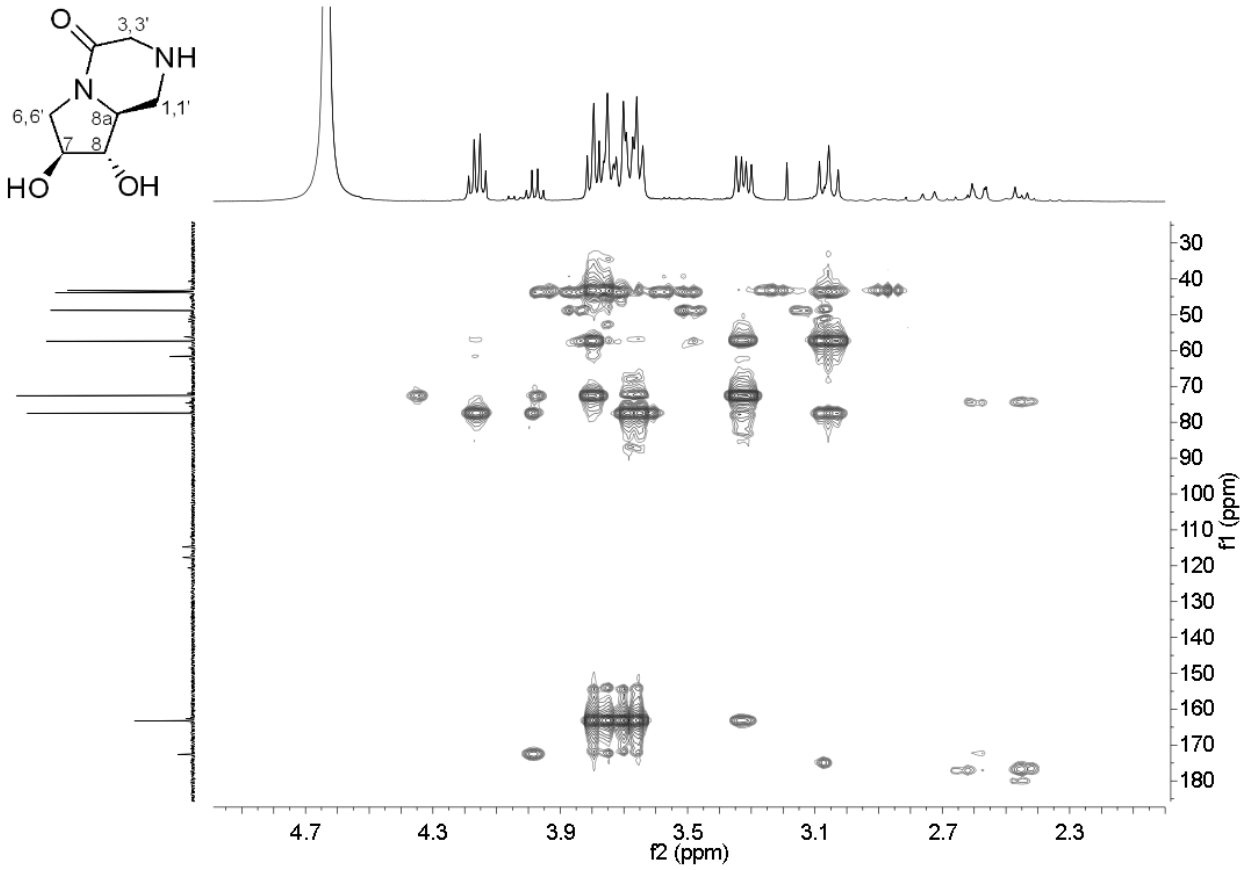

Figure 28. Observed NMR spectra of **29n**: a) ^{1}H, b) ^{13}C, c) 2D ^{1}H-^{1}H COSY and 2D multiplicity-edited HSQC, d) selective 1D NOESY spectra, e) magnitude-mode ge-2D HMBC.

a)

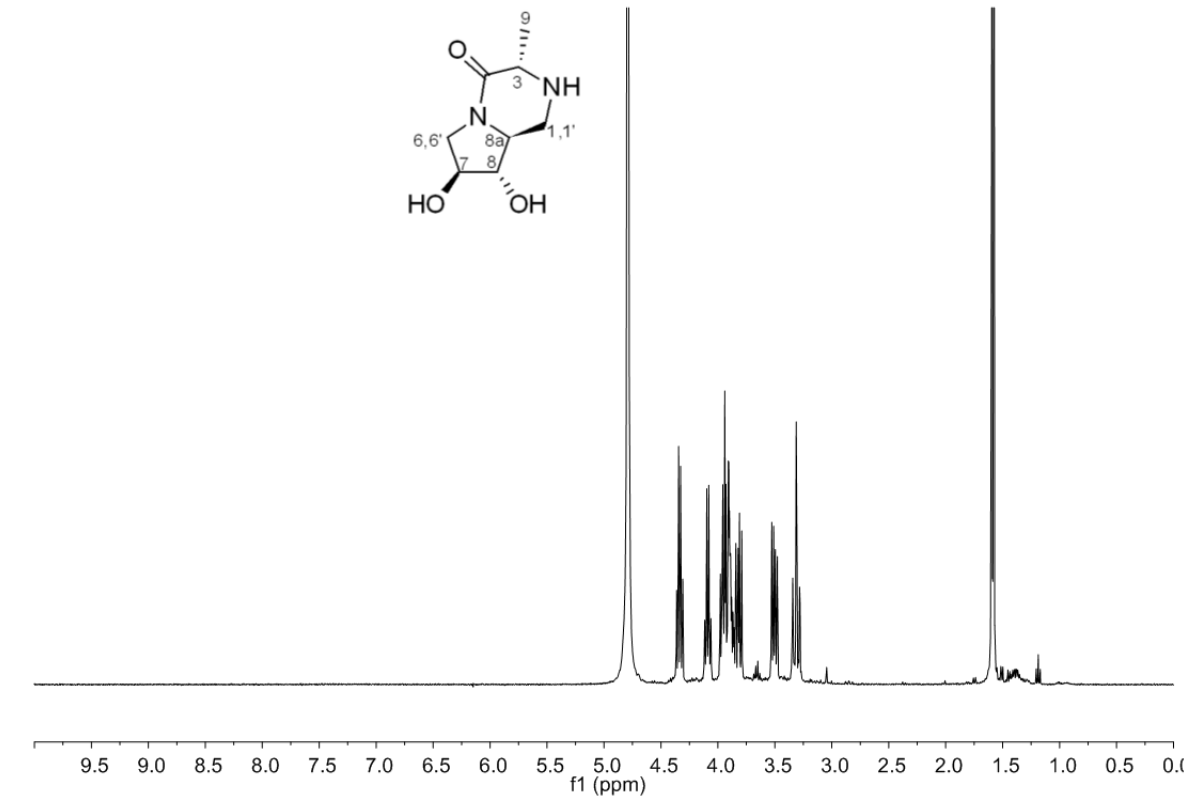

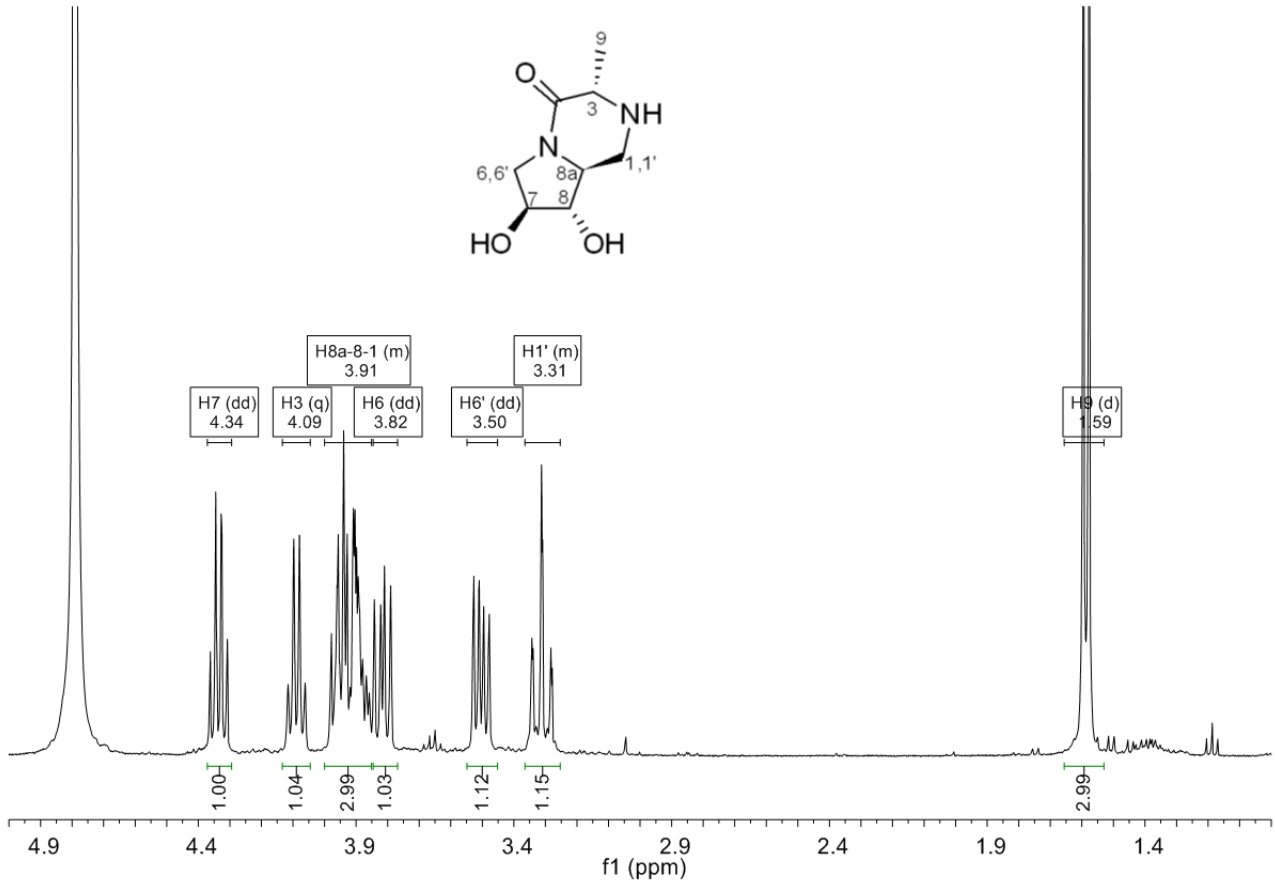

b)

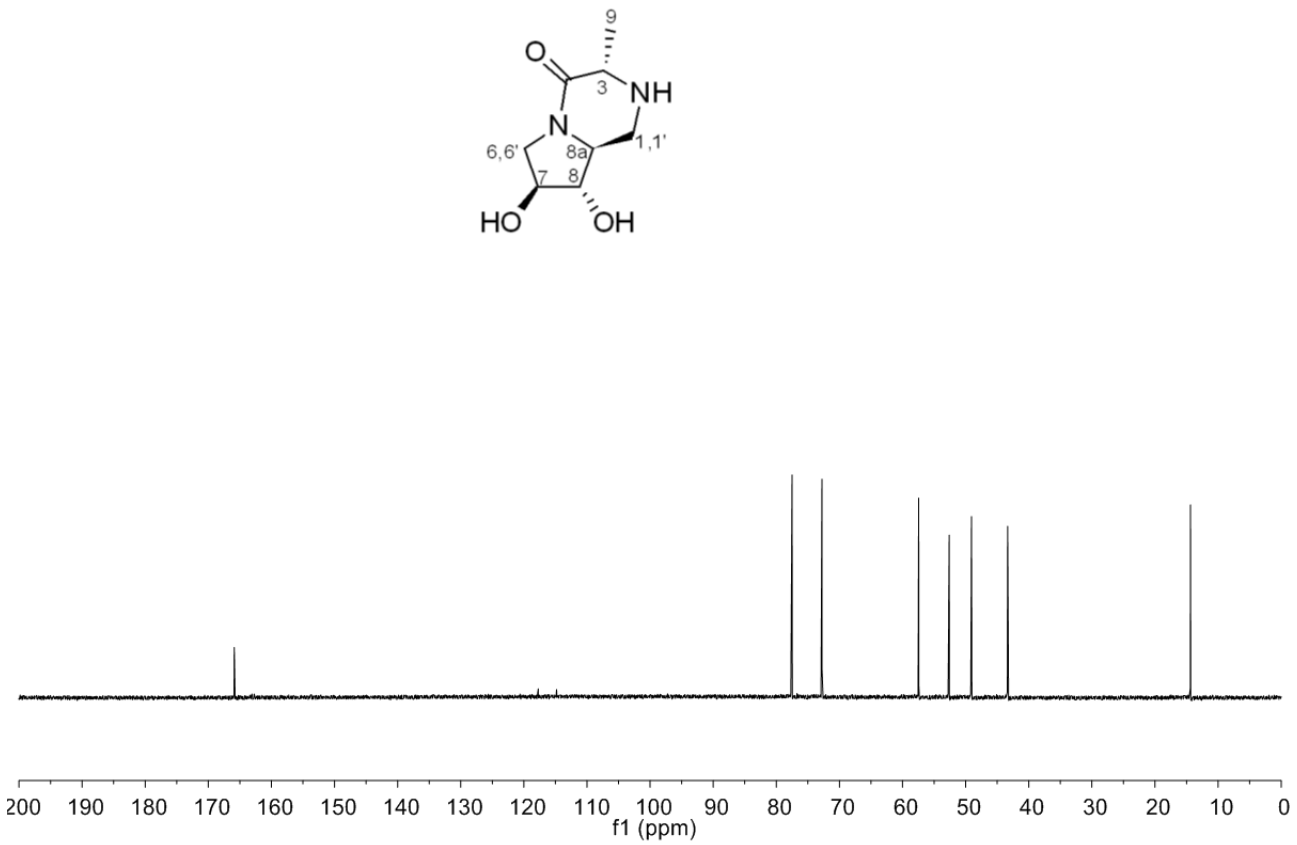

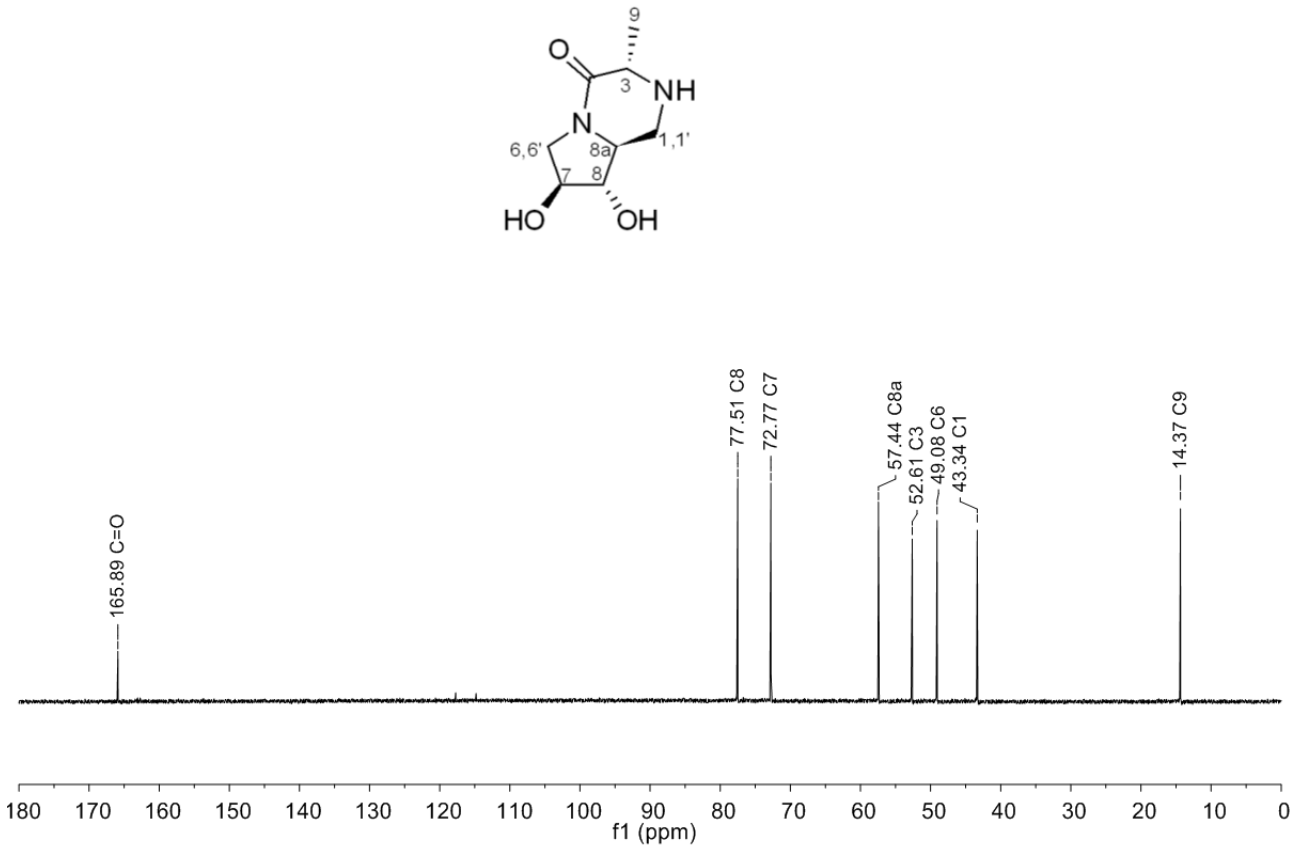

c)

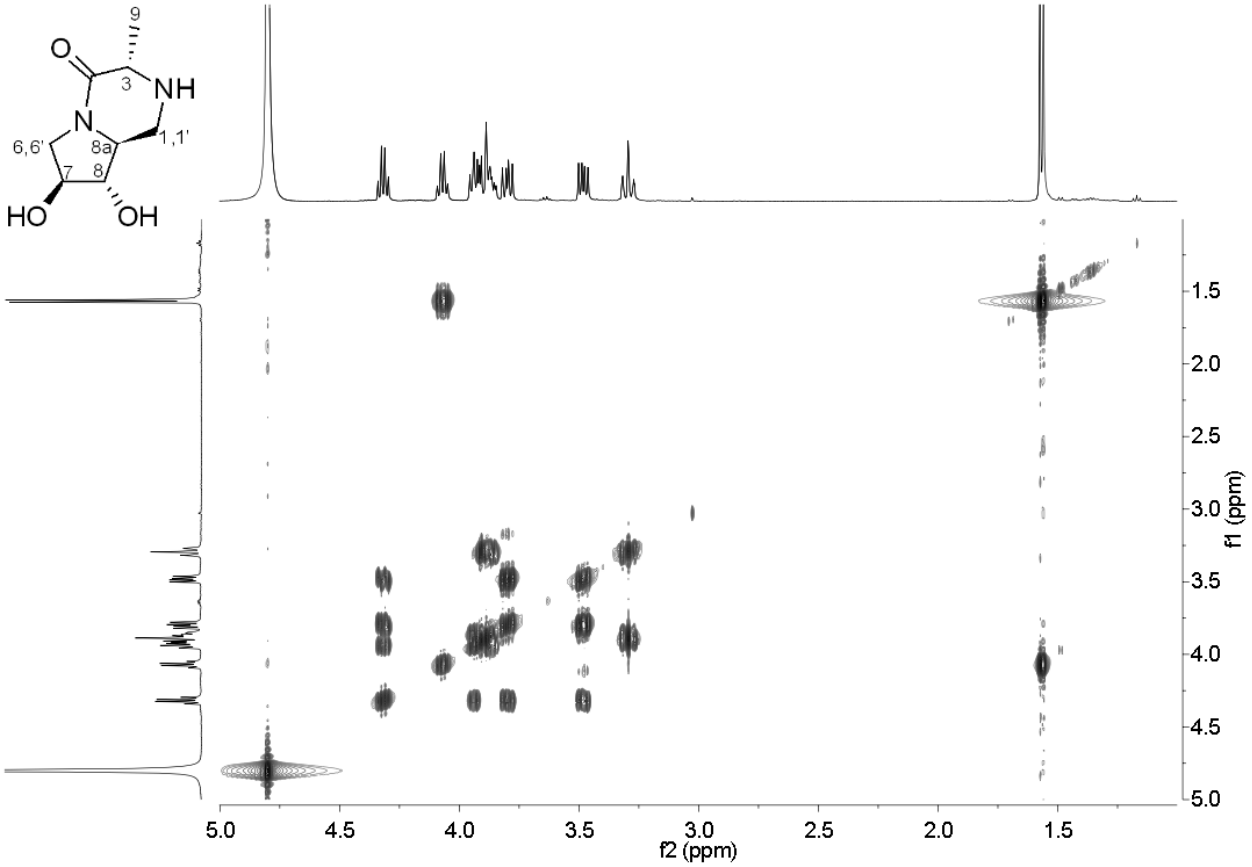

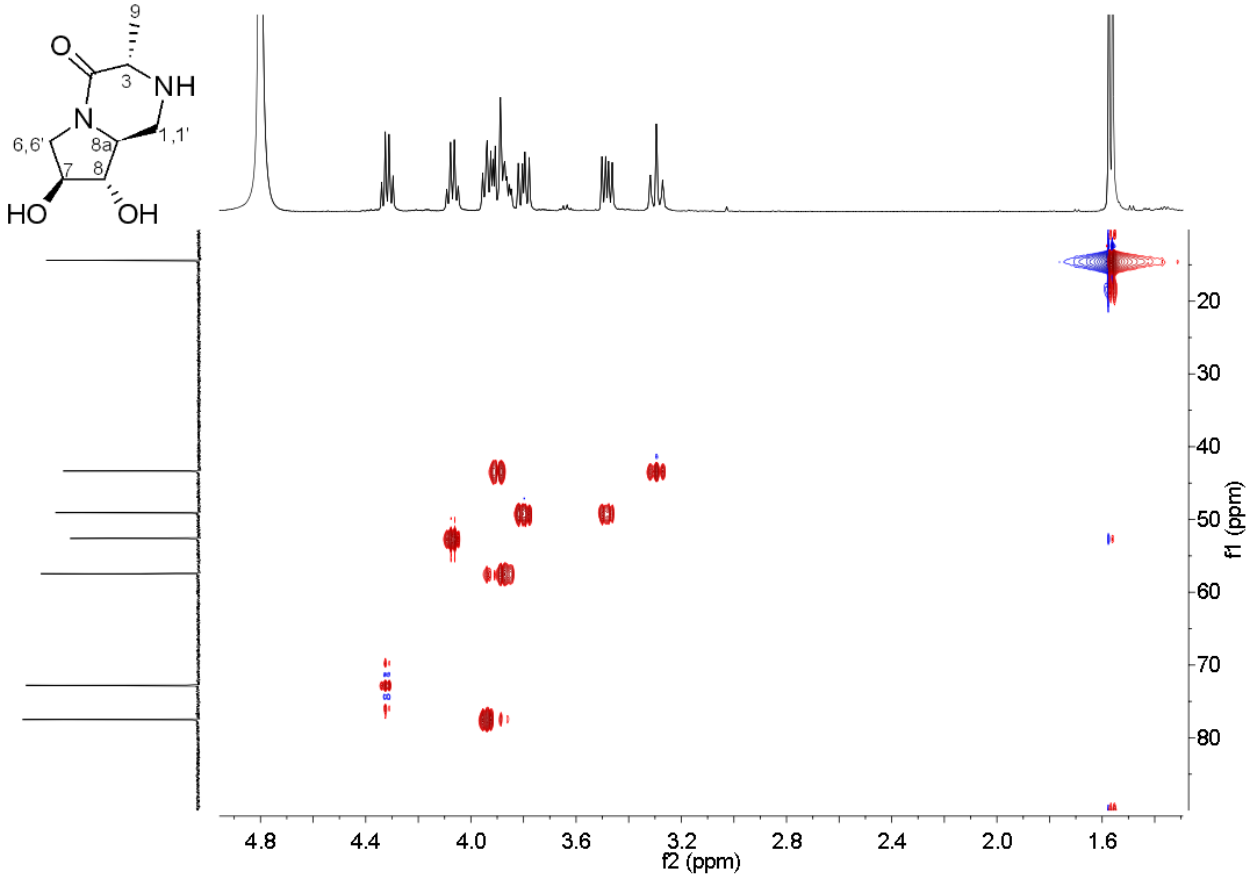

d)

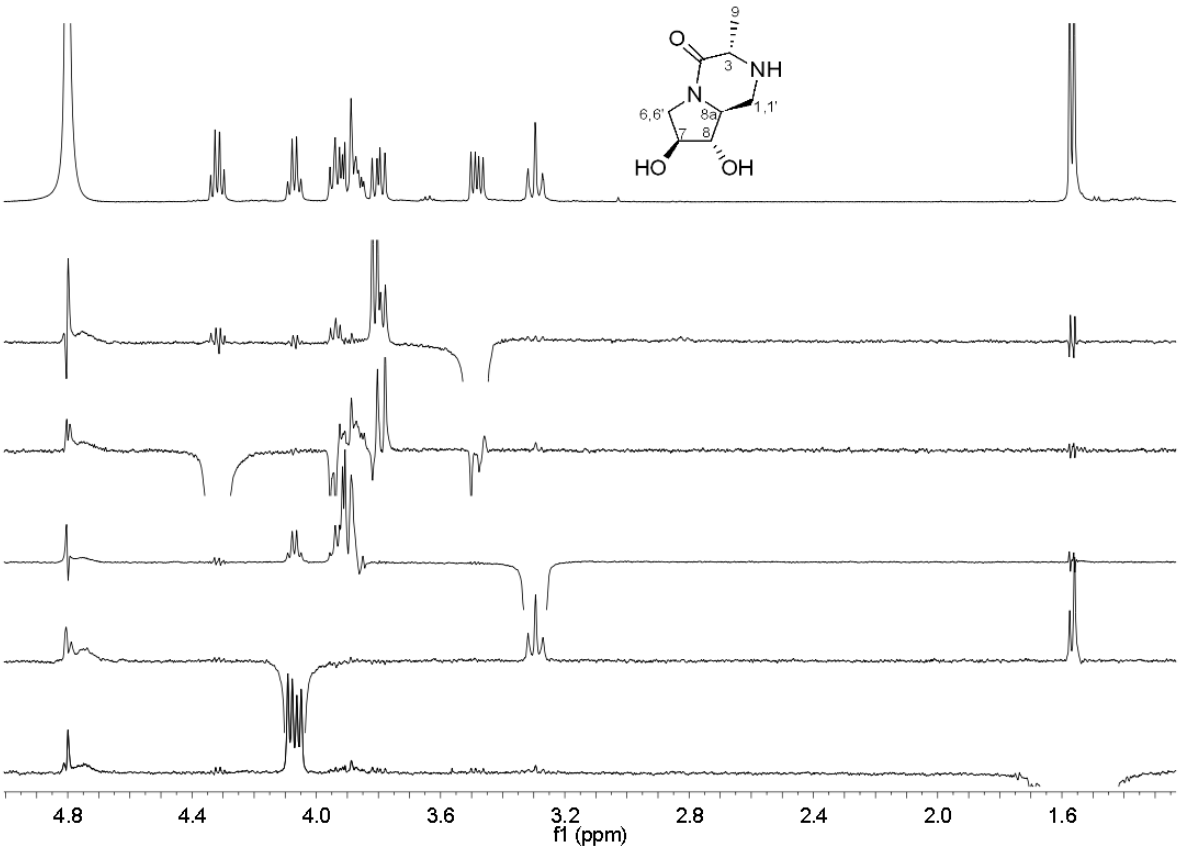

e)

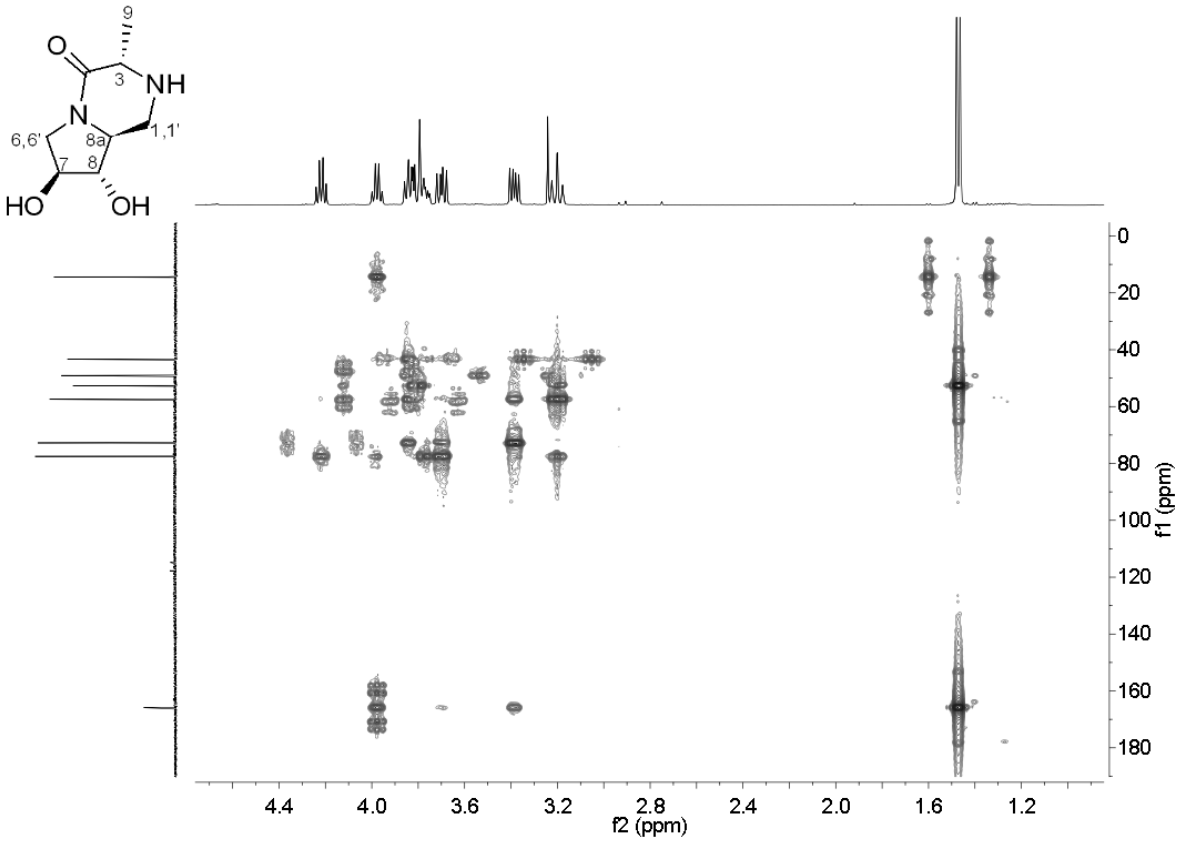

Figure 29. Observed NMR spectra of **29p**: a) ^{1}H, b) ^{13}C, c) 2D ^{1}H-^{1}H COSY and 2D multiplicity-edited HSQC, d) magnitude-mode ge-2D HMBC.

a)

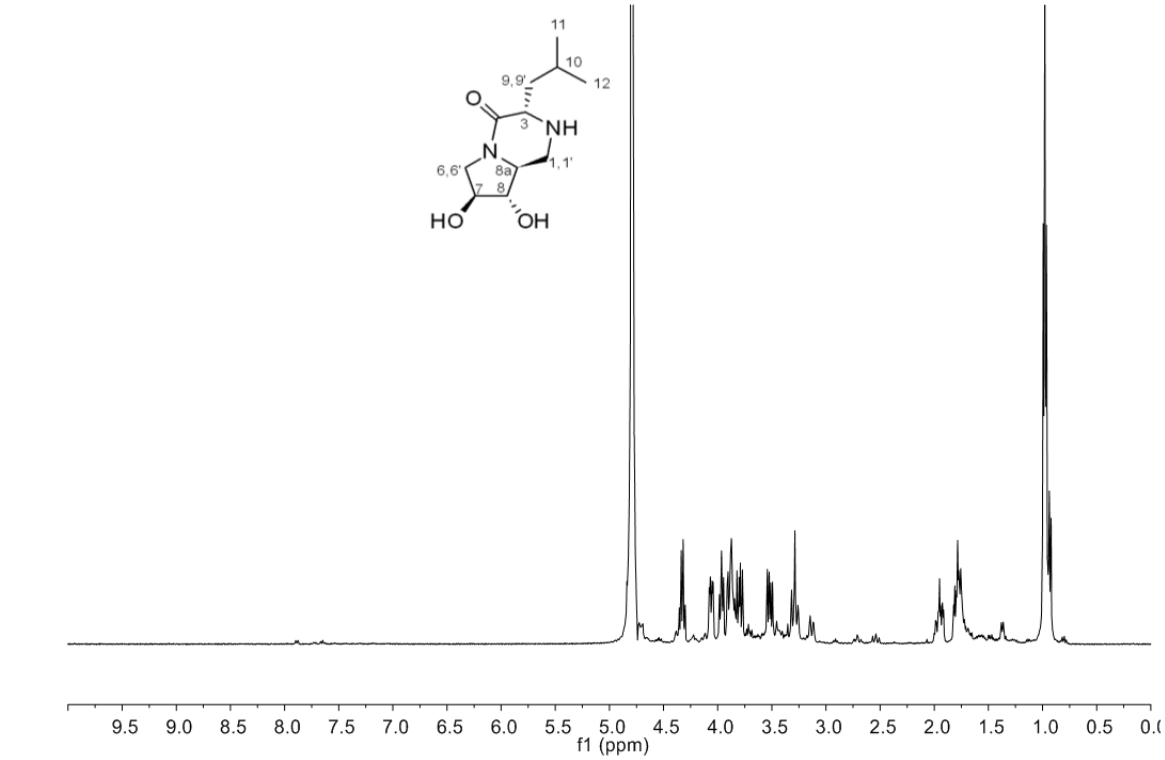

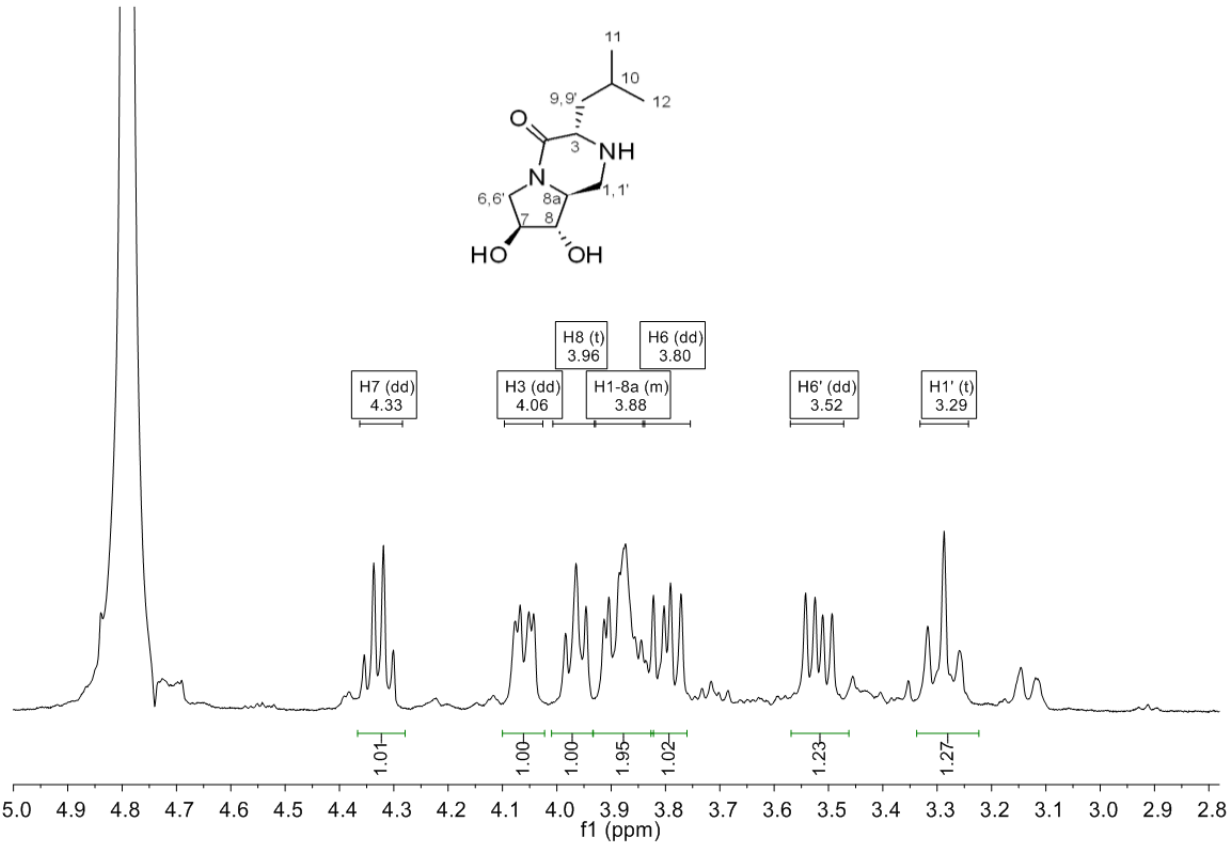

b)

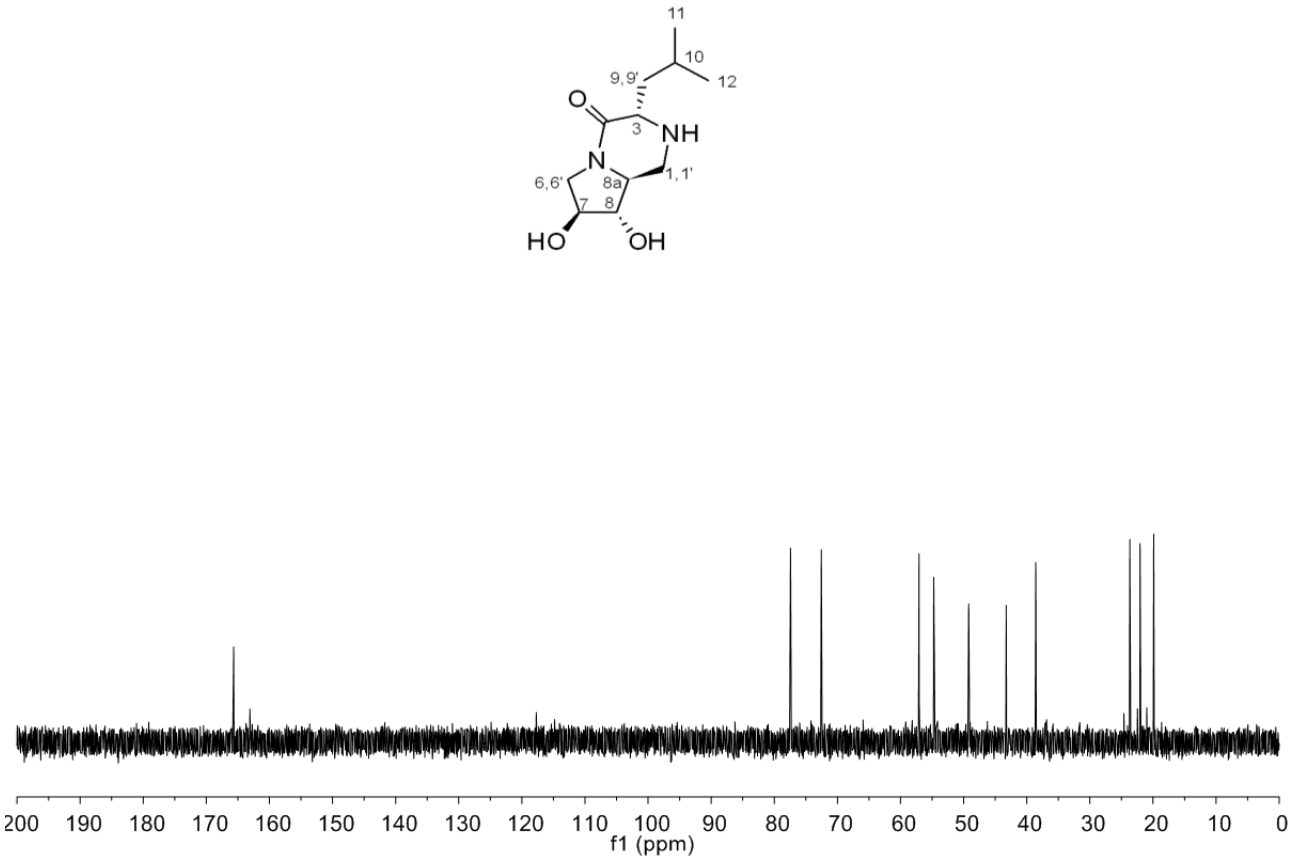

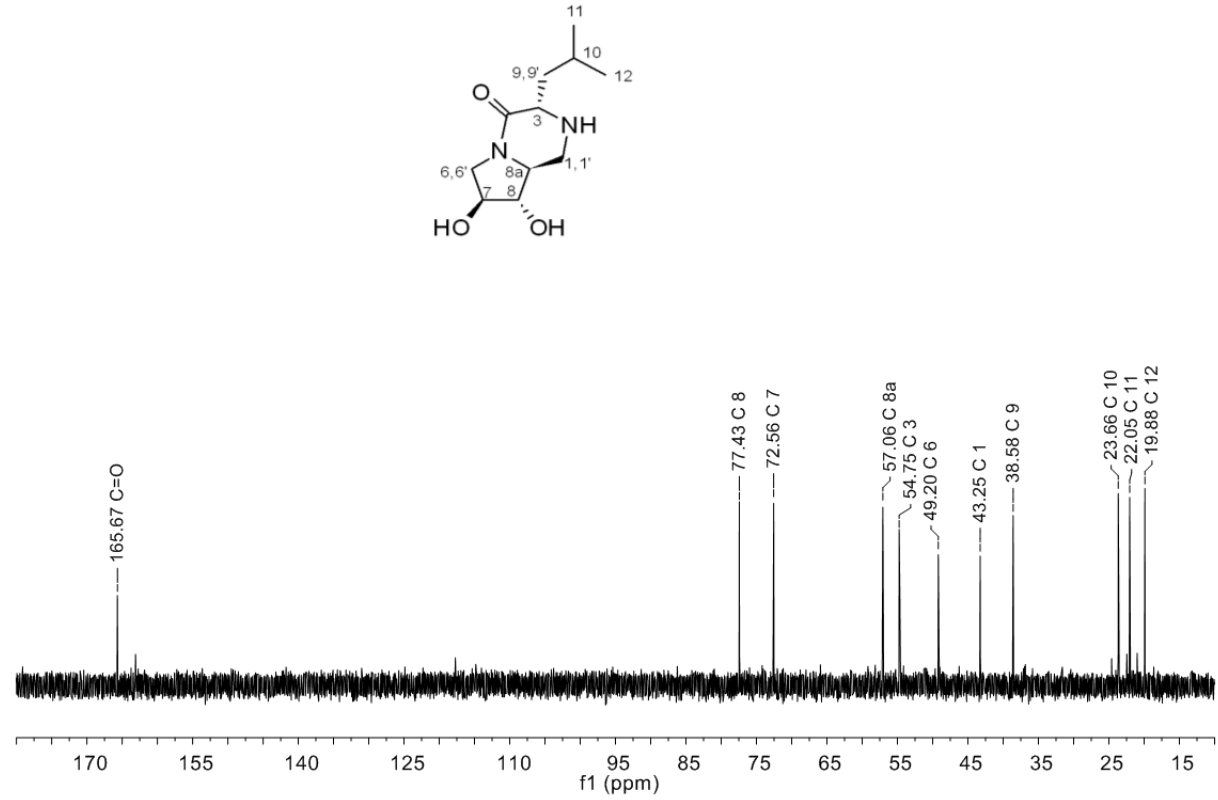

c)

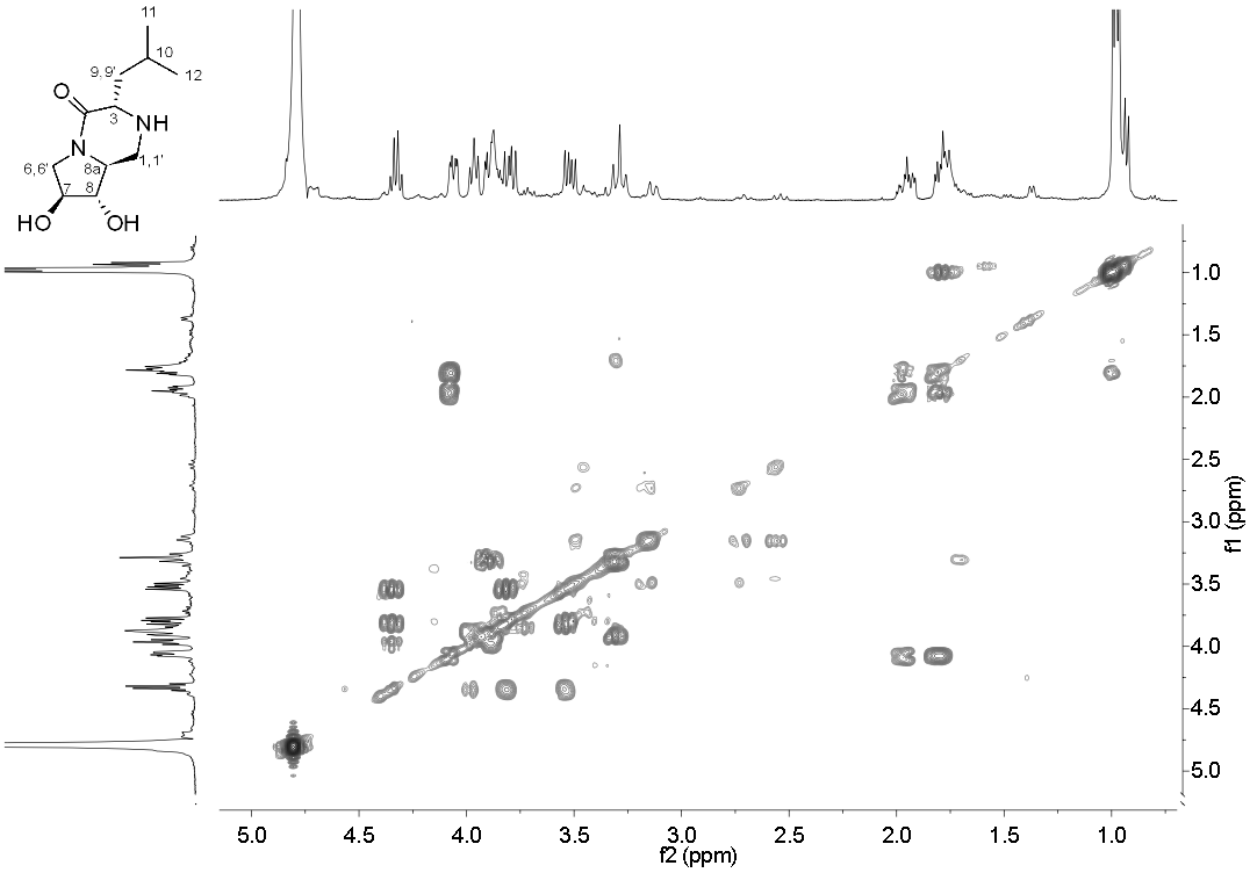

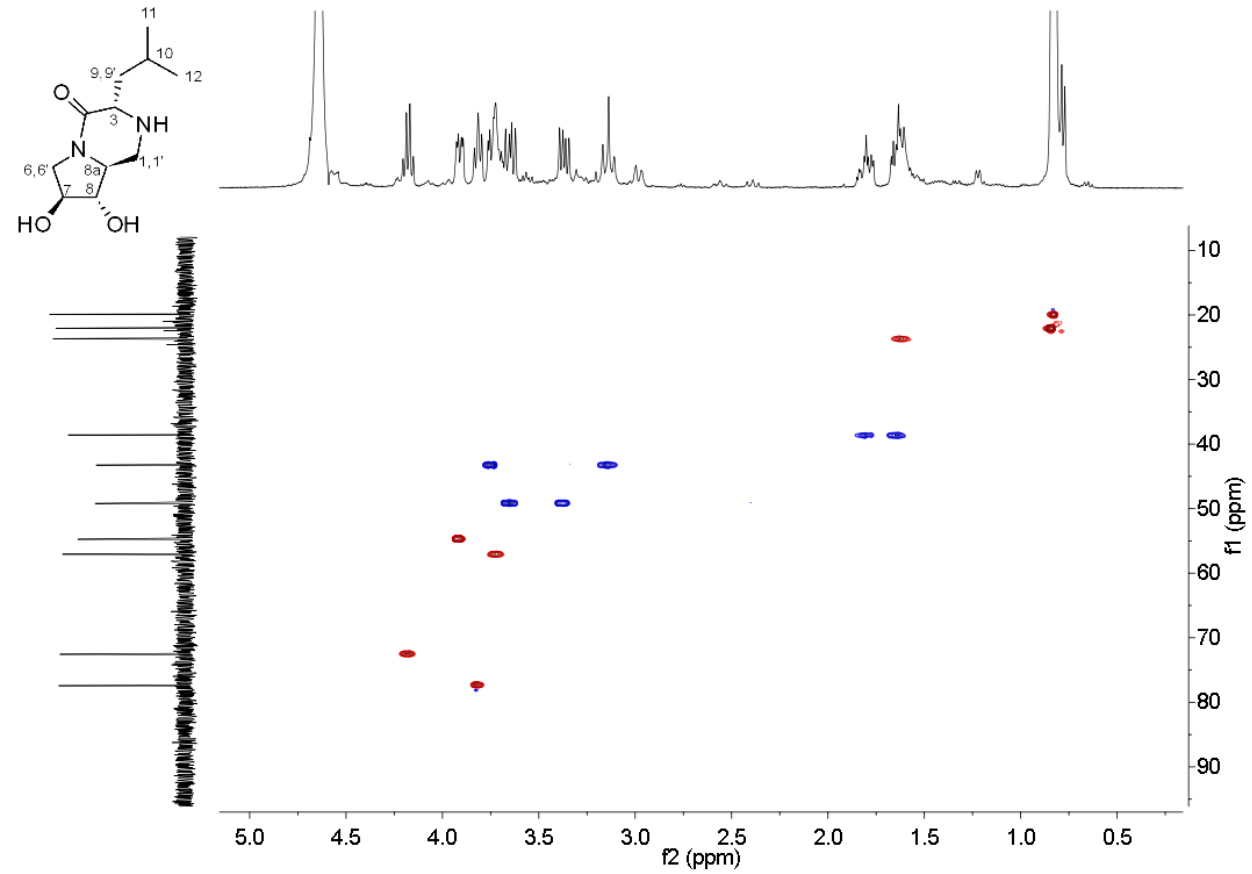

d)

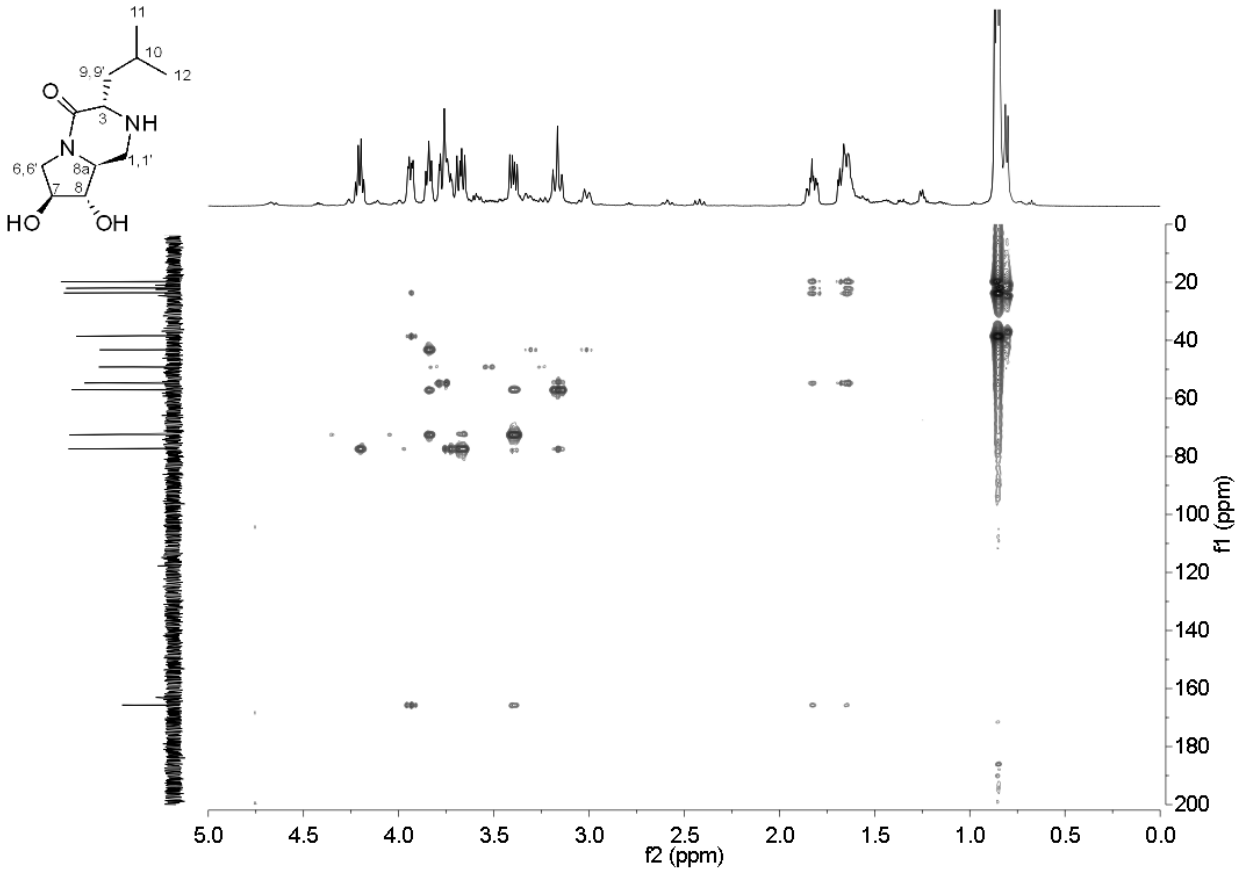
11
10
12
9,9'
O
3
NH
N
1,1'
6,6'
8a
7
8
HO
OH
0
20
40
60
80
100
120
140
160
180
200
f1 (ppm)
5.0
4.5
4.0
3.5
3.0
2.5
2.0
1.5
1.0
0.5
0.0
f2 (ppm)

Figure 30. Observed NMR spectra of **29q**: a) ^{1}H, b) ^{13}C, c) 2D ^{1}H-^{1}H COSY and 2D multiplicity-edited HSQC, d) magnitude-mode ge-2D HMBC.

a)

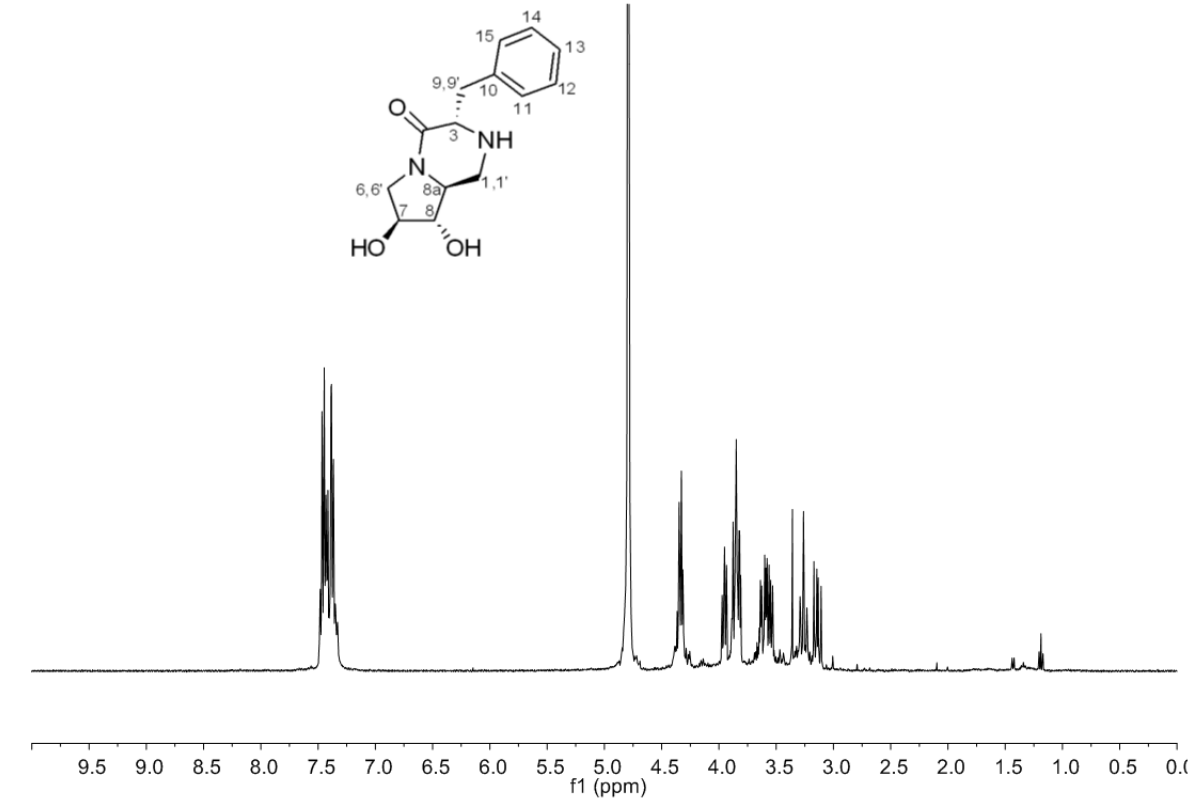

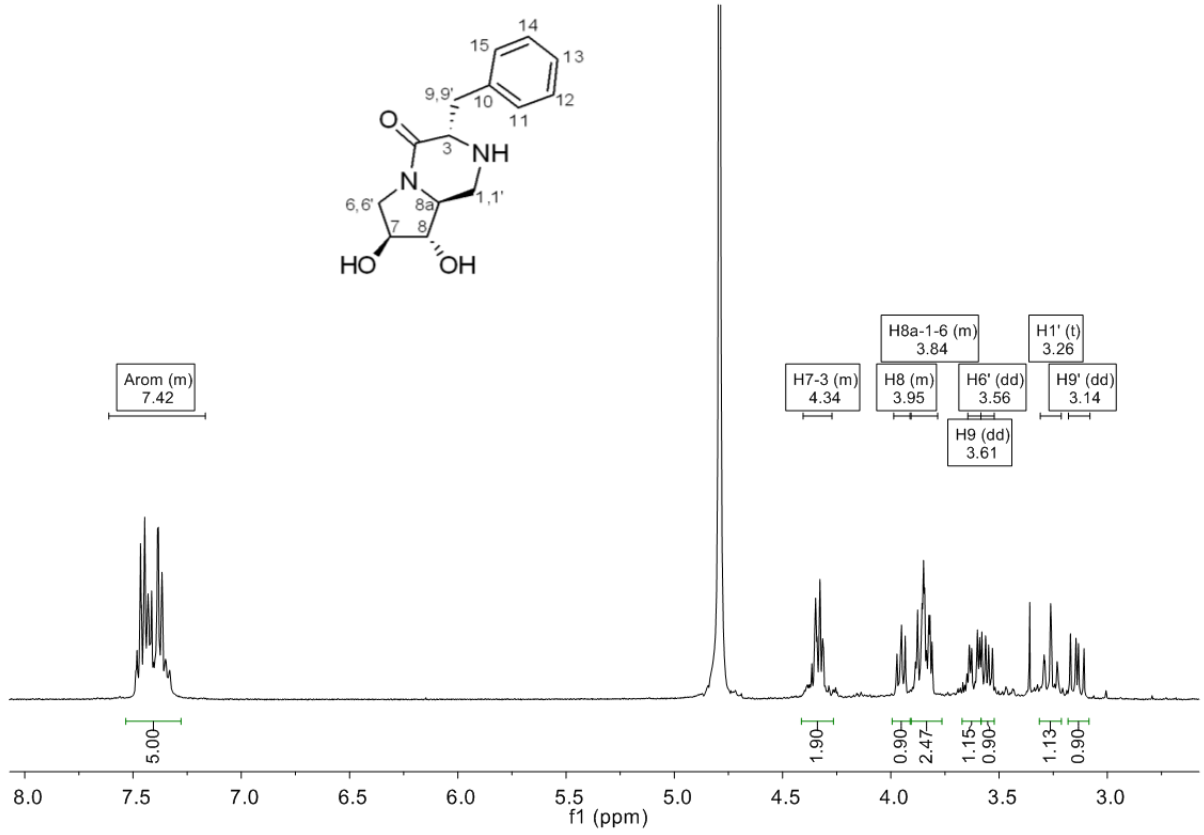

b)

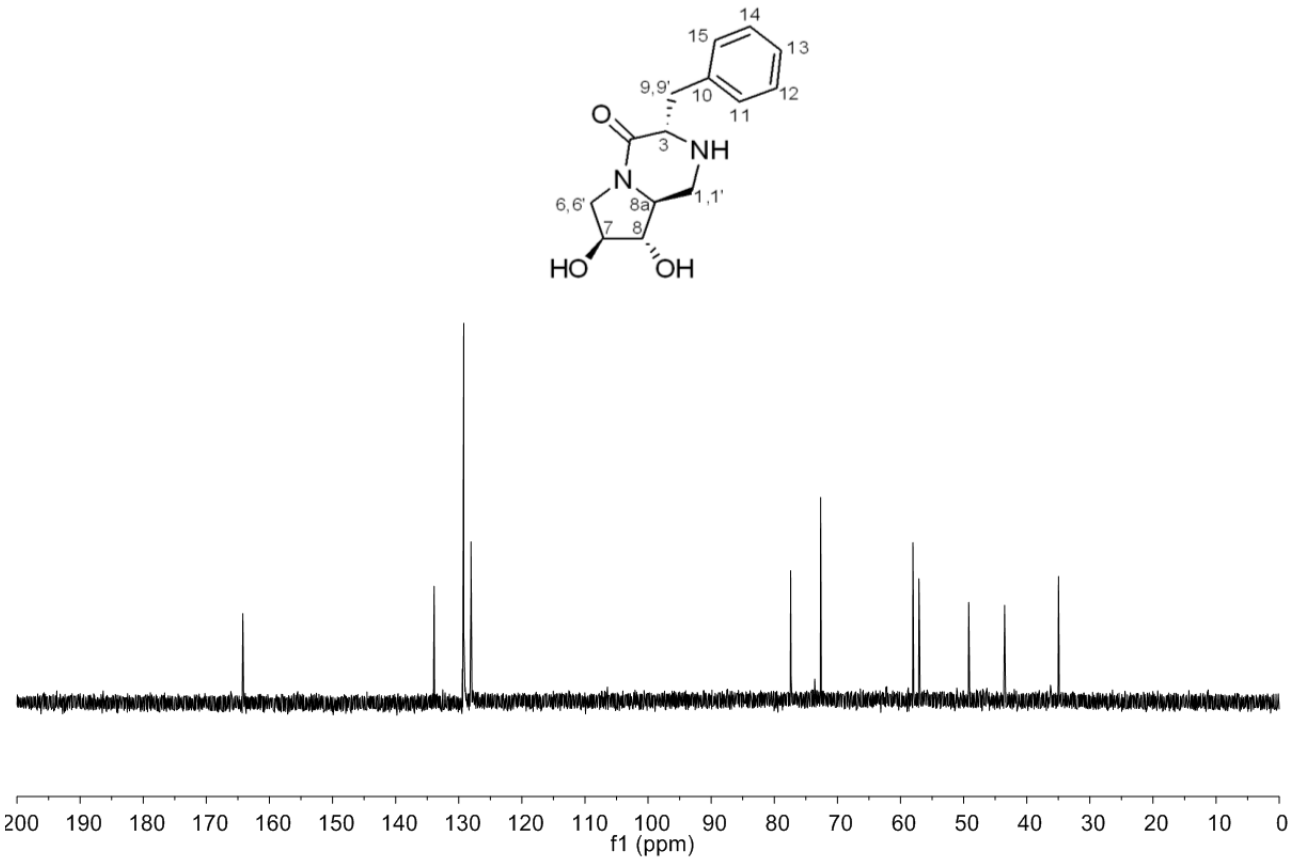

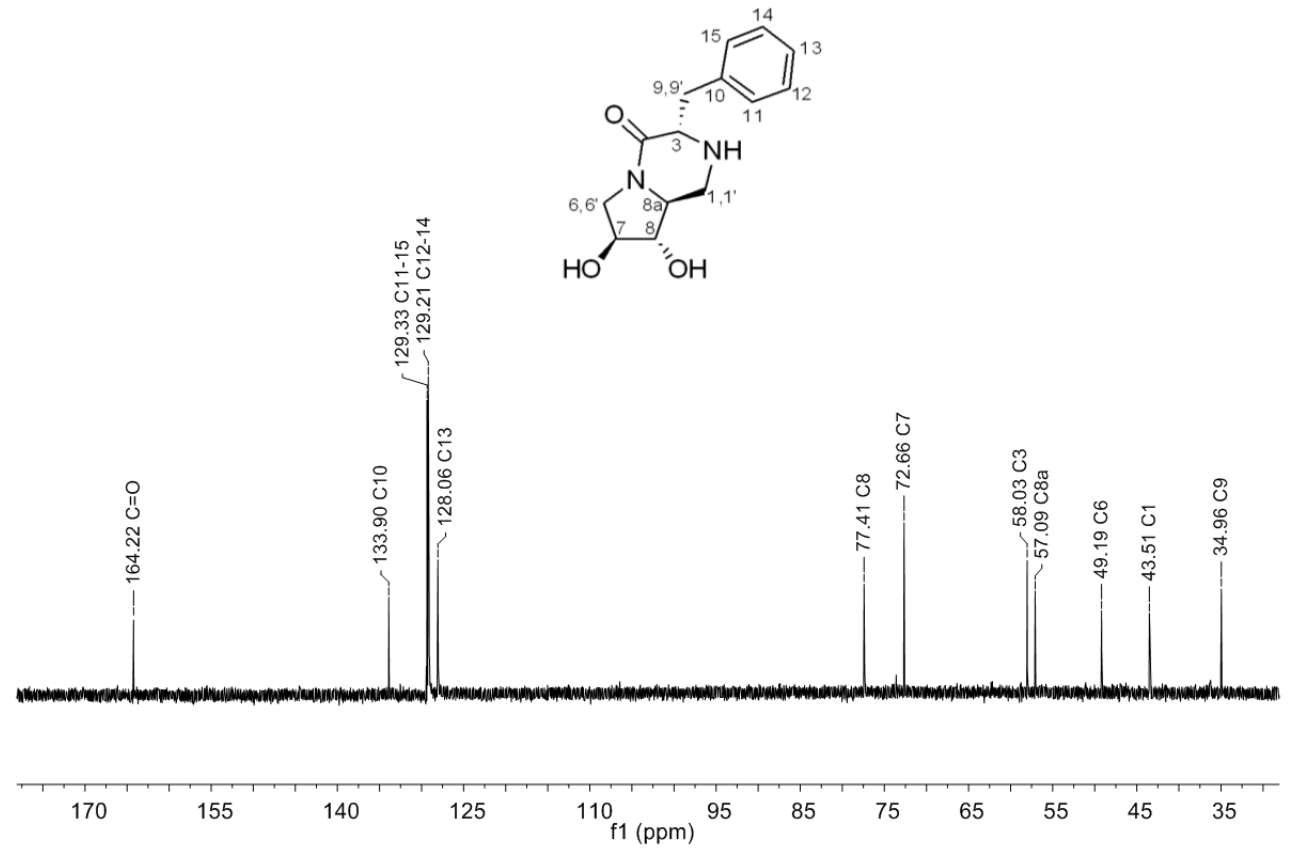

c)

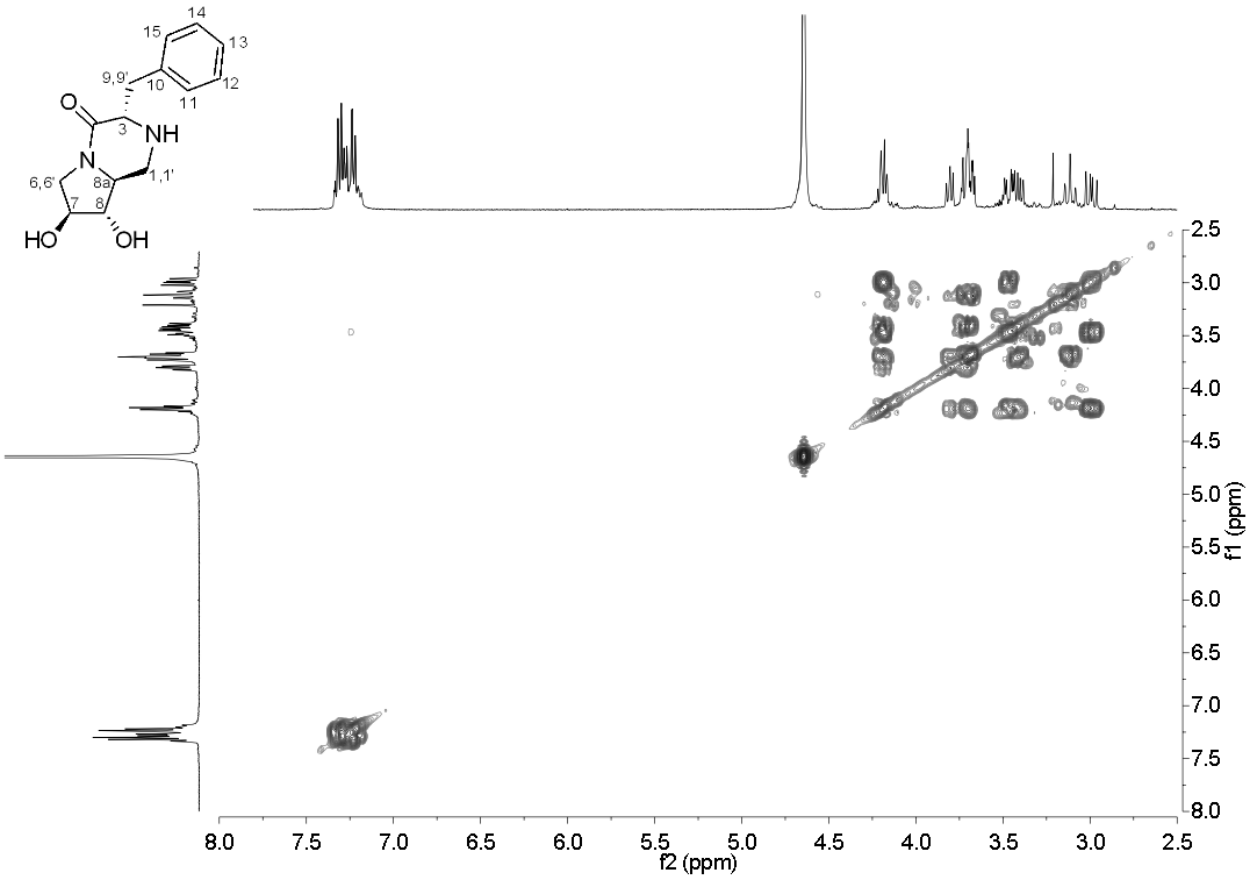

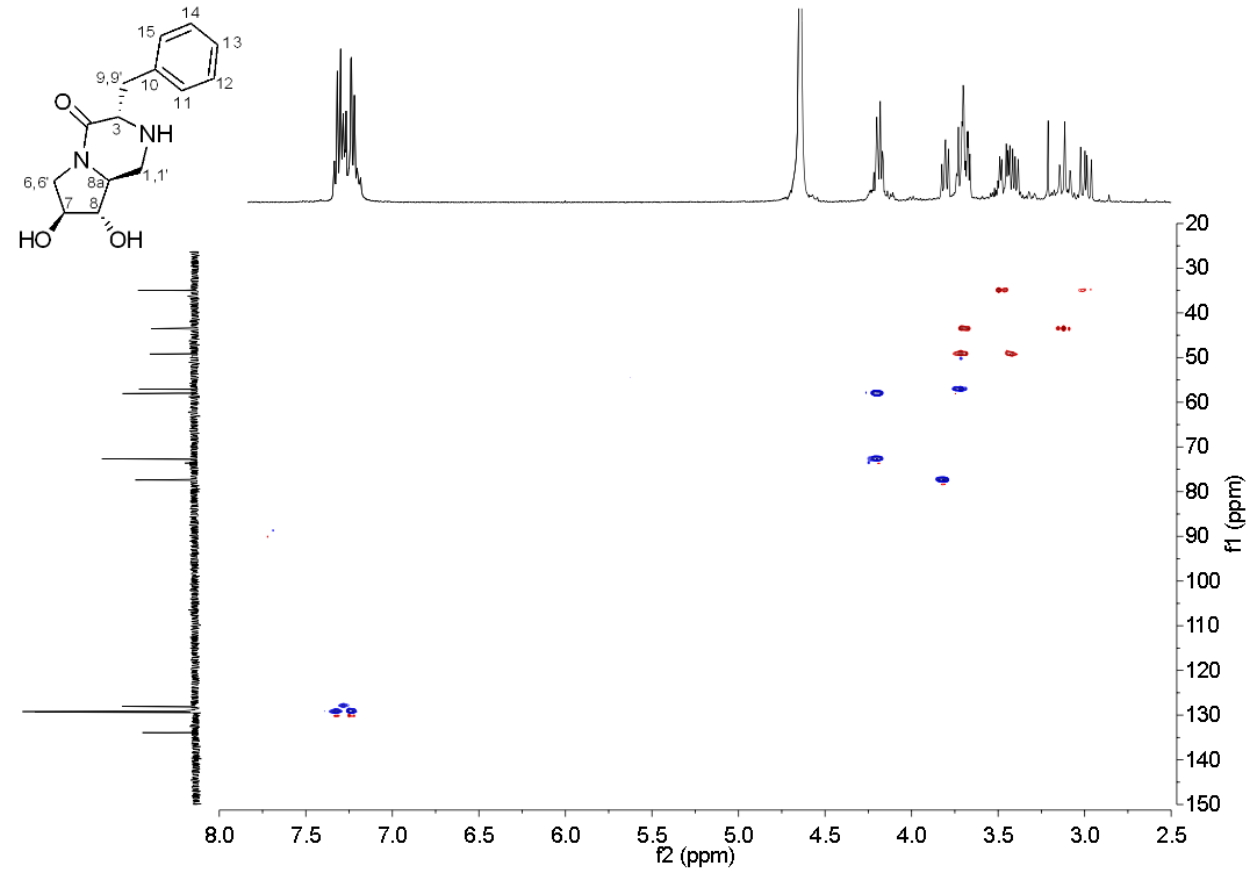

d)

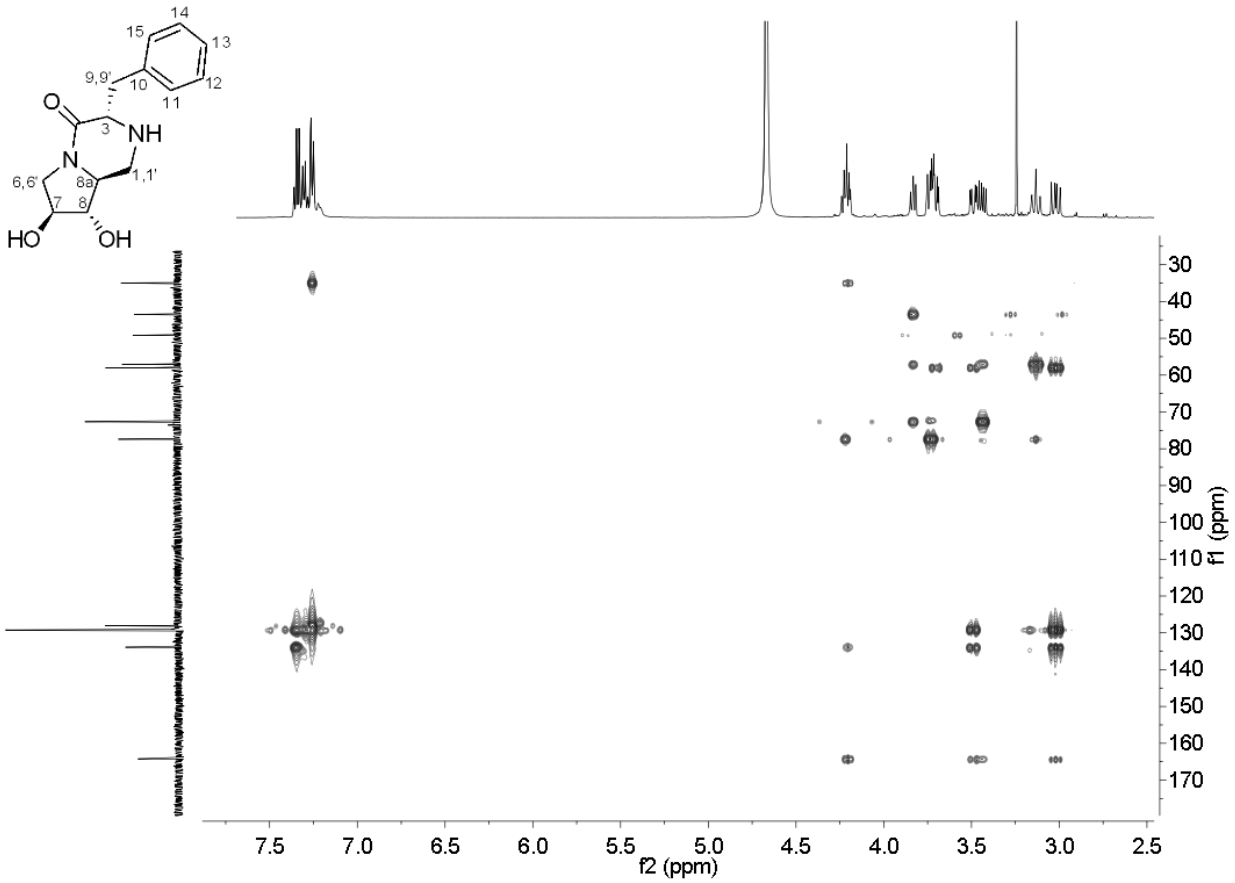

Figure 31. Observed NMR spectra of **29s**: a) ^{1}H, b) ^{13}C, c) 2D ^{1}H-^{1}H COSY and 2D multiplicity-edited HSQC, d) magnitude-mode ge-2D HMBC.

a)

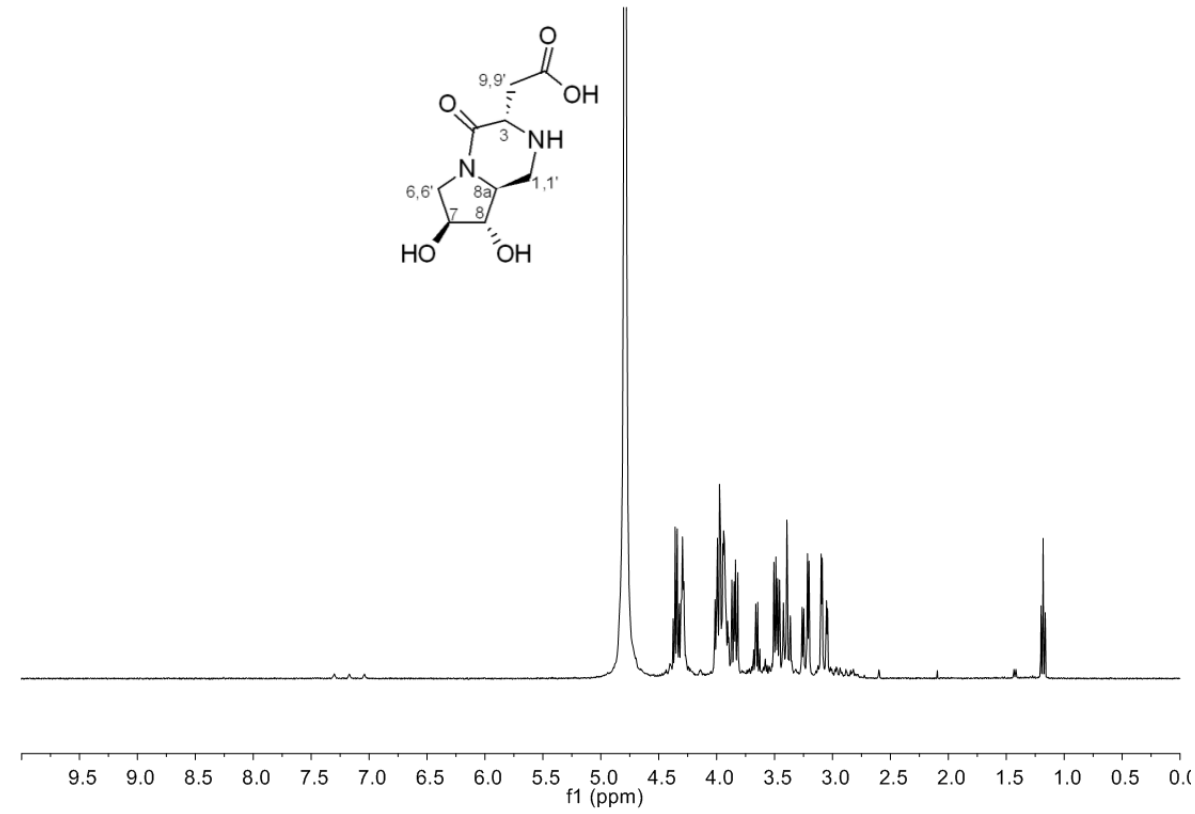

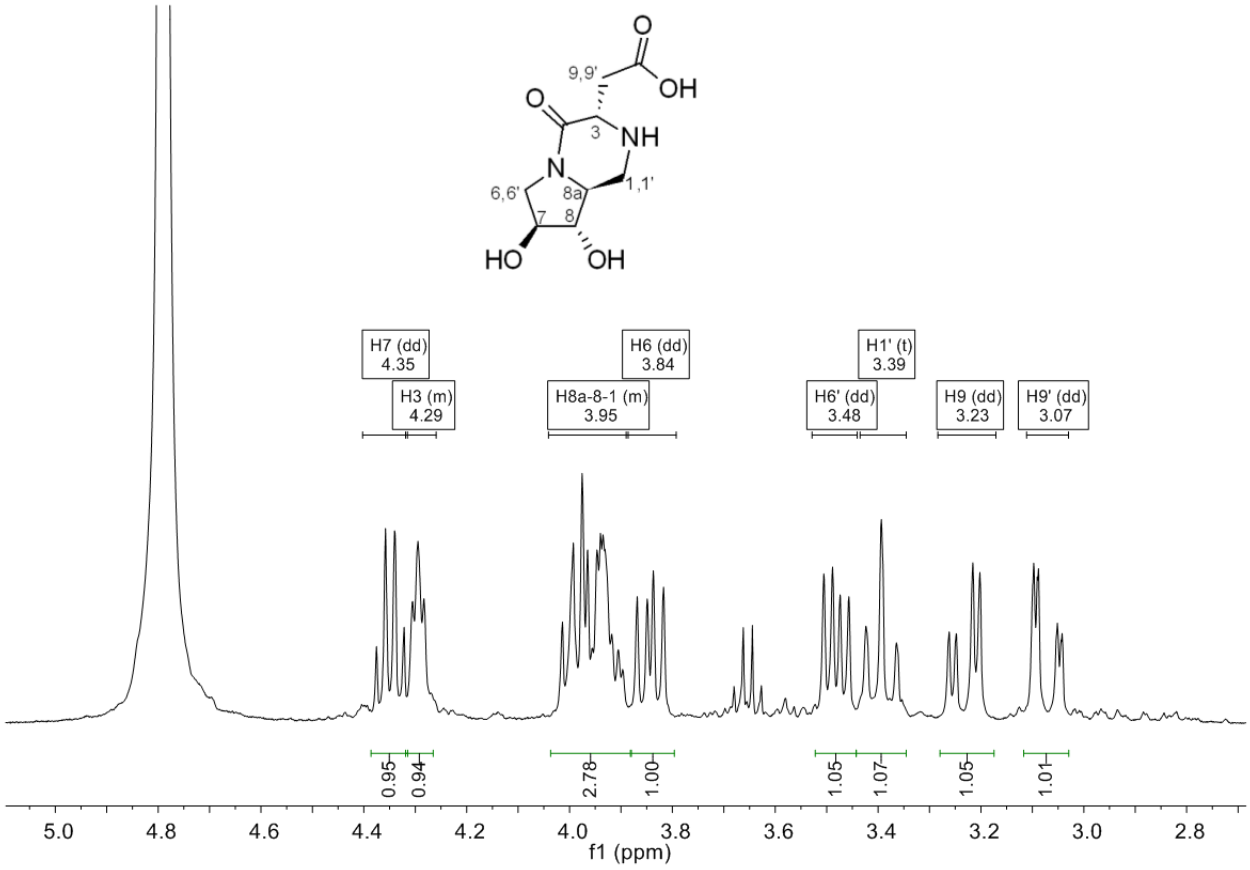

b)

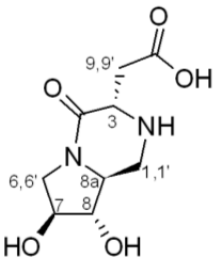

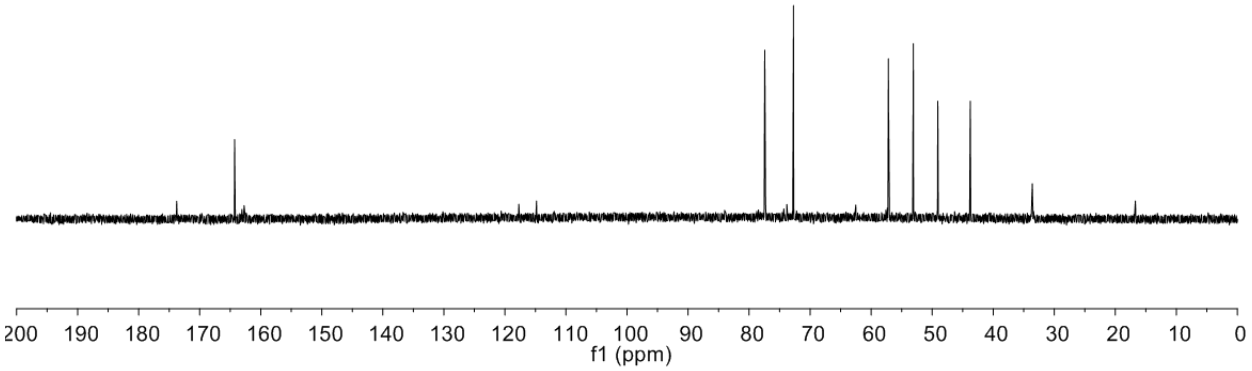

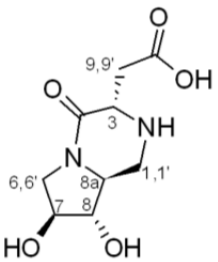

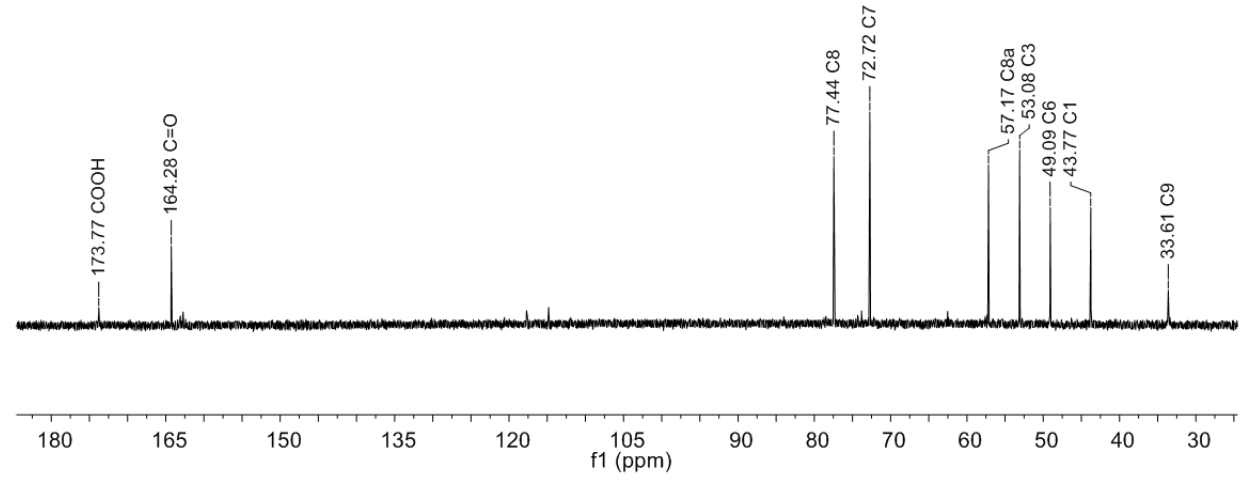

c)

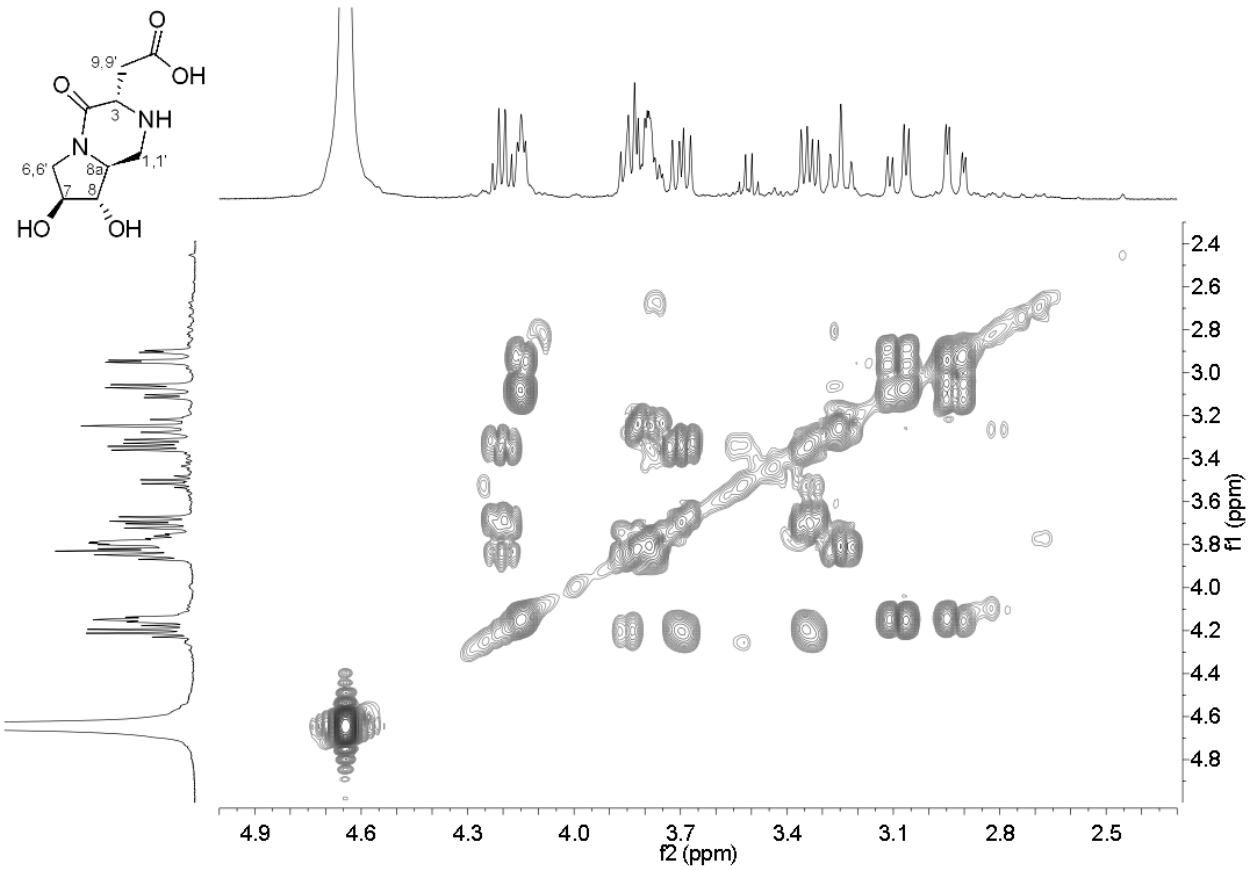

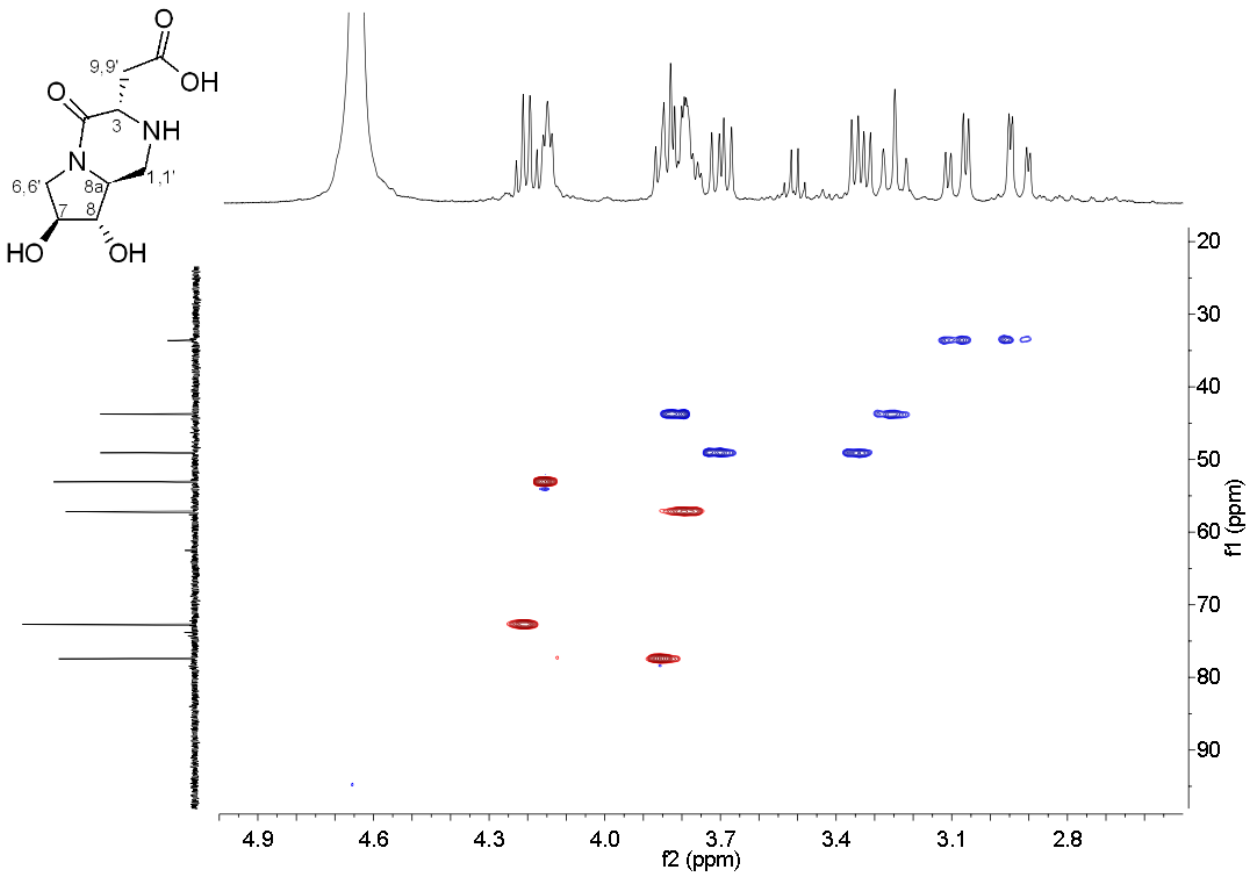

d)

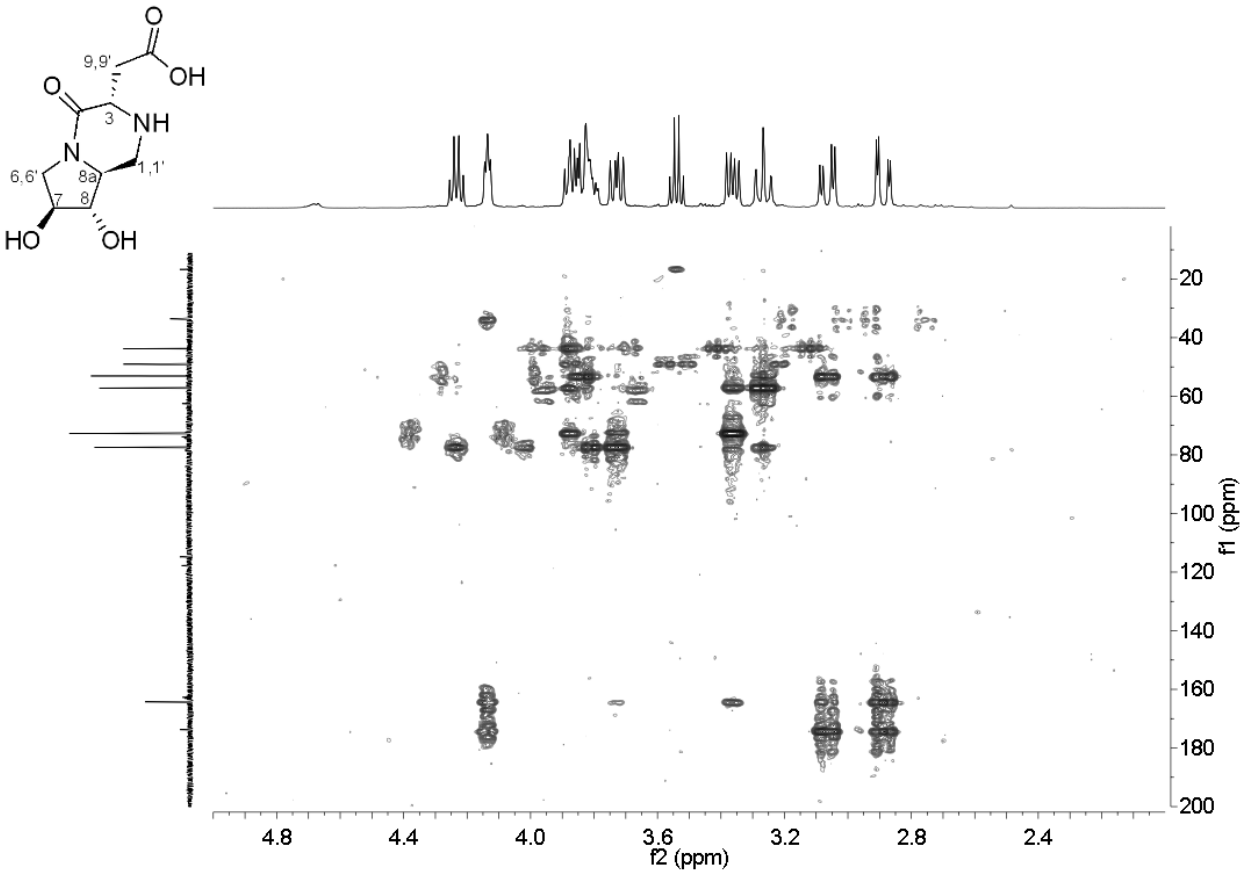

Figure 32. Observed NMR spectra of **29u**: a) ^{1}H, b) ^{13}C, c) 2D ^{1}H-^{1}H COSY and 2D multiplicity-edited HSQC, d) magnitude-mode ge-2D HMBC.

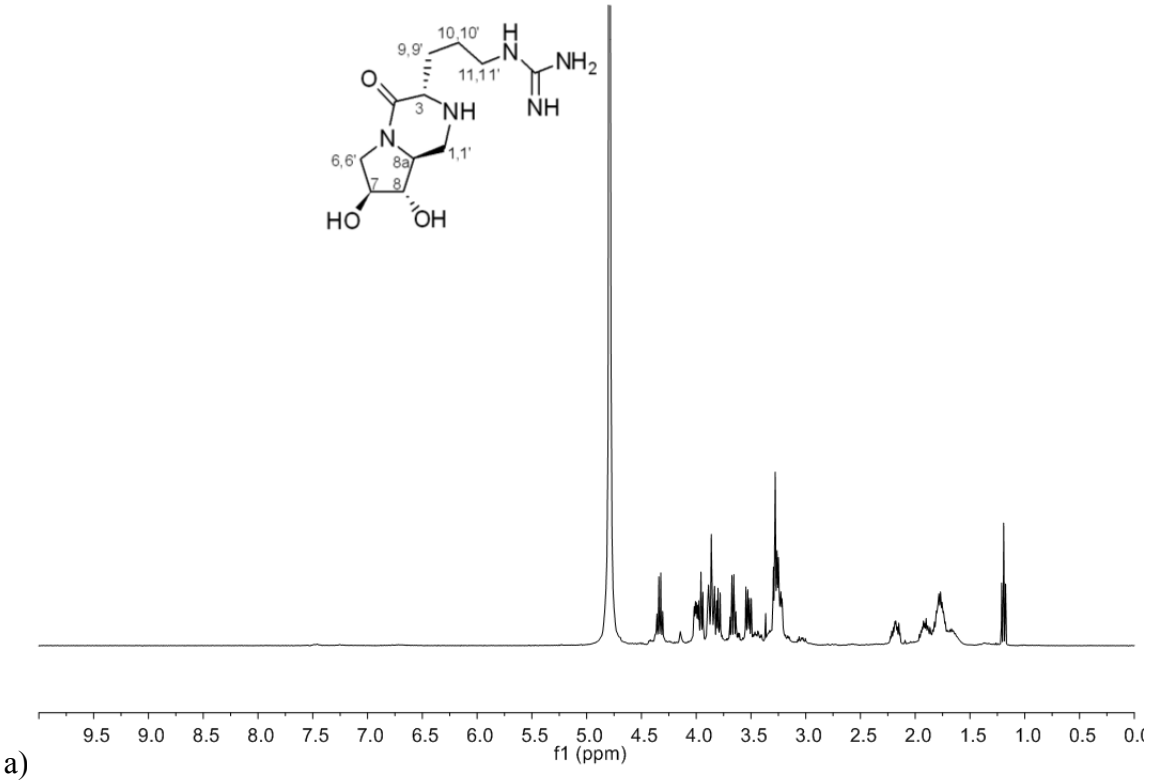

a)

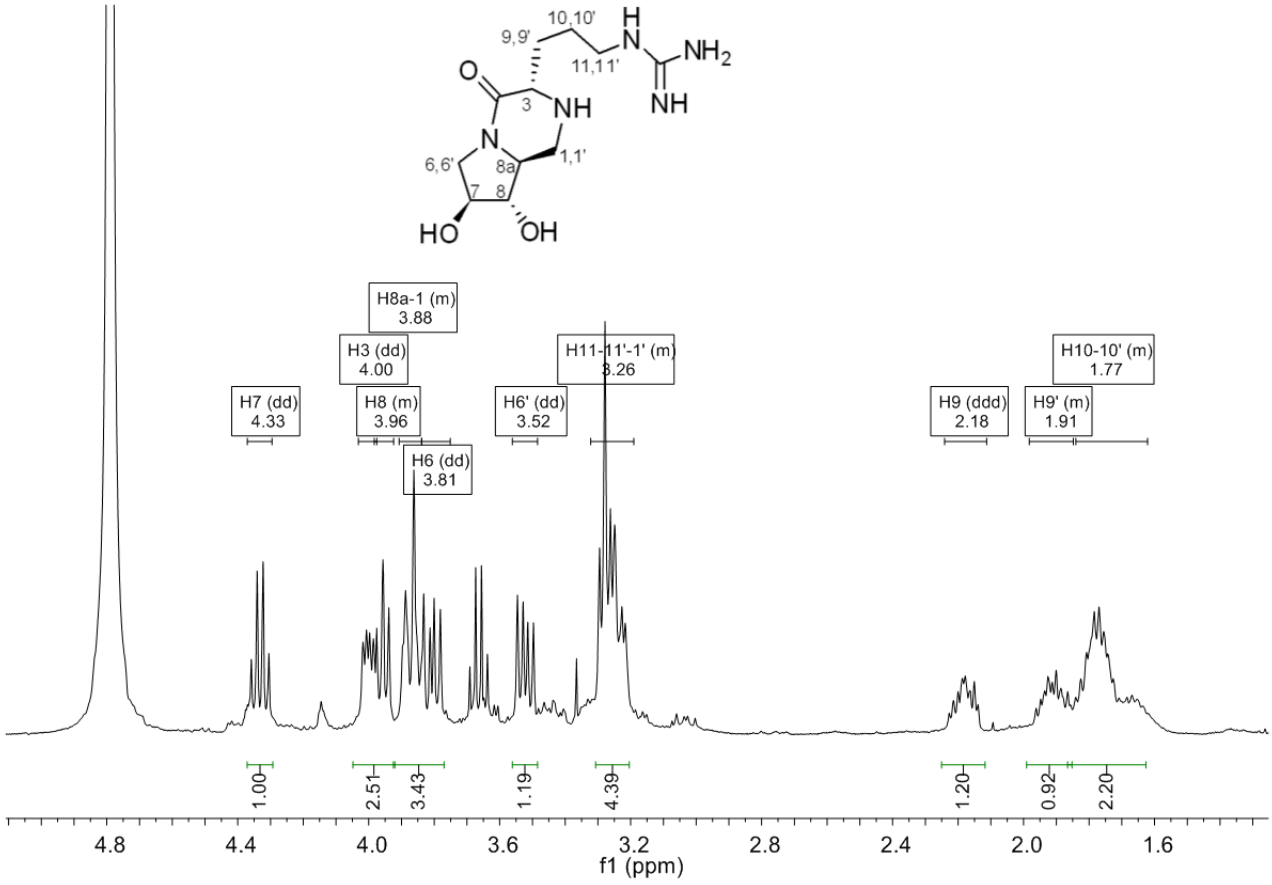

b)

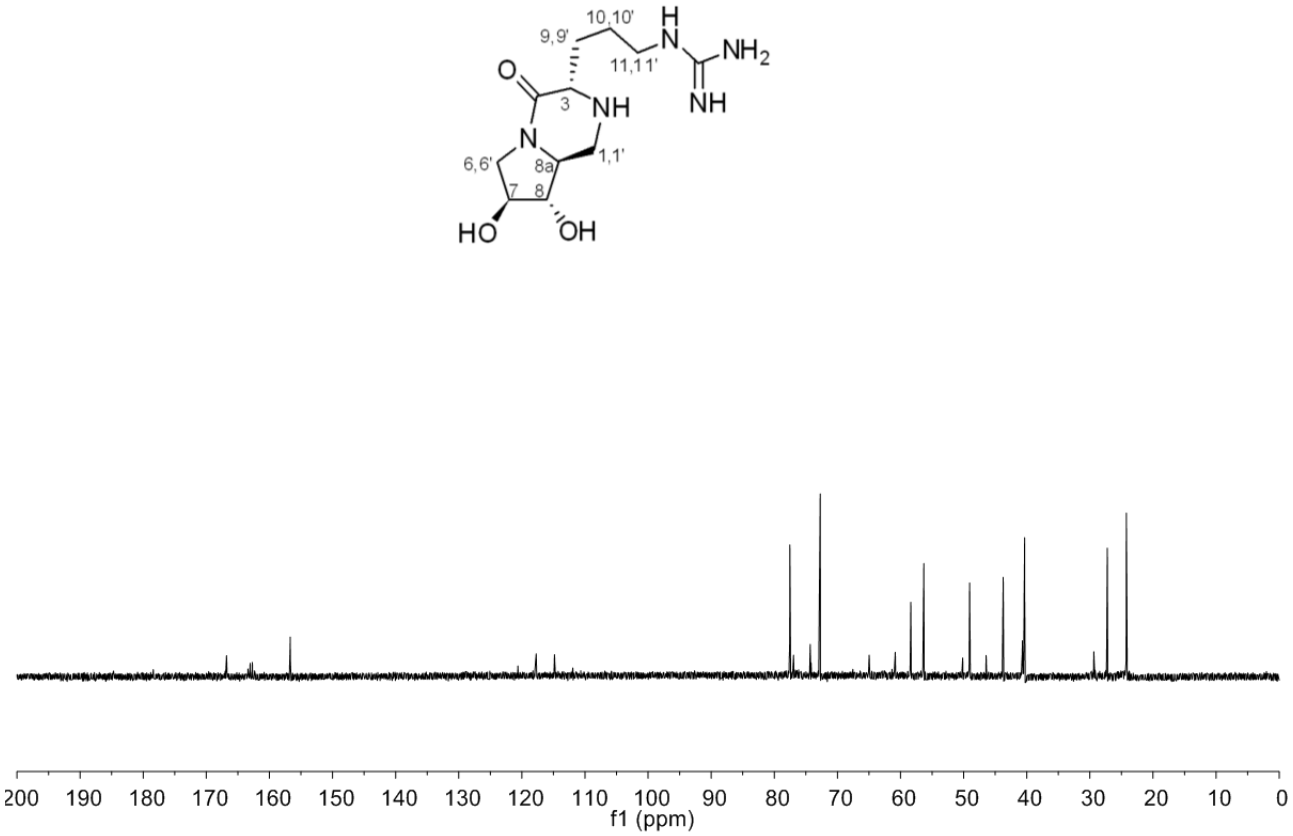

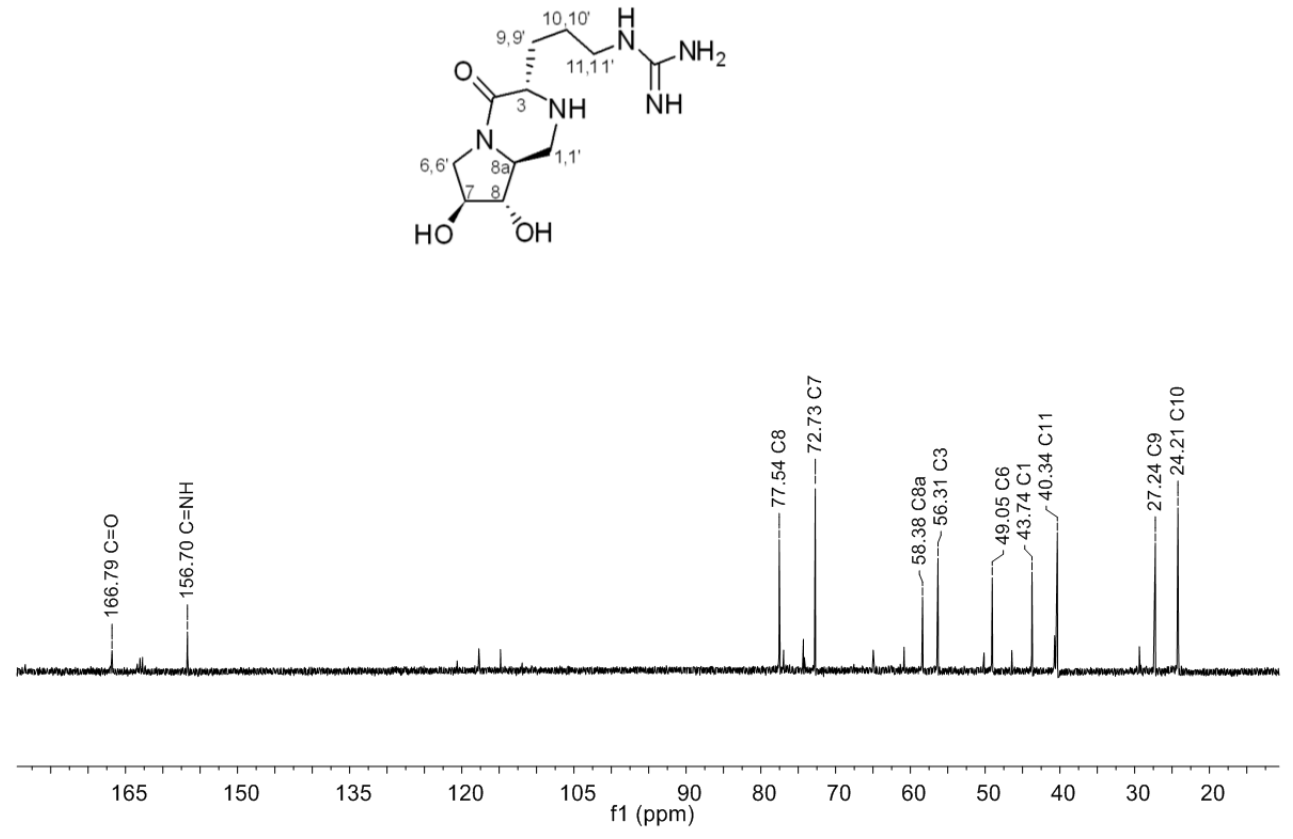

c)

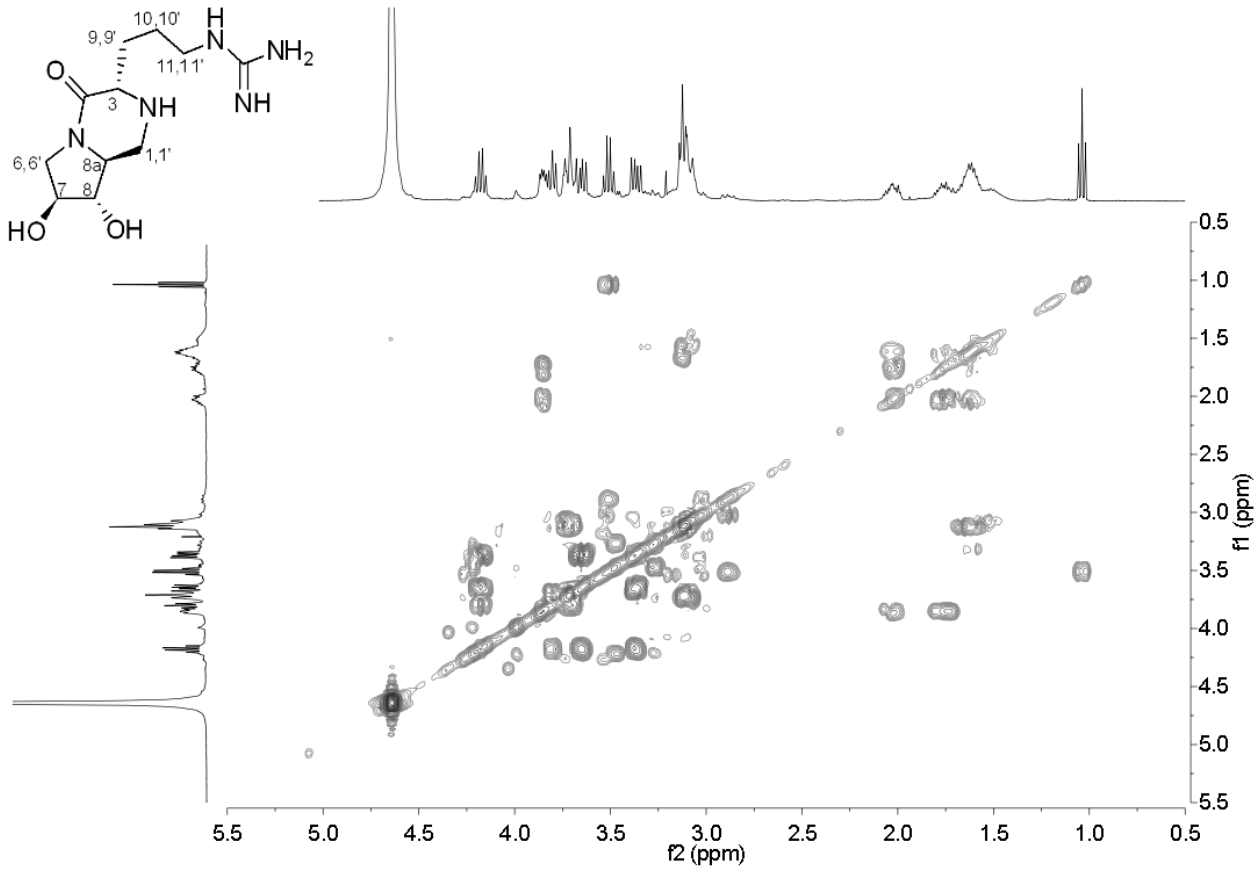

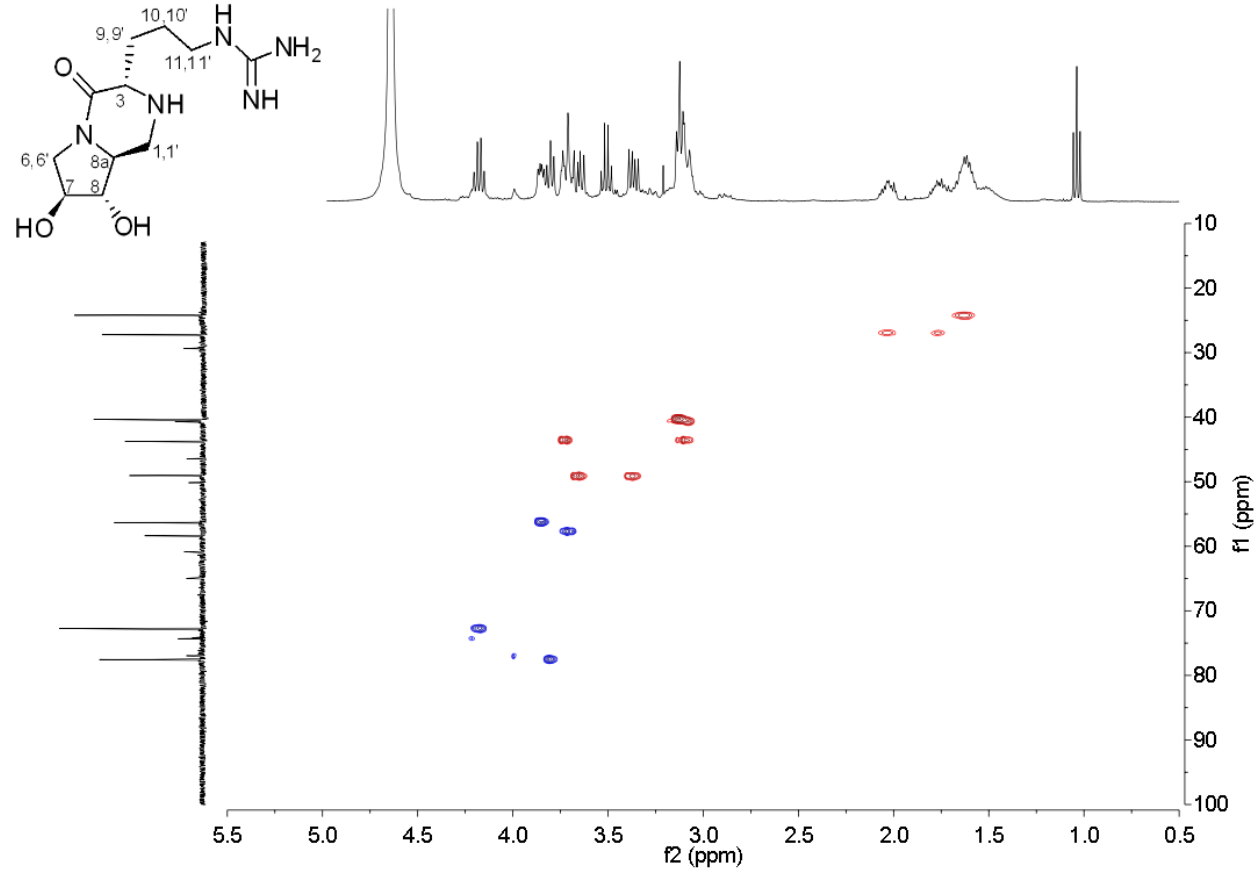

d)

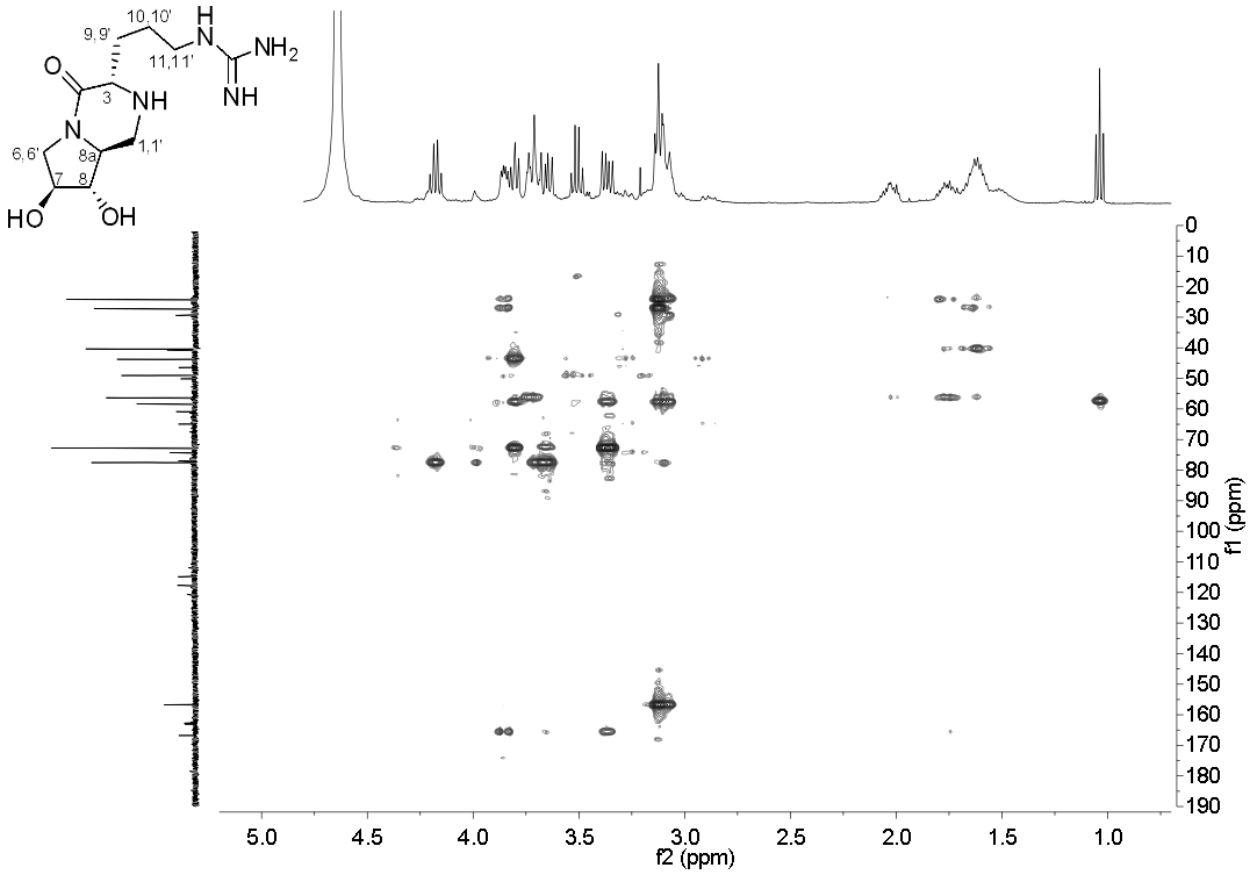

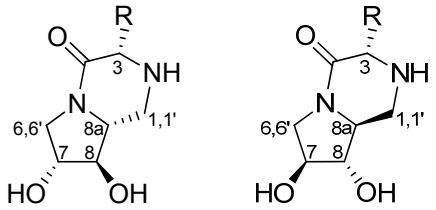

Product	Structure		H8a (C8a)	H8 (C8)	H7 (C7)	H6, 6' (C6)	H1, 1' (C1)	H3 (C3)	α_D	MS (oa-TOF) *m/z* $[M + H]^+$
28m	**DAB**		3.83 (57.94)	3.96 (77.60)	4.33 (72.70)	3.83, 3.49 (48.84)	3.83, 3.15 (44.36)	3.83 (43.51)	+ 2.3 (*c* = 1.4 in MeOH)	173.0923
29m	**LAB**		3.83 (57.37)	3.94 (77.46)	4.31(72.58)	3.83, 3.47 (48.80)	3.83, 3.18 (43.88)	3.83 (43.28)	– 2.5 (*c* =2 in MeOH)	173.0930
28n	**DAB**		3.85 (57.28)	4.04 (77.50)	4.34 (72.78)	3.85, 3.51 (49.17)	3.85, 3.40 (40.46)	4.22 (51.22)	+ 22.2 (*c* =1.2 in MeOH)	187.1089
29n	**LAB**		3.91 (57.44)	3.91 (77.51)	4.34 (72.77)	3.82, 3.50 (49.08)	3.91, 3.31 (43.34)	4.09 (52.61)	+ 26.0 (*c* =1 in MeOH)	187.1085
28p	**DAB**		3.81 (57.68)	4.00 (77.67)	4.32 (72.90)	3.81, 3.50 (49.28)	3.81, 3.30 (41.05)	4.00 (53.63)	– 9.0 (*c* =1 in MeOH)	229.1538
29p	**LAB**		3.88 (57.06)	3.96 (77.43)	4.33 (72.56)	3.80, 3.52 (49.20)	3.88, 3.29 (43.25)	4.06 (54.75)	– 3.78 (*c* =0.9 in MeOH)	229.1545
28q	**DAB**		3.80 (57.19)	3.80 (77.66)	4.28 (72.75)	3.80, 3.52 (49.34)	3.65, 2.91 (41.48)	4.41 (55.77)	– 11.4 (*c* =1.2 in MeOH)	263.1377
29q	**LAB**		3.84 (57.09)	3.95 (77.41)	4.34 (72.66)	3.84, 3.56 (49.19)	3.84, 3.26 (43.51)	4.34 (58.03)	– 5.7 (*c* =1.1 in MeOH)	263.1399
28u	**DAB**		3.82 (57.77)	4.03 (77.66)	4.32 (72.90)	3.82, 3.53 (49.29)	3.82, 3.26 (41.61)	4.03 (54.71)	– 2.0 (*c* =1 in MeOH)	272.1726
29u	**LAB**		3.88 (58.38)	3.96 (77.54)	4.33 (72.73)	3.81, 3.52 (49.05)	3.88, 3.26 (43.74)	4.00 (56.31)	+16.9 (*c* =1.2 in MeOH)	272.1716
29s	**LAB**		3.95 (57.17)	3.95 (77.44)	4.35 (72.72)	3.84, 3.48 (49.09)	3.95, 3.39 (43.77)	4.29 (53.08)	+46.6 (*c* =0.8 in MeOH)	231.0995
28v	**DAB**	**Major 70**	3.86 (58.15)	3.99 (77.04)	4.33 (72.62)	3.83, 3.47 (48.66)	3.93, 3.23 (50.55)	4.38 (62.08)	– 19.0 (*c* = 1 in MeOH)	213.1226
		Minor 30	4.04 (51.79)	4.07 (74.14)	4.40 (68.04)	3.83, 3.52 (51.62)	3.47, 3.33 (48.50)	4.22 (61.00)		

Figure 34. Lineweaver-Burk double reciprocal plots of inhibitions of a) α-D-glucosidase from baker's yeast, b) α-D-glucosidase from rice, c) β-D-glucosidase from sweet almonds, d) β-D-galactosidase from bovine liver and e) α-L-rhamnosidase from *Penicillium decumbens*.

a) α-D-Glucosidase from baker's yeast

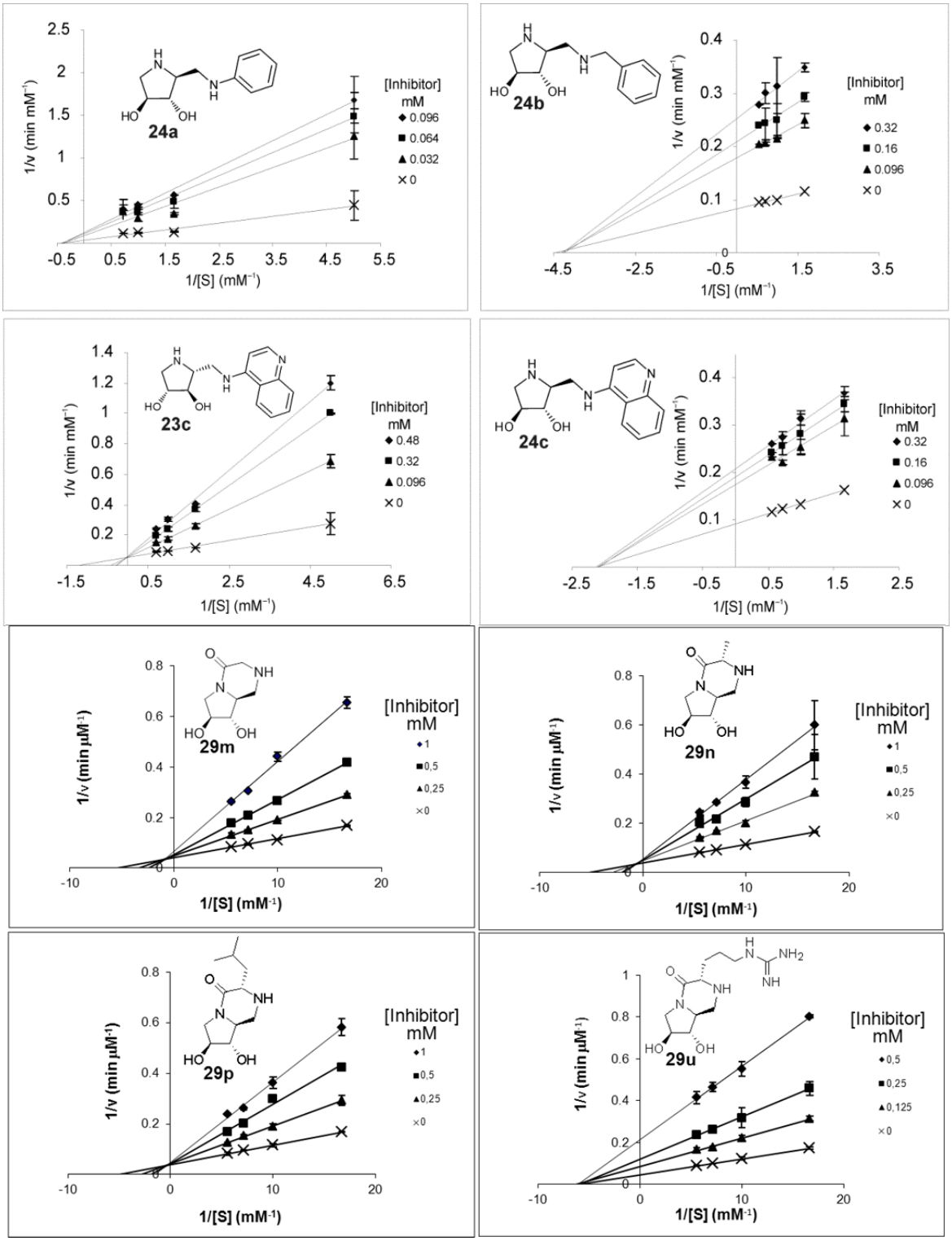

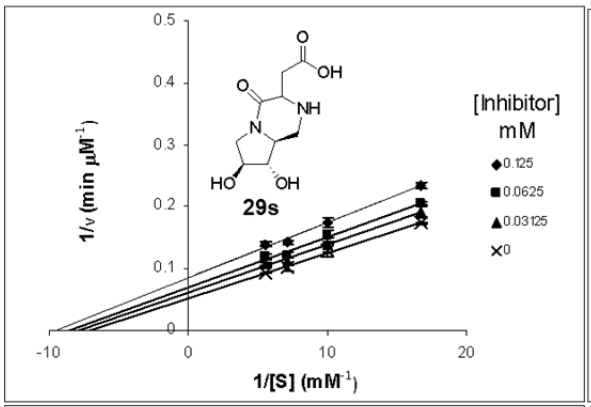

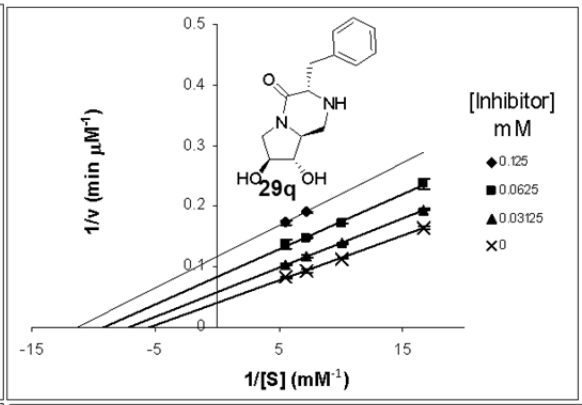

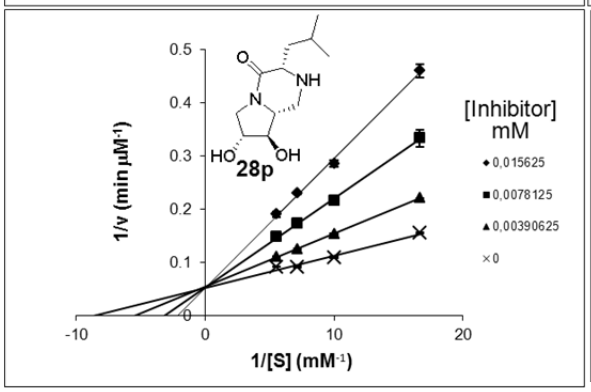

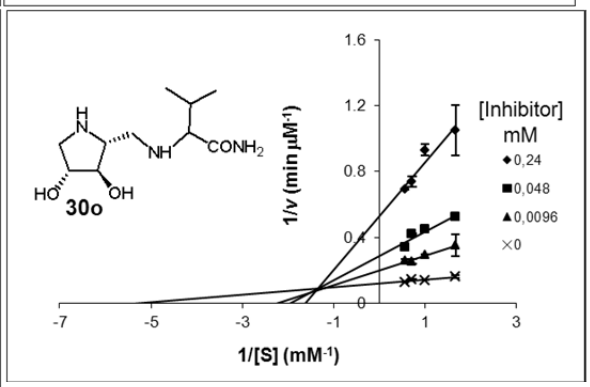

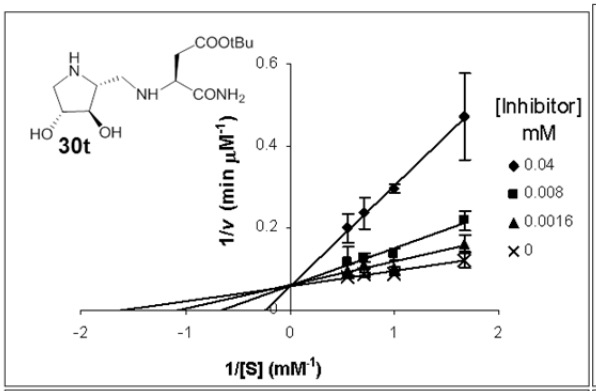

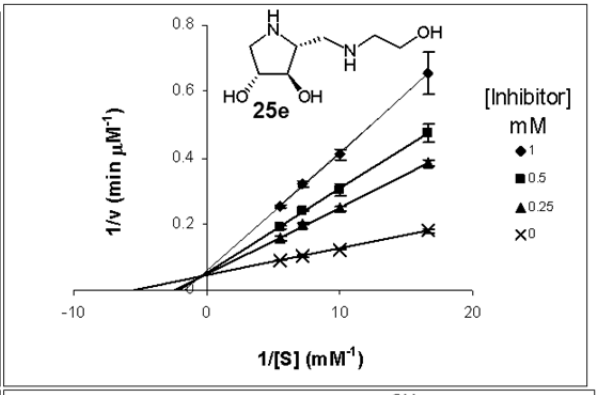

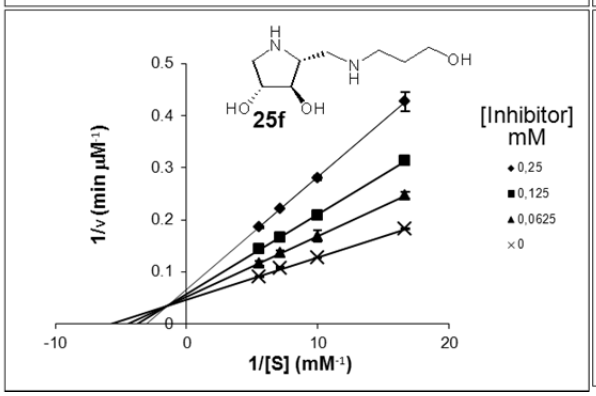

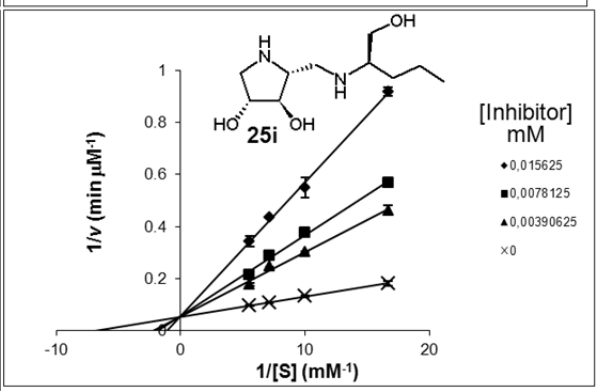

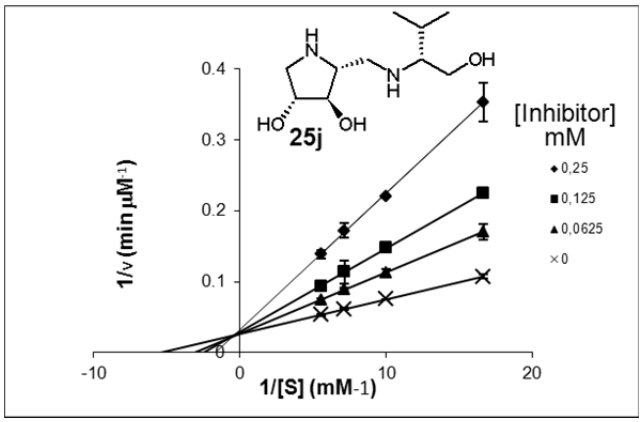

b) α-D-Glucosidase from rice

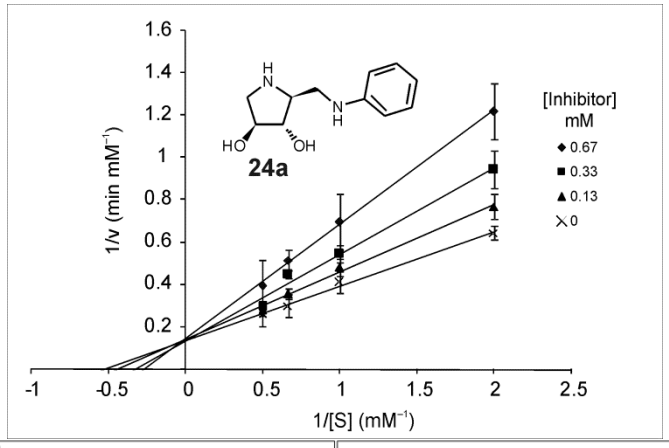

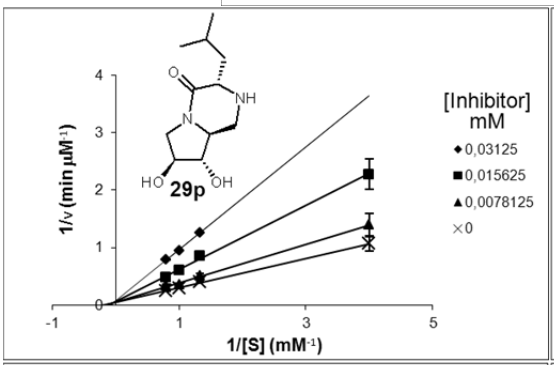

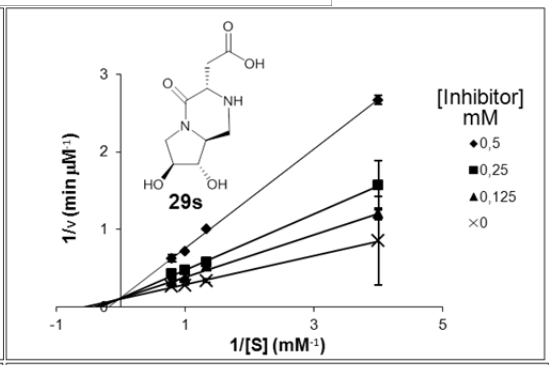

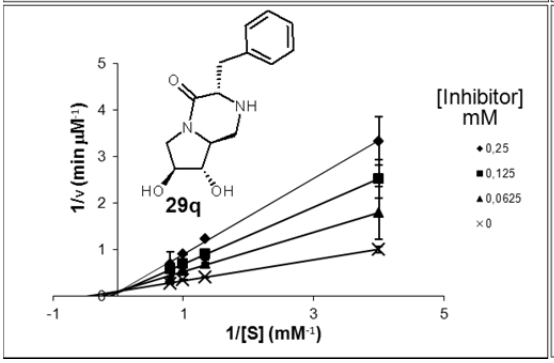

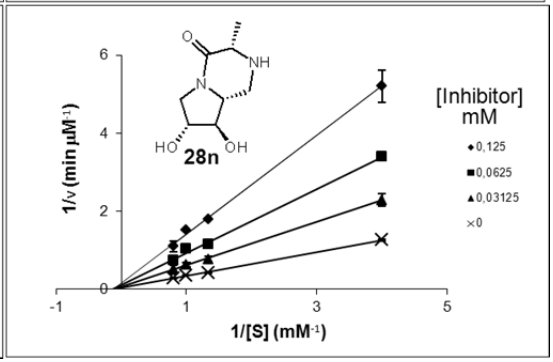

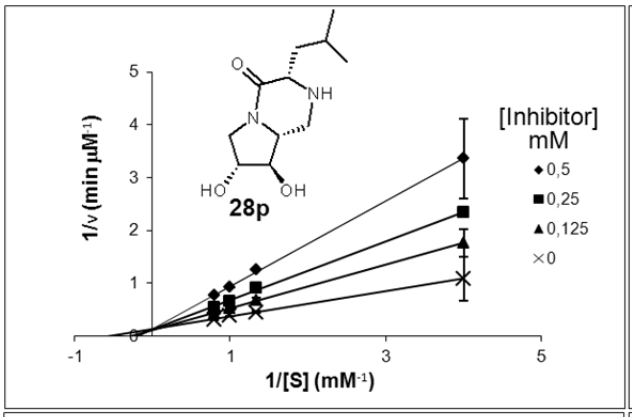

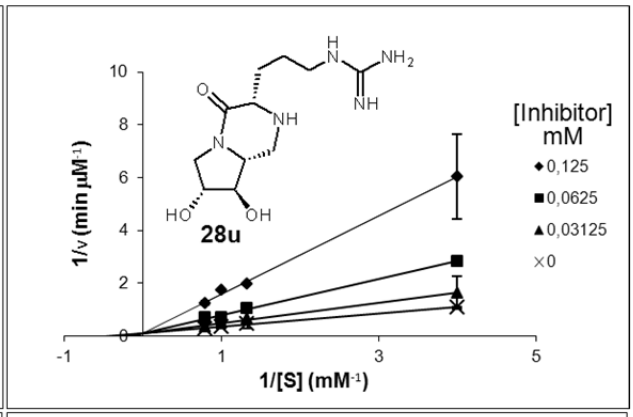

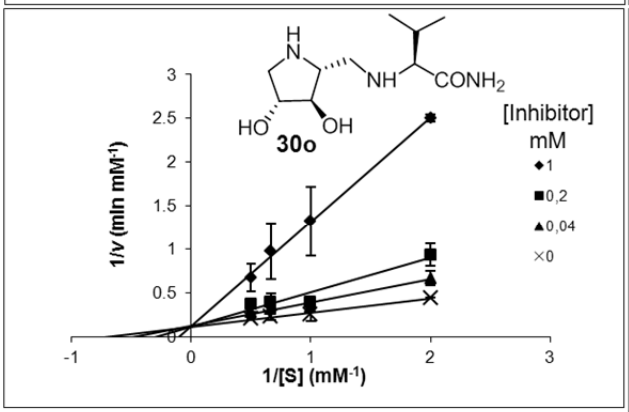

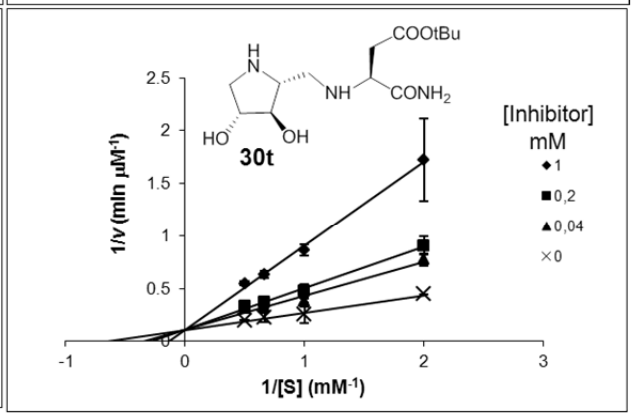

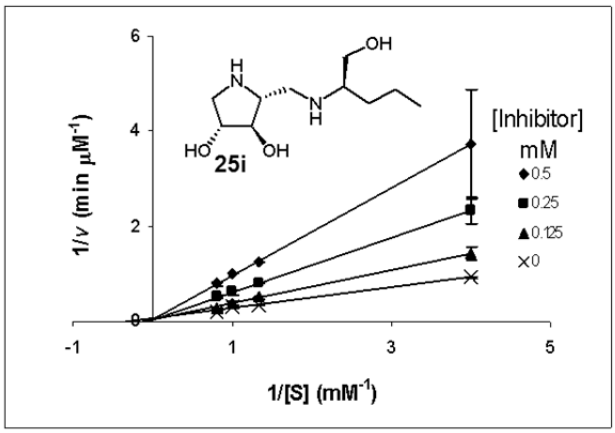

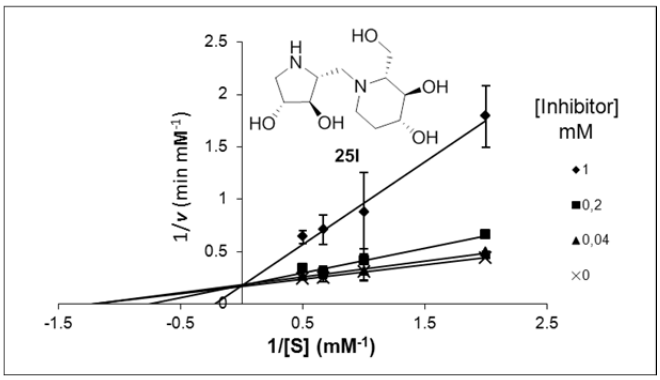

c) β-D-Glucosidase from sweet almonds.

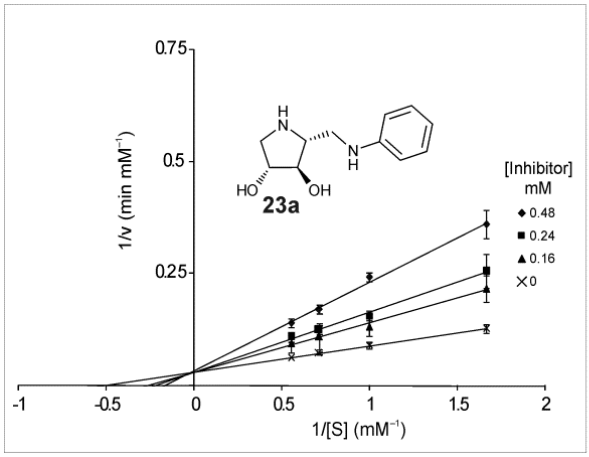

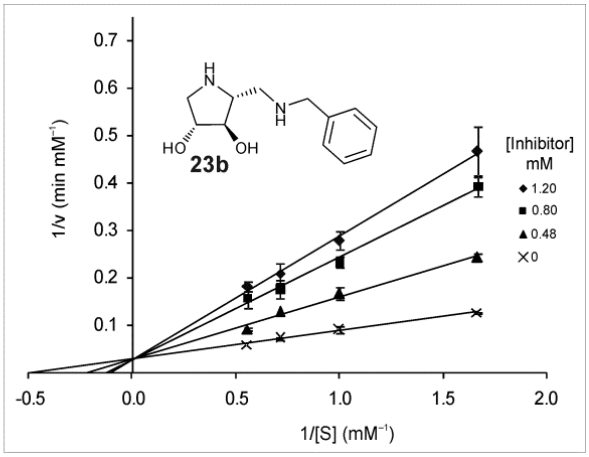

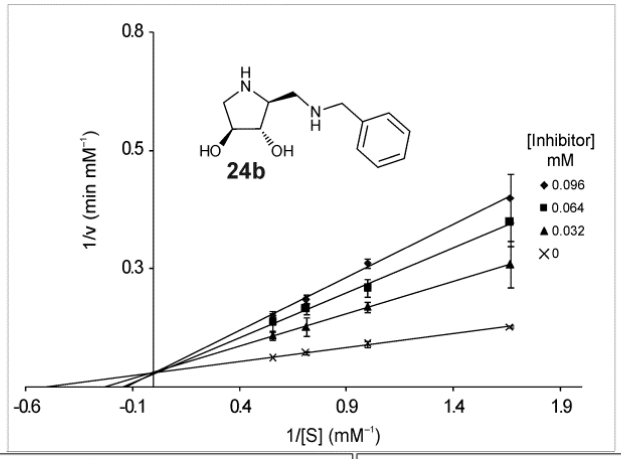

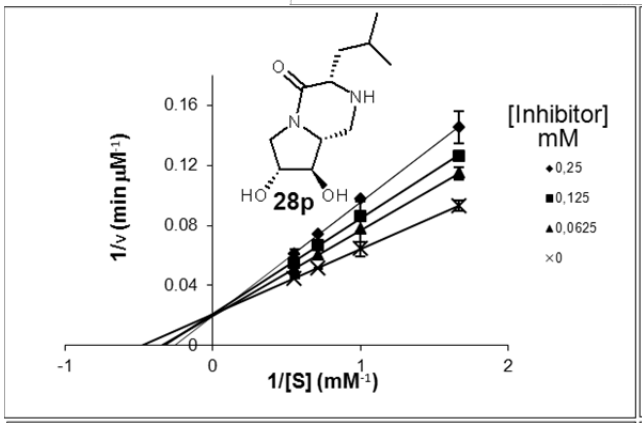

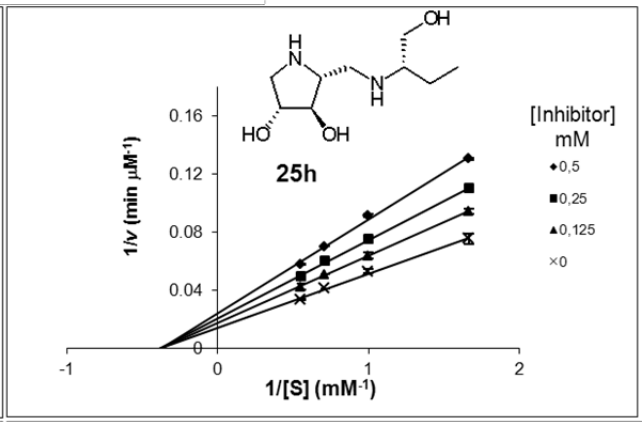

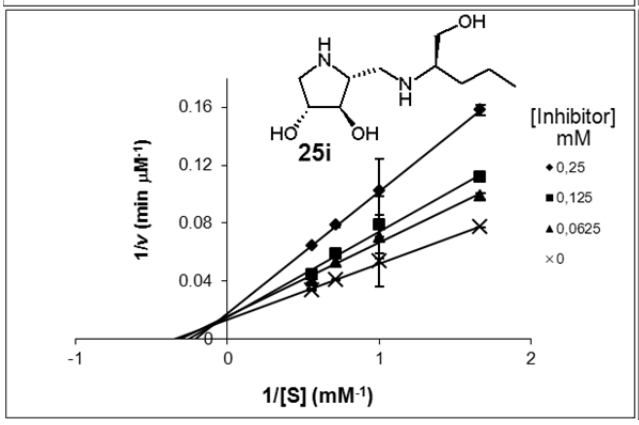

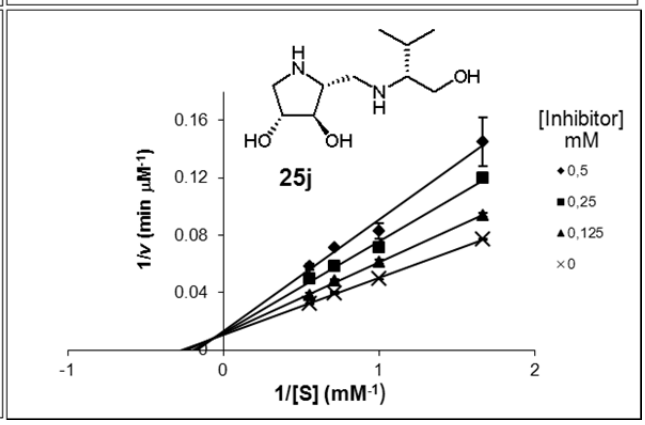

d) β-D-Galactosidase from bovine liver

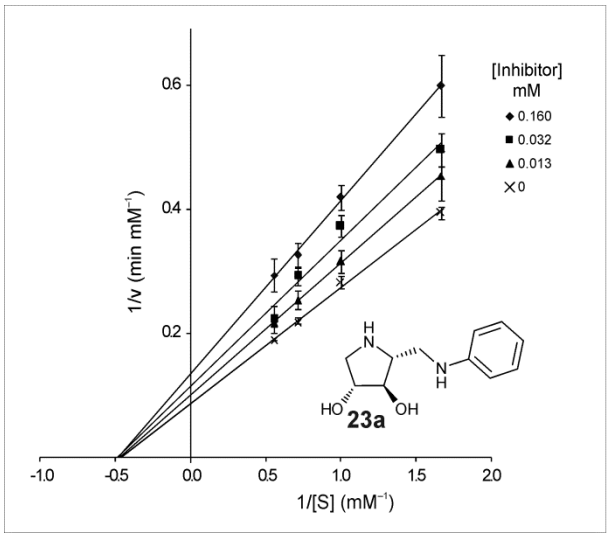

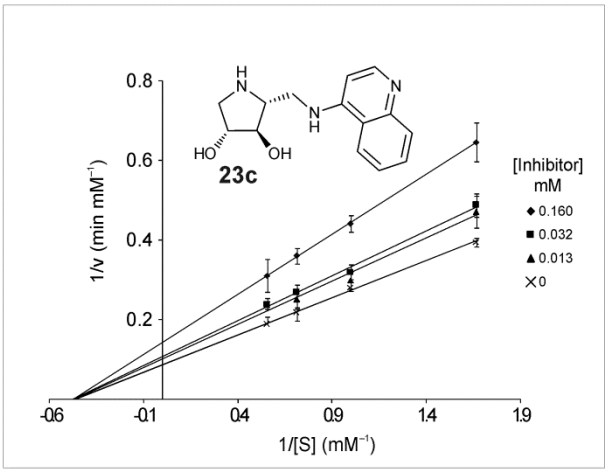

e) α-L-Rhamnosidase from *Penicillium decumbens*

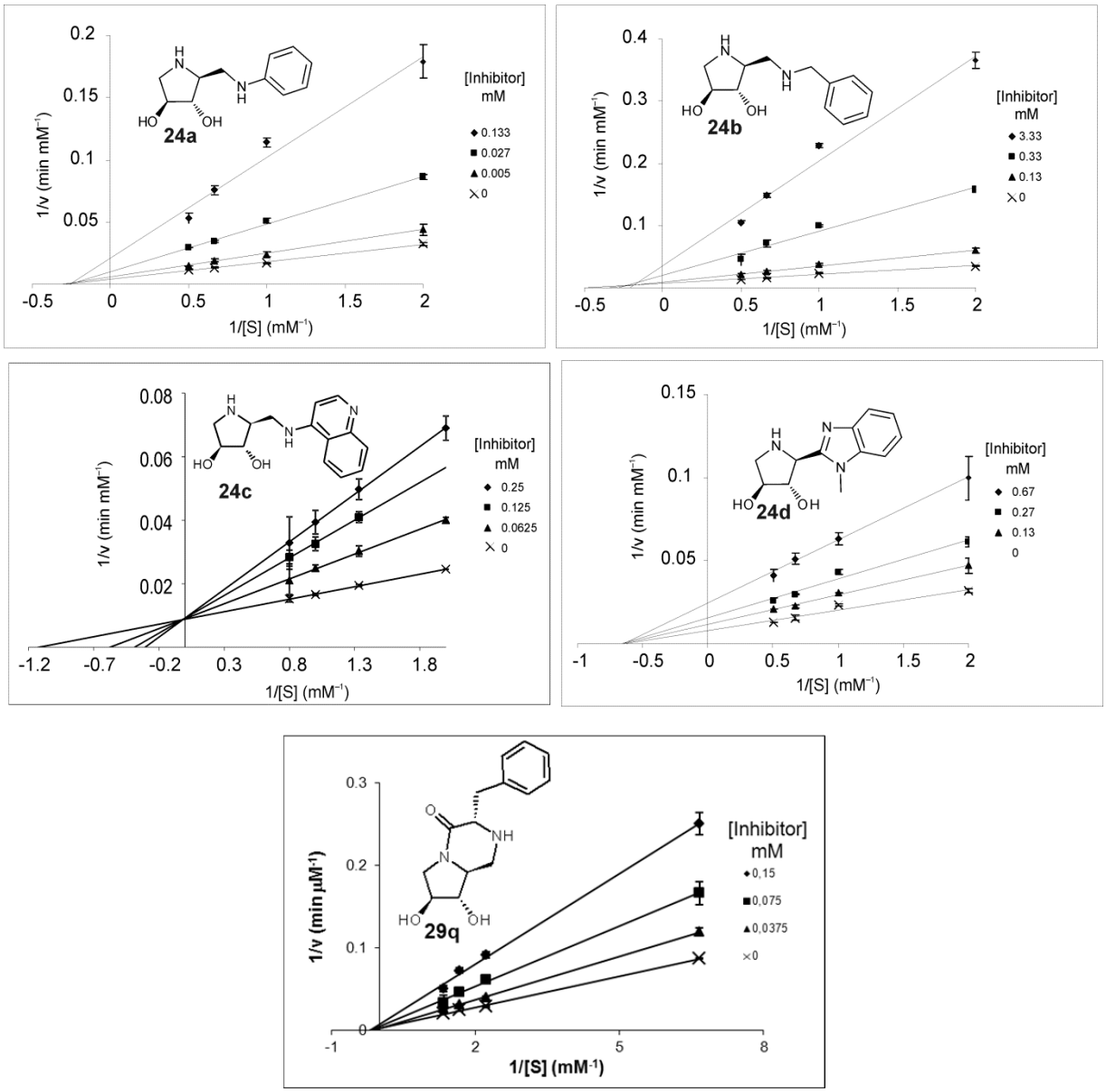

References

1. L. Espelt, T. Parella, J. Bujons, C. Solans, J. Joglar, A. Delgado and P. Clapés, *Chem. Eur. J.*, 2003, 9, 4887-4899; J. Calveras, M. Egido-Gabás, L. Gómez, J. Casas, T. Parella, J. Joglar, J. Bujons and P. Clapés, *Chem. Eur. J.*, 2009, 15, 7310-7328.

2. L. Vidal, O. Durany, T. Suau, P. Ferrer, M. D. Benaiges and G. Caminal, *J. Chem. Tecnol. Biotechnol.*, 2003, 78, 1171-1179; X. Garrabou, J. Joglar, T. Parella, J. Bujons and P. Clapés, *Adv. Synth. Catal.*, 2011, 353, 89-99.

3. M. Gutierrez, T. Parella, J. Joglar, J. Bujons and P. Clapés, *Chem. Commun.*, 2011, 47, 5762-5764.

4. A. Dahlqvist, *Anal. Biochem.*, 1964, 7, 18-25.

5. M. M. Bradford, *Anal. Biochem.*, 1976, 72, 248-254.

6. J.-C. Palomino, A. Martin, M. Camacho, H. Guerra, J. Swings and F. Portaels, *Antimicrob. Agents Chemother.*, 2002, 46, 2720-2722.